N° d'ordre : XXXX **ANNÉE 2013**

THÈSE / UNIVERSITÉ DE RENNES 1
sous le sceau de l'Université Européenne de Bretagne

pour le grade de

DOCTEUR DE L'UNIVERSITÉ DE RENNES 1

Mention : Traitement du Signal et Télécommunications

Ecole doctorale: Mathématiques, Télécommunications, Informatique, Signal, Systèmes, Electronique (MATISSE)

présentée par

Yuan WANG

préparée à l'unité de recherche LTSI – INSERM UMR 1099
Laboratoire Traitement du Signal et de l'Image
UFR Informatique et Electronique (ISTIC)

Heart Rate Variability and Respiration Signal as Late Onset Sepsis Diagnostic Tools in Neonatal Intensive Care Units

Thèse soutenue à Rennes le 19 Décembre 2013

devant le jury composé de :

Catherine MARQUE
Professeur, Université de Technologie de Compiègne (UTC) / *rapporteur*

Jocelyne FAYN
Ingénieur de Recherche, HDR, INSERM Lyon / *rapporteur*

Huazhong SHU
Professeur, Université du Sud-Est, Nankin, Chine / *examinateur*

Lotfi SENHADJI
Professeur, Université de Rennes 1 / *directeur de thèse*

Guy CARRAULT
Professeur, Université de Rennes 1 / *co-directeur de thèse*

Abstract

Late-onset sepsis, defined as a systemic infection in neonates older than 3 days, occurs in approximately 7% to 10% of all neonates and in more than 25% of very low birth weight infants who are hospitalized in Neonatal Intensive Care Units (NICU). In view of the high morbidity and mortality associated with infection, reliable markers are needed.

Recurrent and severe spontaneous apneas and bradycardias is one of the major clinical early indicators of systemic infection in the premature infant. It requires prompt laboratory investigation so that treatment can start without delay. Various hematological and biochemical markers have been evaluated for this indication but they are invasive procedures that cannot be repeated several times.

The objective of this dissertation was to determine if heart rate behavior, respiratory amplitude and the analysis of their relationships help to the diagnosis of infection in premature infants with cardiac decelerations via non-invasive ways in a NICU context. Therefore, we carried out two parts of research work in two selected groups of premature infants (sepsis vs. non-sepsis):

- Analysis for RR series
- Analysis for relationship between RR series and respiration

First of all, we studied the RR interval series not only by distribution methods (moy, varn, skew, kurt, med, SpAs), by linear methods — time domain (SD, RMSSD) and frequency domain (p_VLF, p_LF, p_HF), but also by non-linear methods – chaos theory (alphaS, alphaF) and information theory (AppEn, SamEn, PermEn, Regul). For each method, we attempt three sizes of window 1024/2048/4096, and then compare these methods in order to find the optimal ways to distinguish sepsis premature infants from non-sepsis ones. The results show that **alphaS**, **alphaF** and **SamEn** are optimal parameters to recognize sepsis from the diagnosis of late neonatal infection in premature infants with unusual and recurrent apnea-bradycardia.

The question about the functional coupling of heart rate variability and nasal respiration is addressed. Linear and non-linear relationships have been explored. Linear indexes were correlation (r^2), coherence function (*Cohere*) and time-frequency index ($r^2_{t,f}$), while a non-linear regression coefficient (h^2) was used to analyze non-linear relationships. We calculated two directions during evaluate the index h^2 of non-linear regression. Finally, from the entire analysis process, it is obvious that the three indexes (**r2tf_rn_raw_0p2_0p4**, **h2_rn_raw** and **h2_nr_raw**) were complementary ways to diagnosticate sepsis in a non-invasive way, in such delicate patients.

Furthermore, feasibility study is carried out on the candidate parameters selected from Mono-Channel Analysis in Chapter B1 and Bi-Channel Analysis in Chapter B2 respectively. We discovered that the proposed test based on optimal fusion of 6 features (alphaS, alphaF, SamEn, r2tf_rn_raw, h2_rn_raw and h2_nr_raw) shows good performance with the largest Area Under Curves (AUC) and the least Probability of False Alarm (P_{FA}).

As a conclusion, we believe that the selected measures from Mono-Channel and Bi-Channel signal analysis have a good repeatability and accuracy to test for the diagnosis of sepsis via non-invasive NICU monitoring system, which can reliably confirm or refute the diagnosis of infection at an early stage.

Keywords:

Neonatal intensive care units (NICU), premature newborns, sepsis, non-sepsis, autonomic nervous system (ANS), heart rate variability (HRV), respiratory system, respiration, linear methods, non-linear methods, statistical analysis, feasibility study, optimal fusion, receiver operating characteristic (ROC), clinical decision making, medical informatics, prediction

Acknowledgments

Pursuing Ph.D is a Journey of Odyssey, long and tough, tears and smiles, pain but happiness with sense of accomplishments.

First of all, I would like to thank Prof. **Jean-Louis COATRIEUX**. He selected me from a lot of Chinese students and introduced me to Prof. Lotfi SENHADJI. His approval motivates me to continue on the path of scientific research, which is a turning point in my life. I always regard him as my academic grandfather from the bottom of my heart, and furthermore, I am proud to be one of his academic offspring for ever.

I would like to thank my advisor Prof. **Lotfi SENHADJI**, who accepted me as his Ph.D student. His kind heart and charming personality made me feel warm and comfortable in a foreign country. Particularly, his acumen, chariness and diligence gave me a deep impression. He has been and will continue to be a role model for me to struggle abroad.

I would also like to thank my co-advisor Prof. **Guy CARRAULT**, for his in-depth guidance and fruitful discussions during the course of my Ph.D study. He taught me how to manage time, solve problems, and present the results in an informative and interesting way. His deep and sharp thinking had a tremendous impact both on this work and on my academic development. The problem solving skills I learned from him will be invaluable for my career as a scientist. He also taught me to be conscientious, independent, rigorous and hard-working in performing research.

I might never have entered the world of Digital Signal Processing (DSP) would it not be for Prof. **Huazhong SHU** of Southeast University (SEU) in Nanjing. I am extremely fortunate to have met Prof. SHU while an undergraduate at SEU. After participating in the course "Digital Signal Processing" taught by Prof. SHU, I knew that DSP is what I would want to do! I express my sincerest gratitude to Prof. SHU for exposing me to DSP, for believing in me when I was still green and for encouraging me to come to University of Rennes 1 (UR1). I am looking forward to a lifetime of collaboration back in China.

I am extremely grateful to Prof. **Catherine MARQUE** and Prof. **Jocelyne FAYN** who accepted to be "Rapporteur". They took a lot of time to review my Ph.D dissertation very carefully. In their reports, they gave me not only highly perceptive comments but also a great deal of encouragement.

Most of my time during this Ph.D study was spent at Laboratoire Traitement du Signal et de l'Image (LTSI). It was in this exceptional lab that I had the great opportunity to work with some really intelligent and supportive colleagues, especially in the group of "Surveillance Explication et Prévention de l'Insuffisance cardiaque et des Apnée-bradycardies" (SEPIA). I am extremely grateful to Dr. **Alain BEUCHEE** for the medical fundamentals of neonatology, autonomic nervous system and respiratory system from the very beginning of my research at UR1. He also provided me with clinical neonatal database. I am most grateful to Dr. **Nathalie COSTET** for her generous sparing of her time to discuss with me about statistical analysis, data interpretation and the usage of SAS software. Assist. Prof. **Fabienne POREE** explained to me how to use software "CardioRR" with great patience when my oral French is not fluent enough during the first year. Dr. **Alfredo HERNANDEZ** shared the proprietary software of MAC OS X with me without hesitation.

I am indebted to Assoc. Prof. **Christine TOUMOULIN** for her care and concern for my life in France. She reserved a comfortable studio for me before I arrived in France, so that I can quickly put all my heart into research work without disturbance. When I was sick during the first month in France, she drove me to the doctor as soon as possible. Everything she did made me feel more like "French mother".

I also want to thank Prof. **Limin LUO** from Southeast University in Nanjing, who always pay attention to my growth since undergraduate. His persistent encouragements give me much more confidence.

I thank the excellent technical support from **Guillaume JEHENNE**. Whenever there is something wrong with my desktop, he constantly came to me in a quick manner and save a lot of research time for me. During coffee break, he was friendly to talk with me and willing to correct my French pronunciation and expression. In addition, he taught me how to play Belote and Sudoku, which let me better integrate into French social circle.

I also thank the considerate and polite administrative support from **Muriel DIOP**, **Patricia BERNABE** and **Soizic CHARPENTIER**.

Many thanks go to my labmates ---- the LTSIers. Although we come from different countries, from different cultures, we are friendly to each other and learn from each other under the atmosphere of equality and harmony. Dr. **Jérôme DUMONT** was supportive to me from the very beginning of my journey at LTSI. He was dedicated to help me not only in improving my French, but also in research. The advice and words of wisdom from him will continue to influence me. When I was suffering from illness in my legs, he was warm-hearted to drive me to shopping. Dr. **Xavier NAVARRO**, I thank him for his real empathy for me. We encourage each other and help each other in the final stages of our Ph.D studies. Due to the space limit here, I cannot list everyone who stimulated my thinking, gave me a favor or said words of consolation to me. LTSI looks like a little United Nations. The international environment broadens my eyes and opens my minds, which will have deep and long-term effects on me regardless of academic research or other aspects in my life.

I would also like to acknowledge the financial support of Egide Ph.D Scholarship of French Government.

Finally, I give my deepest thanks to my loving and lovely family---- Mom **Lili MA** and Dad **Jia-lin WANG**, who give me continuous encouragement, strong support, unconditional love and unending patience. They always believe in me and cheer me up when I have doubts about myself. Their high expectations are important parts of my motivation. I feel so lucky that I was born in such an enlightened family.

Dedicated to my dear mother Lili MA and father Jia-lin WANG for their endless love and strong support.

献给我亲爱的母亲马琍琍与父亲王家林，感谢你们给予我无尽的关爱与强有力的支持。

God gives answers in three ways:

He says yes and gives you what you want.
He says no and gives you something better.
He says wait and gives you the best.

Pursuing Ph.D is a Journey of Odyssey

Résumé étendu du mémoire de Thèse

Contexte de la thèse et objectifs (Chap. 1)

Le sepsis tardif, défini comme une infection systémique chez les nouveaux nés âgés de plus de 3 jours, survient chez environ 7% à 10% de tous les nouveau-nés et chez plus de 25% des nouveau-nés de très faible poids de naissance qui sont hospitalisés dans les unités de soins intensifs néonatals (USIN). Les manifestations cliniques du sepsis néonatal, quelle que soit la source de l'infection, ne sont pas toujours si évidentes et par suite, les interventions précoces et adaptées ne sont pas toujours mises en route au risque de complications sévères pour le patient. Par conséquent, cette maladie est un problème majeur de santé publique entraînant une morbidité et la mortalité des nouveau-nés prématurés.

Les bébés prématurés malades ne montrent aucun signe de fièvre, c'est seulement avec une analyse de culture sanguine que les signes de septicémie peuvent être détectés. Cependant, d'une part, les marqueurs hématologiques et biochimiques qui sont utilisés pour ce symptôme, non seulement s'appuient sur des procédures invasives qui ne devraient pas être souvent répétées, mais ont des valeurs prédictives faibles dans la phase précoce du sepsis. D'autre part, il a été observé expérimentalement que les phénomènes d'apnée-bradycardie surviennent plus souvent chez les prématurés atteints de sepsis que chez les prématurés sans sepsis. Cependant, il est encore difficile de savoir si ces changements dans le comportement des signaux physiologiques cardiorespiratoires peuvent être utilisés pour diagnostiquer une septicémie chez les prématurés. Par conséquent, l'objectif de cette thèse est de trouver des critères objectifs (descripteurs quantitatifs) pour distinguer les nouveau-nés prématurés avec un sepsis des nouveau-nés sains ouvrant ainsi la voie à une approche de surveillance non-invasive en USIN.

Pour atteindre cet objectif, deux types d'analyses ont été réalisés :

- Analyse monovoie de la variabilité cardiaque par le biais de la série RR
- Analyse bi-voies considérant la série RR et le signal respiratoire

Dans la suite de ce chapitre, une revue bibliographique est présentée concernant les techniques d'analyse de la série RR dans le cas particulier des nouveau-nés de même que l'analyse conjointe de la série RR et du signal respiratoire.

La suite du document est organisée de la manière suivante.
La thèse a été divisée en deux parties. La partie A concerne les connaissances médicales et regroupe 3 chapitres. Dans le chapitre A1, nous présentons certains problèmes cliniques associés à la prématurité. Surtout, nous passons en revue séparément les manifestations cliniques de sepsis d'apparition précoce et d'infection d'apparition tardive chez les nouveau-nés.
Dans le chapitre A2, nous passons en revue les fondements physiologiques du système nerveux autonome, qui contrôlent la variabilité du rythme cardiaque. Après, nous discutons du comportement du système de contrôle cardio-vasculaire, en particulier, nous nous concentrons sur le comportement anormal lié au sepsis néonatal qu'est la bradycardie.
Dans le chapitre A3, nous présentons les concepts cliniques liés au système respiratoire et qui sont à l'origine de la régulation du signal de respiration. Ensuite, nous discutons de la variabilité respiratoire et, en particulier, nous nous concentrons sur le phénomène déviant

observé lors d'un sepsis néonatal qu'est l'apnée. La relation entre l'apnée et la bradycardie est également discutée.

La partie B regroupe 3 chapitres. Dans le chapitre B1, nous étudions des méthodes linéaires et non linéaires dédiées à l'analyse de la série RR chez les nouveau-nés. Une analyse comparative a été considérée : les patients du groupe « sepsis » ont été comparés au groupe « non-sepsis », selon l'âge post-conception (PCA) et l'âge post-natal (PNA), dont les valeurs sont assez proches pour être comparées. Ceci nous permet de mettre en évidence les meilleurs moyens d'établir une discrimination entre les nouveau-nés prématurés infectés et non infectés.
Dans le chapitre B2, nous nous intéressons au traitement bi-voies de mesure de relations linéaires ou non linéaires entre les séries RR et les signaux respiratoires chez les nouveau-nés. De la même cohorte explorée pour l'analyse des signaux RR, les nourrissons ont été retenus, ceux ayant des signaux respiratoires enregistrés. Ceci nous permet d'envisager un autre moyen pour diagnostiquer d'une manière non-invasive le sepsis.
Dans le chapitre B3, nous avons effectué une étude de faisabilité sur les descripteurs sélectionnés aux chapitres B1 et B2, par rapport à leur fusion optimale, afin d'identifier l'approche ou les approches susceptible(s) d'être explorée(s) dans un système de surveillance en USIN.

Le document se termine par une conclusion qui résume brièvement les travaux de recherche et les principaux résultats présentés dans cette thèse, et par une perspective pointant les orientations futures à donner à ce travail.

Prématurité et sepsis (Chap. A1)

L'objet de notre étude est le nouveau-né prématuré, de sorte que dans ce chapitre nous discutons principalement de considérations médicales le concernant. Tout d'abord, la notion de prématurité est introduite et les définitions des symptômes des sepsis sont données.

Les bébés prématurés sont nés entre la 24^{e} et 37^{e} semaines après la dernière menstruation contrairement aux bébés nés à terme, qui ont un âge post-menstruel entre 37 et 42 semaines (Fig. A1 1). Un nouveau-né pesant moins de 1500 grammes à la naissance est considéré comme un bébé de très faible pesée (VLWB « very low weigh baby »).

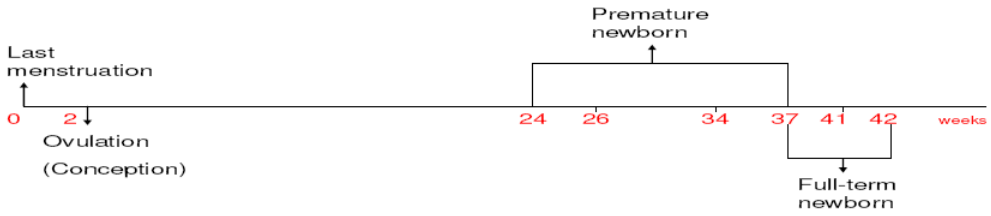

Fig. A1-1 Gestational ages from the last menstrual period

Comme les nouveau-nés subissent des changements rapides après la naissance, et en précisant l'importance du degré de prématurité, il est important de définir clairement l'âge dans les termes suivants, tel que recommandé par la terminologie standard (Fig. A1 -2):
• L'âge gestationnel (AG) : temps écoulé entre le premier jour de la dernière période menstruelle et le jour de la délivrance.
• L'âge chronologique (CA) : temps écoulé après la naissance.
• L'âge post-menstruel (PMA) : l'âge gestationnel plus l'âge chronologique.

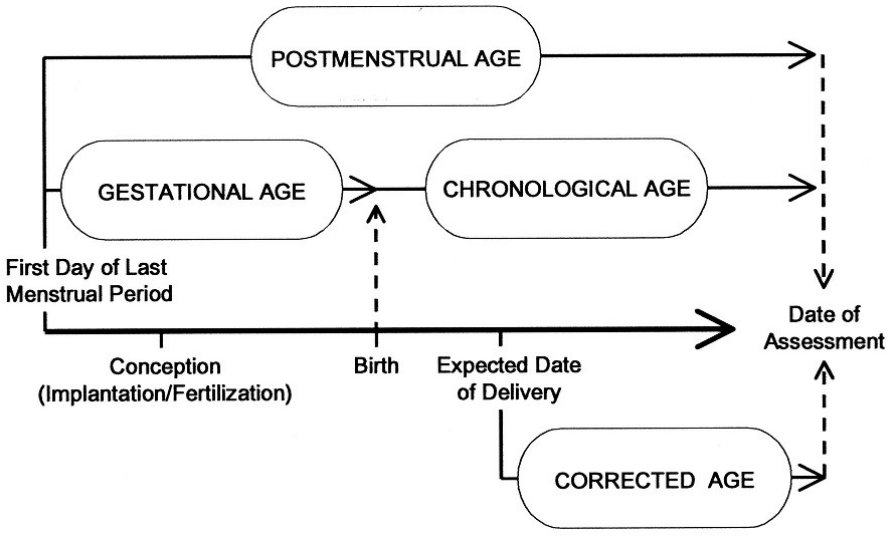

Fig. A1-2 Standard terminology according the AAP

Les nouveau-nés grands prématurés doivent se battre pour survivre, depuis le premier instant de leur vie extra-utérine. Pendant la gestation, de l'oxygène et de la nourriture sont fournis par le placenta, la température est toujours confortable et constante, les effets de la pesanteur sont

imperceptibles et le bébé est bercé par le rythme des activités de la mère. Ses organes sensoriels, en partie déjà formés, ne sont pas soumis à des sollicitations directes comme des sons, des lumières ou des contacts, les anticorps de la mère le protègent et ils vont passer dans son corps dans les dernières semaines de la grossesse. Le grand prématuré de ce fait arrive donc dans un environnement pas très approprié pour lui, et des complications peuvent survenir tels que les sepsis.

Les Sepsis

Les manifestations cliniques de sepsis (ou septicémies néonatales), quelle que soit la source de l'infection, sont souvent non spécifiques et comprennent la détresse respiratoire, l'instabilité de la température et la dépression cardio-vasculaire. Un gonflement de la fontanelle peut être aussi observé. Le sepsis et la méningite peuvent également être précoces ou tardifs. Il est difficile de diagnostiquer les sepsis en raison de la multiplicité des facteurs de risque associés et les manifestations cliniques.
Le sepsis est défini comme la combinaison d'une réaction inflammatoire, à savoir un CRP supérieure à 5 mg par litre, 24 heures après l'enregistrement, et d'hémocultures positives. Alors que la non-sepsie est définie comme l'association d'une absence de réaction inflammatoire, à savoir la CRP inférieure à 5 mg par litre 24 heures après l'enregistrement, et d'une hémoculture négative.

Les bébés de tout âge gestationnel sont à risque élevé d'infections bactériennes aiguës et ce pour plusieurs raisons, à la fois innées et extrinsèques. Les facteurs de risque d'infection sont inversement proportionnels à la GA. En conséquence, les nouveau-nés prématurés sont plus exposés. D'un point de vue clinique, deux types de sepsis sont définis en fonction de la période de survenue : infection précoce et infection tardive.

Sepsis (à début) précoce

Une infection bactérienne aiguë pendant les 3 premiers jours après la naissance survient chez 1 à 10 pour 1000 de naissances. Bien que la majorité survienne chez les nouveau-nés à terme, le risque d'infection est plus élevé chez les prématurés. Le sepsis précoce va se développer dans environ 2% de tous les nourrissons avec un poids de naissance <1500 grammes, bien que 10 fois ce nombre soit traité comme s'il était infecté. La détection rapide en vue d'une prise en charge approfondie est essentielle pour la réussite du traitement médicamenteux.
La septicémie à début précoce est associée à un risque accru du syndrome de détresse respiratoire, une maladie pulmonaire chronique, une hémorragie intraventriculaire sévère, et une leucomalacie périventriculaire (LPV). Malgré les progrès en matière de diagnostic et de traitements thérapeutiques, le sepsis précoce est associé à une forte mortalité et une morbidité importante, les nouveau-nés prématurés sont plus sévèrement touchés : parmi les grands prématurés, la mortalité est d'environ 35%.

Sepsis tardif (après l'âge de 3 jours)

Son incidence chez les nourrissons sains nés à terme est beaucoup plus importante que le sepsis précoce. Toutefois, les prématurés et les enfants nés à terme avec diverses conditions médicales ou chirurgicales sont plus à risque de sepsis tardif. Il survient dans environ 10% des

cas des nouveau-nés et dans plus de 25% des nourrissons de très faible poids de naissance qui sont hospitalisés dans les unités néonatales de soins intensifs.

Comme le sepsis précoce, le sepsis tardif est associé à une morbidité et une mortalité importantes ; les nourrissons prématurés sont plus sévèrement touchés avec un taux de mortalité allant jusqu'à 20%. Le sepsis tardif est associé à un risque accru de persistance du canal artériel, la dysplasie broncho-pulmonaire, l'entérocolite nécrosante et la mort.

Le sepsis tardif en USIN est un problème majeur en termes de risques de morbidité et de mortalité. Des marqueurs fiables permettant de l'identifier sont donc nécessaires.

Les épisodes d'apnées et de bradycardies spontanés, par leurs récurrences et leurs gravités révèlent souvent une infection systémique chez le prématuré. Les marqueurs hématologiques et biochimiques obtenus par des procédures invasives, qui ne peuvent être répétées fréquemment, ont une faible valeur prédictive dans la phase précoce du sepsis. Néanmoins, le manque d'intervention précoce et adaptée peut conduire l'enfant à risquer sa vie, et, en outre, la répétition des épisodes d'apnée-bradycardie compromet l'oxygénation et la perfusion des tissus.

Système nerveux autonome et variabilité cardiaque (Chap. A2)

Les fondements physiologiques du système nerveux autonome (SNA) et de la variabilité du rythme cardiaque (VRC) sont présentés dans le chapitre A2. En particulier, une analyse des systèmes et mécanismes de contrôle est proposée ainsi que la description des influences cardio-vasculaires qu'ils induisent.
Tout d'abord, les sections A2.2 et A2.3 introduisent le système nerveux autonome et la variabilité de la fréquence cardiaque séparément. Secondairement, le rythme cardiaque, son contrôle par le SNA sont discutés dans les section A2.4 et A2.5. Finalement, la définition clinique de la bradycardie et ses manifestations chez les nouveau-nés prématurés sont rapportés dans la section A2.6. Ici quelques éléments clefs sont mentionnés au sujet du SNA et de la bradycardie chez le nouveau-né.

Le système nerveux autonome n'est pas consciemment contrôlé. Il est communément divisé en deux sous-systèmes antagonistes : le système nerveux sympathique et parasympathique, et implique l'homéostasie des organes et fonctions physiologiques. En général, le système nerveux parasympathique (PNS) participe à la digestion et à la conservation de l'énergie, alors que le système nerveux sympathique (SNS) participe à la dépense énergétique. Le PNS et SNS créent souvent des effets opposés dans les mêmes organes ou systèmes physiologiques, et peuvent agir comme une aide à la création d'équilibre (homéostasie) dans le corps. Il est bien connu que le SNA a une influence majeure sur le système cardio-vasculaire, et la variabilité de la fréquence cardiaque en est un exemple.
Le principal moyen par lequel le rythme cardiaque est régulé est l'innervation parasympathique via le nerf vague. En fait, le système nerveux parasympathique fournit un niveau de fond constant d'activité au nœud sinusal. Cela signifie que si cette activité subit une accélération, le cœur ralentit (l'activité parasympathique agit comme un frein). Inversement, lorsque l'activité de fond ralentit la fréquence cardiaque est tirée vers le haut.
Ce dernier effet peut être également obtenu par l'activation du système nerveux sympathique. Normalement, le PNS est le principal déterminant du rythme cardiaque basal. Mais, dans des conditions particulières, comme le stress, la douleur ou la peur, le système sympathique peut accélérer le rythme cardiaque.
Le SNA peut trouver rapidement la façon de se conformer aux changements de la pression artérielle (par l'intermédiaire du baroréflexe) afin de réguler ou de s'adapter à des stimulations à la fois endogènes ou exogènes). L'influence mutuelle entre les composantes sympathique et parasympathique agit comme un mécanisme de commande en boucle fermée de la variabilité de la fréquence cardiaque. C'est la raison pour laquelle la fréquence cardiaque (FC) et sa variabilité (VFC) constituent l'un des quatre principaux signes vitaux (température, pression artérielle et rythme respiratoire). Généralement, la fréquence cardiaque est déterminée à partir du nombre de contractions du cœur (battements cardiaques) en une minute et exprimée par "BPM" (battements par minute). Le développement neurologique est l'un des premiers mécanismes à commencer et le dernier à être complet, générant la structure la plus complexe au sein de l'embryon. Puis il se poursuit tout au long de la vie embryonnaire, foetale, après la naissance, et il continue à être remodelé au niveau synaptique.
Comme il a été dit précédemment, la VFC est régulée par les systèmes sympathique et vagal. Ainsi, une bradycardie peut être due à une augmentation du contrôle vagal ou à une diminution de l'activité sympathique, ou à leur interaction. Ce contrôle autonome joue un rôle plus important dans les mécanismes d'adaptation cardio-vasculaires chez le fœtus et le nouveau-né. Les interactions entre les systèmes nerveux sympathique et vagal sont assez complexes, et modérées par les effets de la maturation. Ce processus normal de maturation

implique des mécanismes de capture (barorécepteurs, chimio-récepteurs, volo-récepteurs, stretch-récepteurs), le développement de l'innervation cardiaque autonome, des médiateurs impliqués dans la régulation du rythme cardiaque (neuropeptide Y, l'adénosine, la sérotonine, les opioïdes), l'expression de différents types de récepteurs adrénergiques et muscariniques, la transduction des signaux des cellules pacemaker au niveau du nœud sinusal (modulation adrénergique de la réponse à une stimulation muscarinique) l'expression et le fonctionnement des canaux ioniques.

Un outil intéressant pour évaluer les mécanismes de contrôle du SNA de la FC est l'analyse spectrale de la variabilité du RR. Classiquement, quatre bandes spectrales sont considérées :
• Ultra basse fréquence (ULF) : de 0,0001 à 0,003 Hz chez l'adulte. Rythmes spontanés très lents, calculés par conséquent sur des enregistrements très longs (au moins 24h).
• Très basse fréquence (VLF) : de 0,003 à 0,04 Hz chez l'adulte. De 0,002 à 0,02 Hz pour le nouveau-né. Ces rythmes sont liés à la thermorégulation et à la régulation vasomotrice périphérique.
• Basse fréquence (LF): de 0,04 à 0,15 Hz chez l'adulte. De 0,02 au 0,2 Hz chez le nouveau-né. Les variations dans cette bande dépendent principalement du comportement du système sympathique.
• Haute Fréquence (HF): de 0,15 à 0,4 Hz chez l'adulte. De 0,2 à 1,5 Hz chez le nouveau-né. La VFC dans cette bande est essentiellement due à la respiration (fluctuation de la fréquence cardiaque autour de la fréquence respiratoire). Cette variabilité est liée principalement à l'activité du système parasympathique (action du nerf vague sur le cœur).

Ces bandes permettent l'observation du comportement du SNA par le spectre de puissance de la fréquence cardiaque. En particulier, le rapport LF/HF peut être évalué pour refléter de manière non invasive la balance sympathovagale, utile pour mieux comprendre la réponse du système nerveux à différentes stimulations. Ce rapport est couramment utilisé comme un indice de l'équilibre entre la modulation sympathique et parasympathique du nœud sinusal. Nous verrons dans le chapitre 5 que d'autres paramètres extraits du domaine temporel, et en exploitant notamment des approches non linéaires, peuvent être utilisés pour quantifier la VFC et les influences du SNA.

L'analyse spectrale de la variabilité du RR a été étudiée chez les nouveau-nés prématurés et à terme. Le ratio LF/HF diminue progressivement avec l'âge postnatal, ce qui indique une augmentation de la contribution parasympathique pour le contrôle de la FC. Néanmoins, pour une meilleure compréhension de ce type de relations, il est nécessaire d'aborder une analyse multivariée des signaux cardiorespiratoires, comme celle menée dans ce travail et qui sera abordée plus loin dans ce document.

La bradycardie chez les prématurés est définie comme une baisse de la fréquence cardiaque sous 100 bpm, soit une baisse de 33% par rapport à la ligne de base, pour au moins 4 secondes. Pour le nouveau-né, l'amplitude des bradycardies médiées par le système vague, diminue avec la maturation. Avec l'augmentation de l'âge post-conception (somme de l'âge gestationnel et post-natal), une diminution de la réponse de la fréquence cardiaque aux stimulations vagales, comme la compression oculaire, a été observée. Une augmentation du tonus vagal apprécié via la fréquence cardiaque de base et la VFC : Hautes fréquences, moyennes fréquences, basses fréquences, ainsi que la fréquence cardiaque moyenne est observée avec l'âge. Les différences entre le nouveau-né prématuré et le nouveau-né à terme sont plus marquées dans leur ensemble, dans le sommeil paradoxal (REM) que dans le sommeil non-REM. En particulier, il a été constaté une forte augmentation du tonus vagal à 37-38 semaines

d’aménorrhée (CA), avec une stabilité par la suite, et une hausse plus régulière du tonus sympathique à 31-41 semaines CA. Ces résultats suggèrent une évolution inverse des bradycardies et de l'importance du tonus vagal en période néonatale. Toutefois, les parts respectives de l'activité sympathique ou parasympathique dans la survenue des bradycardies sont encore peu connues. La survenue des bradycardies chez les nouveau-nés prématurés est un événement fréquent. Elles peuvent débuter à tout moment d'une apnée, et plus souvent dans les dix premières secondes, donc trop tôt pour être due à une hypoxie.

Le système respiratoire (Chap. A3)

Dans le chapitre A2, nous avons abordé la question de l'influence du SNA sur le système cardiovasculaire. Ici, nous présentons le système respiratoire qui est également susceptible d'être affecté par un sepsis. Tout d'abord, la section A3.2 présente le système respiratoire. Puis, la section A3.3 décrit la fréquence respiratoire et sa variabilité. Dans la section A3.4, l'apnée du prématuré est abordée. Finalement, la relation entre l'apnée et la bradycardie est discutée dans la section A3.5. Dans ce qui suit, quelques éléments clés sont brièvement résumés.

Le système respiratoire est composé des voies aériennes respiratoires et des poumons. Le diaphragme et les mouvements des muscles de la poitrine permettent l'expansion de la cavité pulmonaire, ce qui provoque une dépression qui permet à l'air de se déplacer à partir de la bouche ou du nez dans la trachée, dans les bronches et dans les alvéoles.
La régulation de la respiration est le résultat d'une interaction avec plusieurs capteurs formant un système de commande complexe : un centre de contrôle de la respiration, un système effecteur pour activer les muscles et les organes participant à la respiration. La régulation de la respiration est un mécanisme de contrôle homéostatique, ce qui signifie qu'il cherche constamment à maintenir la stabilité de l'environnement interne via des mécanismes de rétroaction négative. Un haut niveau de dioxyde de carbone dans le corps (augmentation du pH dans le sang veineux) implique une respiration rapide et profonde, qui à son tour diminue le niveau de CO 2 en augmentant l'apport d'oxygène.

La respiration est un processus automatique déclenché dans un domaine complexe du cerveau, le tronc cérébral, qui relie la moelle épinière et ses nerfs. Il contient le centre de contrôle respiratoire involontaire. Sinon, la respiration peut être activée par un processus volontaire lorsque le système nerveux central prend le contrôle du mécanisme respiratoire.
Le centre de contrôle respiratoire, au niveau du tronc cérébral, régule la respiration à l'aide d'effecteurs (nerfs et muscles) et de capteurs (Chémorécepteurs et cellules spécialisées) capables de détecter les substances chimiques dans le corps et transmettre l'information aux centres de contrôle.

Le signal respiratoire est l'enregistrement de l'évolution temporelle de la respiration avec un certain nombre de paramètres permettant de décrire cette activité, tels que la pression, le volume d'air ou la tension produite par les muscles.
L'activité respiratoire peut être monitorée de différentes façons, à la fois invasives et non invasives : la mesure du flux d'air (pneumotachometry, spirométrie), l'enregistrement de l'activité électrique des muscles avec des électrodes (pletismography ou même indirectement en extrayant le signal d'un électrocardiogramme) ou en utilisant des capteurs de mouvement pour mesurer la distension du thorax.
Des variables caractéristiques permettent de scruter la fonction respiratoire d'un individu. Elles sont utiles pour identifier des anomalies ou des pathologies. Un ensemble important de paramètres caractérisant la fonction respiratoire est répertorié dans la figure ci-dessous.

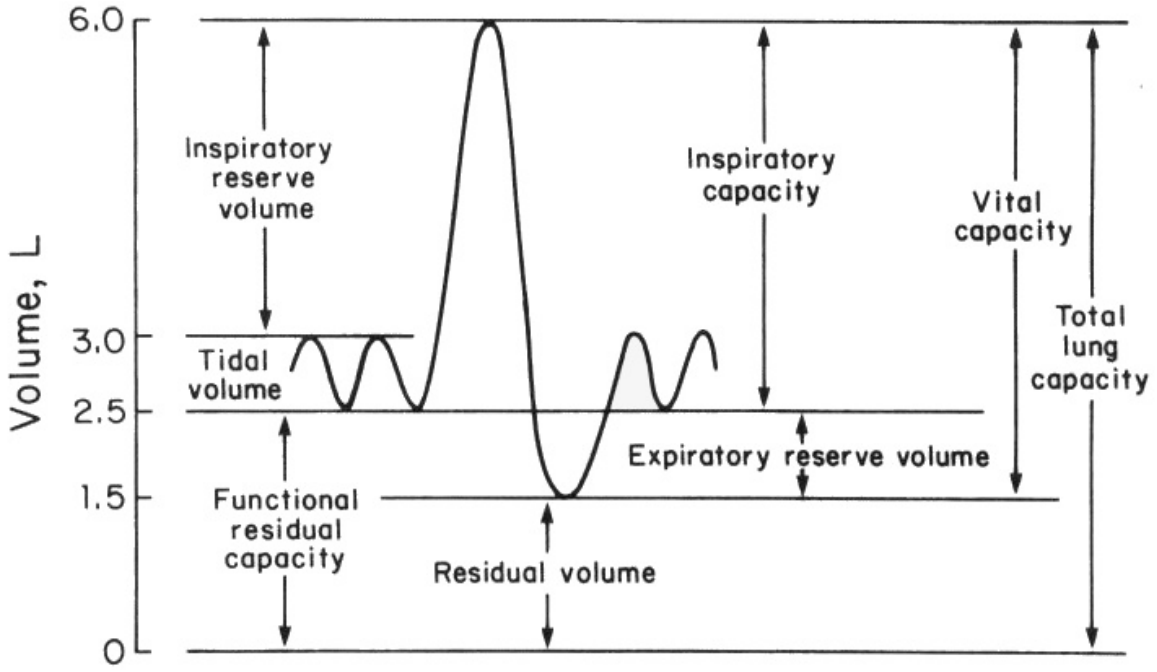

Respiratory volumes

La fréquence respiratoire est un des signes vitaux mesurés lorsque les médecins et les infirmières vérifient l'état de santé. La respiration est commandée par le cerveau. Une variété de facteurs peut influer sur la respiration, comme un traumatisme crânien, une hémorragie, le stress et la fièvre, l'hypothermie, les médicaments, le contrôle volontaire ou l'effort lors d'une activité.

Arythmie sinusale respiratoire (RSA) est la variabilité de la fréquence cardiaque induite par la respiration (l'intervalle RR est raccourci pendant l'inspiration et prolongé durant l'expiration). La VRC à court terme, à la fréquence respiratoire (bande HF), est principalement due aux fluctuations mécaniques du volume d'éjection systolique. Pendant l'inspiration, en raison de la diminution de la pression intra-thoracique et de l'interdépendance ventriculaire, le débit cardiaque (CO) et la pression artérielle diminuent tandis que la FC augmente. La bande HF est donc essentiellement liée à l'activité du système vagal. Plusieurs mécanismes sont impliqués dans cette modulation (baroréflexe artérielle, baroréflexe cardio-pulmonaires, …). Cependant, il est toujours possible d'avoir une modulation sympathique de la fréquence cardiaque à la fréquence respiratoire dans la bande LF, si la fréquence respiratoire est lente ou périodique, comme cela arrive généralement chez les prématurés. Par ailleurs, l'administration de β1 bloquants cardiosélectifs augmente la RSA indépendamment de la fréquence respiratoire : cela signifie que la RSA dans la bande HF ne peut être considérée comme purement vagal, mais elle est également modulée par l'activité sympathique.

La fréquence respiratoire normale pour une personne adulte au repos est de 15 à 20 respirations (cycles) par minute. Les fréquences respiratoires de plus de 25 cycles par minute ou moins de 12 cycles par minute (au repos) peuvent être considérées comme anormales. Les nouveau-nés respirent plus rapidement que les enfants plus âgés et les adultes, ils ont une fréquence respiratoire normale de près de 40 cycles par minute. Cela peut ralentir à 20 cycles par minute quand le bébé dort (quand la plupart des troubles respiratoires apparaissent). La forme du signal de respiration chez un bébé peut également être différente de celle d'un adulte.

Un nouveau-né peut respirer rapidement sur plusieurs cycles puis marquer une pose respiratoire et reprendre de nouveau. C'est ce qu'on appelle la respiration périodique : les pauses respiratoires durent plus de 3 secondes et sont séparées par des respirations normales de moins de 20 secondes. Ce phénomène est la conséquence du contrôle de la respiration immature du bébé dans le cerveau, ce qui répond à la forte concentration de CO2 dans le sang. La respiration rapide superficielle expulse le dioxyde de carbone à partir du sang et le centre de contrôle respiratoire reste inactif jusqu'à ce que ce gaz augmente à nouveau. Ensuite, le cycle global se répète. La respiration périodique est un phénomène normal, plus fréquent chez les nouveau-nés prématurés, mais s'estompe progressivement pendant l'enfance. Il ne doit pas être confondu avec l'apnée, traitée dans la section A3.4.

L'apnée est généralement définie comme l'arrêt de la respiration pendant plus de 20 secondes ou la cessation de la respiration pendant moins de 20 secondes si elle est accompagnée par une bradycardie ou une désaturation en oxygène. La bradycardie, pour un nouveau-né prématuré, est considérée comme significative lorsque la fréquence cardiaque diminue d'au moins de 30 battements par minute de la fréquence cardiaque au repos. Par ailleurs, parmi les spécialistes, il est communément admis qu'un épisode d'arrêt respiratoire est considéré comme une apnée si au moins l'une des deux situations suivantes est avérée : Il y a un arrêt de la respiration équivalent à au moins trois cycles respiratoires consécutifs ; Il y a un arrêt de la respiration durant trois fois la moyenne d'un cycle respiratoire complet. Dans le présent travail, ces définitions seront prises en considération pour trouver des épisodes d'apnée dans le signal respiratoire.
Trois types d'apnée peuvent être distingués :
• L'apnée centrale : Cessation du flux d'air et de l'effort respiratoire. Il n'y a pas de mouvement thoracique. Elle est causée par des irrégularités dans les signaux névralgiques du centre respiratoire.
• Apnée obstructive : Cessation du flux d'air en raison d'une obstruction des voies respiratoires supérieures. Il y a persistance d'un effort respiratoire continu. Elle est due à la relaxation des tissus mous dans le fond de la gorge qui bloque le passage de l'air.
• Apnée mixte : Contient des éléments des deux apnées : centrale et obstructive.

L'apnée du prématuré (AOP) est le trouble le plus important du contrôle de la respiration dans la période néonatale. Il se produit dans environ 7% des enfants nés à 34-35 semaines de gestation, 14% à 32 à 33 semaines, 50 % à 30 et 31 semaines, et il est presque universelle chez les nourrissons nés à moins de 28 semaines de gestation ou avec un poids inférieur à 1000 grammes à la naissance.

L'AOP cesse habituellement à 37 semaines d'âge gestationnel, mais persiste parfois plusieurs semaines après terme. En général, la gravité et la fréquence diminuent avec l'augmentation de la maturité. Bien que l'apnée du prématuré soit généralement associée à des neurones incomplètement organisés et interconnectés dans le tronc cérébral, elle peut aussi être le signe d'autres maladies qui affectent souvent les prématurés.
La répétition d'épisodes d'apnée-bradycardie compromet l'oxygénation des tissus et la perfusion et induit des facteurs de risque pour le développement futur du bébé. Les épisodes de bradycardie chez les nouveau-nés sont fréquents et normalement liés à des apnées et / ou désaturations d'oxygène. La bradycardie peut commencer à moins de 1,5 à 2 secondes après le début de l'apnée. Cette diminution de la fréquence cardiaque (30% en dessous de la ligne de base) peut être produite indirectement, par la stimulation des chémorécepteurs carotidiens ou directement, sous l'effet de l'hypoxie sur le cœur.

On observe également que l'apnée-bradycardie peut apparaître spontanément en attribuant ce phénomène à la simple condition de la prématurité. Néanmoins, elle peut être provoquée ou devenir plus sévère lorsqu'une infection ou l'hypoxémie ou encore une pathologie cérébrale est présente.

L'apnée-bradycardie peut compromettre la perfusion tissulaire et l'oxygénation. Une diminution de la circulation sanguine cérébrale a été constatée, au moyen de flux Doppler dans l'artère cérébrale antérieure ou par spectrométrie dans le proche infrarouge (NIRS), en même temps que l'apnée-bradycardie. La répétition d'apnée-bradycardie sur plusieurs jours semble être à l'origine d'altérations neuropsychiatriques perceptibles à l'âge de trois ans. L'incapacité de prévoir la survenue d'une apnée-bradycardie grave rend nécessaire une surveillance cardiorespiratoire continue des nouveau-nés prématurés (monitoring polygraphique) et le maintien d'un niveau d'alerte élevé qui permette une aide rapide (stimulation kinesthésique, oxygénation, ventilation au masque ou intubation), à chaque instant. La prédiction sur un court terme de la survenue et de la gravité de tels événements permettrait de mettre en œuvre des mesures de prévention ou de thérapie afin de minimiser les risques d'apnée-bradycardie profonde et prolongée, de diminuer le recours à des manœuvres de réanimation (pouvant inclure une assistance respiratoire), de réduire le temps d'hospitalisation (ou encore les besoins de surveillance à domicile), avec comme résultat final l'amélioration de la qualité de vie à court et moyen termes du nouveau-né prématuré.

En conclusion pour cette première partie (Partie A), dans le premier chapitre, nous nous concentrons sur les aspects médicaux fondamentaux concernant les nouveau-nés prématurés et ceux avec un sepsis. En outre, nous indiquons de nombreux aspects de la septicémie, non seulement l'apparition précoce de l'infection, mais aussi son apparition tardive. De toute évidence, l'apnée-bradycardie est la manifestation fréquente chez les prématurés atteints de sepsis tardif.
Ensuite, nous décrivons le système nerveux autonome et son influence sur le système cardiovasculaire. En outre, nous discutons le comportement du système de contrôle cardiovasculaire. Une attention particulière a été accordée à la bradycardie, surtout chez les nouveaux nés. Le dernier chapitre a été consacré au système respiratoire. En particulier, nous expliquons l'apnée du prématuré dans le signal respiratoire et nous avons parlé de la relation entre l'apnée et la bradycardie. Après cette brève revue de la littérature et des connaissances médicales, nous voyons clairement que le sepsis est renforcé par deux facteurs : la bradycardie et l'apnée. Le premier peut être caractérisé par la variabilité du RR tandis que le second peut être étudié à travers la respiration et sa relation avec la VFC.

C'est l'objet principal des prochains chapitres dans la partie B. Le chapitre B1 essaye de montrer comment la HRV peut être utilisée pour le diagnostic du sepsis et plusieurs paramètres sont étudiés dans une perspective d'utilisation dans l'unité de soins intensifs néonatale. Le chapitre B2 s'inscrit dans la même perspective mais s'étend aux relations cardiorespiratoires. Enfin, le chapitre B3 étudie la mise en œuvre en temps différé des paramètres extraits des chapitres B1 et B2 dans une perspective de déploiement sur le terrain clinique.

Analyse de la série RR de nouveau-nés prématurés (Chap. B1)

L'objectif de ce chapitre est d'identifier les meilleurs éléments qui sont en mesure de distinguer un nouveau-né avec sepsis d'un nouveau-né sans sepsis. Pour cela, nous étudions à la fois des méthodes linéaires et non linéaires pour l'analyse et la caractérisation de la VFC, puis nous comparons toutes ces méthodes (i.e. les descripteurs qui en sont issus) afin de trouver les meilleures approches candidates à la discrimination entre les nouveau-nés prématurés infectés et non infectés.

Ce chapitre est organisé de la manière suivante. Tout d'abord, les méthodes de traitement du signal et l'analyse statistique sont présentées respectivement dans les sections B1.2 et B1.3. Deuxièmement, nous proposons un protocole expérimental dans la section B1.4. Troisièmement, d'une part, les résultats de l'analyse mono-variée sont présentés et discutés dans la section B1.5, d'autre part, ceux de l'analyse multivariée sont présentés dans les section B1.6 et B1.7. Enfin, nous concluons avec un résumé dans la section B1.8.

Un large panel de méthodes de traitement du signal et d'analyses statistiques est considéré dans ce chapitre. Sans revenir dessus dans ce résumé, nous décrivons dans la suite les conditions expérimentales et les résultats obtenus.

Tous les enregistrements ont été réalisés en USIN du CHU de Rennes dans les conditions standard de monitoring. Les enregistrements ont été obtenus via le système « Powerlab system ®, AD Instruments » et incluaient un enregistrement numérique (avec une fréquence d'échantillonnage de 400 Hz) d'une heure de deux voies de l'électrocardiogramme (ECG), un electrooculogram (EOG), une voie d'électroencéphalogramme (EEG), une voie pour l'oxymétrie (SaO2), et une voie pour la respiration (le flux) nasale. Les données ont été obtenues à partir de deux groupes de nouveau-nés prématurés (13 sepsis et 13 non sepsis) hospitalisés en USIN entre 2004 et 2007. Cette recherche a été approuvée par le comité d'éthique local (03/05-445). En outre, les parents de ces enfants ont été informés et ont donné leur consentement. Il n'y avait pas de différences significatives entre les sexes, l'âge gestationnel, l'âge chronologique (> 72 heures), l'âge post-menstruel (<33 semaines), le poids et l'hématocrite entre les groupes « sepsis » et « non-sepsis ».

Les séquences de la série RR avec bradycardie ont été extraites des enregistrements ECG, puis ré-échantillonnées à 4 Hz (Fig. B1 3 a) et nettoyées par le filtre Kaplan (Fig. B1 3 b). Après, elles ont été employées dans les domaines temporel, fréquentiel, de la théorie du chaos et de la théorie de l'information.

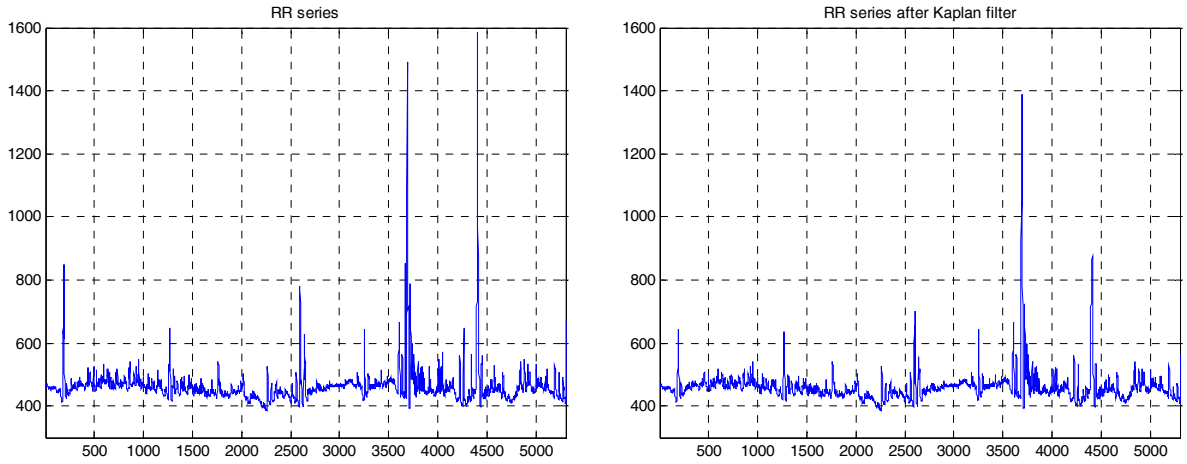

a) RR series extracted from ECG and resampled b) RR series after Kaplan filter

Fig. B1-3. RR series

Les descripteurs ont été calculés à partir de la série RR sur des fenêtres (fenêtres d'analyse) dont l'horizon est 1024/2048/4096. Nous avons comparé toutes les méthodes fournissant les descripteurs en termes de classification de sepsis (S) versus non-Sepsis (NS) pour les trois horizons.

En conclusion de ce chapitre, les manifestations cliniques de septicémie néonatale, quelle que soit la source de l'infection, sont souvent non spécifiques. Dans ce chapitre, l'objectif du travail était de trouver des descripteurs quantitatifs permettant d'identifier les prématurés avec sepsis par un moyen non invasif.
L'analyse de la série RR permet de répondre à cet objectif. La caractérisation de la VFC par des descripteurs issus de l'analyse temporelle ou fréquentielle ne permet pas de trouver des corrélations significatives avec le sepsis. Le recours à des indices (descripteurs) issus de la théorie du chaos (alphaS, alphaF) et de la théorie de l'information (AppEn, SamEn, PermEn et Regul) permet d'améliorer les résultats.

Le paramètre alphaF qui caractérise les corrélations à court terme (4-40 battements) dans la série RR, ne change guère avec l'âge et est presque stable à environ 1,5. Cette valeur indique que le comportement à court terme du RR est similaire à un mouvement Brownien. D'autre part, le paramètre alphaS caractérisant les corrélations à long terme (40-1000 battements) augmente significativement dans le groupe non-sepsis par rapport au groupe sepsis.
En ce qui concerne la théorie de l'information, les résultats ont confirmé la relation entre l'apparition de la maladie et une réduction des informations véhiculées par les signaux cardiovasculaires. AppEn, SamEn et PermEn ont montré qu'une diminution de l'entropie est associée à un sepsis, et de manière cohérente, l'indice Regul a statistiquement des valeurs élevées pour le groupe sepsis.

En outre, toutes les méthodes ont été décryptées à travers des analyses statistiques, non seulement l'analyse univariée, mais aussi l'analyse multivariée (régression logistique, régression pas à pas). Finalement, trois paramètres issus d'analyses non linéaires de la série RR (alphaS, alphaF, SamEn) ont été sélectionnés en tant que candidats à la distinction entre les deux groupes sepsis et non-sepsis quelle que soit la taille de la fenêtre d'analyse.

Analyse de la relation entre la série RR et le signal de respiration chez les nouveau-nés prématurés (Chap. B2)

Différents mécanismes sont impliqués dans la génération de la variabilité cardio-vasculaire. Ils ont été largement étudiés comme marqueurs de l'interaction sympathovagal pour le contrôle des fonctions cardio-vasculaires. Par conséquent, l'application des méthodes d'analyse de signaux multivoies pourrait permettre d'extraire plus d'informations que les techniques d'analyse monovoie à partir des signaux cardiorespiratoires.
Nous considérons dans ce chapitre l'étude du couplage entre les signaux de VFC et de respiration. Ce travail est basé sur une mesure de relations (linéaires ou non linéaires) et le temps de retard entre la série RR et le signal respiratoire. La section B2.2 concerne des méthodes linéaires. Dans la section B2.3, les méthodes non linéaires sont présentées en détail. Le protocole expérimental est introduit dans la section B2.4. Les résultats des méthodes linéaires et des méthodes non linéaires sont proposés et discutés dans les sections B2.5 et B2.6 respectivement. Enfin, nous discutons tous les résultats dans la section B2.7 et une conclusion synthétique est présentée dans la section B2.8.

Ce chapitre constitue une nouvelle façon d'aborder le problème du monitoring du sepsis chez le nouveau-né. Dans la même cohorte explorée par l'analyse de la série RR, les patients ayant des signaux respiratoires enregistrés ont été retenus. Une recherche sur l'influence mutuelle entre la variabilité du système cardiovasculaire et la respiration nasale a été réalisée.
Des relations linéaires et non linéaires ont été mesurées. Les approches linéaires que sont la corrélation linéaire (r^2), la cohérence et la cohérence temps-fréquence $R^2(t, f)$ ont été étudiées pour révéler le couplage entre les signaux cardiorespiratoires. Il en a été de même avec le coefficient de régression non linéaire (h^2).

En ce qui concerne les estimations linéaires, nous confirmons statistiquement ($p < 0,05$ quels que soient les tests statistiques) qu'une corrélation élevée est observée dans la bande de fréquence basse pour le groupe non sepsis entre le RR et la respiration nasale (r2tf_rn_raw). Les résultats montrent que les relations sont circonscrites dans une région particulière du plan temps-fréquence ($0,2 < f < 0,4$ Hz) pour le groupe sepsis et dans une autre pour le groupe non sepsis. Le seuil de 0,8 semble le plus discriminant entre les deux groupes avec comme mesure le $R^2(t, f)$.

En ce qui concerne les estimations non linéaires, les résultats obtenus en utilisant l'indice h^2 de régression non linéaire entre le RR et la respiration nasale dans les deux directions (h2_rn_raw, h2_nr_raw) montrent que les valeurs sont toujours importantes. En outre, l'analyse de la relation non linéaire montre que les courbes présentent un pic dans le groupe non sepsis et que pour le groupe sepsis, les formes des courbes de relation sont arbitraires. Ces faits ont été observés pour tous les patients.

En conclusion, trois descripteurs sont présentés et étudiés. Ils peuvent être considérés comme complémentaires :

- R2tf_rn_raw_0p2_0p4 : la quantité $R^2(t, f)$ entre le RR et la respiration nasale supérieure à un seuil fixé à 0,8 dans la sous-bande $0,2 < f < 0,4$ Hz)
- H2_rn_raw (h^2 entre le RR et la respiration nasale)
- H2_nr_raw (h^2 entre la respiration nasale et le RR)

Ils peuvent être choisis comme paramètres permettant de distinguer le sepsis du non sepsis chez le grand prématuré et ceci de manière non invasive.

Détection des nouveau-nés avec sepsis par analyse de la VFC et de la relation entre la série RR et le signal de respiration (Chap. B3)

Comme nous l'avons déjà mentionné, les épisodes transitoires de l'apnée et la bradycardie sont fréquents chez les prématurés. Ces épisodes peuvent compromettre sérieusement l'oxygénation et la perfusion tissulaire, et quand ils deviennent prolongés et répétitifs, ils peuvent conduire à une morbidité neurologique ou même à la mort infantile. Les bébés prématurés dans les unités de soins intensifs néonatals (USIN) sont surveillés en permanence par l'enregistrement polygraphique, afin de détecter des événements de bradycardie et d'initier des actions de soins rapides (stimulation manuelle ou vibrotactile, oxygénation, ventilation à travers un masque, ou intubation). Généralement, quand un enfant présente un cas de bradycardie, une alarme est générée par un dispositif de surveillance et une infirmière ou un médecin disponible applique une stimulation manuelle à l'enfant en détresse. Le délai d'intervention moyen entre l'activation de l'alarme et l'application de la thérapie a été estimé à environ 33 secondes, avec une durée de stimulation manuelle moyenne de 13 secondes afin de mettre fin à l'événement d'apnée - bradycardie. Cependant, même si les algorithmes de détection de bradycardie ont été développés, ils sont inefficaces et produisent généralement de fausses alarmes ou des retards à la détection.
L'objectif de ce chapitre est d'ajouter une nouvelle fonctionnalité aux dispositifs utilisés pour la détection et le monitoring des apnées bradycardies. La fonctionnalité est focalisée sur la détection du sepsis en USIN. Donc, nous étudions la faisabilité de sa mise en œuvre en USIN avec les fonctionnalités proposées aux chapitres B1 et B2. Ici, une nouvelle architecture pour la prise de décision par fusion est proposée. Ce principe de Fusion optimale est d'abord décrit dans la section B3.2. Dans la section B3.3, les principes de la courbe de réception optimale (ROC) sont rappelés. Le protocole expérimental pour les tests est présenté dans la section B3.4. Les résultats exploitants les approches mono-voie et bi-voies sont illustrés et discutés dans les sections B3.5 et B3.6 respectivement. Puis, la fusion de toutes les caractéristiques est menée dans la section B3.7. Enfin, une conclusion est dressée dans la section B3.8.

En conclusion, ce chapitre a pour but de vérifier que la détection du sepsis en temps réel est possible sur la base des deux chapitres précédents :

(i) Le chapitre B1 basé sur VFC ;
(ii) Le chapitre B2 basé sur VFC et la respiration.

L'étude de faisabilité est réalisée sur les paramètres candidats choisis parmi les analyses conduites précédemment. Tout d'abord, nous générons de longues séries temporelles mélangeant du sepsis et du non sepsis. Ensuite, nous conduisons 5 tests en vue d'une prise de décision sur l'hypothèse d'un sepsis sur tous les segments d'observation en considérant 3 horizons différents. Enfin, nous résumons les caractéristiques des courbes ROC tels que PFA, PD et AUC dans les tableaux B3-2, B3-3 et B3-4 afin de comparer les 5 tests et d'identifier la meilleure solution. En outre, le contraste entre les trois tailles de fenêtre 1024/2048/4096 indique que l'horizon de 4096 points a la plus faible PFA et la plus grande valeur de l'AUC.

Globalement, parmi les cinq tests, le test n°5, basé sur la fusion optimale des 6 fonctions (Alphas, alphaF, Samen, r2tf_rn_raw, h2_rn_raw et h2_nr_raw), conduit à de bonnes performances avec la plus grande surface sous les courbes (AUC) et la plus faible probabilité de fausse alarme (PFA). Il peut être utilisé pour fournir une alarme fiable lors de la survenue d'un épisode d'apnée-bradycardie tout en exploitant les systèmes de monitoring actuels en USIN.

Conclusions et perspectives (Chap. 8)

Dans le chapitre 8, nous résumons l'objectif et les méthodes proposées de cette thèse. Nous rappelons également quelques pistes pour améliorer et étendre nos recherches dans les travaux futurs.

Le sepsis tardif, défini comme une infection systémique chez les nouveaux nés âgés de plus de 3 jours, survient chez environ 10% des nouveau-nés et dans plus de 25% des nourrissons de très faible poids de naissance qui sont hospitalisés dans les unités de soins intensifs néonatals (USIN). Compte tenu du taux élevé de morbidité et de mortalité associée à l'infection, des marqueurs fiables de celle-ci sont nécessaires.

Les apnées-bradycardies spontanées graves et récurrentes sont l'un des principaux indicateurs cliniques précoces du sepsis. L'objectif de cette thèse était de déterminer si le comportement de la fréquence cardiaque, l'amplitude respiratoire et l'analyse de leurs relations aident au diagnostic de l'infection chez les nourrissons prématurés par des moyens non invasifs. Par conséquent, nous avons mené des travaux sur deux groupes de patients prématurés (le groupe sepsis et le groupe non sepsis) par le biais de l'analyse des séries RR et des relations entre ce signal et la respiration.

Tout d'abord, nous avons étudié la série RR par des méthodes liées à sa distribution statistique (essentiellement les moments), par des méthodes linéaires - dans le domaine temporel (SD, RMSSD) et dans le domaine fréquentiel (p_VLF, p_LF, p_HF), mais aussi par des méthodes non linéaires - la théorie du chaos (alphas, alphaF) et la théorie de l'information (AppEn, SamEn, PermEn, Regul). Pour chaque méthode, nous avons exploré et comparé trois tailles de fenêtre d'analyse (horizon) 1024/2048/4096 afin de trouver les meilleurs moyens pour distinguer un sepsis d'un non sepsis chez les prématurés. Les résultats montrent que les descripteurs alphaS, alphaF et SamEn sont les paramètres optimaux pour identifier un sepsis tardif. Cependant, chez les prématurés malades, le mécanisme ne se résume probablement pas à un simple changement dans la série RR. Les résultats cliniques montrent clairement que la VFC, la respiration et leurs relations peuvent être des outils de diagnostic efficaces et peuvent aider à identifier le sepsis dans une population de nourrissons atteinte de bradycardies récurrentes.
La question du couplage fonctionnel entre la variabilité du rythme cardiaque et la respiration nasale est abordée. Trois descripteurs complémentaires ont été identifiés et jugés intéressants (r2tf_rn_raw_0p2_0p4 h2_rn_raw, h2_nr_raw) pour le diagnostic non invasif du sepsis.

En outre, une étude de faisabilité a été réalisée en termes de fusion optimale de descripteurs en vue d'une prise de décision sur le sepsis à partir des approches explorées dans les chapitres B1 et B2. Dans ce sens, la fusion optimale des 6 descripteurs alphaS, alphaF, SamEn, r2tf_rn_raw, h2_rn_raw et h2_nr_raw montre de bonnes performances avec la plus grande surface sous les courbes (AUC) et la plus faible probabilité de fausse alarme (PFA) sur un horizon d'analyse de 4096 points.

En termes de perspective, bien sûr, il y a encore de nombreuses possibilités d'amélioration et d'extension de ce travail dans cette thèse. Des perspectives sont dressées concernant de nouvelles approches permettant d'estimer les relations statistiques entre la respiration et la variabilité cardiaque. Ces approches pourraient améliorer la sensibilité de la discrimination

entre les deux groupes et aussi fournir des algorithmes d'estimation plus rapides que ceux exploités dans cette étude. Une dimension importante qui n'a pas été exploitée dans ce travail est celle de l'analyse de l'EEG du nouveau-né dans le contexte du diagnostic du sepsis et comme outil prédictif du devenir neurologique à moyen et long terme des nouveau-nés atteints.

Table of Contents

List of Figures

List of Tables

List of Abbreviations

In alphabetical order

α_{fast} , alphaF	alpha Fast
α_{slow} , alphaS	alpha Slow
aEEG	amplitude integrated EEG
AIF	autonomic information flow
ANOVA	Analysis of Variance
ANS	Autonomic Nervous System
AOP	Apnea of prematurity
AppEn	Approximate Entropy
AUC	Area Under Curve
AV	atrioventricular
bpm	beats per minute
BR	baro-receptor
CA	Chronological Age
CBC	complete blood count
CE	conditional entropy
CCE_x	corrected conditional entropy
ChiSq	Chi-Square
CHU-Rennes	Center of Hospital affiliated to University of Rennes 1
CO	cardiac output
Cohere	Coherence function
CPAP	Continuous Positive Airway Pressure
CRP	C-reactive protein
CSF	cerebrospinal fluid
CTG	cardiotocographic
DF	degree of freedom
DFA	Detrended fluctuation analysis
DSP	Digital Signal Processing
DWT	discrete wavelet transform
ECDF	empirical cumulative distribution function
ECG	electrocardiogram
EDR	ECG-derived respiration
EEG	electroencephalogram
EMIAT	European Myocardial Infarction Amiodarone Trial
EOG	electrooculogram
EPS	Electrophysiological studies
ERV	Expiratory Reserve Volume
FFT	Fast Fourier Transform
FHR	Fetal Heart Rate

FISs	fuzzy inference systems
FMS	Fybromyalgic Syndrome
FN	false negative
FP	false positive
FPR	false positive rate
FRC	Functional Residual Capacity
GA	Gestational Age
GBS	Group B beta-hemolytic Streptococcus
GLM	Generalized Linear Model
h^2	non-linear regression coefficient
HF	High Frequency
HIE	hypoxic-ischemic encephalopathy
HR	heart rate
HRF	heart rate fluctuations
HRV	Heart Rate Variability
IC	Inspiratory Capacity
IRV	Inspiratory Reserve Volume
KruskWall	Kruskal-Wallis test
KS	Kolmogorov–Smirnov
kurt	kurtosis
LF	Low Frequency
LS-SVM	least squares support vector machine
LTSI	Laboratoire Traitement du Signal et de l'Image
LZ	the Lempel Ziv
med	median
moy	arithmetic mean
MSE	multiscale entropy
$NCCE_x$	normalized corrected conditional entropy
NICU	Neonatal Intensive Care Units
NIS	near infrared spectrometry
NR	normal respiration
nr_amp	Amplitude of Nasal Respiration and RR
nr_brut	Original Nasal Respiration and RR
nr_enp	Envelop of Nasal Respiration and RR
NS	Non-Sepsis
OA	obstructive apnea
OCR	oculo-cardiac reflex
OSA	Obstructive sleep apnea
p_HF	power of High Frequency
p_LF	power of Low Frequency
p_VLF	power of Very Low Frequency
PCA	post-conceptional age
PCC	Pearson correlation coefficient
P_D	Probability of Detection

PermEn	Permutation Entropy
P_{FA}	Probability of False Alarm
PMA	Post-menstrual Age
PNA	post-natal age
PNS	parasympathetic nervous system
PPG	photoplethysmograph
Pr	Probability
PSD	power spectral density
PVL	periventricular leukomalacia
r^2	Correlation Index
$r^2_{t,f}$	Local linear correlation coefficient
RDS	Respiratory Distress Syndrome
Regul	Regularity
REM sleep	rapid eye movement sleep
respn	Nasal Respiration
respn_amp	Amplitude of Nasal Respiration
respn_enp	Envelop of Nasal Respiration
RM	respiratory movements
RMSSD	Root Mean Square of Successive Differences
rn_amp	RR and Amplitude of Nasal Respiration
rn_brut	RR and Original Nasal Respiration
rn_enp	RR and Envelop of Nasal Respiration
ROC	Receiver Operating Characteristic
ROP	Retinopathy of Prematurity
RRI	RR intervals
RSA	Respiratory Sinus Arrhythmia
RSS	residual sum of squares
RV	Residual Volume
S	Sepsis
SA	sinoatrial
SamEn	Sample Entropy
SaO2	one pulse oximetry saturation
SCS	squared coherence spectrum
SD	standard deviation
SEPIA	Surveillance Explication et Prévention de l'Insuffisance cardiaque et des Apnée-bradycardies
SEU	Southeast University
skew	skewness
SNS	sympathetic nervous system
SP3	Service Pack 3
SpAs	Sample Asymmetry
STFT	Short-Time Fourier Transform
t_e	Expiratory time
t_i	Inspiratory time

t_i/t_e	Cycle ratio
TLC	Total Lung Capacity
TN	true negative
TP	true positive
TPR	true positive rate
t_{tot}	Total time
UF	uncoupling function
ULF	Ultra Low Frequency
UR1	University of Rennes 1
varn	variance
VC	Vital Capacity
VLF	Very Low Frequency
VLWB	very low weigh baby
VT	Tidal Volume
Wilrs	Wilcoxon rank-sum test

Chapter 1
Introduction

1.1 Objective of this dissertation

Late-onset sepsis, defined as a systemic infection in neonates older than 3 days, occurs in approximately 7% to 10% of all neonates and in more than 25% of very low birth weight newborns who are hospitalized in Neonatal Intensive Care Units (NICU) [1]. The clinical manifestations of neonatal sepsis, whatever the source of infection, are always not so evident. Accordingly, lacking in early and adapted interventions always leads to life risk. Therefore, this disease is a major problem resulting in high morbidity and mortality for premature newborns[2].

As we know, sick preterm infants do not show any fever, only with blood culture, the possible signs of sepsis may be detected. However, on one hand, the hematological and biochemical markers which have been used in this symptom, not only require invasive procedures which should not be frequently repeated, but also have low predictive values in the early phase of sepsis. On the other hand, it has been observed experimentally that phenomena of apnea-bradycardia happened more frequently in sepsis preterm infants than in non-sepsis ones[3].

Now, it is still unclear whether these neonatal changes in behavior of physiological signals can be used to diagnose sepsis in sick premature infants. Therefore, the objective of this dissertation is to find the quantitative mathematical criteria to distinguish sepsis from non-sepsis in premature newborns for non-invasive NICU monitoring system. In order to reach our goal, two kinds of analysis were conducted:

- Mono-channel signal: considering RR series
- Bi-channel signal: considering both RR series and respiration

But before introducing, the general description of the problem, studied in the dissertation. A literature review is first proposed.

1.2 Literature Reviews

1.2.1 Literature Reviews for RR series in newborns

The heart rate variability (HRV) analysis in neonatology is a useful tool to understand the cardiovascular control system behavior in late-onset sepsis of premature newborns. Starting from the obvious increase in apnea-bradycardia crisis related with the state of sickness, a way to evaluate the relationship between the infection and its manifestation was investigated. In particular, since apnea-bradycardia was an indication of altered mechanisms of cardiovascular regulation, the HRV investigation on these subjects is an immediately consequent decision. Therefore, two research groups investigated the RR interval series extracted from ECG signals in newborns.

- Moorman Lab in University of Virginia
- Cerutti Lab in Politecnico di Milano

1.2.1.1 Moorman Lab in University of Virginia

Cao and Lake [3] invented statistical methods for determining stationarity of HR data based on the two-sample Kolmogorov–Smirnov (KS) test, and developed new HR measures based on the empirical cumulative distribution function (ECDF) that are highly significantly associated with sepsis, but are not correlated with HR measures such as moments or sample entropy. They concluded that neonatal HR data cannot be assumed to be stationary, and become even less stationary prior to sepsis.

Xiao and Griffin [4] proposed nearest-neighbor analysis in addition to logistic regression in the early diagnosis of subacute, potentially catastrophic illnesses such as neonatal sepsis, and they recommended it as an approach to the general problem of predicting a clinical event from a multivariable data set.

Flower and Delos [5] developed a formalized wavelet-based template matching algorithm to detect decelerations in HR time series. The new deceleration metrics added independent information to our existing HRC analysis in predicting neonatal sepsis ($p < 0.0001$). Interestingly, some asymptomatic infants had storms of large decelerations unaccompanied by apnea at a rate of several per minute. Storms of frequent decelerations were highly predictive and diagnostic of sepsis, with up to 10 or more-fold increase in severe clinical illness. This new wavelet-based heart rate deceleration analysis improves heart rate characteristics monitoring in predicting neonatal sepsis.

Methods for estimation of the entropy of a system represented by a time series are not, however, well suited to analysis of the short and noisy data sets encountered in cardiovascular and other biological studies. Pincus [6] introduced approximate entropy (AppEn), a set of measures of system complexity closely related to entropy, which is easily applied to clinical cardiovascular and other time series. AppEn statistics, however, lead to inconsistent results. Richman and Moorman [7] developed a new and related complexity measure, sample entropy (SamEn), and have compared AppEn and SamEn by using them to analyze sets of random numbers with known probabilistic character. They also evaluated cross-AppEn and cross-SamEn, which use cardiovascular data sets to measure the similarity of two distinct time series. SamEn agreed with theory much more closely than AppEn over a broad range of conditions. The improved accuracy of SamEn statistics should make them useful in the study of experimental clinical cardiovascular and other biological time series.

Abnormal heart rate characteristics of reduced variability and transient decelerations are present early in the course of neonatal sepsis. To investigate the dynamics, Lake and Richman [8] calculated sample entropy, a similar but less biased measure than the popular approximate entropy. Both calculate the probability that epochs of window length m that are similar within a tolerance r remain similar at the next point. They studied 89 consecutive admissions to a tertiary care neonatal intensive care unit, among whom there were 21 episodes of sepsis, and they performed numerical simulations. They addressed the fundamental issues of optimal selection of m and r and the impact of missing data. The major findings are that entropy falls before clinical signs of neonatal sepsis and that missing points are well tolerated. The major mechanism, surprisingly, is unrelated to the regularity of the data: entropy estimates inevitably fall in any record with spikes. They proposed more informed selection of parameters and re-examination of studies where approximate entropy was interpreted solely

as a regularity measure. Richman and Lake [9] also proposed closed form estimates of the variance of Sample Entropy.

1.2.1.2 Cerutti Lab in Politecnico di Milano

Signorini and De Angelis [10] proposed new classifiers based on fuzzy inference systems (FISs) for analysis of the Fetal Heart Rate (FHR) signal. They include standard cardiotocographic (CTG) parameters together with a set of frequency domain and nonlinear indices. Results showed FISs predict normal and pathological fetal states even with 100% of correct classifications. Their performance however is always higher than 80% in the whole population, depending on the rule number. This approach can strongly help the automatic CTG signal analysis improving the early discrimination among normal and pathological fetal conditions.

Signorini and Marchetti [11] proposed an enhancement of these HRV components through the application of a noise-reduction method in state space. The method works directly in an embedding space and corrects noisy trajectories, projecting them onto local subspaces that are a good approximation of the original surface of the system attractor. At any iteration, the procedure returns a new time series with the relevant amount of subtracted noise. An empirical criterion, originally proposed, estimates the optimum iteration number to reach a good result in terms of signal-to-noise ratio. Ultimately, our goal is to verify a possible improvement of the diagnostic and prognostic power of HRV analysis through the use of new nonlinear approaches that appear as a promising tool in the early identification of dangerous cardiovascular events.

The estimation of nonlinear parameters in time series whose model is unknown has to consider the use of advanced analysis methods. Cerutti and Signorini [12] introduced time-domain indexes, monofractal characteristics and a regularity statistic. Multifractal approaches such as generalized structure functions have been also used to characterize the HRV signal. A determinism test on the time series assesses the presence of nonlinear structures by a hypothesis test based on surrogate data. In most cases, the multifractal spectrum of the original HRV series significantly differs (t-test), from those obtained from surrogate signals. Results in the HRV signal analysis confirm the presence of a nonlinear deterministic structure in time series. Moreover, nonlinear parameters can be used to separate normal subjects from patients suffering from cardiovascular diseases.

Antepartum fetal monitoring based on the classical cardiotocography is a non-invasive and simple tool for checking fetal status. Its introduction in the clinical routine limited the occurrence of fetal problems leading to a reduction of the precocious child mortality. Nevertheless, very poor indications on fetal pathologies can be inferred from the even automatic CTG analysis methods, which are actually employed. The feeling is that fetal heart rate signals and uterine contractions carry much more information on fetal state than is usually extracted by classical analysis methods. In particular, FHR signal contains indications about the neural development of the fetus. However, the methods actually adopted for judging a CTG trace as "abnormal" give weak predictive indications about fetal dangers. Signorini and Magenes [13] proposed a new methodological approach for the CTG monitoring, based on a multiparametric FHR analysis, which includes spectral parameters from autoregressive models and nonlinear algorithms (approximate entropy). This preliminary study considers 14 normal fetuses, eight cases of gestational (maternal) diabetes, and 13 intrauterine growth retarded fetuses. A comparison with the traditional time domain analysis is also included.

They showed that the proposed new parameters are able to separate normal from pathological fetuses. Results constitute the first step for realizing a new clinical classification system for the early diagnosis of most common fetal pathologies.

Ferrario and Signorini [14] proposed to study the heart rate variability time series complexity by computing the Lempel Ziv (LZ) complexity measure. LZ is sensitive to the rate of pattern recurrences in a time series. Analysis considers 24 h HRV time series of healthy subjects and patients with cardiovascular diseases. Analysis with simulated signals showed the LZ measure can vary depending on the adopted coding process. The binary coding, proposed in this work, is sensitive to the different dynamical systems generating the time series, as the ternary coding is sensitive to the presence of stationary states, i.e. a consecutive repetition of the same RR interval value. LZ method reliably differentiates healthy vs. disease group. Further clinical investigations on the LZ complexity and on its relationship to the risk of sudden death, can supply new diagnostic indications.

Ferrario and Signorini [15] considered the multiscale entropy (MSE) approach for estimating the regularity of time series at different scales. Sample entropy and approximate entropy are evaluated in MSE analysis on simulated data to enhance the main features of both estimators. They applied the approximate entropy and the sample entropy estimators to fetal heart rate signals on both single and multiple scales for an early identification of fetal sufferance antepartum. Their results show that the ApEn index significantly distinguishes suffering from normal fetuses between the 30th and the 35th week of gestation. Furthermore, their data shows that the MSE entropy values are reliable indicators of the fetal distress associated with the presence of a pathological condition at birth.

1.2.2 Literature Reviews for RR series and Respiration in newborns

Different mechanisms are involved in the generation of cardiovascular variability rhythms which have been extensively studied as markers of the sympathovagal interaction controlling cardiovascular functions. Therefore, the application of methods of bi-channel signal analysis can extract more information than it can be obtained by the usual techniques of mono-channel analysis of variability signals. This is why the mono-channel approaches used to analyze heart rate variability have been extended by several bi-channel approaches with respect to cardiorespiratory coordination. In the second part of this study, Bi-channel analysis was attempted, using both RR and respiratory signal.

An increase of apnea-bradycardia crisis is reported during sepsis manifestation, and they are considered among the most relevant symptoms of sepsis. So both respiratory and cardiovascular systems give their response to the sepsis onset. This is why, the relationship between respiration and heart rate variability has to be investigated. Several research groups carried on Bivariate Analysis for these two physiological signals in newborns.

Episodes of apnea, desaturation and bradycardia are a common occurrence in preterm infants and are known to persist after hospital discharge. These events are typically detected by clinical bedside monitoring, but the type and number of events depend on alarm settings, the inclusion of continuous pulse oximetry and the mode of respiratory monitoring used. The long-term effects of cardiorespiratory events remain controversial; however, some studies have suggested an association between prolonged apnea and morbidity such as impaired neurodevelopmental outcome. Common clinical practice requires an event-free period before

hospital discharge, although the specific length of time varies between institutions. Therefore, with the current demand to shorten hospital stay, the possible persistence of cardiorespiratory events after hospital discharge and the potential consequences of these events, cardiorespiratory monitoring remains a subject of considerable interest. Since cardiorespiratory event detection is dependent on the mode of monitoring used, Di Fiore [17] focused on both the respiratory patterns and types of cardiorespiratory events that occur in the infant population and the modalities of cardiorespiratory monitoring currently available to detect these events.

The diagnosis of late onset sepsis in premature infants remains difficult because clinical signs are subtle and non-specific and none of the laboratory tests, including CRP and blood culture, have high predictive accuracy. Heart rate variability analysis emerges as a promising diagnostic tool. Entropy and long-range fractal correlation are decreased in premature infants with proven sepsis. Besides this, respiration and its relations to HRV appear to be less. An estimator of the linear relationship between nonstationary signals, recently introduced, is explored. Carrault and Beuchée [18] found that the correlation in the low frequency band tended to be higher in the sepsis group. The results told us that the analysis of time-frequency correlations between the heart rate and respiration amplitude may help for the diagnosis of infection in premature infants.

Maier and Rodler [19] compared the difference in these traces' phase relation found during and after each obstructive apnea (OA) episode to the difference between the first and second half of the OA and between split halves of epochs of normal respiration (NR), in order to identify the potential indicators of OA in the ECG, based on the traces of QRS area from multiple ECG leads.

Rassi and Mishin [20] investigated the correlation between heart rate variability and other physiological parameters such as blood pressure and respiration in preterm neonates with the aim of developing a numerical model to explain and predict heart rate variability. All the required data are readily available for premature babies who are routinely monitored while being nursed in intensive care, and they have collected large data sets for a random group of such neonates. For the quantitative analysis of the data, they have developed a time domain correlation method, which has a number of advantages over the more commonly used power spectral analysis. They have been able to study the dynamics of the different frequency components of HRV by this method. Highly correlated behavior of the different HRV components, previously observed in their work on fetal HRV, is also present in the neonate, with similar characteristic time constants. Furthermore, the correlation of High Frequency (HF) oscillations of HRV with respiration and that of Low Frequency (LF) oscillations of HRV with blood pressure are demonstrated on timescales of a single oscillation. In neonates receiving artificial ventilation, the correlation between HRV and respiration depends on the type of ventilation involved and assumes opposite polarities for the two main types of equipment currently in use. They demonstrated that it is possible to analyze HRV quantitatively by calculating the relative gains and characteristic time constants for the correlated parameters and components.

It is not known on which time scales the nonlinear respirocardial interactions occur. This work’s aim is to quantitatively assess functional respirocardial organization during quiet and active sleep of healthy full-term neonates by autonomic information flow (AIF) without limitation on specific time scales. Representing respirocardial interactions on a global time scale AIF carries information on a wider scope of interdependencies than known linear and

nonlinear measures described. It assesses the complexity of heart rate fluctuations (HRF) and respiratory movements (RM) and their interaction comprising both linear and nonlinear properties. Thus, Frasch and Zwiener [21] hypothesized AIF to characterize novel aspects of sleep state-dependent respirocardial interaction. RM and ECG-derived HRF of six healthy full-term neonates were studied. They analyzed their power spectra, coherence, auto- and cross-correlation and complexity estimated on local ("next sample" prediction) and global time scales (an integral over AIF predicting for all time lags in HRF and RM). They found the global AIF of HRF and RM to differ significantly between active and quiet sleep in all neonates, whereas on a local time scale this applied to the HRF AIF only. HRF complexity was larger in quiet than in active sleep. Respirocardial interaction was less complex in quiet versus active sleep in the high frequency band only. Complex sleep state-related changes of respirocardial interdependencies cannot be identified completely on the local time scale. Considering the global time scale of respirocardial interactions allows a more complete physiological interpretation with regard to the underlying autonomic dynamics.

1.3 Dissertation outline

As already mentioned in our introduction, our aim is to discover the benchmark to discriminate between the sick and the healthy infants. Therefore this dissertation is organized as follows, and Fig. 1-1 summarizes the organization of the Ph.D works.

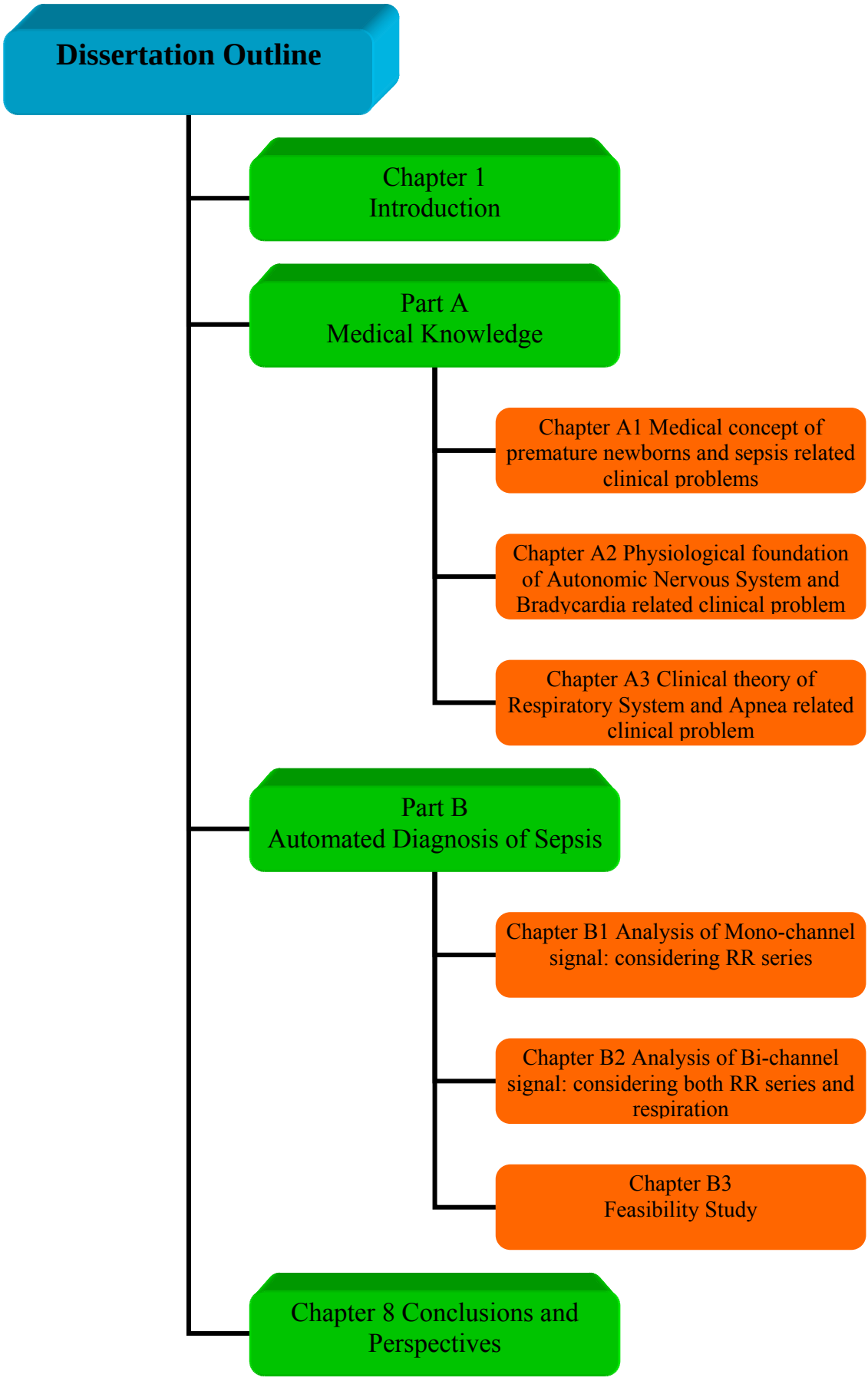

Fig. 1-1 Dissertation Outline

In Chapter 1, first of all, we introduce our aim of this dissertation. Around this topic, literature reviews are addressed and dissertation outline is sketched out.

Then the PhD thesis has been divided into two parts, the first part medical knowledge (called Part A) regroup 3 chapters:
In Chapter A1, we present the medical concept of premature newborns and clinical problems associated with prematurity. Especially, we review the clinical manifestations of early onset sepsis and late onset sepsis in neonatal infants separately.

In Chapter A2, we introduce the physiological foundation of Autonomic Nervous System, which control Heart Rate Variability. After, we discuss the cardiovascular control system behavior, in particular, we focus on the abnormal behavior in neonatal sepsis —Bradycardia.

In Chapter A3, we evince the clinical theory of respiratory system, which regulate breathing signal. Next, we discuss about the respiration rate, in particular, we concentrate on the deviant phenomenon in neonatal sepsis —— Apnea. The relationship between apnea and bradycardia is also mentioned.

The second part (called Part B) regroups 3 chapters:
In Chapter B1, we study both linear methods and non-linear methods on RR analysis in newborns. A comparative analysis was attempted: patients from sepsis group were compared to the non-sepsis' according to the post-conceptional age (PCA) and post-natal age (PNA), whose values are close enough to be compared. Finally, we discover the optimal ways to discriminate between infected and non-infected premature newborns.

In Chapter B2, we carry out the research of Bi-channel signals based on a measurement of linear and non-linear relationships between RR series and Respiratory signals in Newborns. From the same cohort used for RR analysis, infants were retained, those having respiratory signals recorded. Eventually, we find out another valuable way to diagnosticate sepsis in a non-invasive way.

In Chapter B3, we effectuate feasibility study among candidate parameters selected from Chapter B1 and Chapter B2, compared with their optimal fusion, in order to help to decide which of these methods is a reasonable diagnostic scheme for NICU monitoring system.

Conclusions and Perspectives briefly summarize the research work and the main results presented in this dissertation, and then point out the future directions to extend our research.

1.4 Bibliography

[1] C. Beck-Sague, P. Azimi, S. Fonseca*, et al.*, "Bloodstream infections in neonatal intensive care unit patients: results of a multicenter study," *Pediatr Infect Dis,* vol.13, pp.1110-1116, 1994.

[2] A. Philip, "Diagnostic tests for bacterial infection in the new-born," *Infection in the Newborn,* vol.6, pp.49-59, 1990.

[3] H. Cao, D. E. Lake, M. P. Griffin*, et al.*, "Increased Nonstationarity of Neonatal Heart Rate Before the Clinical Diagnosis of Sepsis," *Annals of Biomedical Engineering,* vol.32*(2)*, pp.233-244, 2004.

[4] Yuping Xiao, M. Pamela Griffin, Douglas E. Lake*, et al.*, "Nearest-Neighbor and Logistic Regression Analyses of Clinical and Heart Rate Characteristics in the Early Diagnosis of Neonatal Sepsis," *Medical Decision Making,* vol.30*(2)*, pp.258-266, 2010 March/April.

[5] A. A. Flower, J. B. Delos, Y. Xiao*, et al.*, "Abstract 1769: Storms of Heart Rate Decelerations in Asymptomatic Infants Prior to Neonatal Sepsis," *Circulation,* vol.114*(18_MeetingAbstracts)*, pp.II_348-e-349, October 31, 2006.

[6] S. M. Pincus, "Approximate entropy as a measure of system complexity," *Proc Natl Acad Sci U S A,* vol.88*(6)*, pp.2297-2301, Mar 15, 1991.

[7] J. S. Richman and J. R. Moorman, "Physiological time-series analysis using approximate and sample entropy," *Am J Physiol Heart Circ Physiol,* vol.278, pp.H2039–H2049, 2000.

[8] D. E. Lake, J. S. Richman, M. P. Griffin*, et al.*, "Sample entropy analysis of neonatal heart rate variability," *American Journal of Physiology - Regulatory, Integrative and Comparative Physiology,* vol.283*(3)*, pp.789-797, September 1, 2002.

[9] J. S. Richman, D. E. Lake, and J. R. Moorman, "Sample entropy," *Methods Enzymol,* vol.384, pp.172-184, 2004.

[10] M. G. Signorini, A. de Angelis, G. Magenes*, et al.*, "Classification of fetal pathologies through fuzzy inference systems based on a multiparametric analysis of fetal heart rate," in *Computers in Cardiology 2000*, 2000, pp. 435-438.

[11] M. G. Signorini, F. Marchetti, and S. Cerutti, "Applying nonlinear noise reduction in the analysis of heart rate variability," *Engineering in Medicine and Biology Magazine, IEEE,* vol.20*(2)*, pp.59-68, 2001.

[12] S. Cerutti and M. G. Signorini, "Nonlinear advanced methods for biological signal analysis," in *[Engineering in Medicine and Biology, 2002. 24th Annual Conference and the Annual Fall Meeting of the Biomedical Engineering Society] EMBS/BMES Conference, 2002. Proceedings of the Second Joint*, 2002, 1, pp. 23-24 vol.21.

[13] M. G. Signorini, G. Magenes, S. Cerutti*, et al.*, "Linear and nonlinear parameters for the analysisof fetal heart rate signal from cardiotocographic recordings," *Biomedical Engineering, IEEE Transactions on,* vol.50*(3)*, pp.365-374, 2003.

[14] M. Ferrario, M. G. Signorini, and S. Cerutti, "Complexity analysis of 24 hours heart rate variability time series," in *Engineering in Medicine and Biology Society, 2004. IEMBS '04. 26th Annual International Conference of the IEEE*, 2004, 2, pp. 3956-3959.

[15] M. Ferrario, M. G. Signorini, G. Magenes*, et al.*, "Comparison of entropy-based regularity estimators: application to the fetal heart rate signal for the identification of fetal distress," *Biomedical Engineering, IEEE Transactions on,* vol.53*(1)*, pp.119-125, 2006.

[16] R. Sassi, S. Cerutti, K. Hnatkova*, et al.*, "HRV scaling exponent identifies postinfarction patients who might benefit from prophylactic treatment with amiodarone," *Biomedical Engineering, IEEE Transactions on,* vol.53*(1)*, pp.103-110, 2006.

[17] J. M. Di Fiore, "Neonatal cardiorespiratory monitoring techniques," *Semin Neonatol,* vol.9*(3)*, pp.195-203, Jun, 2004.

[18] G. Carrault, A. Beuchée, P. Pladys*, et al.*, "Time Frequency Relationships between Heart Rate and Respiration: A Diagnosis Tool for Late Onset Sepsis in Sick Premature Infants. ," *Proceedings of the IEEE Computers in Cardiology; Park City, Utah, USA*, pp.369-372, Sept 13-16, 2009.

[19] C. Maier, V. Rodler, H. Wenz*, et al.*, "ECG fingerprints of obstructed breathing in sleep apnea patients," *Engineering in Medicine and Biology Magazine, IEEE,* vol.28*(6)*, pp.41-48, 2009.

[20] D. Rassi, A. Mishin, Y. E. Zhuravlev*, et al.*, "Time domain correlation analysis of heart rate variability in preterm neonates," *Early Human Development,* vol.81*(4)*, pp.341-350, 2005.

[21] M. G. Frasch, U. Zwiener, D. Hoyer*, et al.*, "Autonomic organization of respirocardial function in healthy human neonates in quiet and active sleep," *Early Human Development,* vol.83*(4)*, pp.269-277, 2007.

[22] A. Yildiz, M. Akin, and M. Poyraz, "An expert system for automated recognition of patients with obstructive sleep apnea using electrocardiogram recordings," *Expert Systems with Applications,* vol.38*(10)*, pp.12880-12890, 2011.

Part A

Medical Knowledge

Chapter A1
Premature newborns and some related clinical problems

A1.1 Introduction

The subject of our study is premature newborns, so that we mainly discuss its medical background in this chapter. First of all, section A1.2 introduces the concept of premature newborns. Secondly, section A1.3 describes clinical problems associated with prematurity. Thirdly, section A1.4 presents the definition of sepsis and related symptoms, furthermore, it tries to enhance the main characteristic of the disease.

A1.2 Premature newborns

Premature or preterm infants are born between 24 and 37 weeks after the last menstrual period in contrast to full-term infants, which have a post-menstrual age between 37 and 42 weeks (Fig. A1-1). A neonate weighing less than 1500 grams at birth is considered as a very low weigh baby (VLWB).

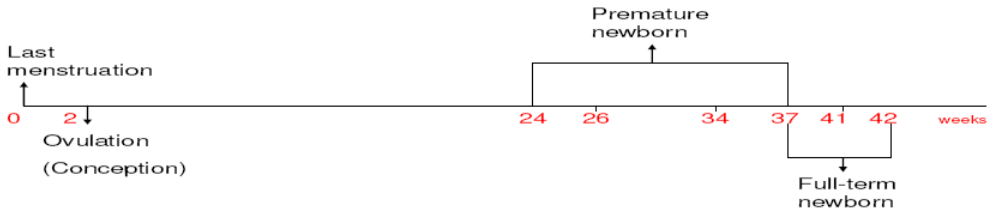

Fig. A1-1 Gestational ages from the last menstrual period [1]

Since newborns undergo rapid changes as they are born, and stating the significance of the degree of prematurity, it is important to clearly define the age in the following terms, as recommended by the standard terminology [1] (Fig. A1-2):

- Gestational Age (GA): time elapsed between the first day of the last menstrual period and the day of delivery.
- Chronological Age (CA): time elapsed after birth.
- Post-menstrual Age (PMA): gestational age plus chronological age.

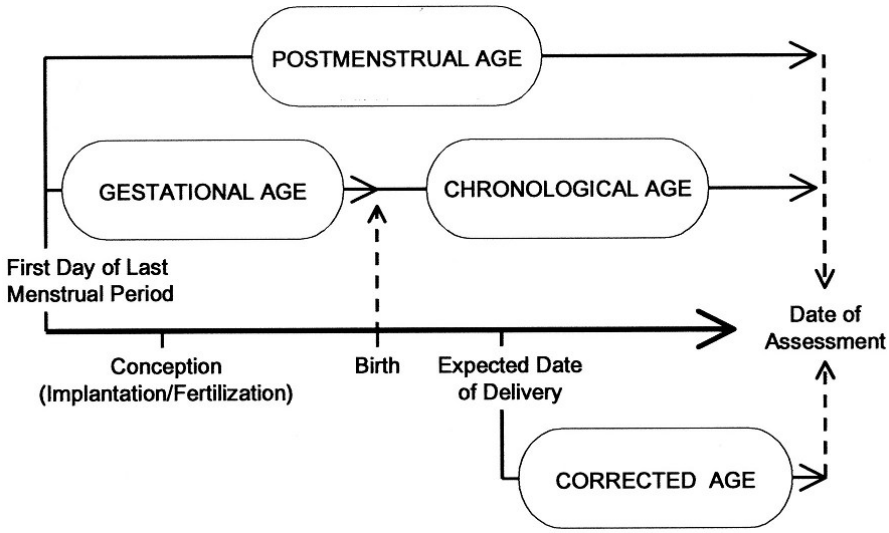

Fig. A1-2 Standard terminology according the AAP

A1.3 Clinical problems associated with prematurity

These newborns have to fight to survive, since the first moment of their extra-uterine life. During gestation, oxygen and food are provided by mother's placenta, and it is not necessary to breathe or digest; temperature is always comfortable and constant, gravity effects are imperceptible and the baby is rocked by mother's activities rhythm. His or her sensorial organs, although partly already formed, are not submitted to direct solicitations as sounds, lights or contacts, mother's antibodies protect him/her and they will pass in his/her body in the last pregnancy weeks.

Preterm newborns hit on living in a world not much appropriate to them, and they can go toward several problems described briefly in the next subsections:

A1.3.1 Low body temperature

They are not able to maintain an appropriate body temperature, thus they are put in an incubator, for trying to recreate, at least partially, the ideal conditions for their survival.

A1.3.2 Sepsis infection

They are at high risk of infections, provoked by bacteria, in the most common case, virus or fungi; when the infection is generalized or concerns the blood circulation, it is called sepsis.

Premature newborns are particularly exposed because they have a still incomplete immune system, since the majority of antibodies passes from placenta to the baby during the last months of pregnancy. Besides, catheters and respirators, always present in the Neonatal Intensive Care Units (NICU), can be bacterial vectors.

A baby suffering from an infection is less reactive, more prone to apneas and respiration problems, pale and feeding intolerant. Usually infections should be defeated quickly by focused antibiotics administration, and they should not leave permanent problems. Since the problem of sepsis is of central interest for this work, it is going to be developed further in the next section.

A1.3.3 Respiratory Distress Syndrome

They are at risk of respiration problems, which are mainly caused by incomplete lungs development. The most frequent trouble is the Respiratory Distress Syndrome (RDS). This pathology arises because of scarce quantity of surfactant, produced by mature lungs: a surface-active agent helping to maintain alveoli open. Lack of surfactant makes alveoli collapse and makes respiration difficult. The pathology interests mainly extreme premature babies, long period intubated, with an incidence between 4.2% and 40%. Usually, even the most serious situations have the tendency to improve in the first years of baby's life, with the growing lung development.

A1.3.4 Anemia

Premature newborns are particularly subjects to anemia (a deficiency of red blood cells), because in neonatal period, the red blood cells have a shorter life and during the first weeks their production is limited. Also the infections decrease the number of blood cells, as it does the small blood control collecting necessary for monitoring the newborn clinical situation.

A1.3.5 Apnea and Bradycardia

They develop episodes of apnea and bradycardia. An apneic pause is as a cessation of breathing movements and/or airflow for at least 4 seconds. It can be associated with bradycardia (defined as a decrease in heart rate of 33% from the baseline, for at least 4 seconds) and desaturation (a fall in oxygen quantity in blood, SaO2, under 80%) [2].

The respiratory pause may be central (i.e., no respiratory effort), obstructive (usually due to upper airway obstruction), or mixed.

Periodic breathing[1] and apnea are common in all the neonates, and the physiological mechanisms involved are not clear yet [3]. A low arterial PO_2 might magnify peripheral chemoreceptor contribution to breathing, with its baseline variability inducing major changes in ventilation, leading to instability of the respiratory control system. It has been hypothesized as following:

(1) Neonates would depend on the peripheral chemoreceptor contribution to breathing much more than adult subjects.
(2) Their baseline arterial PO_2 would sit on the steep portion of the ventilation/arterial PO_2 relationship on the adult nomogram, making breathing prone to oscillate [4].

Moreover, premature babies have apneas because they have immature respiratory centers in the brain. Preemies normally have bursts of big breaths followed by periods of shallow breathing or pauses. Apnea is most common when the baby is sleeping. Although there is considerable variation in incidence and severity of apnea in premature infants, both are inversely related to gestational age.

Approximately 50% of infants less than 1500 grams birth weight require either pharmacologic intervention or ventilatory support for recurrent prolonged apneic episodes. The peak incidence occurs between 5 and 7 days postnatal age.

[1] Cluster of breaths separated by intervals of apnea or near-apnea. It tends to occur during sleep, it can occur in healthy persons but it is typical in patients with congestive heart failure. The apnea in periodic breathing is usually central rather than obstructive.

Apnea of Prematurity is a specific diagnosis and usually resolves with the growth of the newborn, disappearing in proximity of the presumed date of birth, but until this moment apneas represent an high risk factor for mortality and morbidity of the baby.

Newborns with this pathology can be treated in several ways:

- Medications that stimulate breathing (as caffeine).
- CPAP or Continuous Positive Airway Pressure. This is air or oxygen delivered under pressure through little tubes into the baby's nose.
- Mechanical ventilation (breathing machine). If apnea is severe, the baby may need a few breaths from the ventilator every minute. These might be given at regular intervals or only if apnea occurs.
- Periodic stimulation. [5]

Continuous monitoring allows the staff to realize the problem and intervene immediately.

A1.3.6 Others

Other pathologies correlated with prematurity are: Retinopathy of Prematurity (ROP), open Bottallo's duct, jaundice, brain troubles. [6] This is the reason why premature newborns need to be put into an incubator for trying to recreate, at least partially, the ideal conditions for their survival.

A1.4 Sepsis

The clinical manifestations of neonatal sepsis, whatever the source of infection, are frequently nonspecific and include respiratory distress, unstable temperature and cardiovascular depression. A bulging or tense fontanel may be observed in meningitis. Neonatal septicemia and meningitis are also classified into early onset and late onset. It may be difficult to diagnose because of the multiplicity of associated risk factors and clinical manifestations [7] [8].

"Sepsis" is defined as the combination of an inflammatory response, i.e. CRP higher than 5mg/l 24 hours after the recording, and positive blood cultures. While "No-sepsis" is defined as the association of an absence of inflammatory response, i.e. CRP less than 5mg/l 24 hours after the recording, and negative blood cultures.

Infants of any gestational age are at high risk for acute bacterial infections for several reasons, both innate and extrinsic. Risk factors for infection are inversely related to GA. As a consequence, preterm infants acquire bacterial infections more readily than term infants, and morbidity and mortality are greater for those born earlier in gestation. From a clinical point of view, two kinds of sepsis are defined, depending on the onset period: Early Onset and Late Onset sepsis.

- ★ Early Onset Sepsis (Section A1.4.1)
- ★ Late Onset Sepsis (Section A1.4.2)

A1.4.1 Early Onset Sepsis

Acute bacterial infection during the first 3 days after birth occurs in 1 to 10 per 1,000 live births. Although the majority occurs in term infants, the likelihood of infection is greater among preterm

infants. Culture proven early onset sepsis will develop in about 2% of all infants with birth weight <1500 grams, although 10 times that number are treated as if they are infected.

Risk Factors interconnected with vertical transmission of causative organisms include:

- Premature and/or prolonged rupture of chorioamniotic membranes
- Maternal colonization with Group B beta-hemolytic Streptococcus (GBS)
- Intrapartum maternal fever
- Prematurity
- Chorioamnionitis (infection of mother's placenta)

Since the advent of intrapartum antibiotic prophylaxis to prevent neonatal GBS infection, Gram-negative organisms have become the most common pathogens, accounting for nearly 2/3 of all infections. Among these, Escherichia coli are the most common. Among Gram-positive causative organisms, GBS is most common. It is associated with rapid onset of respiratory disease and shock being often fatal.

Signs are nonspecific and may include any of the following:

- Lethargy
- Hypotonia
- Irritability with hyperreflexia
- Seizures
- Apnea
- Cyanosis
- Respiratory distress
- Metabolic acidosis
- Hypoglycemia
- Hyperglycemia
- Shock

Early, rapid and thorough evaluation is essential for successful treatment. An asymptomatic-term or near-term newborn with even one risk factor for sepsis requires careful physical examination and a screening complete blood count (CBC) with differential and platelet count. In the presence of multiple risk factors, also a blood culture is required, and it is considered to start antibiotic therapy.

For a preterm infant with any risk factors, and for any symptomatic newborn, CBC is made, and then blood culture and antibiotics have to be started.

As soon as cultures have been obtained, antibiotic therapy begins.

Early onset sepsis is associated with an increased likelihood of respiratory distress syndrome, chronic lung disease, severe intraventricular hemorrhage, and periventricular leukomalacia (PVL)[2]. Despite diagnostic and therapeutic advances, early onset sepsis is associated with a high

[2] Periventricular leukomalacia (PVL) is characterized by the death of the white matter of the brain due to softening of the brain tissue. Premature babies are at the greatest risk of the disorder. PVL is caused by a lack of oxygen

mortality and substantial morbidity; preterm newborns are more severely affected. Among very preterm infants, mortality is about 35%.

A1.4.2 Late Onset Sepsis (After age 3 days)

Incidence among healthy term infants is much less than early onset sepsis. However, preterm infants and term infants with various medical or surgical conditions are at greater risk for late onset sepsis. It occurs in approximately 7% to 10% of all neonates and in more than 25% of very low birth weight infants who are hospitalized in neonatal intensive care units [9].

Risk Factors for late onset bacterial infection are closely related to horizontal transmission of causative organisms and include endotracheal intubation, indwelling urinary and vascular catheters (especially venous catheters), lack of enteric feeding and exposure to broad- spectrum antibiotics, which may alter normal flora and permit overgrowth and dissemination of fungal species and resistant bacteria.

In contrast to early onset infections, Gram-positive organisms predominate and account for approximately 2/3 of cases. Coagulase-negative Staphylococcus species (common skin flora) are the most common isolates, especially among very preterm infants. However, Gram-negative bacteria (e.g., E. Coli, Klebsiella pneumonias, Pseudomonas aeruginosa) also cause a significant proportion of late onset disease. Fungal infections (with Candida species) occur frequently in small preterm infants

Presentation in most cases of late onset sepsis is gradual, rather than fulminant. The first indications may be subtle signs such as feeding intolerance, need for increased environmental oxygen. However, some infants become gravely sick very quickly and the presentation may include any signs mentioned above in Early Onset Sepsis.

As with early onset sepsis, it is imperative to perform an early and thorough diagnostic evaluation that should include CBC with differential and platelet count. Unlike early onset disease, urine infection is frequent. Urine should be collected for urinalysis and culture. To prevent contamination of the specimen, urine should be obtained by suprapubic needle aspiration. Urine by bag collection should never be sent for culture. Also, in contrast to early onset sepsis, serial C-reactive protein (CRP)[3] levels may be useful to rule out late onset sepsis among infants of any gestational age. If the CRP is <1.0 mg/dL at 12 and 36 hours after the onset of symptoms, the likelihood of proven or probable sepsis is 2.4%.

As soon as cultures have been obtained, antibiotic therapy should be instituted without delay. While the spectrum of causative organisms differs from early onset sepsis, ampicillin and gentamicin are appropriate initial antibiotic therapy.

As with early-onset infection, late-onset disease is associated with significant morbidity and mortality, thus preterm infants are more severely affected with a mortality of up to 20%. Late-onset sepsis is associated with an increased likelihood of patent ductus arteriosus,

[3] C-reactive protein (CRP) is a special type of protein produced in the liver that is present during episodes of acute inflammation or infection.

bronchopulmonary dysplasia, necrotizing enterocolitis and death. That is why we prefer to study late-onset sepsis rather than early-onset sepsis.

Late-onset sepsis in the NICU is a major problem associated with high morbidity and mortality, so reliable markers are needed.

Recurrent and severe spontaneous apneas and bradycardias frequently reveal systemic infection in the premature infant [10]. It requires prompt laboratory investigation so that treatment can start without delay.

The hematological and biochemical markers that have been described require invasive procedures that cannot be frequently repeated and have low predictive value in the early phase of sepsis [11] .

Nevertheless, lack of early and adapted intervention can lead the baby to risk his life, and, besides, apnea-bradycardia' episodes repetition compromises tissue oxygenation and perfusion.

Having considered this kind of risk, prolonged hospitalization periods are up to babies that have already had a long hospital path. Sometimes a house monitoring is also necessary [12].

A1.5 Bibliography

[1] W. A. Engle, "Age terminology during the perinatal period," *Pediatrics,* vol.114*(5)*, pp.1362-1364, Nov, 2004.

[2] C. F. Poets, V. A. Stebbens, M. P. Samuels*, et al.*, "The relationship between bradycardia, apnea, and hypoxemia in preterm infants," *Pediatr Res,* vol.34*(2)*, pp.144-147, Aug, 1993.

[3] *Medical dictionary definitions of popular medical terms*. Available: www.medterms.com/script/main/art.asp?articlekey=10902

[4] A. Al-Matary, I. Kutbi, M. Qurashi*, et al.*, "Increased peripheral chemoreceptor activity may be critical in destabilizing breathing in neonates," *Semin Perinatol,* vol.28*(4)*, pp.264-272, Aug, 2004.

[5] *Childrens specialists of San Diego- Division of Neonatology*. Available: http://www.childrensspecialists.com/

[6] *Sepsis in the Newborn*. Available: http://www.merckmanuals.com/home/sec23/ch264/ch264t.html

[7] A. G. S. Philip, *Neonatal sepsis and meningitis*, pp.1-5, Boston: GK Hall & Co, 1985.

[8] A. G. S. Philip, *Diagnostic tests for bacterial infection in the newborn.*, vol.6, pp.49-59, Chichester: John Wiley & Sons, 1990.

[9] C. M. Beck-Sague, P. Azimi, S. N. Fonseca*, et al.*, "Bloodstream infections in neonatal intensive care unit patients: results of a multicenter study," *Pediatr Infect Dis J,* vol.13*(12)*, pp.1110-1116, Dec, 1994.

[10] H. Cao, D. E. Lake, M. P. Griffin*, et al.*, "Increased Nonstationarity of Neonatal Heart Rate Before the Clinical Diagnosis of Sepsis," *Annals of Biomedical Engineering,* vol.32*(2)*, pp.233-244, 2004.

[11] A. Malik, C. P. Hui, R. A. Pennie*, et al.*, "Beyond the complete blood cell count and C-reactive protein: a systematic review of modern diagnostic tests for neonatal sepsis," *Arch Pediatr Adolesc Med,* vol.157*(6)*, pp.511-516, Jun, 2003.

[12] E. C. Eichenwald, M. Blackwell, J. S. Lloyd*, et al.*, "Inter-neonatal intensive care unit variation in discharge timing: influence of apnea and feeding management," *Pediatrics,* vol.108*(4)*, pp.928-933, Oct, 2001.

Chapter A2
Autonomic Nervous System and Heart Rate Variability

A2.1 Introduction

The physiological foundation of Autonomic Nervous System (ANS) and Heart Rate Variability (HRV) are introduced in Chapter A2. In particular, a control systems behavior analysis is approached, thus involving the cardiovascular and other mutual influences description.

First of all, section A2.2 and section A2.3 introduce the Autonomic Nervous System and Heart Rate Variability separately. Secondly, Heart Rate controlled by ANS and its behaviour are demonstrated in section A2.4 and section A2.5. Thirdly, the clinical definition of bradycardia and its manifestation in premature newborns are reported in section A2.6.

A2.2 The Autonomic Nervous System

It is the part of the nervous system of the higher life forms that is not consciously controlled (Fig. A2-1). It is commonly divided into two, usually antagonistic, subsystems: the sympathetic and parasympathetic nervous system, and involves the homeostasis of organs and physiological functions. A third and less commonly considered part of the autonomic nervous system is the enteric nervous system, which controls the digestive organs, and is, for the most part, independent of ANS input.

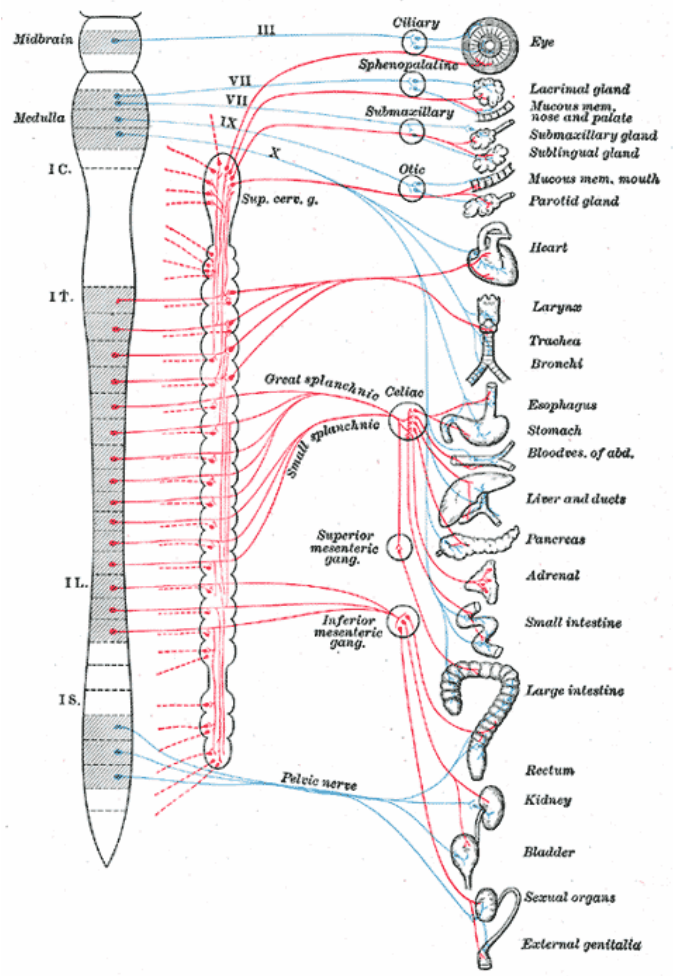

Fig. A2-1 Autonomic nervous system innervation,
showing the sympathetic and parasympathetic systems, in red and blue respectively.
From Gray's Anatomy

In general, parasympathetic nervous system (PNS) is involved with digestion and energy conservation, while the sympathetic nervous system (SNS) is involved with energy expenditure and the 'fight or flight' response. The PNS and SNS often create opposite effects in the same organs or physiological systems, and can act as an aid in creating balance (homeostasis) within the body.

It remains open to debate whether the term "involuntary" nervous system is a precise description of the ANS. Many autonomic functions are beyond conscious control, but others are impacted voluntarily including the sphincters in urination (micturition). It is well known that ANS has a major influence of the cardiovascular system, and the heart rate variability is an example.

A2.3 Heart Rate Variability

Heart rate variability is a physiological phenomenon where the time interval between heart beats varies. It is measured by the variation in the beat-to-beat interval [1].

Other terms used include: "cycle length variability", "heart period variability" and "RR variability", where R is a point corresponding to the peak of the QRS complex of the ECG wave (Fig. A2-2), and RR is the interval between successive Rs (Fig. A2-3).

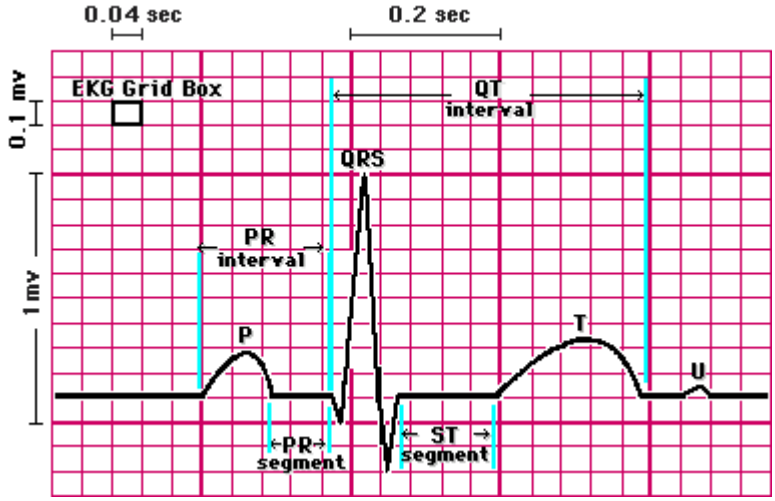

Fig. A2-2 QRS complex [2]

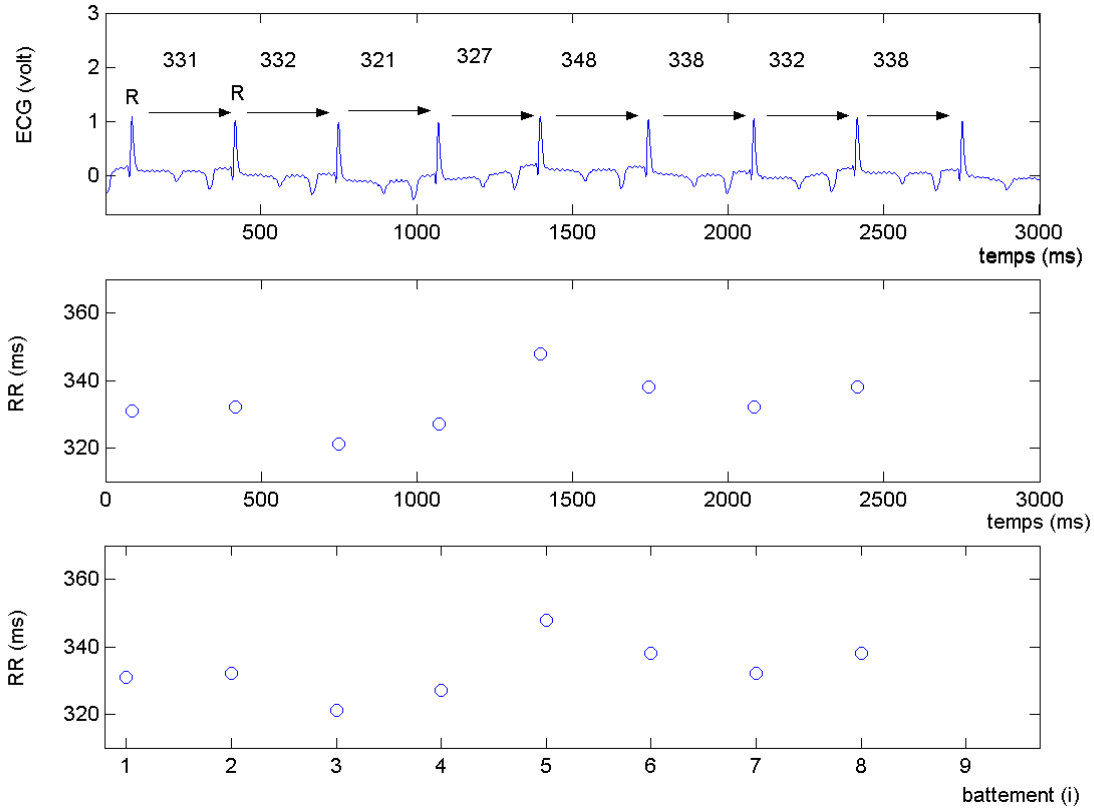

Fig. A2-3 RR extracted from ECG

Methods used to detect beats include: ECG, blood pressure, and the pulse wave signal derived from a photoplethysmograph (PPG). ECG is considered superior because it provides a clear waveform, which makes it easier to exclude heartbeats not originating in the sinoatrial (SA) node.

The term "NN" is used in place of RR to emphasize the fact that the processed beats are "normal" beats.

Reduced HRV has been shown to be a predictor of mortality after myocardial infarction [2] [3] although others have shown that the information in HRV relevant to acute myocardial infarction survival is fully contained in the mean heart rate (HR) [4]. A range of other outcomes/conditions may also be associated with modified (usually lower) HRV, including congestive heart failure, diabetic neuropathy, depression post-cardiac transplant, susceptibility to SIDS and poor survival in premature babies.

HRV studies have also been used to examine autonomic function in the context of bodily pain. Studies of patients with Fybromyalgic Syndrome (FMS) demonstrate reduced general ANS activity and markedly reduced nocturnal ANS activity [5], increased baseline SNS activity [6], and impaired SNS reactivity to stimuli including orthostatic and mental stress. [6]

A2.4 Heart Rate controlled by ANS

The primary means by which heart rate is regulated is that one through parasympathetic innervations via the vagus nerve. In fact, the parasympathetic nervous system provides a constant background level of activity to the sinoatrial node. It means that if it speeds up its activity, the heart slows down (parasympathetic activity leads to rest). Conversely, when background activity slows down, heart rate speeds up.

The latter effect can be also obtained through activation of the sympathetic nervous system. Normally, the PNS is the major determinant of the basal HR. But, in particular conditions such as stress, pain, or fear, the sympathetic system can speed up the heart rate. The postganglionic axons of the sympathetic nervous system arrive at the heart through nerves that have been called accelerator nerves.

The medulla of the brain contains a "cardiac center": it determines how to change the heart rate and which system to use. Since it is in the brain, it receives lots of other information upon which to base its decision.

The ANS can find quickly the way to comply with changes in arterial pressure (via the baroreflex) in order to regulate it or to adjust to stimulations both endogenous (chemoreflexes) or exogenous (stress, emotions, etc).

The mutual influence between vagal and SNS acts as a closed loop control mechanism for heart rate variability (Fig. A2-4).

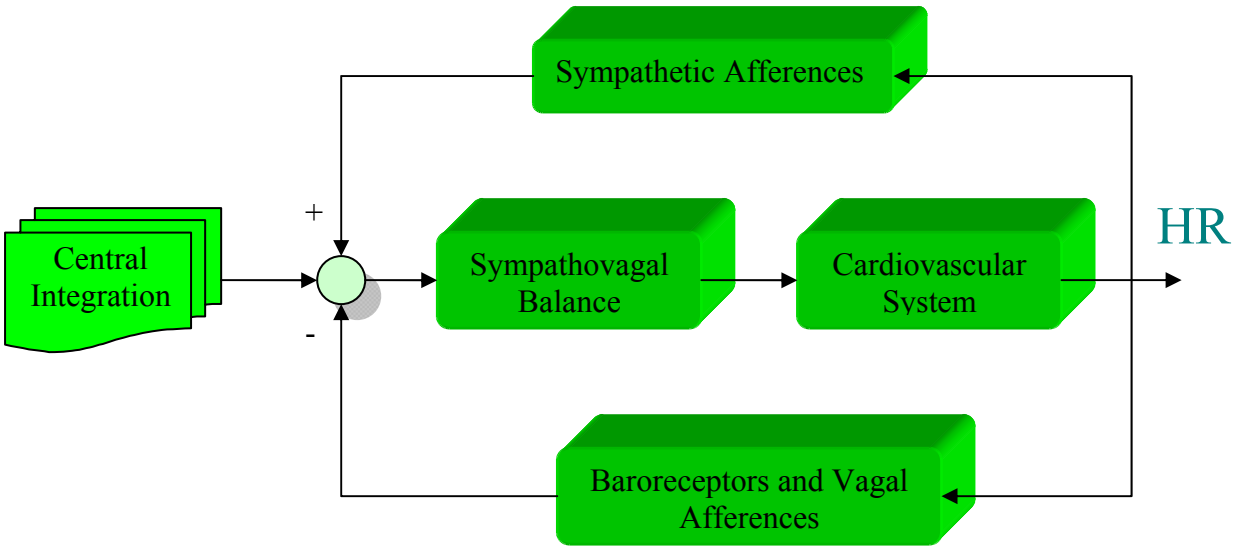

Fig. A2-4 Cardiovascular regulation loop model

This is the reason why HR and its variability constitute one of the main four vital signs (together with temperature examination, blood pressure and respiratory rate): usually it is calculated as the number of contractions (heart beats) of the heart in one minute and expressed in "bpm" (beats per minute).

Neural development is one of the earliest to begin and the last to be complete, generating the most complex structure within the embryo. Then it continues throughout our entire life, through embryonic, fetal, newborn, postnatal, and it keeps being remodeled at the synaptic level.

A2.5 HRV and Cardiovascular control system behavior

As it has been said before, in physiologic conditions HRV is regulated by the sympathetic and vagal system.

Thus, a bradycardia can be due to an increase in vagal control or to a decrease in sympathetic activity, or to their interaction. This autonomic control of HR and vascular tone, plays a more important role in cardiovascular adaptation mechanisms in the fetus [7] [8] and in the newborn [9] [10] [11]. Interactions between sympathetic and vagal systems are quite complex, and subdued to maturation effects. This normal process of maturation involve sensor mechanisms (baro-receptors, chemo-receptors, volo-receptors, stretch-receptors) [12] [13], the development of the autonomic heart innervations [14], mediators implicated in heart rhythm regulation (neuropeptide Y, adenosine, serotonin, opioids) [15] [16] [17] [18], the expression of different kinds of receptors adrenergic and muscarinic [14], the electrophysiology and the sinusal knot pacemaker cells' signal transduction (adrenergic modulation of the response to a muscarinic stimulation) [14] [19],

the expression and functioning of ionic channels, especially the different potassium ones. [20] [21] [22] [23].

A useful tool for assessing ANS mechanisms controlling HR is the spectral analysis of RR variability. According to previous HRV frequency analysis studies, four frequency bands have been defined:

- Ultra Low Frequency (ULF): 0.0001 — 0.003 Hz in adult. The very slow spontaneous rhythms are calculated on long recordings (24h at least).
- Very Low Frequency (VLF): 0.003 — 0.04 Hz in adult. 0.002 — 0.02 Hz in newborn [24]. These rhythms are bound with thermoregulation and peripheral vasomotor regulation.
- Low Frequency (LF): 0.04 — 0.15 Hz in adult. 0.02 — 0.2 Hz in newborn [24]. A LF spectral peak, synchronous with Mayer waves in BP, occurs around 0.1 Hz and is attributed to the BR (baro-receptor reflex) [25]: thus, this variability depends mainly by the sympathetic system behavior.
- High Frequency (HF): 0.15 — 0.4 Hz in adult. 0.2 — 1.5 Hz in newborn [24] [26]. The HRV in this band is essentially the RSA, which is the heart rate fluctuation around the respiratory frequency. This variability is bound mainly to the parasympathetic system activity, which is to the vagus nerve action on heart. [27]

This kind of definition, allows observing the ANS behavior through the heart rate power spectrum. In particular, the so called $\frac{LF}{HF}$ can be valued, reflecting the "sympathovagal balance", useful to better understand the nervous system response to different stimulations. Though there is no definite evidence that the autonomic nervous system exclusively affects the ratio $\frac{LF}{HF}$ of HR variability, this ratio is commonly used as an index of the balance between sympathetic and parasympathetic modulation of the sinoatrial node [27] [28]. We will see in Chapter B1 that other parameters extracted from the temporal domain and the non-linear theory can be used to quantify HRV and the influence of PNS and ANS.

Cardiovascular reflexes using spectral power analysis of RR interval have been studied in preterm and full-term infants [29] [30].

The $\frac{LF}{HF}$ ratio progressively decreases with postnatal age, indicating an increase in parasympathetic contribution to control HR [24] [30] [31].

Power spectral analysis of beat-to-beat HR variability is a non-invasive method to assess autonomic nervous system regulation of cardiovascular activity, of the degree of interconnectivity and coupling between these two organ systems.

Nevertheless, for better understanding these kinds of relations, it is necessary to approach a multivariate signal analysis, as the one conducted in this work and later explained.

A2.6 Bradycardia

A2.6.1 Definition of Bradycardia

Bradycardia, in the context of medicine, is a slowness of the heart rate [32]. Normal heart rate is showed in Fig. A2-5 and bradycardia in Fig. A2-6

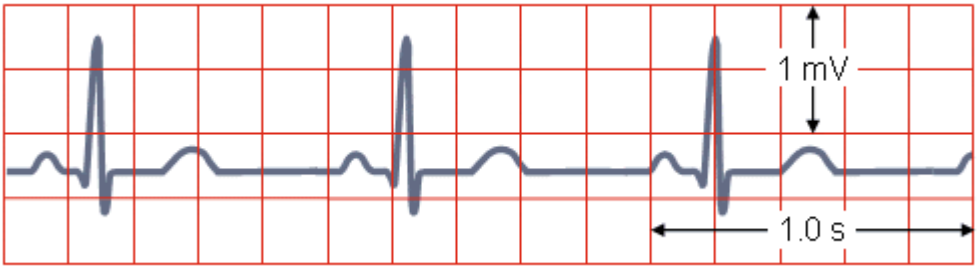

Fig. A2-5 Normal heart rate (evenly spaced)

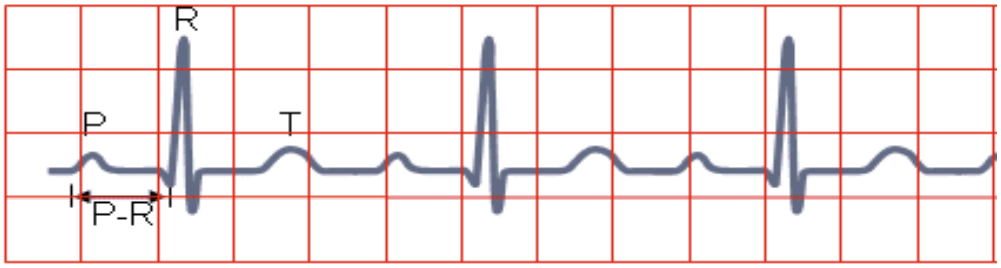

Fig. A2-6 Heart rate with bradycardia (First-degree A-V block) [32]

It may cause cardiac arrest in some patients, because those with bradycardia may not be pumping enough oxygen to their heart. It sometimes results in fainting, shortness of breath, and if severe enough, death.

Trained athletes or young healthy individuals may also have a slow resting heart rate. Resting bradycardia is often considered normal if the individual has no other symptoms such as fatigue, weakness, dizziness, light-headedness, fainting, chest discomfort, palpitations or shortness of breath associated with it.

A2.6.2 Classification of Bradycardia

A2.6.2.1 Atrial Bradycardia

Atrial bradycardias come in three different types. One of types is sinus bradycardia, which is usually found in young and healthy adults. The symptoms are linked with the individual's respirations. Each inhalation corresponds with the heart rate decrease. Expiration causes an increase in the heart rate. This is thought to be caused by changes in the vagal tone during respiration. [33]

Sinus bradycardia is a sinus rhythm of less than 60 bpm. It is a common condition found in both healthy individuals and those who are considered well conditioned athletes. Studies have found

that 50 - 85 percent of conditioned athletes have benign sinus bradycardia, as compared to 23 percent of the general population studied [34]. The reason for this is that their heart muscle has become conditioned to have a higher stroke volume and therefore requires fewer contractions to circulate the same volume of blood. [33]

Sick sinus syndrome covers conditions that include severe sinus bradycardia, sinoatrial block, sinus arrest, and bradycardia-tachycardia syndrome (atrial fibrillation, flutter, and paroxysmal supraventricular tachycardia). [33]

A2.6.2.2 Atrioventricular nodal

An atrioventricular (AV) nodal bradycardia or AV junction rhythm is usually caused by the absence of the electrical impulse from the sinus node. This usually appears on an ECG with a normal QRS complex accompanied with an inverted P wave before, during, or after the QRS complex. [33]

An AV junctional escape is a delayed heartbeat originating from an ectopic focus somewhere in the AV junction. It occurs when the rate of depolarization of the SA node falls below the rate of the AV node [33]. This dysrhythmia also may occur when the electrical impulses from the SA node fail to reach the AV node because of SA or AV block [35]. This is a protective mechanism for the heart, to compensate for a SA node that is no longer handling the pace making activity, and is one of a series of backup sites that can take over pacemaker function when the SA node fails to do so. This would present with a longer PR interval. A junctional escape complex is a normal response that may result from excessive vagal tone on the SA node. Pathological causes include sinus bradycardia, sinus arrest, sinus exit block, or AV block. [33]

A2.6.2.3 Ventricular Bradycardia

A ventricular bradycardia, also known as ventricular escape rhythm or idioventricular rhythm, is a heart rate of less than 50 beats a minute. This is a safety mechanism that arises when there is lack of electrical impulse or stimuli from the atrium [33]. Impulses originating from or below the bundle, also known as ventricular, will produce a wide QRS complex with heart rates between 20 and 40 beats a minute. Those above the bundle, also known as junctional, will typically range between 40 and 60 bpm with a narrow QRS complex [36] [37]. In a third degree heart block, approximately 61% take place at the bundle branch-Purkinje system, 21% at the AV node, and 15% at the bundle [37]. AV block maybe ruled out with an ECG indicating "a 1:1 relationship between P waves and QRS complexes." [36] Ventricular bradycardias occurs with sinus bradycardia, sinus arrest, and AV block. Treatment often consists of the administration of atropine and cardiac pacing. [33]

A2.6.3 Bradycardia in adults

During bradycardia the heart beats at a rate slower than normal. A normal heart rate ranges from 60-100 bpm. Sometimes, like during sleep or in some athletes, the heart rate may be lower than 60 bpm, being completely normal. But often a slow beating heart is a medical condition that requires treatment. A slower heart rate means less oxygen-rich blood is being pumped through the body, and symptoms are related to this lack of oxygen.

Most bradyarrhythmias are due to one of the two following of problems:

- ❖ Sinus bradycardia
- ❖ Heart block.

Sinus bradycardia occurs when the SA node develops an abnormally slow rate of impulse generation. The heartbeat is slow because the heart's "natural pacemaker" is operating slowly.

"Heart block" is a term for delay or interruption in the heart's conduction system, causing the electrical impulses to travel too slowly or to be stopped. There are several different kinds of heart block, classified according to location (where in the conduction system the block occurs) and according to degree (whether the block is mild, causing delayed conduction or severe, causing conduction to stop). [38]

Bradycardia can be caused by a variety of factors, including:

- Hypotension
- Acutely altered mental status
- Signs of shock
- Ischemic chest discomfort
- Congenital defect - Irregular heartbeat present at birth.
- Aging - Degenerative process of aging can cause the heart to slow down.
- Medication - Some cold medicines and diet pills have been known to cause arrhythmia.
- Acute heart failure - Dysfunction of the electrical pathways of the heart can cause bradycardia.

Tests for diagnosing bradycardias may include analysis of ECG signals, either during long-term monitoring (portable ECG) or during provocative tests (stress test ECG or Electrophysiological studies-EPS).

Treatment for bradycardia varies from person to person and depends upon the severity, frequency and cause of the bradycardia. Medication to prevent blood clots, to control low blood pressure or to control other medical conditions (such as thyroid disease) can be effective in preventing bradycardia.

Various surgical procedures can also be effective in preventing bradycardia. Procedures include:

- Electric shocks - electrical shocks given to reset the heart rate
- Pacemaker - surgically inserted to regulate the heart beat

If for some reason severe bradycardia is not treated, it can lead to other serious problems, including fainting and injuries from fainting, seizures[4], and death [39] [40].

Reflected bradycardias are a common event in human clinic, especially in vaso-vagal syncope in adult. These bradycardias have been studied according to different models, tilt test and oculo-cardiac reflex (OCR) [41] [42] [43] [44] [45] [46], but they follow unfully explained mechanisms [47].

[4] Seizures are sudden bursts of abnormal electrical activity in the brain that may affect a person's muscle control, movement, speech, vision, or awareness (consciousness).

A2.6.4 Bradycardia in newborns

The pathogenesis of bradycardias in preterm infants is poorly understood. Bradycardia in preterm infants is defined as a fall in heart rate under 100 bpm, or a decrease of 33% from the baseline, for at least 4 seconds. In the newborn the amplitude of vagus-mediated bradycardias, decreases with maturation. With the increase of post-conceptional age (sum of gestational and post-natal age), a decrease of heart rate response to vagal stimulation, as ocular compression, has been observed, and a rise in vagal tone valued in the baseline heart rate [15], and HRV : High Frequencies, Medium Frequencies, Low Frequencies, and mean RR all increase with age; the differences from the premature to the full-term are more marked, as a whole, in REM sleep (rapid eye movement sleep) than in non-REM sleep. In particular, it has been noticed a steep increase in vagal tone at 37-38 weeks CA, with stability afterwards, and a more regular increase in sympathetic tone from 31 to 41 weeks CA [48]. These results suggest an inverse evolution of reflected bradycardias and vagal tone importance in neonatal period. However, the respective parts of sympathetic or parasympathetic activity in reflected bradycardias' onset is still not much known.

A2.7 Bibliography

[1] Wikipedia. *Heart rate variability*. Available: http://en.wikipedia.org/wiki/Heart_rate_variability

[2] J. T. Bigger, Jr., J. L. Fleiss, R. C. Steinman*, et al.*, "Frequency domain measures of heart period variability and mortality after myocardial infarction," *Circulation,* vol.85*(1)*, pp.164-171, Jan, 1992.

[3] R. E. Kleiger, J. P. Miller, J. T. Bigger, Jr.*, et al.*, "Decreased heart rate variability and its association with increased mortality after acute myocardial infarction," *Am J Cardiol,* vol.59*(4)*, pp.256-262, Feb 1, 1987.

[4] S. Z. Abildstrom, B. T. Jensen, E. Agner*, et al.*, "Heart rate versus heart rate variability in risk prediction after myocardial infarction," *J Cardiovasc Electrophysiol,* vol.14*(2)*, pp.168-173, Feb, 2003.

[5] M. Martinez-Lavin, A. G. Hermosillo, M. Rosas*, et al.*, "Circadian studies of autonomic nervous balance in patients with fibromyalgia: a heart rate variability analysis," *Arthritis Rheum,* vol.41*(11)*, pp.1966-1971, Nov, 1998.

[6] H. Cohen, L. Neumann, M. Shore*, et al.*, "Autonomic dysfunction in patients with fibromyalgia: application of power spectral analysis of heart rate variability," *Semin Arthritis Rheum,* vol.29*(4)*, pp.217-227, Feb, 2000.

[7] A. M. Nuyt, J. L. Segar, A. T. Holley*, et al.*, "Autonomic adjustments to severe hypotension in fetal and neonatal sheep," *Pediatr Res,* vol.49*(1)*, pp.56-62, Jan, 2001.

[8] A. L. Portbury, R. Chandra, M. Groelle*, et al.*, "Catecholamines act via a beta-adrenergic receptor to maintain fetal heart rate and survival," *Am J Physiol Heart Circ Physiol,* vol.284*(6)*, pp.H2069-2077, Jun, 2003.

[9] H. Lagercrantz, D. Edwards, D. Henderson-Smart*, et al.*, "Autonomic reflexes in preterm infants," *Acta Paediatr Scand,* vol.79*(8-9)*, pp.721-728, Aug-Sep, 1990.

[10] J. Ramet, B. Hauser, M. Dehan*, et al.*, "Effect of state of alertness on the heart rate response to ocular compression in human infants," *Biol Neonate,* vol.68*(4)*, pp.270-275, 1995.

[11] J. Ramet, J. P. Praud, A. M. D'Allest, *et al.*, "Effect of maturation on heart rate response to ocular compression test during rapid eye movement sleep in human infants," *Pediatr Res,* vol.24*(4)*, pp.477-480, Oct, 1988.
[12] J. L. Segar, "Ontogeny of the arterial and cardiopulmonary baroreflex during fetal and postnatal life," *Am J Physiol,* vol.273*(2 Pt 2)*, pp.R457-471, Aug, 1997.
[13] J. L. Segar, A. Minnick, A. M. Nuyt, *et al.*, "Role of endogenous ANG II and AT1 receptors in regulating arterial baroreflex responses in newborn lambs," *Am J Physiol,* vol.272*(6 Pt 2)*, pp.R1862-1873, Jun, 1997.
[14] R. B. Robinson, "Autonomic receptor--effector coupling during post-natal development," *Cardiovasc Res,* vol.31 Spec No, pp.E68-76, Feb, 1996.
[15] A. M. Fenton, S. C. Hammill, R. F. Rea, *et al.*, "Vasovagal syncope," *Ann Intern Med,* vol.133*(9)*, pp.714-725, Nov 7, 2000.
[16] B. P. Grubb and B. Karas, "Diagnosis and management of neurocardiogenic syncope," *Curr Opin Cardiol,* vol.13*(1)*, pp.29-35, Jan, 1998.
[17] A. Pelleg, G. Katchanov, and J. Xu, "Autonomic neural control of cardiac function: modulation by adenosine and adenosine 5'-triphosphate," *Am J Cardiol,* vol.79*(12A)*, pp.11-14, Jun 19, 1997.
[18] J. C. Shryock and L. Belardinelli, "Adenosine and adenosine receptors in the cardiovascular system: biochemistry, physiology, and pharmacology," *Am J Cardiol,* vol.79*(12A)*, pp.2-10, Jun 19, 1997.
[19] S. S. Demir, J. W. Clark, and W. R. Giles, "Parasympathetic modulation of sinoatrial node pacemaker activity in rabbit heart: a unifying model," *Am J Physiol,* vol.276*(6 Pt 2)*, pp.H2221-2244, Jun, 1999.
[20] E. Cerbai, R. Pino, L. Sartiani, *et al.*, "Influence of postnatal-development on I(f) occurrence and properties in neonatal rat ventricular myocytes," *Cardiovasc Res,* vol.42*(2)*, pp.416-423, May, 1999.
[21] G. Malfatto, L. S. Sun, and T. S. Rosen, "Bradycardia and long QT interval in neonate rats with delayed cardiac sympathetic innervation," *J Auton Nerv Syst,* vol.30 Suppl, pp.S101-102, Jul, 1990.
[22] L. Protas, D. DiFrancesco, and R. B. Robinson, "L-type but not T-type calcium current changes during postnatal development in rabbit sinoatrial node," *Am J Physiol Heart Circ Physiol,* vol.281*(3)*, pp.H1252-1259, Sep, 2001.
[23] G. T. Wetzel and T. S. Klitzner, "Developmental cardiac electrophysiology recent advances in cellular physiology," *Cardiovasc Res,* vol.31 Spec No, pp.E52-60, Feb, 1996.
[24] U. Chatow, S. Davidson, B. L. Reichman, *et al.*, "Development and maturation of the autonomic nervous system in premature and full-term infants using spectral analysis of heart rate fluctuations," *Pediatr Res,* vol.37*(3)*, pp.294-302, Mar, 1995.
[25] M. A. Cohen and J. A. Taylor, "Short-term cardiovascular oscillations in man: measuring and modelling the physiologies," *J Physiol,* vol.542*(Pt 3)*, pp.669-683, Aug 1, 2002.
[26] T. Aarimaa, R. Oja, K. Antila, *et al.*, "Interaction of heart rate and respiration in newborn babies," *Pediatr Res,* vol.24*(6)*, pp.745-750, Dec, 1988.
[27] S. Akselrod, D. Gordon, F. Ubel, *et al.*, "Power spectrum analysis of heart rate fluctuation: a quantitative probe of beat-to-beat cardiovascular control," *Science,* vol.213*(4504)*, pp.220-222, July 10, 1981.
[28] M. Pagani, N. Montano, A. Porta, *et al.*, "Relationship between spectral components of cardiovascular variabilities and direct measures of muscle sympathetic nerve activity in humans," *Circulation,* vol.95*(6)*, pp.1441-1448, Mar 18, , 1997.
[29] H. Witte and M. Rother, "High-frequency and low-frequency heart-rate fluctuation analysis in newborns--a review of possibilities and limitations," *Basic Res Cardiol,* vol.87*(2)*, pp.193-204, Mar-Apr, 1992.

[30] J. E. Mazursky, C. L. Birkett, K. A. Bedell, *et al.*, "Development of baroreflex influences on heart rate variability in preterm infants," *Early Hum Dev,* vol.53*(1)*, pp.37-52, Nov, 1998.
[31] C. Van Ravenswaaij-Arts, J. Hopman, L. Kollee, *et al.*, "Spectral analysis of heart rate variability in spontaneously breathing very preterm infants," *Acta Paediatr,* vol.83*(5)*, pp.473-480, May, 1994.
[32] Wikipedia. *Bradycardia*. Available: http://en.wikipedia.org/wiki/Bradycardia
[33] A. B. Wolfson, *Harwood-Nuss' Clinical Practice of Emergency Medicine*, 4th ed., pp.260, 2005.
[34] B. G. Ward and J. M. Rippe, "Athletic Heart Syndrome," *Clinical Sports Medicine,* vol.11, p.259, 1992.
[35] "AV Junctional Rhythm Disturbances (for Professionals)," *American Heart Association*, Dec 04, 2008.
[36] *Arrhythmias and Conduction Disorders*: Merck Sharp and Dohme Corp, 2008 Jan.
[37] M. Adams and M. Pelter, "Ventricular Escape Rhythms," *American Journal of Critical Care,* vol.12, pp.477–478, 2003.
[38] *UpToDate Patient information*. Available: http://www.uptodate.com/patients/index.html?file=hrt_dis/9666
[39] *Strong Health*. Available: http://www.urmc.rochester.edu/cardiology/patient-care/conditions/bradycardia.cfm
[40] *Bradycardia (Slow Heart Rate)*. Available: http://www.healthbanks.com/patientportal/MyPractice.aspx?UAID={245E31C8-DEFF-4BF8-90E6-8FDB07A10710}&ID=HW5aa107571
[41] B. C. Galland, R. M. Hayman, B. J. Taylor, *et al.*, "Factors affecting heart rate variability and heart rate responses to tilting in infants aged 1 and 3 months," *Pediatr Res,* vol.48*(3)*, pp.360-368, Sep, 2000.
[42] M. M. Massin, V. Henrard, and P. Gerard, "Heart rate variability and the outcome of head-up tilt in syncopal children," *Acta Cardiol,* vol.55*(3)*, pp.163-168, Jun, 2000.
[43] M. M. Massin, K. Maeyns, N. Withofs, *et al.*, "Circadian rhythm of heart rate and heart rate variability," *Arch Dis Child,* vol.83*(2)*, pp.179-182, Aug, 2000.
[44] C. Miwa, Y. Sugiyama, T. Mano, *et al.*, "Effects of aging on cardiovascular responses to gravity-related fluid shift in humans," *J Gerontol A Biol Sci Med Sci,* vol.55*(6)*, pp.M329-335, Jun, 2000.
[45] G. A. Ruiz, C. Madoery, F. Arnaldo, *et al.*, "Frequency-Domain Analysis of Heart Rate Variability During Positive and Negative Head-Up Tilt Test: Importance of Age," *Pacing and Clinical Electrophysiology,* vol.23*(3)*, pp.325-332, 2000.
[46] R. Sutton and D. M. Bloomfield, "Indications, methodology, and classification of results of tilt-table testing," *Am J Cardiol,* vol.84*(8A)*, pp.10Q-19Q, Oct 21, 1999.
[47] M. Brignole, "Randomized clinical trials of neurally mediated syncope," *J Cardiovasc Electrophysiol,* vol.14*(9 Suppl)*, pp.S64-69, Sep, 2003.
[48] J. Clairambault, L. Curzi-Dascalova, F. Kauffmann, *et al.*, "Heart rate variability in normal sleeping full-term and preterm neonates," *Early Hum Dev,* vol.28*(2)*, pp.169-183, Feb, 1992.

Chapter A3
The Respiratory System

A3.1 Introduction

In the previous chapter, we have seen the influence of ANS on the cardiovascular system. Here, we present the respiratory system which is also affected by sepsis. First of all, section A3.2 introduces the respiratory system. Secondly, section A3.3 describes respiration rate. Thirdly, apnea of prematurity is demonstrated in section A3.4. Finally, the relationship between apnea and bradycardia is discussed in section A3.5.

A3.2 The respiratory system

A3.2.1 Physiology of the respiratory system

The respiratory system consists in the respiratory airways and the lungs, which are composed by left and right lung. The diaphragm and the chest muscles movements allow expanding the pulmonary cavity, causing a negative pressure which allows the air to move from the mouth or nose into the trachea, into the bronchi and eventually into the alveoli. (Fig. A3-1)

This process (inspiration) provides fresh air, rich in oxygen, and the inverse (exhalation) permits to emit the waste air, rich in carbon dioxide, produced by the metabolic reactions of the organism.

The alveoli are the smallest functional structures into the lungs where takes place the gas exchange: the oxygen contained in the air enters the blood and the carbon dioxide, comes out through the capillary by a diffusion process.

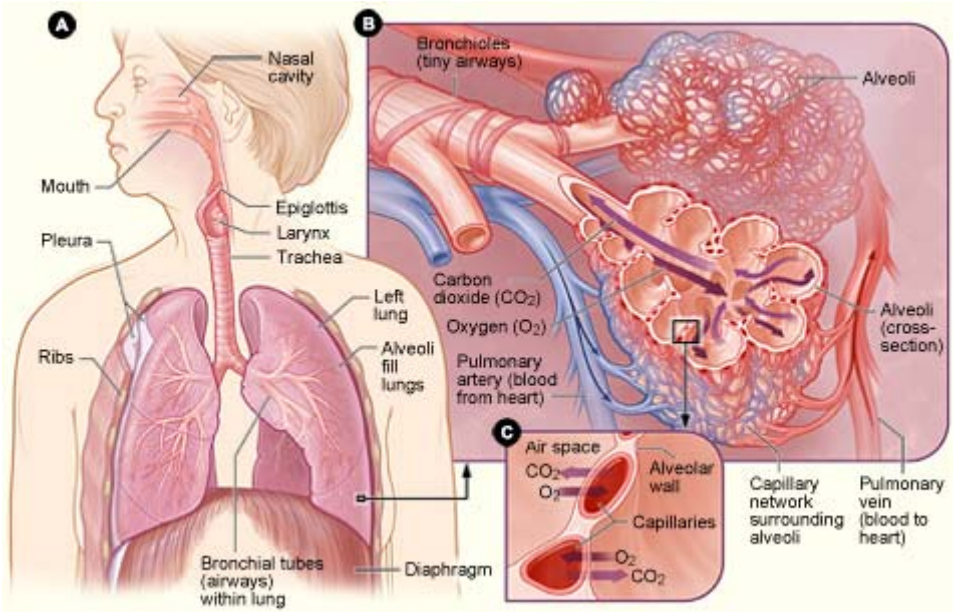

Fig. A3-1 A: Lung and airways; B: alveoli; C: gas exchange at capillaries level [1]

A3.2.2 Respiratory regulation

The regulation of respiration is the result of an interaction with several sensors forming a complex control system: A respiratory control center, an effector system to activate the muscles and organs involved in breathing. The regulation of breathing is a homeostatic control mechanism, meaning that it seeks constantly to maintain the stability of the internal environment via negative feedback mechanisms. High level of carbon dioxide in the body (increased *p*H in the venous blood) implies a quicker and deeper breathing, which in turn decreases the level of CO_2 by increasing the intake of oxygen.

Breathing is an automatic process triggered in a complex area of the brain, the brain stem, which connects the spinal cord and its nerves. It contains the involuntary respiratory control center. Otherwise, the respiration can be activated by a voluntary process when the central nervous system takes control of the ventilatory mechanism.

The brain stem respiratory control center regulates breathing with the help of effectors (nerves and muscles) and sensors (Chemoreceptors and specialized cells capable to detect chemical substances in the body and pass the information to the control centers).

The respiratory control is the central controlling area for breathing (Fig. A3-2). It receives information from other parts of the body and produces an automatic coordinated response, which consists in a reaction triggering the various organs and muscles to act together. It is located in the medulla oblongata, and there are two types of neurons: the inspiratory (active during inhaling and inactive during exhaling) and the expiratory neurons (active during exhaling and inactive during inhaling). This pair of neurons generates an automatic succession of ventilatory cycles which can be modified (or even temporally stopped) depending on the information received by the respiratory control from a variety of origins. The most important parts are:

- Central chemoreceptors: located at the bottom of the fourth ventricle (region of the brain stem), they respond to the acidity of the cerebrospinal fluid (CSF). When the *p*H changes (alteration in the concentration of blood hydrogen ions) this chemoreceptors send the information to the respiratory control center so it can have an effect on breathing.
- Peripheral arterial chemoreceptors: They are the carotid and aortic bodies, placed in the carotid artery and aorta. It is a small specialized tissue that responds to the concentration of the arterial blood O_2 and CO_2, sending the information to the respiratory control center with nerves.
- Brain: The cerebral cortex can activate the ventilatory mechanism consciously.
- Lung: Some receptors located in the bronchi can be irritated by inhaled substances provoking responses as coughing and sneezing. There are also other receptors in the flexible tissues of the lung and the chest wall (mechanoreceptors) related with various reflexes.

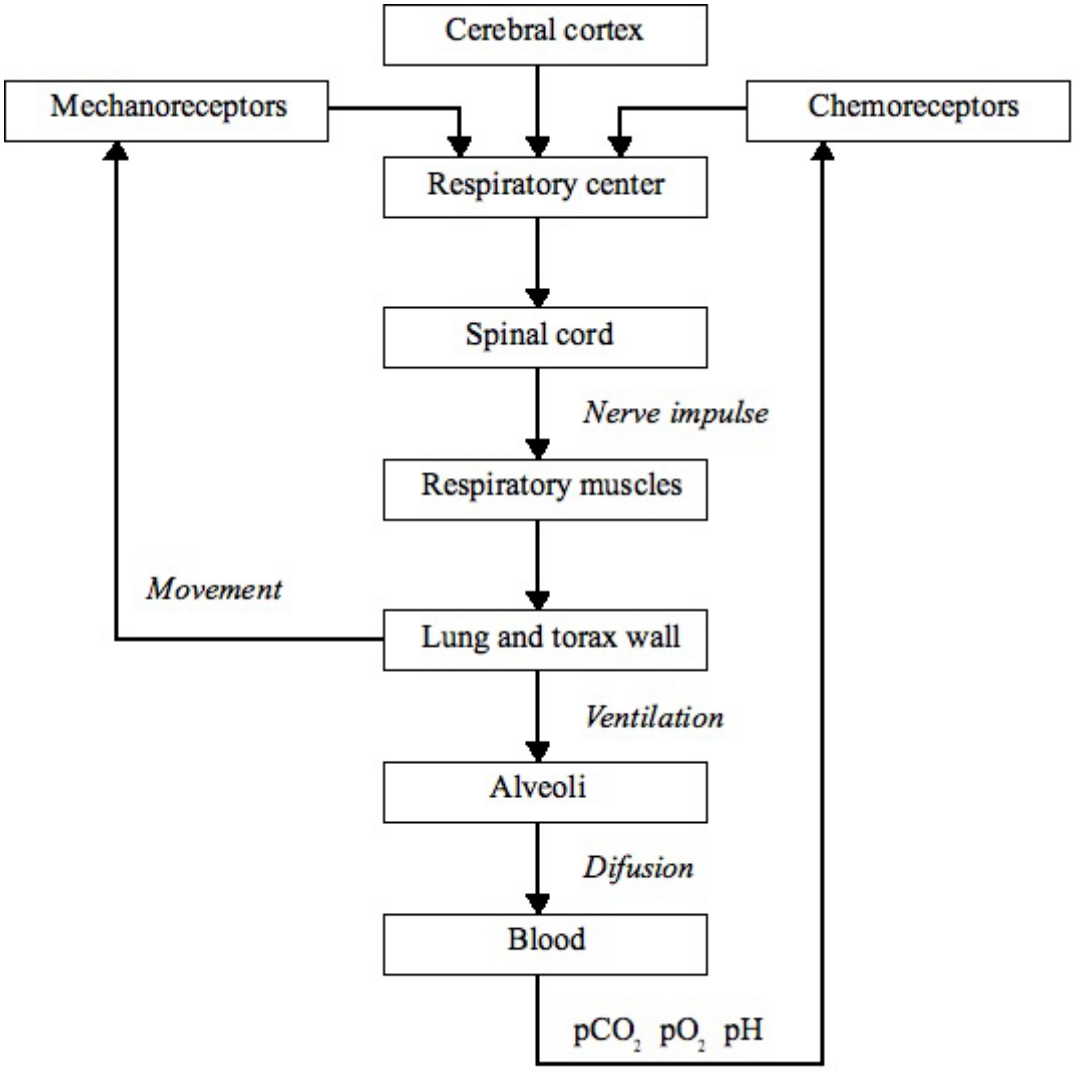

Fig. A3-2 Respiratory control diagram [1]

A3.2.3 The breathing signal

The respiratory signal is the registration of the temporal breathing evolution with some parameter to describe its activity, such as the air pressure, volume or voltage generated by the muscles.

The breathing activity can be monitored in several ways, both invasive and noninvasive: measuring the airflow (pneumotachometry, spirometry), registering the electrical activity of the muscles with electrodes (pletismography or even indirectly by extracting the signal from an electrocardiogram) or using movement sensors to measure the thorax distention.

The respiratory variables characterize the breathing features and pattern of an individual, and they are useful to find abnormalities and pathology [1]. An important set of parameters to determine the ventilatory function are the static lung volumes (see Fig. A3-3) [2]

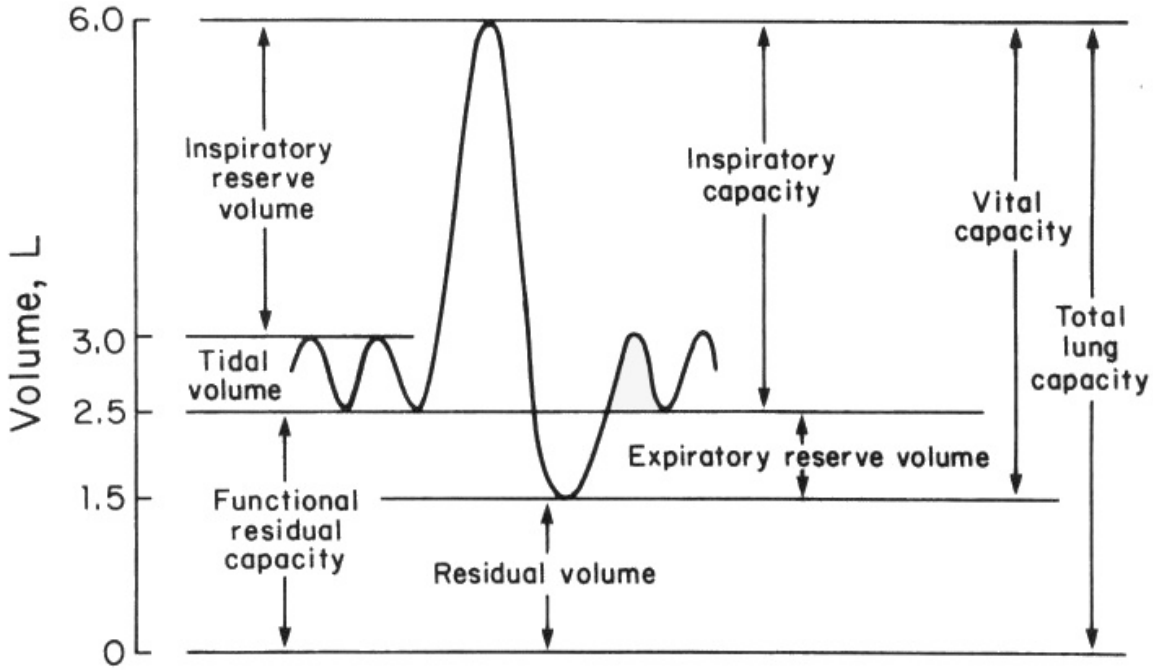

Fig. A3-3 Respiratory volumes [2]

These parameters are:

- Vital Capacity (VC): The maximal volume that can be expired.
- Tidal Volume (VT): Volume inspired in each breath.
- Inspiratory Capacity (IC): The maximal volume that can be inspired from resting expiratory level.
- Inspiratory Reserve Volume (IRV): The maximal volume of air inspired from end-tidal inspiration.
- Expiratory Reserve Volume (ERV): The maximal volume expired from the resting expiratory level.
- Functional Residual Capacity (FRC): The volume of air in lungs at resting expiratory level.
- Residual Volume (RV): Volume of gas in lungs at end of maximal expiration.
- Total Lung Capacity (TLC): Volume in lungs at end of maximal inspiration.

The variables concerns breathing in a resting state and they are extracted from a piezoelectric transducer signal (See Fig. A3-4):

- **Inspiratory time** (t_i): The air enters the lung increasing the thorax volume to reach the tidal volume. The signal has normally a rising value.
- **Expiratory time** (t_e): The air comes out from the lung decreasing its volume to the functional residual capacity. The signal has a downward trend.
- **Total time** (t_{tot}): The sum of t_i and t_e, completing a entire respiratory cycle.
- **Cycle ratio** (t_i/t_e): Inspiratory to expiratory time ratio. Measure of the symmetry of the breathing cycle: a value under the unity implies longer expiratory time.

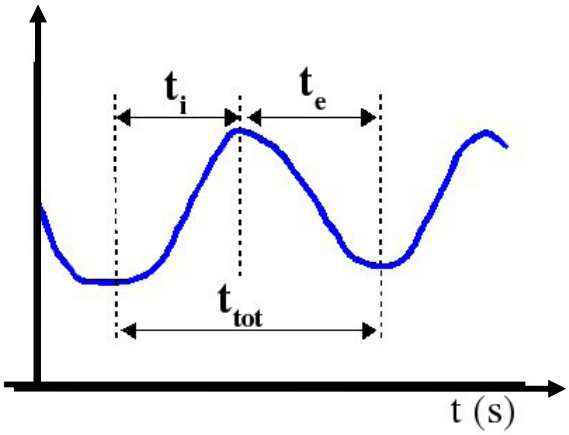

Fig. A3-4 The definitions of t_i, t_e and t_{tot} [2]

A3.3 Respiration Rate

The respiration rate is one of the vital signs measured when physicians and nurses check health status. Respiration (breathing) is controlled by the brain. A variety of factors can influence respiration such as head injury, bleeding, stress and fever, hypothermia, medications, voluntary control or exertion from an activity.

Respiration rate is the number of breath per minute. This rate is usually determined by counting the number of times the chest raises (inspirations) or falls (expirations) for one minute.

Respiration rate is also named as respiratory rate, pulmonary ventilation rate, ventilation rate or breathing frequency. [3]

The human respiration rate is usually measured when a person is at rest and simply involves counting the number of breaths for one minute by counting how many times the chest rises. Respiration rates may increase with fever, illness, or other medical conditions. When checking respiration, it is important to also note whether a person has any difficulty breathing.

It is ideal to measure the Respiration Rates for a full minute. Often times, respiration is observed for only 30 seconds and then the doubled count represents the rate per minute. If pressed for time, respiration can be observed for 15 seconds and then multiplying it by four to get the rate per minute.

Respiratory Sinus Arrhythmia (RSA) is heart rate variability in synchrony with respiration, by which the R-R interval is shortened during inspiration and prolonged during expiration. Short term HRV, at the respiratory frequency (High Frequency band), is mainly due to mechanical fluctuations of the stroke volume [4] [5]. During inspiration, because of the decrease in intrachest pressure and of the ventricular inter-dependence, the cardiac output (CO) and the Arterial Pressure decrease, while the HR increases [6]. HF band results are related to the vagal system activity. Several mechanisms are involved in this modulation (arterial baroreflex, cardio-pulmonary baroreflex, non reflexes mechanisms).

However, it is still possible to have a sympathetic modulation of the heart rate at the respiratory frequency in LF band, if the respiratory frequency is slow or periodic [7], as usually happens in premature newborns. Besides, the administration of β1 cardioselective blockers increases the RSA whatever it is the respiratory frequency: it means that RSA in HF band can not be considered as purely vagal, but it is equally modulated by sympathetic activity [8].

The normal respiration rate for an adult person at rest is from 15 to 20 breaths per minute. Respiration rates of more than 25 breaths per minute or under 12 breaths per minute (when at rest) may be considered abnormal. Abnormal breathing may be characterized as deep breathing, shallow breathing and rapid breathing [9].

The primary function of the respiratory system is to obtain oxygen for use by body cells. Change in your respiratory rate happens, for instance, when an examinee is working, RR is 25 breaths per minute; when you are sleeping, RR becomes lower or around 15 breaths per minute.

Newborns breathe much faster than older children and adults, having a normal breathing rate about 40 times per minute. This may slow to 20 times per minute when the baby is sleeping, when most respiratory disorders appear [10]. The pattern of breathing in a baby may also be different.

A neonate may breathe fast several times, then have a brief rest and breathe again. This is called periodic breathing, and it is designated when the breathing pause lasts over 3 seconds in duration separated by regular respirations of less than 20 seconds [11]. This phenomenon is the consequence of the baby's immature breathing control in the brain, which responds to high concentration of CO_2 in the bloodstream. The superficial rapid breathing expels the carbon dioxide from the blood, and the respiratory control center remains inactive until this gas rises again. Then, the cycle repeats.

Periodic breathing is normal occurrence and more prevalent among premature newborns, but gradually resolves during infancy [12]. It is not to be confused with apnea, treated in section A3.4.

A3.4 Apnea of prematurity

A3.4.1 Definitions of “Apnea of prematurity”

Apnea is generally defined as the cessation of breathing for more than 20 seconds or the cessation of breathing for less than 20 seconds if it is accompanied by bradycardia or oxygen desaturation [13].

Bradycardia in a premature neonate is considered significant when the heart rate decreases by least 30 beats per minute from the resting heart rate.

Oxygen desaturation or hypoxemia implies an insufficient amount of oxygen in the bloodstream. Normal oxygen saturation in the arteries is 95 to 100 percent, it is considered pathologic in a neonate when the level is equal or below 80% more than 4 seconds [14].

Even though this definition is accepted to classify severe apnea, there is no consensus about the duration of apnea that should be considered pathologic, and there is no agreement regarding the degree of change in oxygen saturation or severity of bradycardia. So, in the literature other definitions can be found.

Moreover, among respiratory electrophysiologists is commonly accepted that an episode of apnea can be considered if at least one of the two following situations are accomplished:

1. There is a cessation of breathing equivalent to at least three consecutive respiratory cycles.
2. There is a cessation of breathing lasting three times the average of a complete respiratory cycle (t_{tot}).

In the present work, these definitions will be taken in consideration to find episodes of apnea in the respiratory signal.

A3.4.2 Classification of apnea

According to apnea classification, three types can be differentiated: [15] (see Fig. A3-5)

- Central apnea: Cessation of both airflow and respiratory effort. There is no thoracic movement. It is caused by irregularities in the neuralgic signals from the respiratory center.
- Obstructive apnea: Cessation of airflow due to an obstruction in the upper airways. There is a presence of continued respiratory effort. It is caused by relaxation of soft tissue in the back of the throat that blocks the passage of air.
- Mixed apnea: Contains elements of both central and obstructive apnea.

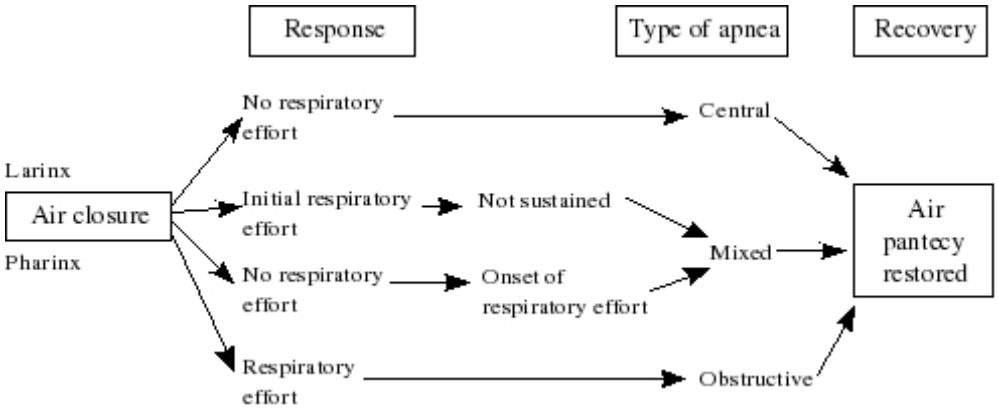

Fig. A3-5 different types of apnea [15]

A3.4.3 Incidence and problems

Apnea of prematurity (AOP) is the most important disorder of the control of breathing in the newborn period. It occurs in approximately 7 percent of infants born at 34 to 35 weeks gestation,

14 percent at 32 to 33 weeks, 50 percent at 30 to 31 week, and it is almost universal in infants born at less than 28 weeks of gestation [16] or below 1000 grams at birth [17].

AOP usually ceases by 37 weeks gestational age, but occasionally persists to several weeks past term. In general, its severity and frequency decreases with increasing maturity.

Although apnea of prematurity typically is associated with incompletely organized and interconnected respiratory neurons in the brainstem, it also may be the presenting sign of other diseases frequently affecting preterm infants.

The repetition of apnea-bradycardia episodes compromises tissue oxygenation and perfusion, risking the future infant's development.

A3.5 Relationship between apnea and bradycardia

Bradycardia episodes in newborns are frequent and normally related to apneas and/or oxygen desaturations. The bradycardia may begin within 1.5 to 2 seconds of the onset of apnea. This decrease in the heart rate (30% below the baseline) can be produced indirectly, by the under stimulation of the carotid body chemoreceptors or directly, by the effect of hypoxia (reduced content of oxygen dissolved in blood) on the heart.

It is also observed that apnea-bradycardia may appear spontaneously, attributing these phenomena to the mere condition of prematurity. Nevertheless, they can be provoked or become more severe when an infection, hypoxemia, an intraskull pathology or cerebral pathology is present [18].

Apnea-bradycardia can compromise tissue perfusion and oxygenation. A decrease in cerebral blood stream has been observed, by means of doppler fluxes in the anterior cerebral artery [19], or near infrared spectrometry (NIS) [20], concurrently with apnea-bradycardia.

Apnea-bradycardia' repetition in several days seems to be associated to a neuropsychiatric evolution's alteration valued at three years old. The inability to predict a serious apnea-bradycardia's arrival makes necessary a continuous cardiorespiratory surveillance on premature newborns with polygraphic monitoring and a high level of alert that makes possible a fast and idoneous aid (manual or kinestetic, oxygenation, mask ventilation or intubation), in every moment. The prediction of such events arrival and gravity, in short times, could be enough to apply preventative or healing measures, thus enabling to minimize deep and prolonged apnea-bradycardia' risk, to diminish the recourse to reanimation manoeuvres and intubation for assisted ventilation, equally decreasing the hospitalization time and the frequency of home monitoring needs, with the final result to improve life quality.

A3.6 Bibliography

[1] R. K. Albert, S. G. Spio, and J. R. Jett, *Comprehensive Respiratory Medicine*, St Louis, MO: Mosby Inc, 1999.

[2] F.-S. F. Yao, *Asthma-Chronic Obstructive Pulmonary Disease (COPY) in Yao and Artusio's Anesthesiology: Problem-Oriented Patient Management*, 4th ed., Chapter 1, pp.3-28, Philadelphia: Lippincott Williams & Wilkins.

[3] Wikipedia. *Respiratory rate*. Available: http://en.wikipedia.org/wiki/Respiratory_rate

[4] A. Beuchee, P. Pladys, L. Senhadji, *et al.*, "Beat-to-beat blood pressure variability and patent ductus arteriosus in ventilated, premature infants," *Pflugers Arch,* vol.446*(2)*, pp.154-160, May, 2003.

[5] A. Malliani, M. Pagani, F. Lombardi, *et al.*, "Cardiovascular neural regulation explored in the frequency domain," *Circulation,* vol.84*(2)*, pp.482-492, Aug, 1991.

[6] K. Toska and M. Eriksen, "Respiration-synchronous fluctuations in stroke volume, heart rate and arterial pressure in humans," *J Physiol,* vol.472, pp.501-512, Dec, 1993.

[7] G. G. Berntson, J. T. Bigger, Jr., D. L. Eckberg, *et al.*, "Heart rate variability: origins, methods, and interpretive caveats," *Psychophysiology,* vol.34*(6)*, pp.623-648, Nov, 1997.

[8] M. A. Cohen and J. A. Taylor, "Short-term cardiovascular oscillations in man: measuring and modelling the physiologies," *J Physiol,* vol.542*(Pt 3)*, pp.669-683, Aug 1, 2002.

[9] *Normal Adult Respiration Rate*. Available: http://www.ehow.com/about_5403651_normal-adult-respiration-rate.html

[10] S. Kotagal, "Sleep and breathing disturbances in infancy and early childhood," *Seminars in Pediatric Neurology,* vol.10*(4)*, pp.281-288, 2003.

[11] K. J. Barrington and N. N. Finer, "Periodic breathing and apnea in preterm infants," *Pediatr Res,* vol.27*(2)*, pp.118-121, Feb, 1990.

[12] M. Albani, K. H. Bentele, C. Budde, *et al.*, "Infant sleep apnea profile: preterm vs. term infants," *Eur J Pediatr,* vol.143*(4)*, pp.261-268, Mar, 1985.

[13] "Apnea, sudden infant death syndrome, and home monitoring," *Pediatrics,* vol.111*(4 Pt 1)*, pp.914-917, Apr, 2003.

[14] D. Richard, C. F. Poets, S. Neale, *et al.*, "Arterial oxygen saturation in preterm neonates without respiratory failure," *J Pediatr,* vol.123*(6)*, pp.963-968, Dec, 1993.

[15] N. R. RUGGINS, *Pathophysiology of apnoea in preterm infants*, vol.66, pp.70-73, London, ROYAUME-UNI: BMJ Publishing Group, 1991.

[16] D. J. Henderson-Smart, "The effect of gestational age on the incidence and duration of recurrent apnoea in newborn babies," *Aust Paediatr J,* vol.17*(4)*, pp.273-276, Dec, 1981.

[17] E. R. Alden, T. Mandelkorn, D. E. Woodrum, *et al.*, "Morbidity and mortality of infants weighing less than 1,000 grams in an intensive care nursery," *Pediatrics,* vol.50*(1)*, pp.40-49, Jul, 1972.

[18] R. J. Martin, J. M. Abu-Shaweesh, and T. M. Baird, "Apnoea of prematurity," *Paediatr Respir Rev,* vol.5 Suppl A, pp.S377-382, 2004.

[19] J. M. Perlman and J. J. Volpe, "Episodes of apnea and bradycardia in the preterm newborn: impact on cerebral circulation," *Pediatrics,* vol.76*(3)*, pp.333-338, Sep, 1985.

[20] O. G. JENNI, M. WOLF, M. HENGARTNER, *et al.*, *Impact of central, obstructive and mixed apnea on cerebral hemodynamics in preterm infants*, vol.70, Basel, SUISSE: Karger, 1996.

Part A Conclusion

In the first chapter of Part A, we focus on the fundamentals of preterm infants and those with sepsis. Furthermore, we indicate many aspects of sepsis, not only from early-onset of the infection, but also from late-onset.

Obviously, premature newborns with late-onset sepsis have more frequent apnea-bradycardia than those with early-onset, consequently, the former is associated with higher morbidity and mortality than the latter. Therefore, our research concentrates on late-onset sepsis.

Then, we describe the Autonomic Nervous System and its influence on the cardiovascular system which produce Heart Rate Variability. Furthermore, we discuss the behavior of cardiovascular control system. Particular attention was paid to Bradycardia, especially in newborns.

The ultimate chapter was dedicated to the respiratory system and its functional mechanism. In particular, we explain apnea of prematurity in the respiratory signal and we mention about the relationship between apnea and bradycardia.

In this part, we set all problems stated in this dissertation based on the essential bibliography.

After this brief literature review and medical knowledge, we clearly see that sepsis is enhanced by two factors ---- Bradycardia and Apnea. The former can be characterized by the RR variability while the latter can be studied through the respiration and its relationship with HRV.

This is the main object of the following chapters in Part B. Chapter B1 tries to show how HRV can be used in the diagnosis of sepsis, and how several parameters are studied and can be used in neonatal intensive care units. Chapter B2 takes the same point of view but extended to the cardiorespiratory relationships. Finally, Chapter B3 is the art of this dissertation, which studied the semi real time implementation of the parameters extracted from Chapter B1 and Chapter B2.

Part B

Automated Diagnosis of Sepsis

Chapter B1
Analysis for RR series in Premature Newborns

B1.1 Introduction

In Part A, we showed that the sepsis has a direct influence on a number of bradycardias and then disrupt the HRV. The objective of this chapter is to look for the best features which are able to distinguish sepsis and non-sepsis. For this aim, we study both linear methods and non-linear methods on HRV analysis, and then compare all of these methods in order to find the candidate ways to discriminate between infected and non-infected premature newborns.

First of all, methods for signal processing and statistical analysis are presented respectively in section B1.2 and section B1.3. Secondly, we offer experimental protocol in section B1.4. Thirdly, on the one hand, results of univariate analysis are demonstrated and discussed in section B1.5; On the other hand, those of multivariate analysis are reported in section B1.6 and section B1.7. Finally, we conclude with summary in section B1.8.

B1.2 Methods for Signal Processing

We study the RR series by means of time-domain, frequency domain methods as well as methods issued from non-linear system. We refer to these last methods as “non-linear methods” [1]. After, we compare these methods.

B1.2.1 Time Domain

These methods are measures that can be derived from the RR distribution.

The distribution of a random variable is the relative frequency of such a variable. The distribution of a series can be described by moments (mean, variance, coefficient asymmetry "skewness" and flattening "kurtosis", cf. Table B1-1), the median, and sample asymmetry.

Table B1-1 Distribution parameters based on moments

Moment	Geometry	Formula	Measure
1st moment	$\sum(RR_i)$	$\frac{1}{N}\sum_{i=1}^{N}(RR_i)$	Mean
2nd moment	$\sum(RR_i-\overline{RR})^2$	$\frac{1}{N-1}\sum_{i=1}^{N}(RR_i-\overline{RR})^2$	Variance
3rd moment	$\sum(RR_i-\overline{RR})^3$	$\frac{1}{\sigma^3}\cdot\frac{1}{N-1}\cdot\sum_{i=1}^{N}(RR_i-\overline{RR})^3$	Skewness
4th moment	$\sum(RR_i-\overline{RR})^4$	$\frac{1}{\sigma^4}\cdot\frac{1}{N-1}\cdot\sum_{i=1}^{N}(RR_i-\overline{RR})^4-3$	Kurtosis

B1.2.1.1 Arithmetic Mean (the 1st moment)

In mathematics and statistics, the arithmetic mean (or simply the mean) of a list of numbers is the sum of the entire list divided by the number of items in the list. It is defined as $\overline{RR} = \frac{1}{N}\sum_{i=1}^{N}(RR_i)$.

The mean is the most commonly-used type of average and is often referred to simply as *the* average. The term "mean" or "arithmetic mean" is preferred in mathematics and statistics to distinguish it from other averages such as the median and the mode. The mean is more sensitive than the median and it is not always representative of the signal series (especially when the distribution is not normal).

B1.2.1.2 Variance (the 2nd moment)

In probability theory and statistics, the variance (varn) of a random variable, probability distribution, or sample is one measure of statistical dispersion, averaging the squared distance of its possible values from the mean value. It is defined as the mean value of squared differences between the observed and the mean value over a period given:

$$\sigma^2 = \frac{1}{N-1}\sum_{i=1}^{N}(RR_i - \overline{RR})^2 \qquad (5.1)$$

A simple example of a time domain measure is the calculation of the standard deviation of beat-to-beat intervals. In other words the time intervals between heart beats can be statistically analyzed to obtain information about the autonomic nervous system. In probability and statistics, the standard deviation (SD) is a measure of the dispersion of a collection of numbers. It can apply to a data set as an estimation of global variability. It is defined as the square root of the variance.

$$SD = \sigma = \frac{1}{N-1}\sqrt{\sum_{i=1}^{N}(RR_i - \overline{RR})^2} \qquad (5.2)$$

The standard deviation remains the most common measure of statistical dispersion, measuring how widely spread the values in a data set are. A useful property of standard deviation is that, unlike variance, it is expressed in the same units as the data.

Other time domain measure elects Root Mean Square of Successive Differences (RMSSD), which is estimated as short term beat to beat variability.

$$RMSSD = \frac{1}{N-1}\sqrt{\sum_{i=1}^{N}(RR_i - RR_{i-1})^2} \qquad (5.3)$$

This measure potentially has the property that, provided it proved to be stationary, an equivalently longer duration and more accurate measure can be built up from short segments of heart rhythm.

B1.2.1.3 Skewness (the 3rd moment)

In probability theory and statistics, skewness (skew) is a measure of the asymmetry of the probability distribution of a real-valued random variable. It is defined as the sample third central moment divided by the cube of the standard deviation σ: $\frac{1}{\sigma^3}\cdot\frac{1}{N-1}\cdot\sum_{i=1}^{N}(RR_i-\overline{RR})^3$

It is equal to 0, if the distribution is symmetrical.

less than 0, if the distribution is asymmetric to the left (mean is smaller than median)

greater than 0 if the distribution is asymmetric to the right (mean is greater than median)

B1.2.1.4 Kurtosis (the 4th moment)

In probability theory and statistics, kurtosis (kurt) is a measure of the "peakedness" of the probability distribution of a real-valued random variable. It is independent of the measurement system unit and variance of the distribution. The kurtosis is calculated as the fourth moment around the mean divided by the square of the variance of the probability distribution minus 3: $\frac{1}{\sigma^4}\cdot\frac{1}{N-1}\cdot\sum_{i=1}^{N}(RR_i-\overline{RR})^4-3$

If the bias is corrected (-3 in the formula above) is always greater than -3 and is:

- equal to 0, if the data come from normal distributions
- positive, if the distribution is called leptokurtic pointed "pointed"
- negative, if the distribution is called platykurtic relatively "crushed"
- close to -1.2, for a rectangular distribution
- below -1.2, for a bimodal distribution.

It is difficult to interpret, if the bias is higher than 1.

B1.2.1.5 Median

In probability theory and statistics, a median (med) is described as the number separating the higher half of a sample, a population, or a probability distribution, from the lower half. The *median* of a finite list of numbers can be found by arranging all the observations from lowest value to highest value and picking the middle one. If there is an even number of observations, the median is not unique, so one often takes the mean of the two middle values.

B1.2.1.6 Sample Asymmetry

Sample Asymmetry (SpAs) is a measure of the symmetry of distributions. The method is based on weighting individual deviations of the samples from its median value. More formally, let x be a random variable with values in its sampling space $\boldsymbol{X}$ and unspecified distribution, and let $\boldsymbol{m}$ be a point within the sampling Space $\boldsymbol{X}$. For any $\boldsymbol{m}$, we define a weighting function $w(x;a)=(x-m)^a$, where $a > 0$ is a parameter describing the degree of weighting of deviations from the reference point $\boldsymbol{m}$. For example, if $a = 2$, deviations from $\boldsymbol{m}$ will receive quadratically increasing weights. We further define a left weighting function: whenever $x < \boldsymbol{m}$ and *0* otherwise, and a right weighting function: whenever $x \geq m$ and *0* otherwise. Further, given a sample $x_1, x_2, \cdots x_n$ of $\boldsymbol{n}$ observations on x, we compute the sum of the weighted deviations to the left and to the right from the reference point $\boldsymbol{m}$ as:

$$R_2=\sum_{x_i>m}(x_i-m)^2 \qquad (5.4)$$

$$R_1 = \sum_{x_i < m} (x_i - m)^2 \tag{5.5}$$

respectively, and we define Sample Asymmetry of the random variable x as the ratio R_2/R_1.

- If SpAs is greater than 1, then the distribution has a tail to the right;
- If SpAs is less than 1, the tail is to the left;
- If SpAs equals to 1, the distribution is symmetric.

B1.2.2 Frequency Domain

A common frequency domain method is the application of the discrete Fourier transform to the beat-to-beat interval time series. This provides an estimation of the amount of variation at specific frequencies. According to previous HRV frequency analysis studies, three frequency bands of interest have been defined in newborns [2].

- VLF band between 0.002 and 0.02 Hz. The origin of VLF is not well known, but it had been attributed to thermal regulation of the body's internal systems.
- LF band between 0.02 and 0.2 Hz. LF derives from both parasympathetic and sympathetic activity and has been hypothesized to reflect the delay in the baro-receptor loop [3].
- HF band between 0.2 and 1.5 Hz. HF is driven by respiration and appears to derive mainly from vagal activity or the parasympathetic nervous system [4] [5].

Here, we focus on power of VLF (p_VLF), power of LF (p_LF) and power of HF (p_HF).

B1.2.3 Non-linear Methods

We also use two kinds of non-linear methods: chaos theory and information theory, in order to analyze the degree of correlation and randomness of the time series in cardiovascular studies.

B1.2.3.1 Chaos theory

Detrended fluctuation analysis (DFA) is a modified root-mean-square analysis of a random walk in order to test the scale invariance [6]. In recent years, DFA method has become popular, and has been widely used for detections of long-range correlation in non-stationary time series at various fields [7] [8] [9]. In DFA, the scaling exponent referred to as α represents types and degree of correlation presented in the time series. Let us briefly illustrate the DFA method. The DFA includes the following six steps:

1. For a given correlated signal $B(i)$, where $i = 1, \ldots, N_{\max}$, and $N_{\max}$ is the length of the signal, we first integrate the signal $B(i)$ to obtain $y(k)$ as:

$$y(k) = \sum_{i=1}^{k} (B(i) - \bar{B}) \tag{5.6}$$

where $\bar{B}$ is the mean. In this section, RR intervals (RRI) time series was used as the signal $B(i)$.

2. The integrated signal $y(k)$ is divided into boxes (intervals) of equal length n to obtain M segments (the boxes) of length n (see Fig. B1-1). We basically look at the correlation within the box for various box size (length) n.

3. In each box of length n, we fit $\overline{y}_m(k)$ $(m = 1,\ldots,M)$ using a polynomial function of the order l, which represents the "trend" in that box (a linear fit was used; see Fig. B1-1). When a polynomial fit is of the order l, the algorithm is referred to as DFA(l). In this study, we set l = 1, i.e., we used DFA(1).

4. The integrated signal $y(k)$ is detrended by subtracting the local trend in each box of length n, and variance of fluctuation $F_m^2(n)$ is calculated for each box as:

$$F_m^2(n) = \frac{1}{n}\sum_{k=1}^{n}(y(k) - \overline{y}_m(k))^2 \tag{5.7}$$

5. For a given box size n, the average root-mean-square fluctuation $F(n)$ for this integrated and detrended signal is calculated as:

$$F(n) = \sqrt{\frac{1}{M}\sum_{m=1}^{M} F_m^2(n)} \tag{5.8}$$

6. The above computation is repeated for a broad range of box sizes n to obtain a relationship between $F(n)$ and the box size n.

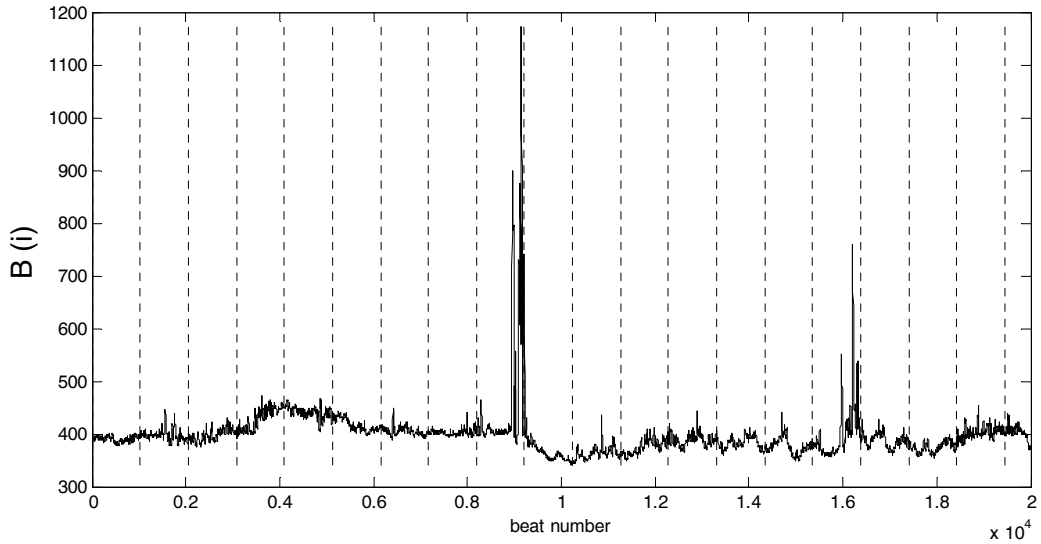

(a) An example of RR time series for 20000 beats from a preterm infant. For DFA methodology, the ith RR interval corresponds to B(i)

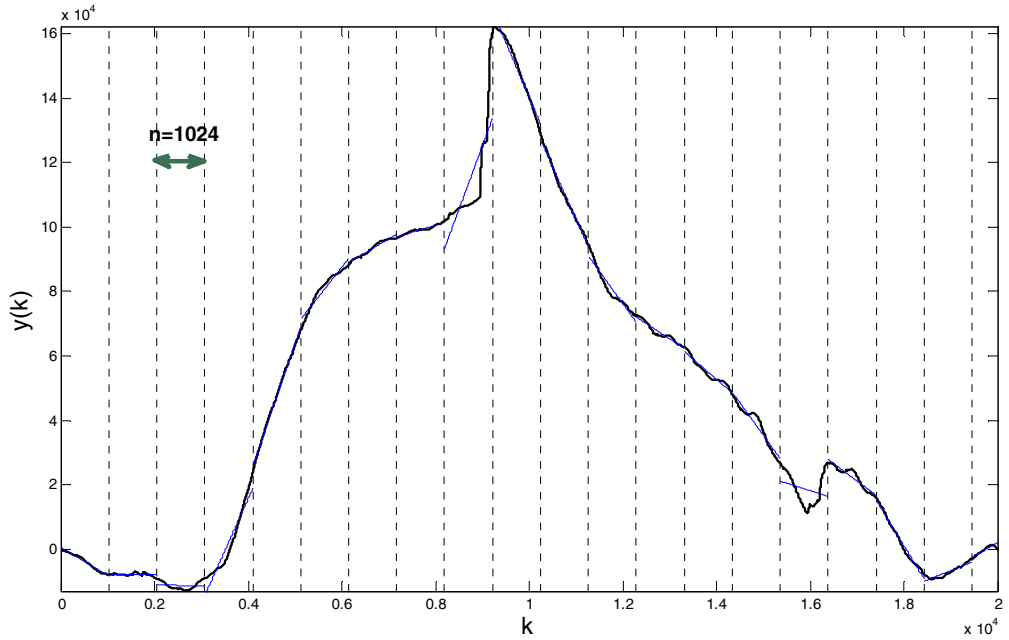

(b) The thick curve represents y(k), the integrated time series of B(i) as the function of the integration interval k (see text). The vertical dotted lines illustrate a box in a case with its size n = 1024. The thin line for each box represents "a trend" of y(k) in each box.

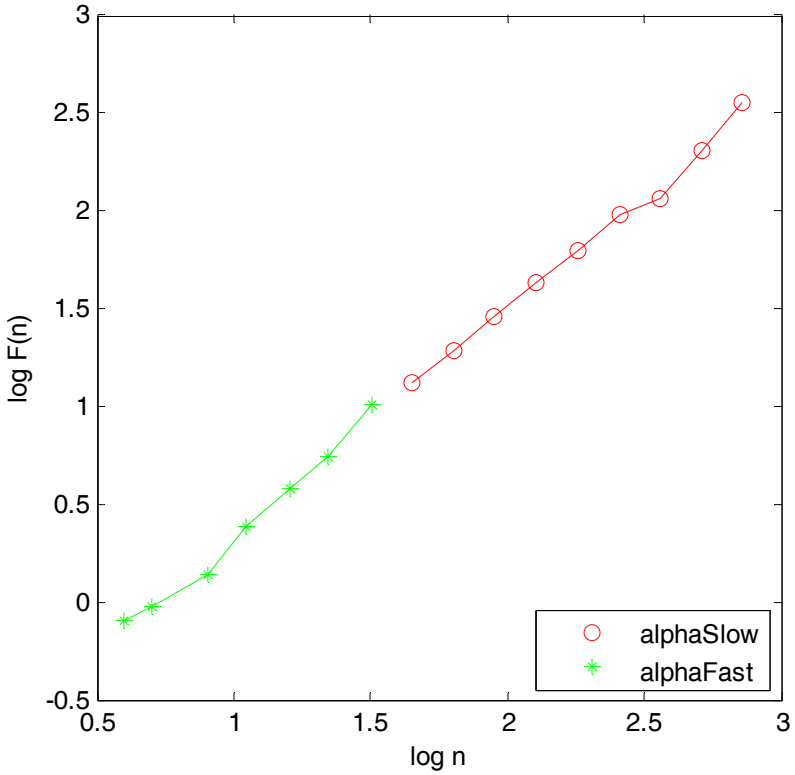

(c) Plot of log F(n) vs. log n for the detrended version of y(k) obtained from (b). The thin and thick regression lines were fitted, respectively, for the range 4–40 beats and for the range 40–1000 beats. The slope of the former was used as the index α_{fast} *representing the short-range correlation of the detrended RRI, and the latter as the index* α_{slow} *representing the long-range correlation.*

Fig. B1-1 Illustration of the behavior of the DFA Algorithm

A power-law relation between the average root mean-square fluctuation $F(n)$ and the box size n indicates the presence of scaling: $F(n) \simeq n^{\alpha}$. The fluctuations can be characterized by the scaling exponent α, a self-similarity parameter representing the long-range fractal correlation properties of the signal. The exponent α

α = 0.5 for white noise with uncorrelated randomness,

α = 1 for 1/*f* noise and long-range fractal correlations,

and α = 1.5 for Brownian motion [10] [11].

According to the preceding study, HRV for healthy adults has different scaling index α in short and long-time scales [10] [11]. In most cases, the log-log plot was not strictly linear but rather consisted of two distinct linear regions of different slopes separating at a break point near 40 beats. Therefore, in this study, we evaluated the fractal scaling exponent α_{fast} from the scale range *n* from 4 to 40 beats, and α_{slow} from 40 to 1000 beats [12]. In addition to the VLF, LF and HF obtained from the spectrum analysis as well as the mean and standard deviation of the RRI time series, the two indices α_{fast} and α_{slow} were used as the indices possibly characterizing autonomic nervous system development in the preterm infants.

B1.2.3.2 Information theory

Information theory is derived from the ideas about entropy of random variables and processes provided by Claude E Shannon. Entropy is defined in terms of a discrete random event *x*, with possible states *1*...*n* as:

$$H(x) = \sum_{i=1}^{n} p(i)\log_2\left(\frac{1}{p(i)}\right) = -\sum_{i=1}^{n} p(i)\log_2(p(i)) \qquad (5.9)$$

The concept of entropy in information theory describes how much 'uncertainty' there is in a signal or random event. An alternative way to look at this notion is to talk about how much information is carried by the signal.

So, according to the same reasoning that led to the definition of entropy, it is possible to find the same quantity for pairs of random events, which is called the joint entropy, written as $H[x, y]$.

Then, when the state of one of the two variables, let us say, *y* is known, the possible states for the *x* variable are expressed by the cross-conditional entropy, i.e. the entropy of *x* conditioned on *y*, written as $H[x/y]$.

Entropy, as it relates to dynamical systems, is the rate of information production. However, methods for estimating the entropy of a system represented by a time series are not well suited to analysis of the short and noisy data sets encountered in cardiovascular and other biological studies.

Recently, it has been observed that non-linear indexes based on information theory may be useful to discern sepsis from non-sepsis babies [13]. Thus, analysis of non-linear variables has been performed in order to assess randomness of the series. Four metrics were considered: Approximate Entropy, Sample Entropy, Permutation Entropy and Regularity.

B1.2.3.2.1 Approximate Entropy

Pincus [14] introduced Approximate Entropy (AppEn), a set of measures about system complexity closely related to entropy, which has been extensively applied to biological series analysis. It allows discriminating signals depending on their regularity without considering the model of the system. Consequently, regardless of their nature, whatever it is stochastic or purely deterministic, linear or non-linear, AppEn allows calculating indirectly signal correlation and persistence: low values of AppEn suggest high regularity and correlation.

Given a sequence S_N, consisting of N instantaneous Heart Rate measurements $HR(i)$, $i=1,\ldots,N$. We must choose values for two input parameters—m and r, to compute the $AppEn(S_N,m,r)$ of the sequence, where m refers to the pattern length, and r defines the criterion of similarity. We denote a pattern of m HR measurements, beginning at i within S_N, by the vector $x_m(i)$. Two patterns, $x_m(i)$ and $x_m(j)$, are similar if the difference between any pair of corresponding measurements in the patterns is less than r, i.e., if

$$\left|HR(i+k)-HR(j+k)\right|<r \tag{5.10}$$

In(5.10), $0 \le k < m$

Now given the set x_m of all patterns of length m $[x_m(1), x_m(2), \cdots, x_m(N-m+1)]$ within S_N, it is possible to define

$$C_{im}(r)=\frac{n_{im}(r)}{N-m+1} \tag{5.11}$$

Where $n_{im}(r)$ is the number of patterns in x_m that are similar to $x_m(i)$(given the similarity criterion r). The quantity $C_{im}(r)$ is the fraction of patterns of length m that resemble the pattern of the same length that begins at interval i. We can calculate $C_{im}(r)$ for each pattern in x_m, and we define $C_m(r)$ as the mean value of $C_{im}(r)$. The quantity $C_m(r)$ expresses the prevalence of repetitive patterns of length m in S_N.

Finally, we define the AppEn of S_N, for patterns of length m and similarity criterion r, as following:

$$AppEn(S_N,m,r)=\ln\left[\frac{C_m(r)}{C_{m+1}(r)}\right] \tag{5.12}$$

For example, the natural logarithm of the relative prevalence of repetitive patterns of length m is compared with those of length $m+1$.

Thus, if we find similar patterns in a heart rate time series, AppEn estimates the logarithmic likelihood that the next intervals after each of the patterns will differ (i.e., that the similarity of the patterns is mere coincidence and lacks predictive value). Smaller values of AppEn imply a greater likelihood that similar patterns of measurements will be followed by additional similar measurements. If the time series is highly irregular, the occurrence of similar patterns will not be predictive for the following measurements, and AppEn will be relatively large [15].

B1.2.3.2.2 Sample Entropy

Sample Entropy (SamEn) is derived from approaches developed by Grassberger and his co-workers [16] [17] [18] [19]. *SamEn(m,r,N)* is precisely the negative natural logarithm of the conditional probability that two sequences similar for *m* points remain similar at the next point, where self-matches are not included in calculating the probability. Thus a lower value of SamEn also indicates more self-similarity in the time series. In addition to eliminating self-matches, the SamEn algorithm is simpler than the AppEn algorithm, requiring approximately one-half as much time to calculate. SamEn is largely independent of record length and displays relative consistency under circumstances where AppEn does not.

We began from the work of Grassberger and Procaccia [18], who defined

$$C^m(r) = (N-m+1)^{-1} \sum_{i=1}^{N-m+1} C_i^m(r) \tag{5.13}$$

The average of the $C_i^m(r)$ is defined above. This differs from $\Phi^m(r)$ only in that $\Phi^m(r)$ is the average of the natural logarithms of the $C_i^m(r)$. They suggest approximating the Kolmogorov entropy of a process represented by a time series by

$$\lim_{r\to 0} \lim_{n\to\infty} \lim_{N\to\infty} -\ln[C^{m+1}(r)/C^m(r)] \tag{5.14}$$

Self-matches are counted and

$$C^{m+1}(r)/C^m(r) = (N-m+1) \sum_{i=1}^{N-m} A_i \Big/ (N-m) \sum_{i=1}^{N-m+1} B_i \tag{5.15}$$

Where A_i is the number of vectors $x_{m+1}(j)$ within r of $x_{m+1}(i)$, and B_i is the number of vectors $x_m(j)$ within *r* of $x_m(i)$.

In this form, however, the limits render it unsuitable for the analysis of finite time series with noise. We therefore made two alterations to adapt it to this purpose. Firstly, we followed their later practice in calculating correlation integrals [16] [17] [18] [19] and did not consider self-matches when computing $C^m(r)$. Secondly, we considered only the first *N-m* vectors of length *m*, ensuring that, for $1 \le i \le N-m$, $x_m(i)$ and $x_{m+1}(i)$ were defined.

We defined $B_i^m(r)$ as $(N-m-1)^{-1}$ times the number of vectors $x_m(j)$ within r of $x_m(i)$, where *j* ranges from *1* to *N - m*, and $j \neq i$ to exclude self-matches. We then defined

$$B^m(r) = (N-m)^{-1} \sum_{i=1}^{N-m} B_i^m(r) \tag{5.16}$$

Similarly, we defined $A_i^m(r)$ as $(N-m-1)^{-1}$ times the number of vectors $x_{m+1}(j)$ within *r* of $x_{m+1}(i)$, where *j* ranges from *1* to *N - m* ($j \neq i$), and set

$$A^m(r) = (N-m)^{-1} \sum_{i=1}^{N-m} A_i^m(r) \tag{5.17}$$

$B^m(r)$ is then the probability that two sequences will match for *m* points, whereas $A^m(r)$ is the probability that two sequences will match for *m+1* points. We then defined the parameter

$$SamEn(m,r) = \lim_{N\to\infty} \left\{ -\ln\left[A^m(r)/B^m(r) \right] \right\} \tag{5.18}$$

which is estimated by the statistics

$$SamEn(m,r,N) = -\ln\left[A^m(r)/B^m(r) \right] \tag{5.19}$$

Where there is no confusion about the parameter *r* and the length *m* of the template vector, we set

$$B = \left\{ \left[(N-m-1)(N-m) \right] / 2 \right\} B^m(r) \tag{5.20}$$

And

$$A = \left\{ \left[(N-m-1)(N-m) \right] / 2 \right\} A^m(r) \tag{5.21}$$

So that B is the total number of template matches of length m and A is the total number of forward matches of length $m+1$. We note that $A/B = \left[A^m(r) / B^m(r) \right]$, so SamEn can be expressed as

$$SamEn(m, r, N) = -\ln(A/B) \tag{5.22}$$

The quantity A/B is precisely the conditional probability that two sequences within a tolerance r for m points remain within r of each other at the next point.

B1.2.3.2.3 Permutation Entropy

Permutation Entropy (PermEn) was introduced by Bandt, Keller and Pompe [20] as a convenient means of mapping a continuous time series onto a symbolic sequence. To illustrate the idea, let us first embed a scalar time series $\{x(i), i = 1, 2, \cdots\}$ to a m-dimensional space [21]:

$$X_i = [x(i), x(i+L), \cdots, x(i+(m-1)L)] \tag{5.23}$$

where m is called the embedding dimension and L the delay time. For a given, but otherwise arbitrary i, the m number of real values X_i can be sorted in an increasing order: $[x(i+(j_1-1)L) \le x(i+(j_2-1)L) \le \cdots \le x(i+(j_m-1)L)]$

When an equality occurs, e.g.

$$x(i+(j_{i1}-1)L) = x(i+(j_{i2}-1)L) \tag{5.24}$$

we order the quantities x according to the values of their corresponding j's, namely if $j_{i1} < j_{i2}$, we write

$$x(i+(j_{i1}-1)L) \le x(i+(j_{i2}-1)L) \tag{5.25}$$

This way, the vector X_i is mapped onto $(j_1, j_2, \ldots, j_m)$, which is one of the $m!$ permutations of m distinct symbols $(1, 2, \ldots, m)$. It is clear that each point in the m-dimensional embedding space, indexed by i, can be mapped to one of the $m!$ permutations. When each such permutation is considered as a symbol, then the reconstructed trajectory in the m-dimensional space is represented by a symbol sequence. The number of distinct symbols can be at most $m!$. Let the probability distribution for the distinct symbols be $P_1, P_2, \ldots, P_K$, where $K \le m!$. Then the PermEn for the time series $\{x(i), i = 1, 2, \cdots\}$ is defined [20] as the Shannon entropy for the K distinct symbols

$$H_p(m) = -\sum_{j=1}^{K} P_j \ln P_j \tag{5.26}$$

When $P_j = 1/m!$, then $H_p(m)$ attains the maximum value ln(m!). For convenience, we always normalize $H_p(m)$ by ln(m!), and denote

$$0 \le \bar{H}_p = H_p(m) / \ln(m!) \le 1 \tag{5.27}$$

Thus H_p gives a measure of the departure of the time series under study from a complete random one: the smaller the value of H_p, the more regular the time series is.

B1.2.3.2.4 Regularity

Regularity (Regul) can be defined as the degree of recurrence of a pattern in a signal. The evaluation of the regularity for a process *x* is based on the calculation of the conditional entropy (*CE*) over a normalized realization of *x* [22]. The CE_x function measures the amount of information carried by the most recent sample of *x* when its past *L-1* samples are known: the more informative are the past samples to predict the future behavior, the smaller is CE_x. CE_x is a function of the number (*L*) of past samples used in the prediction and it is defined as:

$$CE_x(L) = -\sum_{L} p_L \log p_L + \sum_{L-1} p_{L-1} \log p_{L-1} \tag{5.28}$$

where p_L is probability of the patterns of length *L* which may be extracted from *x*.

Unfortunately, when *L* increases, (5.28) produces unreliable estimation of CE_x. To avoid this problem, it has been proposed [22] to add a corrective term, thus defining a new function (the corrected conditional entropy, CCE_x):

$$CCE_x(L) = CE_x(L) + perc(L) \bullet E(x) \tag{5.29}$$

Where *perc*(*L*) is the percentage of single points in the *L*-dimensional phase space and $E(x)$ is the Shannon Entropy of the process. When the CE_x estimate becomes unreliable, the corrective term forces the CE_x to increase and to tend to the *CE* pattern of a white noise with the same probability distribution of *x*. The minimum value of the CCE_x is taken as an index of complexity [22]: the larger the index, the more unpredictable and complex the series. To derive an index of complexity which is independent of the different probability distribution of the processes, the CCE_x is normalized by the Shannon entropy of the process [23], thus obtaining the normalized corrected conditional entropy ($NCCE_x$). Independently of the distribution of the process, the $NCCE_x$ ranges from 0 to 1. Therefore, the minimum of the $NCCE_x$ appears more useful than that of the CCE_x when processes with different probability distribution are analyzed. In this case, the regularity index of the process *x* is defined as

$$\mathrm{Re}\,gul = 1 - \min(NCCE_x(L)) \tag{5.30}$$

From(5.30), it is obvious that regularity ranges from 0 to 1. In detail, regularity tends to 0, if the series is a fully unpredictable process. On the contrary, it tends to 1, if the series is a really periodic signal. Besides, regularity assumes intermediate values for those processes that can be partially predicted by the knowledge of the past samples. Applications of the regularity index to cardiovascular variability series can be found in [23].

B1.3 Methods for Statistical Analysis

The previous paragraph has underlined the features that we could use. This section demonstrates the interest of each feature for a diagnosis purpose. It also tries to enhance the best parameter through Univariate Analysis or the best set of parameters through Multivariate Analysis. These two approaches are described in this section.

B1.3.1 Univariate Analysis

In univariate analysis, p value is calculated to test whether these parameters can discriminate between the two groups—Sepsis vs. Non-Sepsis.

The following three hypothesis tests are chosen to calculate the p value for each method in order to look for the best window size

- Analysis of Variance
- Kruskal-Wallis test
- Wilcoxon rank-sum test

In statistics, analysis of variance (ANOVA) is a collection of statistical models, and their associated procedures, in which the observed variance in a particular variable is partitioned into components attributable to different sources of variation. In its simplest form ANOVA provides a statistical test of whether or not the means of several groups are all equal, and therefore generalizes *t*-test to more than two groups. ANOVAs are helpful because they possess an advantage over a two-sample t-test. Doing multiple two-sample t-tests would result in an increased chance of committing a type I error. Other details are in Appendix I. [24]

The statistical analysis was carried out using Kruskal-Wallis test in order to evaluate p-value for each method. The level of significance was set to $p < 0.05$. The Kruskal-Wallis test (KruskWall) is a nonparametric version of one-way Analysis of Variance. The low p-value means the Kruskal-Wallis test results agree with the one-way ANOVA results. The Kruskal-Wallis test evaluates the **null hypothesis H0** (all samples come from populations that have the same median) against the **alternative hypothesis H1** (the medians are not all the same).

The Kruskal-Wallis test makes the following assumptions about the test data:

- All samples come from populations having the same continuous distribution, apart from possibly different locations due to group effects.
- All observations are mutually independent.

The Kruskal-Wallis test is based on an analysis of variance using the ranks of the data values, not the data values themselves. It is preferable to perform a test to determine which pairs are significantly different, and which are not.

The nonparametric Wilcoxon rank-sum test (Wilrs) is generally used to quantify the test of equal medians. It tests if two independent samples come from identical continuous (not necessarily normal) distributions with equal medians, against the alternative that they do not have equal medians.

B1.3.2 Multivariate Analysis

The purpose of multivariate analysis is to select candidate parameters and estimate the relationship between these parameters. Here, we consider two methods:

- Logistic Regression
- Stepwise Regression

B1.3.2.1 Logistic Regression

In statistics, logistic regression (sometimes called the logistic model or logit model) is used for prediction of the probability of occurrence of an event by fitting data to a logit function logistic curve. It is a Generalized Linear Model (GLM) used for binomial regression. Like many forms of regression analysis, it makes use of several predictor variables that may be either numerical or categorical. For example, the probability that a person has a heart attack within a specified time period might be predicted from knowledge of the person's age, sex and body mass index. Logistic regression is used extensively in the biological sciences and medical fields. [25]

An explanation of logistic regression begins with an explanation of the logistic function, which, like probabilities, always takes on values between zero and one:

$$f(z) = \frac{e^z}{e^z + 1} = \frac{1}{1 + e^{-z}} \tag{5.31}$$

A graph of the function is shown in Fig. B1-2. The input is z and the output is $f(z)$. The logistic function is useful because it can take as an input any value from negative infinity to positive infinity, whereas the output is confined to values between 0 and 1. The variable z represents the exposure to some set of independent variables, while $f(z)$ represents the probability of a particular outcome, given that set of explanatory variables. The variable z is a measure of the total contribution of all the independent variables used in the model and is known as the logit.

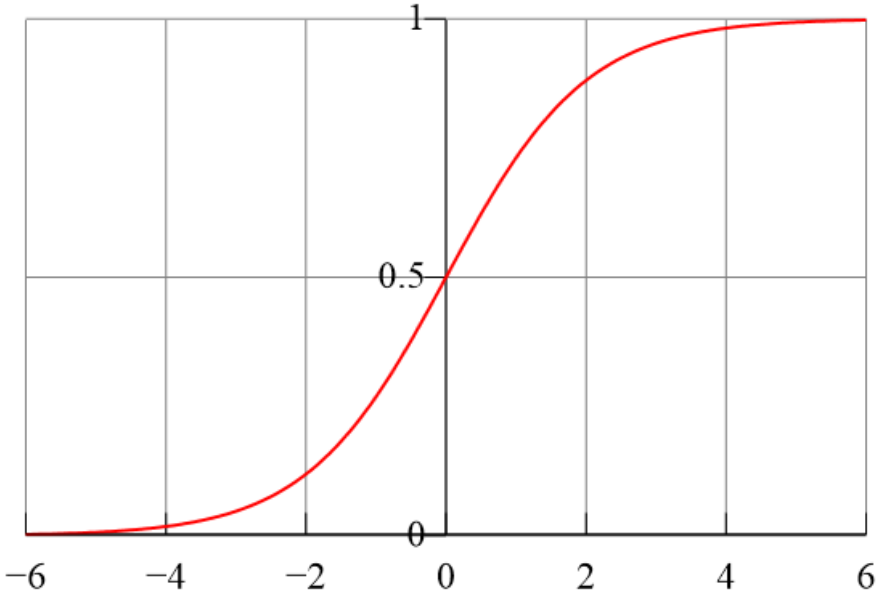

Fig. B1-2 The logistic function, with z on the horizontal axis and f(z) on the vertical axis

The variable z is usually defined as

$$z = \beta_0 + \beta_1 x_1 + \beta_2 x_2 + \beta_3 x_3 + \cdots + \beta_k x_k \tag{5.32}$$

Where β_0 is called the "intercept" and β_1, β_2, β_3, and so on, are called the "regression coefficients" of x_1, x_2, x_3 respectively. The intercept is the value of z when the values of all independent

variables are zeros (e.g. the value of z in someone with no risk factors). Each of the regression coefficients describes the size of the contribution of risk factor. A positive regression coefficient means that the explanatory variable increases the probability of outcome, while a negative regression coefficient means that the variable decreases the probability of outcome; a large regression coefficient means that the risk factor strongly influences the probability of outcome, while a near-zero regression coefficient means that the risk factor has little influence on the probability of outcome.

Logistic regression is a useful way of describing the relationship between one or more independent variables (e.g., age, sex, etc.) and a binary response variable, expressed as a probability, that has only two values, such as having sepsis ("has sepsis" or "doesn't have sepsis").

B1.3.2.2 Stepwise Regression

In statistics, stepwise regression includes regression models in which the choice of predictive variables is carried out by an automatic procedure. [26] [27] [28] Usually, this takes the form of a sequence of F-tests.

The main approaches are:

- Forward selection, which involves starting with no variables in the model, trying out the variables one by one and including them if they are 'statistically significant'.
- Backward elimination, which involves starting with all candidate variables and testing them one by one for statistical significance, deleting any that are not significant.
- Methods that are a combination of the above, testing at each stage for variables to be included or excluded.

A widely used algorithm was first proposed by Efroymson [29]. This is an automatic procedure for statistical model selection in cases where there are a large number of potential explanatory variables, and no underlying theory on which to base the model selection. The procedure is used primarily in regression analysis, though the basic approach is applicable in many forms of model selection. This is a variation on forward selection. At each stage in the process, after a new variable is added, a test is made to check if some variables can be deleted without appreciably increasing the residual sum of squares (RSS). The procedure terminates when the measure is locally maximized, or when the available improvement falls below some critical value.

B1.4 Experimentation

All recordings were performed in the NICU and data were recorded in standard conditions. The monitoring (Powerlab system®, AD Instruments) included one-hour recording of two electrocardiogram (ECG), electrooculogram (EOG), electroencephalogram (EEG) leads, one pulse oximetry saturation (SaO2), nasal respiration trace.

Data were obtained from two groups of premature newborns (13 sepsis vs. 13 non-sepsis) hospitalized from the NICU in the Center of Hospital affiliated to University of Rennes 1 (CHU-Rennes) between 2004 and 2007. This research was approved by the local ethics committee in France (03/05-445). Furthermore, the parents of these babies were informed and gave common consents.

Continuous electrocardiogram signals were sampled at 400Hz, which was also carried on for the other biological signals. There were no significant differences in gender, gestational age, chronological age (>72 hours), post-menstrual age (<33 weeks), weight and haematocrit between sepsis and non-sepsis groups.

Here are experimental criteria:

- ☞ Inclusion criteria: more than one bradycardia per hour and/or need for bag-and-mask resuscitation and/or the intention of the attending physician to investigate for a suspected infection.

- ☜ Exclusion criteria: ongoing inflammatory response with or without confirmed infection, medication known to influence autonomic nervous system (ANS) including morphine, catecholamine, sedative drugs, intra-tracheal respiratory support, intra-cerebral lesion or malformation.

Data analysis was conducted on home-made signal processing tools designed with the software MATLAB® R2010b (The Mathworks, Inc.) in the system of Windows® 7.

Consecutive sequences of successive RR series with bradycardia were extracted from ECG recordings, and then resampled at 4 Hz[5] (Fig. B1-3 a) and cleaned by Kaplan filter (Fig. B1-3 b). After, they are employed into time domain, frequency domain, chaos theory and information theory.

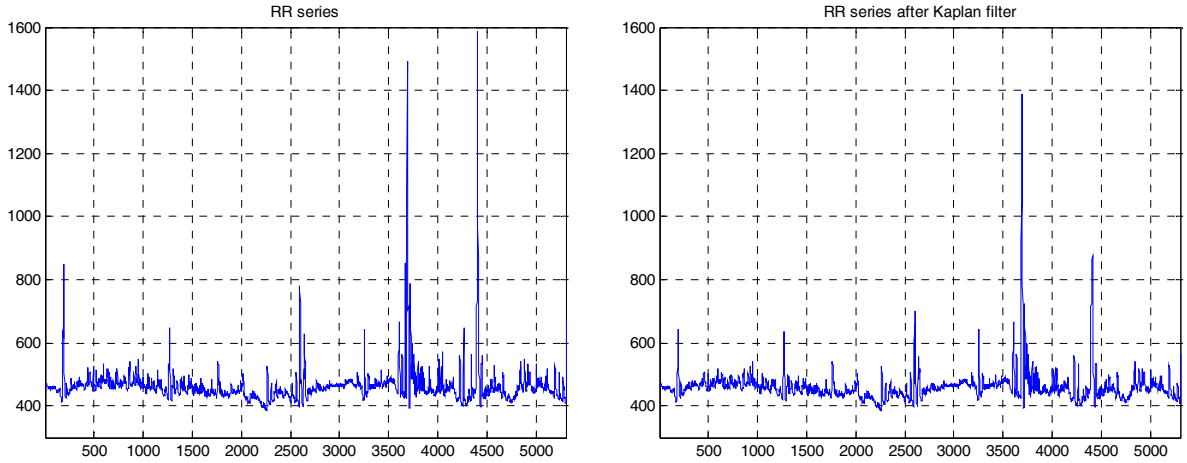

a) RR series extracted from ECG and resampled

b) RR series after Kaplan filter

Fig. B1-3 RR series

The indexes were calculated in analysis windows (Fig. B1-4). Finally, we compared all methods in terms of classification of Sepsis (S) versus Non-Sepsis (NS).

For each baby, analysis windows are used on RR series. The size of analysis window is chosen as 1024/2048/4096, steps have the same length as windows, showed in Fig. B1-4.

[5] RR series was resampled at 4 Hz in this dissertation: the unusual resampling is necessary in premature newborns which exhibits higher heart rate (120-130 bpm) than adults.

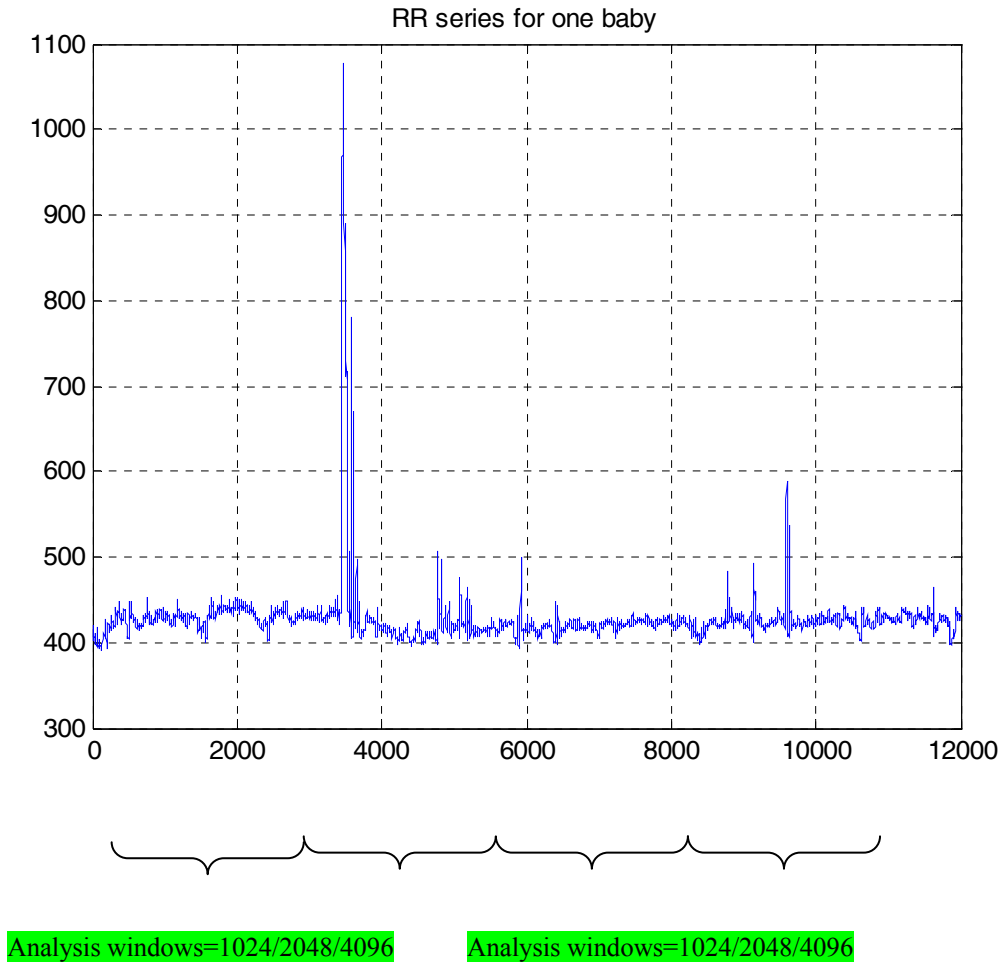

Fig. B1-4 Analysis windows

Therefore, all observations are mutually independent, which makes it accurate to look for the most discriminating parameters in these windows.

B1.5 Results and Discussion for Univariate Analysis —— p value

For this part of results, we consider four aspects:
1. with/without outliers, in order to verify the stability of the results taking into account some outliers. An outlier is defined as the most extreme data point outside boxplot.
2. Analysis windows equal to 1024/2048/4096, in order to identify the best window size for the diagnosis
3. Parameter by parameter, to extract the best features for sepsis discrimination
4. with/without baby effect, we used mixed effect ANOVA in which the baby is a random effect such as the fact that the same baby is used several times is taken into account.

Then we will present our results according to these four points

We carry out the same analysis for three sizes of window with/without outliers in detail. All these results are reported in the Appendix II, and the synthesis of all the results are reported in the following table.

Table B1-2 Univariate Analysis

	With Outliers			Without Outliers		
	1024	2048	4096	1024	2048	4096
moy						
varn						×
skew	×			×	×	
kurt	×			×		
med						
SpAs	×		×	×	×	×
SD						
RMSSD						
p_HF						
p_LF		×			×	
p_VLF						
alphaS	×	×	×	×	×	×
alphaF	×	×	×	×	×	×
AppEn		×	×		×	×
SamEn	×	×	×	×	×	×
PermEn	×	×	×			×
Regul						×

For each case in column, these parameters whose p value less than 0.2 are marked as "×". We use these p values in order to keep a maximum number of significant parameters for the multivariate analysis

From Table B1-2, certain HRV characteristics such as SD, RMSSD, p_HF, p_LF, p_VLF, were unable to find a correlation between these parameters and sepsis. However, three indexes from non-linear methods

- alphaS
- alphaF
- SamEn

are candidate parameters (highlighted in red horizontally) to recognize sepsis from non-sepsis whatever the size of the window analysis. Their p values are shown in following table:

Table B1-3 p values of candidate parameters of Mono-Channel

	With Outliers			Without Outliers		
	1024	2048	4096	1024	2048	4096
alphaS	0.0012	0.0045	0.0003	0.0047	0.01	0.0011

	With Outliers			Without Outliers		
	1024	2048	4096	1024	2048	4096
alphaF	0.0307	0.1154	0.0252	0.0128	0.04	0.0440
SamEn	0.0840	0.0507	0.0410	0.1931	0.03	0.0006

For further details, we also boxplot alphaS, alphaF and SamEn (Fig. B1-5) as following:

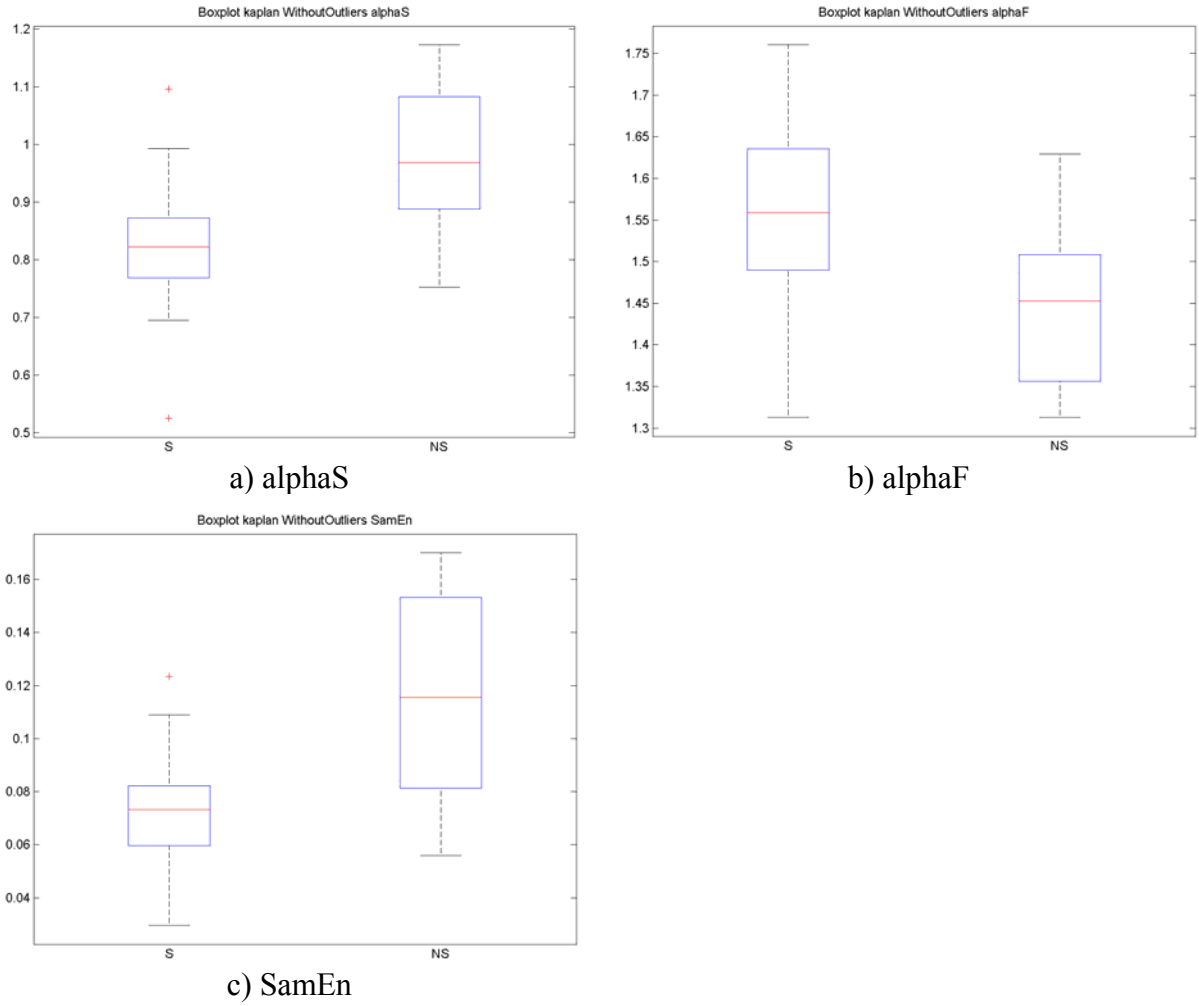

a) alphaS b) alphaF

c) SamEn

Fig. B1-5 Boxplot of optimal parameters

As for the methods of information theory, HRV analysis shows that the mean values of AppEn (Fig. B1-6 a), SamEn (Fig. B1-5 c) and PermEn (Fig. B1-6 b) are lower in sepsis infants than in non-sepsis ones, while, the mean values of Regul index (Fig. B1-6 c) give lower values for non-sepsis than for sepsis. These performances above express a decrease in information content in the newborns suffering from infection, because an increase in regularity coincides with a decrease in entropy from sepsis. Univariate analysis confirmed the previous studies based on entropy analysis, giving higher regularity values in sepsis cases. Results also confirmed the relationship between the occurrence of disease and a reduction of information carried by cardiovascular signals.

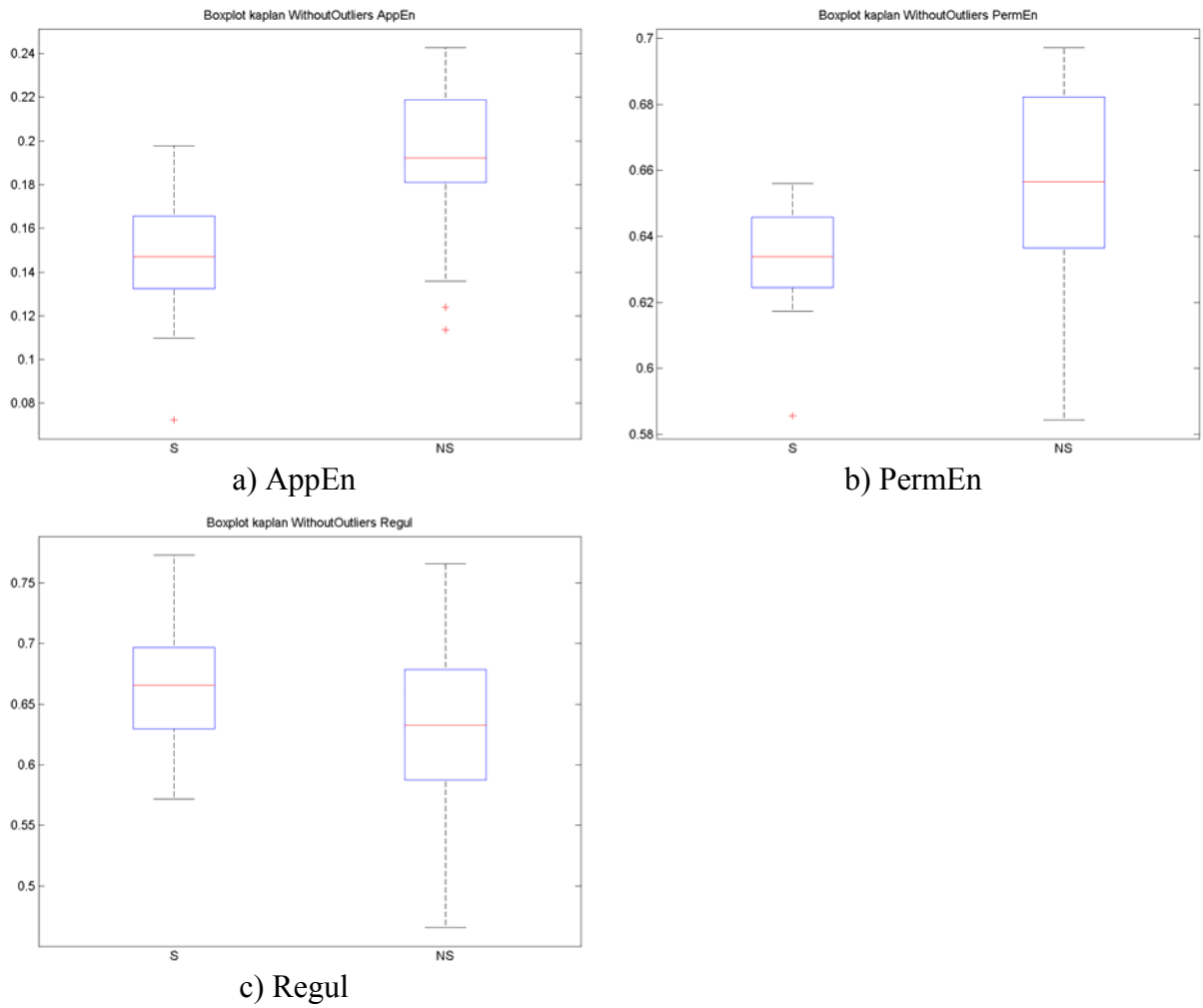

a) AppEn

b) PermEn

c) Regul

Fig. B1-6 Boxplot of parameters from information theory

B1.6 Results and Discussion for Multivariate Analysis —— Logistic Regression

Logistic regression is a useful way of describing the relationship between one or more independent variables (e.g., varn, skew, etc.). In this study, we should focus on the variables that have p-values <0.2.

Each of the regression coefficients describes the size of the contribution of that risk factor. A positive regression coefficient means that the explanatory variable increases the probability of sepsis, while a negative regression coefficient means that the variable decreases the probability of sepsis.

A large regression coefficient means that the risk factor strongly influences the probability of sepsis, while a near-zero regression coefficient means that the risk factor has little influence on the probability of sepsis.

Table B1-4 shows the result of logistic regression, with outliers and with an analysis window=1024.

Table B1-4 Logistic Regression, with outliers, window 1024

Analysis of Maximum Likelihood Estimates					
Parameter	**DF**	**Coefficient**	**Standard Error**	**Wald Chi-Square**	**Pr > ChiSq**
Intercept	1	11.6551	8.0490	2.0967	0.1476
skew	1	-0.1631	0.4663	0.1223	0.7265
kurt	1	-0.00714	0.0453	0.0248	0.8748
SpAs	1	0.0500	0.0576	0.7534	0.3854
alphaS	1	-5.7189	2.2126	6.6811	0.0097
alphaF	1	0.1465	2.8801	0.0026	0.9594
SamEn	1	-9.9756	7.5724	1.7355	0.1877
PermEn	1	-8.5441	9.3547	0.8342	0.3611

- The first column represents the Intercept and the significant parameters chosen from Table II-1 of univariate analysis in Appendix II.
- The second column denotes the degree of freedom (DF) with each parameter.
- The third column denotes the estimated coefficients of the parameter, which are $\beta_1, \beta_2, \beta_3, \ldots, \beta_k$ in Equation (5.32)
- The fourth column denotes the standard error of the coefficient.
- The fifth column denotes the Wald Chi-Square statistic, computed as the square of the value obtained by dividing the parameter estimate by its standard error.
- The sixth column denotes the p-value (Pr > ChiSq) for the Wald Chi-square statistic with 1 DF, with a value below 0.2 indicating a significant effect of the associated model parameter if a 20 percent significance level is chosen.

From Table B1-4, it is observed that the p-values (Pr>ChiSq) of alphaS and SamEn are less than 0.2 (marked in green), that is to say, both of them are significant variables. Since the coefficient for alphaS and SamEn are negative, as alphaS or SamEn increases, the probability of sepsis decreases.

We carry out the same analysis for three sizes of window with/without outliers in detail. All these results are reported in Appendix III, and the synthesis of all the results are reported in the following table.

Table B1-5 Significant Regression Coefficients of Logistic Regression

	With Outliers			Without Outliers		
	1024	2048	4096	1024	2048	4096
moy						
varn						
skew				-3.7032	-2.3937	

	With Outliers			Without Outliers		
	1024	2048	4096	1024	2048	4096
kurt				0.5575		
med						
SpAs				1.8309	0.6450	
SD						
RMSSD						
p_HF						
p_LF						
p_VLF						
alphaS	-5.7189	-6.7654	-12.1747	-7.4428	-18.7639	-11.2460
alphaF				9.6729	16.9458	
AppEn			-16.9164			
SamEn	-9.9756			-37.0885		
PermEn		-23.1268				
Regul						

Table B1-5 lists Significant Regression Coefficients of Logistic Regression selected from Appendix III (marked in green). From this table, we can see:

Firstly, it is obvious that alphaS is most frequently chosen as the significant variable with a negative regression coefficient, which decreases the probability of sepsis. Furthermore, the largest regression coefficient in absolute value means that alphaS strongly influence the probability of sepsis.

Secondly, alphaF and SamEn are selected for two times. Positive regression coefficients mean that alphaF increases the probability of sepsis, while negative regression coefficients mean that SamEn decrease the probability of sepsis.

Thirdly, skew and SpAs are also picked for two times, but their absolute values of regression coefficients are less than 4, so that we do not need to consider their impact.

B1.7 Results and Discussion for Multivariate Analysis —— Stepwise Regression

We carry out the same analysis for three sizes of window with/without outliers in detail, and use all the significant parameters on the whole population. Table B1-6 shows the result of stepwise regression, with outliers and with an analysis window=1024.

Table B1-6 Stepwise Regression, with outliers, window 1024

Summary of Stepwise Selection								
	Effect			Number	Score	Wald		Variable
Step	Entered	Removed	DF	In	Chi-Square	Chi-Square	Pr > ChiSq	Label
1	alphaS		1	1	11.0066		0.0009	alphaS
2	SamEn		1	2	6.6081		0.0102	SamEn

Analysis of Maximum Likelihood Estimates					
Parameter	DF	Estimate	Standard Error	Wald Chi-Square	Pr > ChiSq
Intercept	1	6.1324	1.7289	12.5808	0.0004
alphaS	1	-5.3019	1.5784	11.2835	0.0008
SamEn	1	-11.6893	4.8646	5.7740	0.0163

For the upper table:

- The first column denotes the number of step.
- The second column represents the variables added to the model.
- The third column represents the variables removed from the model.
- The fourth column denotes the degree of freedom (DF) with each parameter.
- The fifth column count on the number of the added variables.
- The sixth column denotes the Score Chi-Square statistic.
- The seventh column denotes the Wald Chi-Square statistic.
- The eighth column denotes the p-value (Pr > ChiSq) for the Score/Wald Chi-square statistic with 1 DF.
- The ninth column denotes Variable Label.

For the down table

- The first column represents the Intercept and the significant parameters chosen from Stepwise Selection in the upper table.
- The second column denotes the DF with each parameter.
- The third column denotes the estimated coefficients of the parameter.
- The fourth column denotes the standard error of the coefficient.
- The fifth column denotes the Wald Chi-Square statistic, computed as the square of the value obtained by dividing the parameter estimate by its standard error.
- The sixth column denotes the p-value (Pr > ChiSq) for the Wald Chi-square statistic with 1 DF.

Stepwise regression is a modification of the forward selection technique in that variables already in the model do not necessarily stay there. As in the forward selection technique, variables are added one at a time to the model, as long as the F statistic p-value is below 0.05. After a variable is added, however, the stepwise technique evaluates all of the variables already included in the

model and removes any variable that has an insignificant F statistic p-value exceeding 0.05. Only after this check is made and the identified variables have been removed can another variable be added to the model. The stepwise process ends when none of the variables excluded from the model has an F statistic significant at 0.05 and every variable included in the model is significant at 0.05. For the case of Table B1-6, among all the parameters, 'alphaS' and 'SamEn' are chosen as significant predictive variables by using stepwise regression. The other results are also reported in Appendix IV.

The synthesis of all the results is reported in the following table.

Table B1-7 Stepwise Regression

	With Outliers			Without Outliers		
	1024	2048	4096	1024	2048	4096
moy						
varn						
skew						
kurt				×		
med						
SpAs						
SD						
RMSSD						
p_HF						
p_LF						
p_VLF				×		
alphaS	×	×	×	×	×	×
alphaF						
AppEn						×
SamEn	×		×			
PermEn		×				
Regul						

For each case in column, these parameters selected from Stepwise Regression are marked as "×". From Table B1-7, firstly, it is obvious that 'alphaS' is the most frequently chosen as a significant predictor, that is to say, alphaS is added to the multi-linear model based on its statistical significance in a regression and always stay in the model for all cases. Secondly, 'SamEn' is selected for two times, so it can be considered as the second frequent choice. Thirdly, other methods are chosen only for one time, or even some of them are not chosen, so that we can ignore them.

B1.8 Conclusion

The clinical manifestations of neonatal sepsis, whatever the source of infection, are frequently nonspecific. In this chapter, the aim of the work was to find quantitative mathematical criteria for the diagnosis of late-onset sepsis happened in premature infants by a non-invasive way.

The aim was achieved by means of RR signal analysis. HRV characteristics such as quantitative estimates in Time Domain and in Frequency Domain, we were unable to find a correlation between these parameters and sepsis. However, chaos indexes (alphaS, alphaF) and four metrics from Information Theory were considered (AppEn, SamEn, PermEn and Regul).

Referring to the methods of Chaos Theory, the index alphaF obtained by DFA and characterizing short-range (4–40 beats) correlation in the detrended RRI time series hardly changed with age and was almost constant at about 1.5 in the mean. The alphaF value greater than unity in the preterm infants indicated that the RRI fluctuation at short range was near to Brownian motion (uncorrelated). On the other hand, the index alphaS characterizing the long-range (40–1000 beats) correlation increased, and showed the high correlation coefficient value and most statistically significant between groups sepsis and non-sepsis, suggesting that alphaS could be a good and robust index characterizing the ANS development.

With regard to the Information Theory, results confirmed the relationship between the occurrence of disease and a reduction of information carried by cardiovascular signals. AppEn, SamEn and PermEn showed that a decrease of entropy is associated with sepsis condition, and coherently, the Regul index measured a higher value for the same group of patients.

Furthermore, all methods are screened through Statistical Analysis, not only Univariate Analysis, but also Multivariate Analysis (Logistic Regression, Stepwise Regression). Finally, three indexes from non-linear methods

- → alphaS
- → alphaF
- → SamEn

are selected as candidate parameters to discriminate between the two groups—Sepsis vs. Non-Sepsis, because these three are frequently significant whatever the size of the window analysis.

In conclusion, the distinctive variation in heart rate behavior related with sepsis could be useful in the field of neonatology.

B1.9 Bibliography

[1] "Heart rate variability: standards of measurement, physiological interpretation and clinical use. Task Force of the European Society of Cardiology and the North American Society of Pacing and Electrophysiology," *Circulation,* vol.93*(5)*, pp.1043-1065, Mar 1, 1996.

[2] U. Chatow, S. Davidson, B. L. Reichman*, et al.*, "Development and maturation of the autonomic nervous system in premature and full-term infants using spectral analysis of heart rate fluctuations," *Pediatr Res,* vol.37*(3)*, pp.294-302, Mar, 1995.

[3] M. A. Cohen and J. A. Taylor, "Short-term cardiovascular oscillations in man: measuring and modelling the physiologies," *J Physiol,* vol.542*(Pt 3)*, pp.669-683, Aug 1, 2002.

[4] T. Aarimaa, R. Oja, K. Antila*, et al.*, "Interaction of heart rate and respiration in newborn babies," *Pediatr Res,* vol.24*(6)*, pp.745-750, Dec, 1988.

[5] S. Akselrod, D. Gordon, F. Ubel*, et al.*, "Power spectrum analysis of heart rate fluctuation: a quantitative probe of beat-to-beat cardiovascular control," *Science,* vol.213*(4504)*, pp.220-222, July 10, 1981.

[6] C. K. Peng, S. V. Buldyrev, S. Havlin, *et al.*, "Mosaic organization of DNA nucleotides," *Phys Rev E Stat Phys Plasmas Fluids Relat Interdiscip Topics,* vol.49*(2)*, pp.1685-1689, Feb, 1994.

[7] S. M. Ossadnik, S. V. Buldyrev, A. L. Goldberger, *et al.*, "Correlation approach to identify coding regions in DNA sequences," *Biophysical Journal,* vol.67*(1)*, pp.64-70, 1994.

[8] J. M. Hausdorff, C. K. Peng, Z. Ladin, *et al.*, "Is walking a random walk? Evidence for long-range correlations in stride interval of human gait," *J Appl Physiol,* vol.78*(1)*, pp.349-358, Jan, 1995.

[9] J. M. Hausdorff, P. L. Purdon, C. K. Peng, *et al.*, "Fractal dynamics of human gait: stability of long-range correlations in stride interval fluctuations," *J Appl Physiol,* vol.80*(5)*, pp.1448-1457, May, 1996.

[10] C. K. Peng, S. Havlin, H. E. Stanley, *et al.*, "Quantification of scaling exponents and crossover phenomena in nonstationary heartbeat time series," *Chaos,* vol.5*(1)*, pp.82-87, 1995.

[11] M.-K. YUM, E.-Y. PARK, C.-R. KIM, *et al.*, "Alterations in irregular and fractal heart rate behavior in growth restricted fetuses," *European Journal of Obstetrics & Gynecology and Reproductive Biology,* vol.94*(1)*, pp.51-58, 2001.

[12] T. Nakamura, H. Horio, S. Miyashita, *et al.*, "Identification of development and autonomic nerve activity from heart rate variability in preterm infants," *Biosystems,* vol.79*(1-3)*, pp.117-124, 2005.

[13] D. E. Lake, J. S. Richman, M. P. Griffin, *et al.*, "Sample entropy analysis of neonatal heart rate variability," *American Journal of Physiology - Regulatory, Integrative and Comparative Physiology,* vol.283*(3)*, pp.789-797, September 1, 2002.

[14] S. M. Pincus, "Approximate entropy as a measure of system complexity," *Proc Natl Acad Sci U S A,* vol.88*(6)*, pp.2297-2301, Mar 15, 1991.

[15] K. K. Ho, G. B. Moody, C. K. Peng, *et al.*, "Predicting survival in heart failure case and control subjects by use of fully automated methods for deriving nonlinear and conventional indices of heart rate dynamics," *Circulation,* vol.96*(3)*, pp.842-848, Aug 5, 1997.

[16] A. Ben-Mizrachi, I. Procaccia, and P. Grassberger, "Characterization of experimental (noisy) strange attractors," *Physical Review A,* vol.29*(2)*, p.975, 1984.

[17] P. Grassberger, "Finite sample corrections to entropy and dimension estimates," *Physics Letters A,* vol.128*(6-7)*, pp.369-373, 1988.

[18] P. GRASSBERGER and I. PROCACCIA, *Estimation of the Kolmogorov entropy from a chaotic signal*, vol.28, pp.2591-2593, New York, NY, ETATS-UNIS: American Institute of Physics, 1983.

[19] P. Grassberger, T. Schreiber, and C. Schaffrath, "Nonlinear time sequence analysis," *Int J Bifur Chaos,,* vol.1*(3)*, pp.521-547, 1991.

[20] C. Bandt, G. Keller, and B. Pompe, "Entropy of interval maps via permutations," *Nonlinearity,* vol.15 *(5)*, pp.1595-1602, 2002.

[21] F. Takens, "Dynamical Systems and Turbulence," in *Lecture Notes in Mathematics* 1980, Warwick In: R. Rand and L. S. Young, Springer, Berlin (1981), vol.898, p. 366.

[22] A. Porta, G. Baselli, D. Liberati, *et al.*, "Measuring regularity by means of a corrected conditional entropy in sympathetic outflow," *Biol Cybern,* vol.78*(1)*, pp.71-78, Jan, 1998.

[23] A. Porta, S. Guzzetti, N. Montano, *et al.*, "Information domain analysis of cardiovascular variability signals: evaluation of regularity, synchronisation and co-ordination," *Med Biol Eng Comput,* vol.38*(2)*, pp.180-188, Mar, 2000.

[24] MathWorld. *ANOVA*. Available: http://mathworld.wolfram.com/ANOVA.html

[25] Wikipedia. *Logistic regression*. Available: http://en.wikipedia.org/wiki/Logistic_regression
[26] R. R. Hocking, "The Analysis and Selection of Variables in Linear Regression," *Biometrics*, p.32, 1976.
[27] N. Draper and H. Smith, *Applied Regression Analysis*, 2nd Edition ed., New York: John Wiley & Sons, Inc., 1981.
[28] "SAS/STAT User's Guide," Version 6, Fourth Edition ed. Cary, NC: SAS Institute Inc., 1989.
[29] M. A. Efroymson, "Multiple regression analysis " in *Mathematical Methods for Digital Computers*, A. Ralston and H. S. Wilf, Eds.: Wiley, 1960.

Chapter B2
Analysis for Relationship between RR series and Respiration in Premature Newborns

B2.1 Introduction

Different mechanisms are involved in the generation of cardiovascular variability rhythms which have been extensively studied as markers of the sympathovagal interaction controlling cardiovascular functions. Therefore, the application of methods of multichannel signal analysis can extract more information than it can be obtained by the usual techniques of single-channel analysis of variability signals [1]. This is why the Mono-channel signal approaches used to analyze heart rate variability have recently been extended by several Bi-channel approaches with respect to cardiorespiratory coordination.

Physiologists had already investigated cardiorespiratory coordination in the human organism as early as the 1960's. Calculating the distance between an inspiratory onset and its preceding R-peak, they found intermittent coordination between heartbeat and respiration. In the 1970's this interesting topic was no longer followed up, presumably because the physiological interpretation of the results was limited, although the last reviews of this period appeared in the late 1980's [2] [3]. The investigation of cardiorespiratory coordination has recently been revived mainly by physicists and mathematicians [4].

The connections between biological control systems can be revealed sometimes by the presence (in terms of concentration in blood) of mediator elements that can be found during infection manifestation. They are vectors used by the control system, helping to regulate, modulate, and "express" in general, the body's response to some internal or external perturbation to the system.

In the examined case, sepsis constitutes the perturbation to the system and the role of the Interleukin 1 (Il-1) as vector was investigated. It is one of the first fever effectors in adults. Some studies have given certain results regarding the role of Il-1 in the connection between infection and respiratory control system: coinciding increase in Interleukin concentration and apnea's crisis was found.

On the other side, instead, no evidence is still present for the relationship between infection and cardiac pacemaker through the Autonomic Nervous System (see Fig. B2-1). The only evidence up to now is that there is an increase in bradycardias together with apneas, during sepsis manifestation.

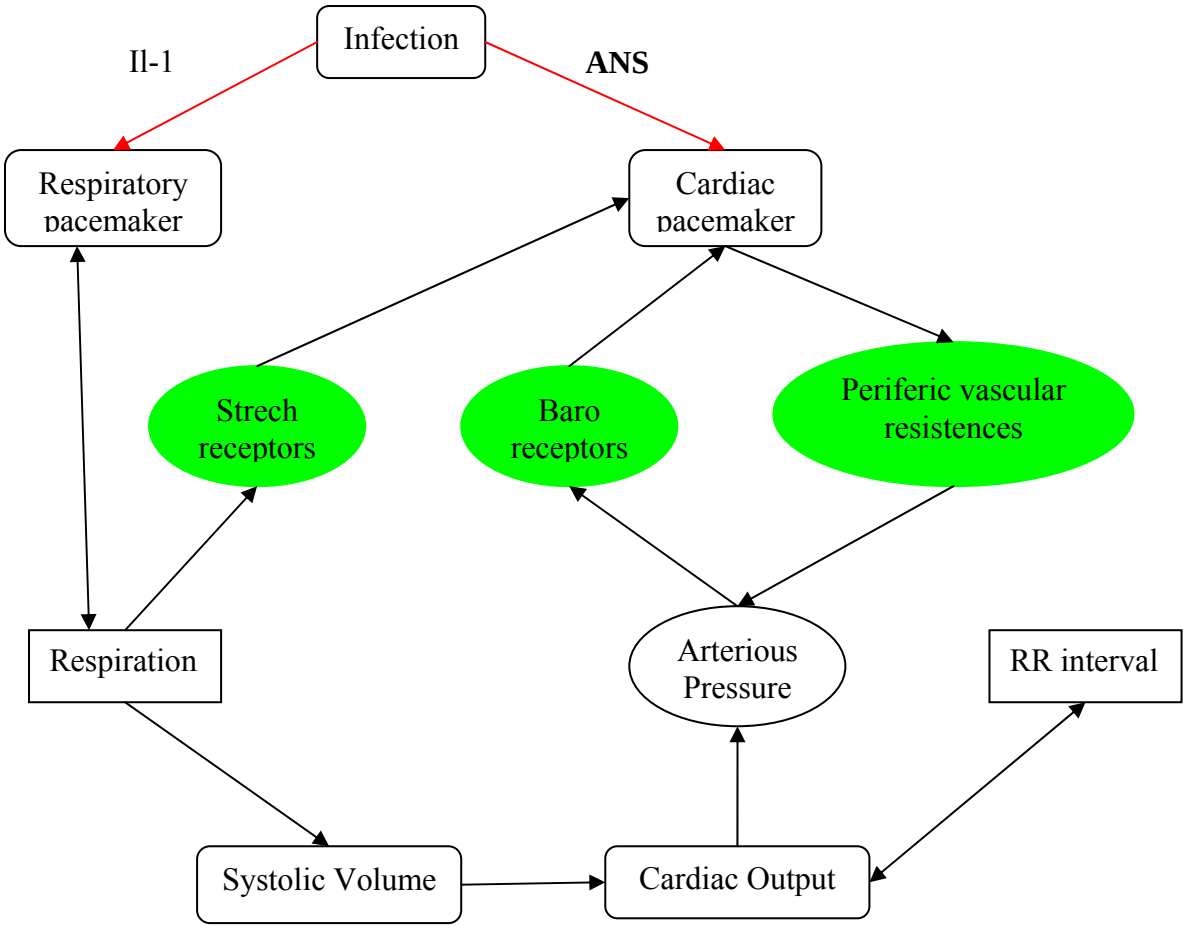

Fig. B2-1 Interconnections between cardiovascular systems and respiration. Bi-channel signal analysis rule in their interpretation, to find the infection – bradycardias possible relation.

Of course, giving an answer to this question, the intervention to be effected would change, depending on the result. And new therapies could be arranged in order to prevent the possible damages of bradycardia' onset. Studies upon the incidence of Il-1 in respiratory pacemaker are in act to find new therapies to prevent apnea by regulating Il-1 concentration.

We consider here the study of Bi-channel signals. This work is based on a measurement of linear and non-linear relationships and delay times assessment between RR and Respiratory signals. There are several techniques that allow discovering the relationship between these two channels of signals. In the following, we review some representative approaches among those existing ones.

Section B2.2 refers to linear methods. In section B2.3, non-linear methods are presented in details. Experimental protocol is explained in detail in section B2.4. Results of linear methods and non-linear methods are demonstrated and discussed in section B2.5 and section B2.6 respectively. Finally, we discuss all results in section B2.7 and conclude with summary in section B2.8.

B2.2 Linear Methods

Linear methods were developed first. Many estimators based on linear cross-correlation were proposed by Chapman *et al* [5]. Works based on the coherence function were initiated by Brazier [6]. They were followed by Gotman [7] who studied interhemispheric relations in partial seizures and by Duckrow *et al.* [8] and Franaszczuk *et al.* [9] [10] who analyzed possible synchronization mechanisms occurring at the seizure onset.

The basic problem, set in literature, is that of trying to estimate the delay and the level of the relationship between two series, presumably generated from an equation model as:

$$\begin{aligned} X_1(t) &= S(t) + b_1(t) \\ X_2(t) &= T_r(s(t-D)) + b_2(t) \end{aligned} \tag{6.1}$$

Where $S(t)$ is the source signal,

$b_1(t)$ and $b_2(t)$ are noises,

T_r is a transformation, linear in this case, which links $X_2(t)$ to $X_1(t)$.

In general, the delay estimator appeals to a function built on several time shifts, and to an algorithm detecting the maximum value in this function, with its time delay. Several approaches have been proposed in the past that are detailed in the following.

B2.2.1 Correlation Index (r^2)

The most classical time-delay estimation method is that of looking for the maximum of the cross-correlation function $R_{X_1X_2}(\tau)$. In fact, under the hypothesis that T_r (in the equation(6.1)) is reduced to a parameter α of attenuation, it can be demonstrated that $R_{X_1X_2}(\tau)$ estimation of cross-correlation function has its maximum in $\tau = D$.

$R_{X_1X_2}(\tau)$ indicates the strength and direction of a linear relationship between two random variables: in general, it refers to the departure of two variables from independence and equals. In this broad sense, there are several coefficients which measure the degree of correlation and are adapted to the nature of data. The best known is the Pearson product-moment correlation coefficient, which is obtained by dividing the covariance of the two variables by the product of their standard deviations:

$$R^2_{1,2}(\tau) = \frac{E\left\{(X_1(t) - E\left\{X_1(t)\right\})(X_2(t-\tau) - E\left\{X_2(t-\tau)\right\})\right\}}{\left[Var(X_1(t)) * Var(X_2(t))\right]^{\frac{1}{2}}} \tag{6.2}$$

$$r^2 = \max_{\tau} R^2_{1,2}(\tau) \tag{6.3}$$

Where $Var(.)$ is the variance;

$E(.)$ is the expected value;

The process $X_2(t)$ can be delayed with the time-lag (τ);

$R^2_{1,2}(\tau)$ is the normalized cross-correlation coefficient.

So that $|r^2| \leq 1$ and the equal is true if $X_1(t)$ and $X_2(t)$ are perfectly correlated.

B2.2.2 Coherence Function (*Cohere*)

Similarly to what it has been said for the correlation index, it is possible to measure the convolutional relation between two signals, by means of the coherence function. The amount of linear coupling between two signals in the frequency domain can be expressed by means of the (squared) coherence function [11].

The coherence function is defined as

$$C_{X_1X_2}(f) = \frac{S_{X_1X_2}(f)}{\sqrt{S_{X_1X_1}(f) S_{X_2X_2}(f)}} \tag{6.4}$$

Where $S_{X_1X_1}(f)$ and $S_{X_2X_2}(f)$ are the power spectral densities of X_1 and X_2 respectively,
$S_{X_1X_2}(f)$ is cross-spectral density between these two signals.
The maximum of $\left\| C_{X_1X_2}(f) \right\|^2$ is computed (k^2).

Coherence is a function of frequency (f) and it ranges between 0 and 1 that indicate how well the input X_1 corresponds to the output X_2 at each frequency. It provides both amplitude and phase information about the frequencies held in common between the two sequences.

In the analysis, the squared coherence spectrum (SCS) is estimated in the system with input X_1 and output X_2 :

$$C^2_{X_1X_2}(f) = \frac{\left| S_{X_1X_2}(f) \right|^2}{S_{X_1X_1}(f) S_{X_2X_2}(f)} \tag{6.5}$$

And Welch's average periodogram method[6] has been used to calculate it [2].

A value of SCS close to 1 indicates that same rhythms in two signals have a constant phase relationship, thus they may have a common origin or they can be linearly synchronized.

[6] One way of estimating the PSD of a process is to simply find the discrete-time Fourier transform of the samples of the process (usually done on a grid with an FFT, Fast Fourier Transform) and take the magnitude squared of the result. This estimate is called the *periodogram*. An improved estimator of the PSD is the one proposed by Welch. The method consists of dividing the time series data into (possibly overlapping) segments, computing a modified periodogram of each segment, and then averaging the PSD estimates. The result is Welch's PSD estimate.

B2.2.3 Local Linear Correlation coefficient ($r^2_{t,f}$)

It is well known that HRV and respiration are non-stationary over time. To overcome these difficulties, a new estimator was recently proposed and can be of interest for our purpose [12]. It uses a local linear correlation coefficient, computed at the outputs of narrow band-pass filter, as the function of frequency and time, which is maximized for time delay. To our knowledge, the application of this latter method in the cardio-respiratory field has never been reported. Let us briefly recall the method:

We consider two observations, *x(t)* the HRV signal and *y(t)* the respiration signal. The problem is to characterize the statistical relationship, simultaneously in the time and frequency domains, between the nonstationary signals *x(t)* and *y(t)*. The estimation of the local linear correlation coefficient is given by:

$$R^2_{x,y}(t,f) = \max_{-\tau_m<\tau<\tau_m} \left(\frac{\left(\sum_{k=-\frac{H}{2}}^{\frac{H}{2}} x_f(k) y_f(k+\tau) \right)^2}{\sum_{k=-\frac{H}{2}}^{\frac{H}{2}} x_f^2(k) \sum_{k=-\frac{H}{2}}^{\frac{H}{2}} y_f^2(k+\tau)} \right) \tag{6.6}$$

Where $x_f(t)$ and $y_f(t)$ are zero-mean and narrow band filtered signals over a sliding window of duration H (Fig. B2-2) of an appropriate filter bank (Fig. B2-3). $R^2_{x,y}(t,f)$ is computed with different delays τ between the two windows. This last one is derived from the Short-Time Fourier Transform (STFT).

The parameter $r^2_{t,f}$ is chosen and defined from $R^2_{x,y}(t,f)$ as:

$$r^2_{t,f} = \max_{\tau} R^2_{x,y}(t,f) \tag{6.7}$$

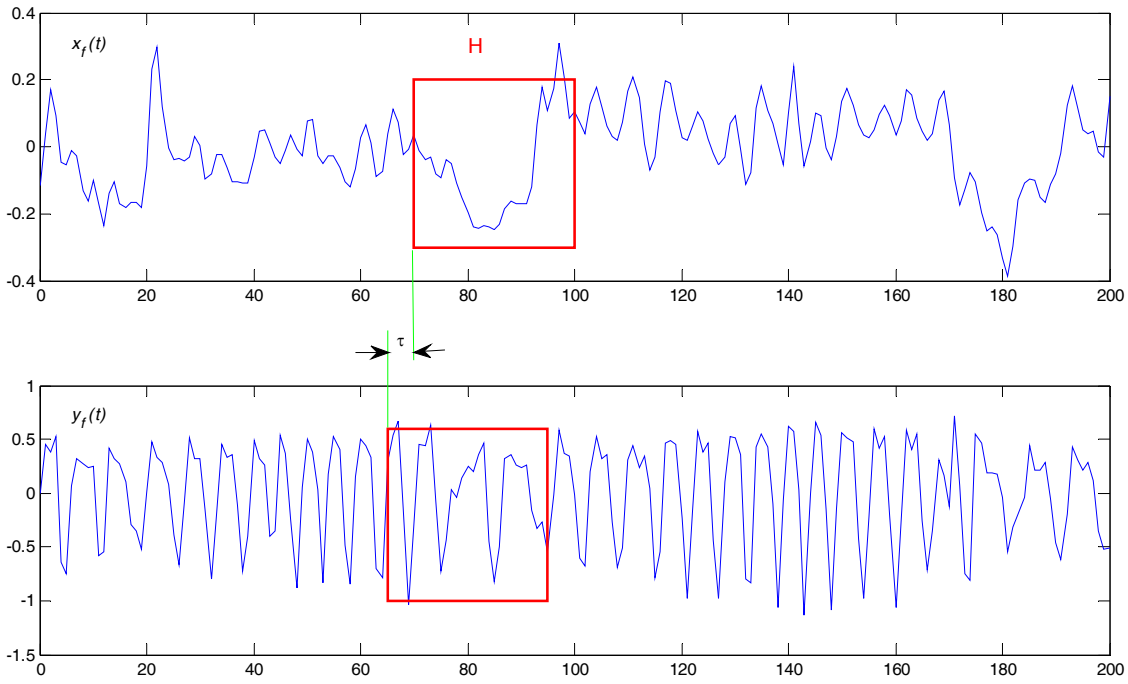

Fig. B2-2 Selection of the temporal support H for the computation of $R^2(t, f)$ with different delays τ

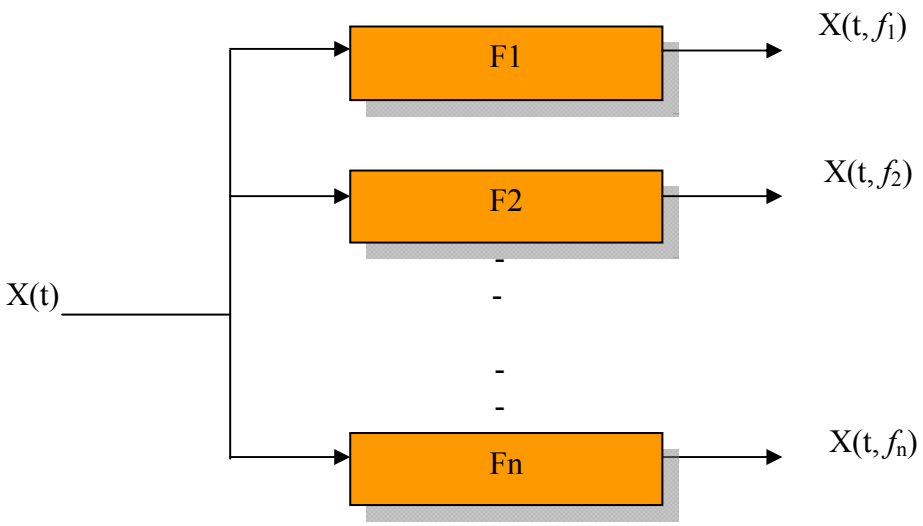

Fig. B2-3 filter bank derived from Short-Time Fourier Transform

B2.3 Non-linear Methods

The previous methods suppose a linear relationship between the HRV and the respiration (see equation(6.1)). In this section, one of non-linear indexes will be used: the non-linear regression coefficient (also known as non-linear association index).

Non-linear regression coefficient (h^2) allows to measure statistical dependence between observations obtained in a bound temporal support. It is defined as:

$$h^2_{X_1X_2} = \frac{E\left\{\left(X_2(t)-E\{X_2(t)\}\right)^2\right\} - E\left\{\left(X_1(t)-f(X_1(t))\right)^2\right\}}{E\left\{\left(X_2(t)-E\{X_2(t)\}\right)^2\right\}} \tag{6.8}$$

$$= \frac{Var(X_2)-\left\|X_2-f(X_1)\right\|^2}{Var(X_2)}$$

Where *f* is a non-linear regression function, allowing to measure the similarity, more or less linear, between the two observed processes X_1 and X_2, thanks to three principal characteristics:

- For a perfectly linear transformation, $h^2_{X_1X_2}$ tends to $r^2_{1,2}$;
- $h^2_{X_1X_2}$ is generally different from $h^2_{X_2X_1}$, whereas we have a non-linear transformation;
- $h^2_{X_1X_2}$ is a quantity that can assume values between 0 and 1, if $\left\|X_2-f(X_1)\right\|^2 \le Var(X_2)$

Practically, we attempt to approximate $f(X_1)$ with treats of linear regression. To do that the X_1 axis is dived into *M* identical intervals, or bins (see Fig. B2-4), and the expectation value of X_2 given a certain value of X_1 is calculated and denoted as E_{X_2/X_1} :

$$E_{X_2/X_1}(x_1^J) = \sum_{i=1}^{N} X_2(i)\,p(X_2(i)/X_1(i) \in x_1^J) \tag{6.9}$$

E_{X_2/X_1} is a function of x_1^J, where *J* indicates the *J*-th bin. The curve described in this way represents the predicted value of X_2 given X_1 and it is, in general, a non-linear relationship.

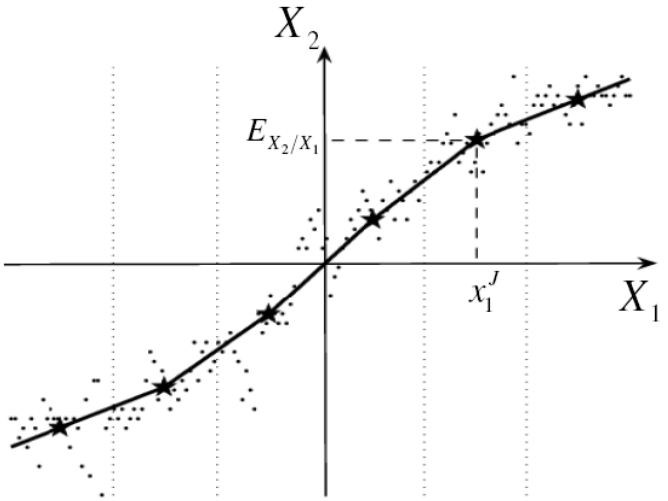

Fig. B2-4 Non-linear regression approximating curve

In particular, for each bin *J*, the average of the X_2-values is calculated, $E(X_2)$, as well as the X_1-value of the midpoint (x_1^J). Then the points $(x_1^J, E_{X_2/X_1}(x_1^J))$ are connected by segments of straight line to approximate the function $f(X_1(t))$, as shown in Fig. B2-4.

The same procedure may also be carried out in the opposite way by subdividing the variable X_2 into bins and computing the expected value of X_1 given a certain X_2 value, in order to test both the causal directions.

The numerator of (6.8) represents the difference between the total variance of X_2 and the part of variance of X_2 not explained by the interpolating function. Consequently, $h^2_{X_1X_2}$ express the reduction of variance of X_2 obtained predicting the X_2 values on basis of X_1 : the better the prediction, the minor the unexplained variance and the major the $h^2_{X_1X_2}$ index results.

The process $X_2(t)$ can be also delayed with the time-lag (τ) and a non-linear $h^2_{X_1X_2}(\tau)$ function can be computed. The maximum of $h^2_{X_1X_2}(\tau)$ is considered (h^2), in other words:

$$h^2 = \max_{\tau} h^2_{X_1X_2}(\tau) \qquad (6.10)$$

B2.4 Experimentation

Experimental protocol and RR series pre-processing are the same as Section B1.4. Respiration can be seen in a different way. This is the purpose of this part to discuss respiration signal pre-processing and analysis window settings.

B2.4.1 Respiration signal pre-processing

Nasal airflow (thermocouples measure air flow into and out of the lungs directly) and abdominal movements (strain gauges measure of thoracic movement) are generally collected. Both of them are useful in order to analyse the respiration pattern, avoiding movement artefacts, and distinguishing obstructive apnea from the central one.

In this study, the abdominal respiration signals have a poor quality and we only use the nasal airflow data. Here, it is calculated in two types:

- Original Nasal Respiration (raw)
- Envelope of Nasal Respiration (enp)

B2.4.1.1 Original Nasal Respiration

One of the original nasal respirations is shown in Fig. B2-5

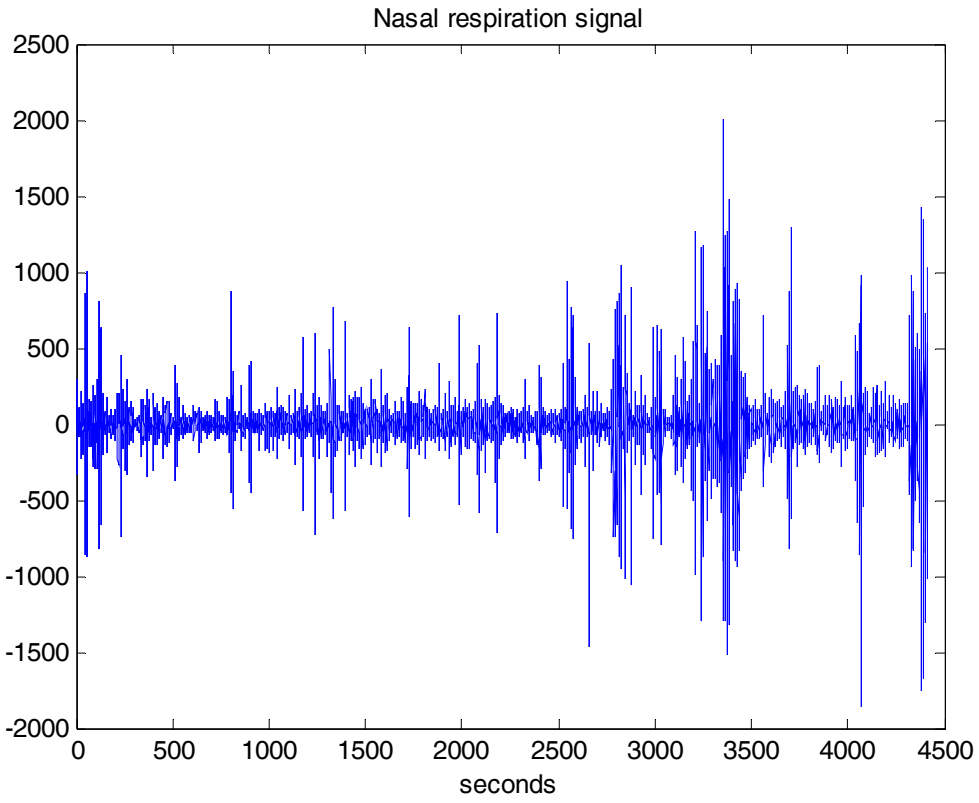

Fig. B2-5 Nasal respiration signal

B2.4.1.2 Envelope extraction

For respiration pattern amplitude modulation analysis, the envelope of the respiratory traces was extracted. To evaluate the envelope, the signals absolute values were taken, and the Hilbert transform was computed. In details, the Hilbert transform of a signal $r(t)$ is defined as:

$$r\%(t) = H(r(t)) = \frac{1}{\pi}\int_{-\infty}^{+\infty}\frac{r(t)}{t-\tau}d\tau \tag{6.11}$$

Being

$$r\%(t) = r(t) * \frac{1}{\pi t} \tag{6.12}$$

The associated analytic signal $z(t)$ is:

$$z(t) = r(t) + ir\%(t) \tag{6.13}$$

And the signal envelope is defined as its module:

$$E(t) = |z(t)| = \sqrt{r(t)^2 + r\%(t)^2} \tag{6.14}$$

As a final step, the envelope was low-pass filtered. A Zero-phase forward and reverse FIR filter was implemented, with a cut-off frequency of 0.02 Hz. This frequency was chosen to focus our analysis on the VLF band of 0.002-0.02 Hz. Lots of studies have been already done on HF band, because this is the typical Respiratory Sinus Arrhythmia (RSA) band. The LF too has been explored: a sympathetic contributes has been found in RSA. Now the VLF band was used for trying to observe the autonomic nervous system control in this new frequency pathway.

Fig. B2-6 is the envelope extracted from Fig. B2-5.

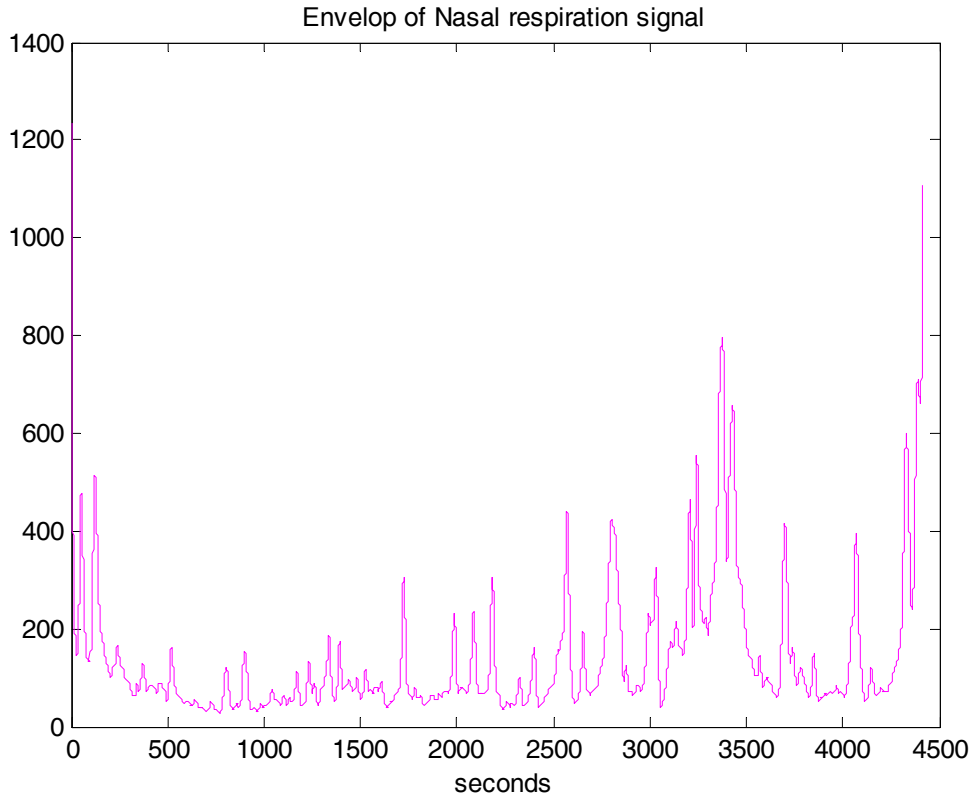

Fig. B2-6 Envelope of Nasal respiration signal

Only for the Coherence analysis the signal was not enveloped: in this case, the entire signal pattern has to be considered, since we don't want to loose any frequency information. Besides, coherence analysis was made to analyse the VLF relations between RR and respiration. Thus, the sampling frequency was reduced to 0.1 Hz, and then no low-pass filtration has been necessary.

B2.4.2 Signal normalized

Both the RR series and respiration signals were normalized before analysis according to the following equation:

$$X(\tau) = \frac{x(\tau) - E\{x(\tau)\}}{\sigma_x^2} \qquad (6.15)$$

That is subtraction of the mean value, and division for the standard deviation of the signal.

Each signal has been divided in several intervals, and analysis has been computed for each interval. Then, for each patient, the mean value on the different segments has been computed.

B2.4.3 Analysis windows

Signals recording lengths were variables: among babies, the longest record was 3 hours recordings (around 45000 points, with a sampling frequency of 4 Hz), but average length was about 1.5 hours.

Fig. B2-7 is the example of Bi-channel signal in 4Hz for one baby, where the blue signal is RR series, and the red one is original nasal respiration.

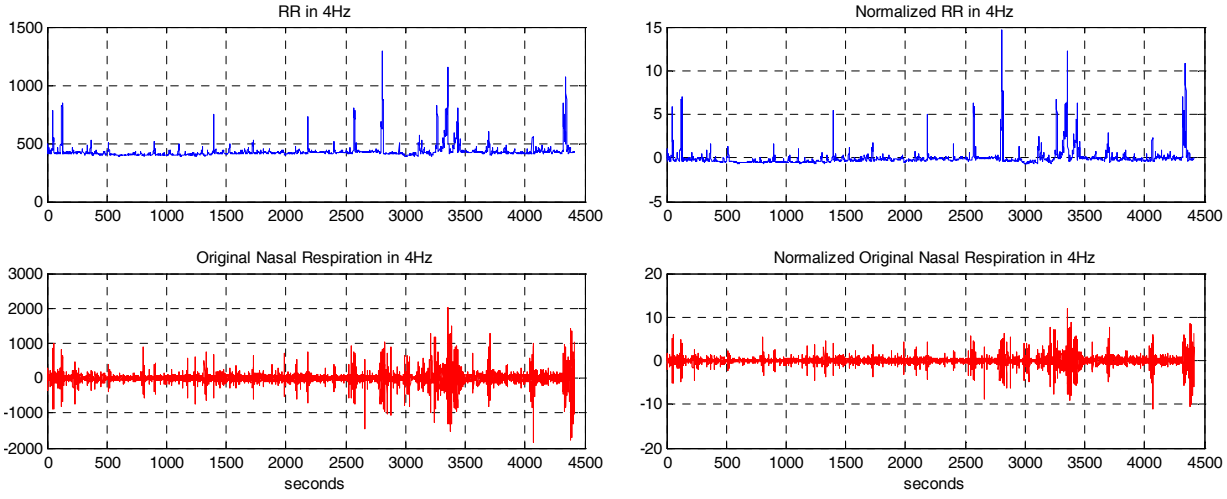

a) Original b) Normalized

Fig. B2-7 RR and Original Nasal Respiration in 4Hz

Analysis was performed on three kinds of window size (1024/2048/4096 points, Fig. B2-8), with the same length of step accordingly. A sensitivity study was made to evaluate the performance of the single segments in comparison to the entire signal, thus evaluating the index performances on different signal's lengths. This was necessary for trying to choose the most appropriate length to consider. The bradycardias exclusion stage took long time in some cases, when the signals were affected by lots of noise, since it is not always so easy to differentiate a spike simply generated by an artefact, from one representing a sudden bradycardia event. This kind of analysis requires long pre-processing time, especially in noisy recordings.

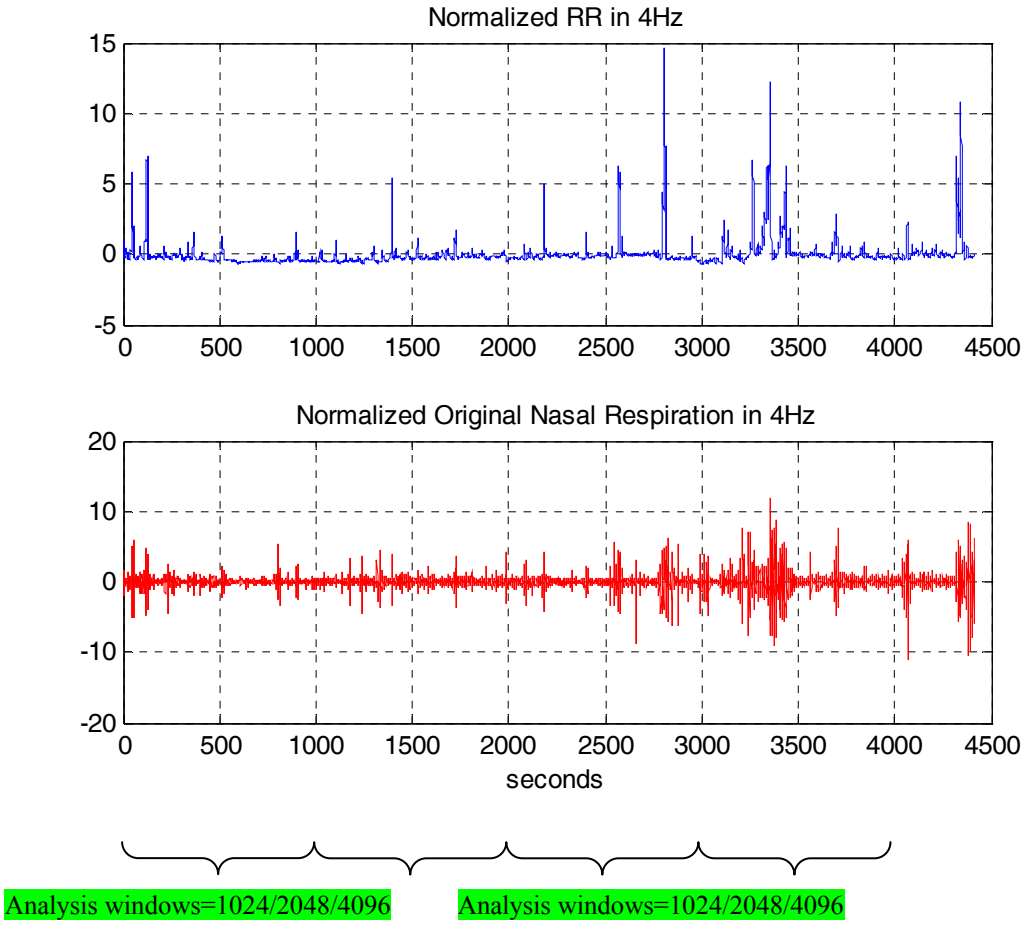

Fig. B2-8 Analysis windows over Normalized RR and Original Nasal Respiration

B2.4.4 Flow chart

The flow chart Fig. B2-9 summarized the experimental procedure:

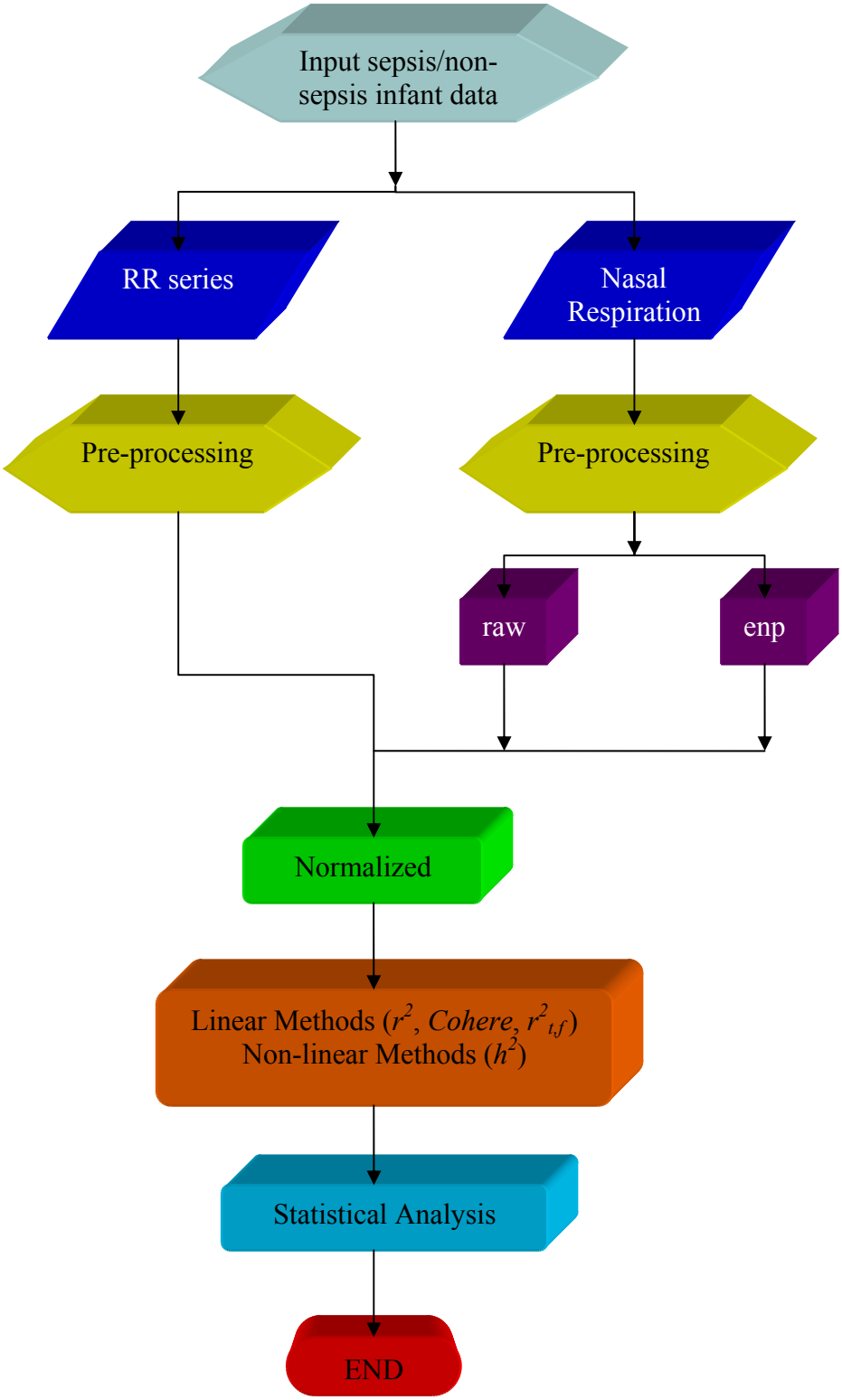

Fig. B2-9 Flow chart of Bi-channel signal analysis: RR series and Nasal Respiration

B2.5 Results and Discussion for Linear Methods

Here, most of the work was focused on the Bi-channel signal analysis, whose results are reported in this section. The Bi-signal analysis includes linear and non-linear indexes and explores the RR and Respiration signals series.

For Bi-signal analysis, all babies with respiration recordings were considered, in total 26 patients: 13 sepsis and 13 non-sepsis. The two groups had comparable post-conceptional age (PCA) and post-natal age (PNA). This is a fundamental criterion for our analysis since in preterm newborns. even small differences in these ages may entail very big differences from a physiological point of view, which invalidate the comparative analysis.

B2.5.1 Correlation Index (r^2)

The cross-correlation (r^2) between the RR and the respiratory series was computed (only for nasal channel) over the range of -240 to 240 sample lags (1 minute) and it was normalized to have $r^2(0)=1$.

The maximum r^2 values for each sequence were registered as well as the delay time at which these values occurred. Table B2-1 reports the results of statistical analysis for r^2 between RR and nasal respiration on the entire population, in the window 1024 with step 1024.

Table B2-1 Results of statistical analysis for r^2 between RR and nasal respiration, Window=1024, Step=1024

r^2	Sepsis	Non Sepsis	ANOVA	KruskWall	Wilrs
rn_raw	0.0800 ± 0.0872	0.0450 ± 0.0383	0.0001	0.0011	0.0011
rn_enp	0.5135 ± 0.1980	0.4953 ± 0.1825	0.4528	0.4374	0.4379

The level of significance was set at p value
$p < 0.05$ is marked in yellow

In Table B2-1, the second and third column present "Mean Value ± Standard Deviation" of sepsis and non-sepsis infants respectively. The fourth, fifth and sixth column bring forth the p value of ANOVA, Kruskal-Wallis test and Wilcoxon rank-sum test respectively in each case.

- For the original nasal respiration and its envelope, correlation index r^2 is higher in sepsis infants than in non-sepsis ones. That is to say, sepsis condition doesn't influence on the original nasal respiration signal and its envelope.

We carry out the same analysis for three sizes of window in detail. All these results are reported in Appendix V.

B2.5.2 Coherence function (*Cohere*)

Coherence is a function of frequency with values between 0 and 1 that indicate how well the input (the RR signal) corresponds to the output (the respiratory signal) at each frequency.

The squared coherence estimate of the system has been computed using Welch's averaged periodogram method.

A vector divides RR and Respiration signals into overlapping sections of 64 or 32 points (depending on the signal length, here 64 is selected), and then windows each section with this vector (hamming window).

As final results, the cumulative sum of the coherence values upon the frequency band of interest (VLF = 0.002 —0.02 Hz), normalized (divided by N points, correspondent to the frequency band points, here N=256) to give a value between 0 and 1, was recorded as:

$$\frac{1}{N}\sum_{f=0.002}^{0.02} C_{RRresp}(f) \tag{6.16}$$

Table B2-2 shows the results of statistical analysis for Coherence between RR and nasal respiration, in the window 1024 with step 1024.

Table B2-2 Results of statistical analysis for *Cohere* between RR and nasal respiration, Window=1024, Step=1024

Cohere	Sepsis	Non Sepsis	ANOVA	KruskWall	Wilrs
rn_raw	0.4375 ± 0.1693	0.4149 ± 0.1542	0.2742	0.2668	0.2672

In Table B2-2, the second and third column present "Mean Value ± Standard Deviation" of sepsis and non-sepsis infants respectively. The fourth, fifth and sixth column bring forth the p value of ANOVA, Kruskal-Wallis test and Wilcoxon rank-sum test respectively in each case.

- For original nasal respiration, coherence index is higher in sepsis infants than in non-sepsis ones. That is to say, sepsis condition doesn't influence on the original nasal respiration signal and its envelope.

We carry out the same analysis for three sizes of window in detail. All these results are reported in Appendix VI.

B2.5.3 Local Linear Correlation Coefficient ($r^2_{t,f}$)

B2.5.3.1 Time-Frequency plot

Representative examples (HRV, respiration signal and Time-Frequency linear correlation coefficient) are displayed in the sepsis and non-sepsis group (Fig. B2-10) separately. Both signals are nonstationary.

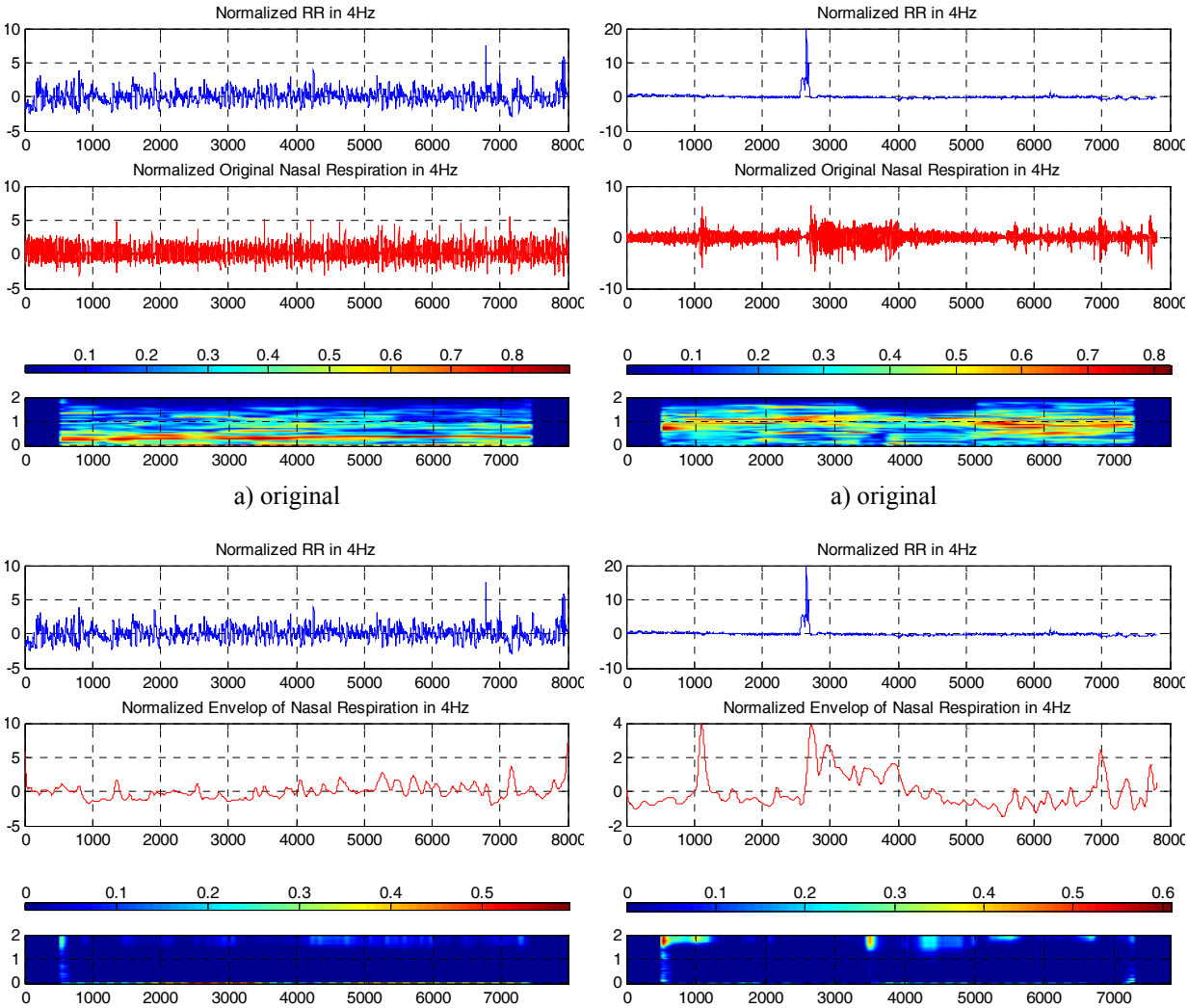

Fig. B2-10 Time-Frequency plot

- In the left column, we demonstrate typical square modulus of Time-Frequency linear correlation coefficient for a sepsis baby. The upper traces represent the Normalized RR and Original/Envelope of Nasal Respiration separately. These Time-Frequency plots indicate that a higher correlation coefficient for the sepsis group in the lower band around 0.5 Hz

- In the right column, we demonstrate typical square modulus of Time-Frequency linear correlation coefficient for a non-sepsis baby. The upper traces represent the Normalized RR and Original/Envelope of Nasal Respiration separately. These Time-Frequency plots indicate that a strong relationship in the higher frequency band for the non-sepsis group.

B2.5.3.2 Multi-Boxplot $r^2_{t,f}$ between RR and original nasal respiration

The following section reports the results of statistical analysis for $r^2_{t,f}$ between RR and original nasal respiration frequency band by band. These qualitative findings were statistically verified. Fig. B2-11 depicts the sub-band distribution of the time-frequency correlation coefficient $r^2_{t,f}$, over a threshold set to 0.8, in the window 1024 with step 1024.

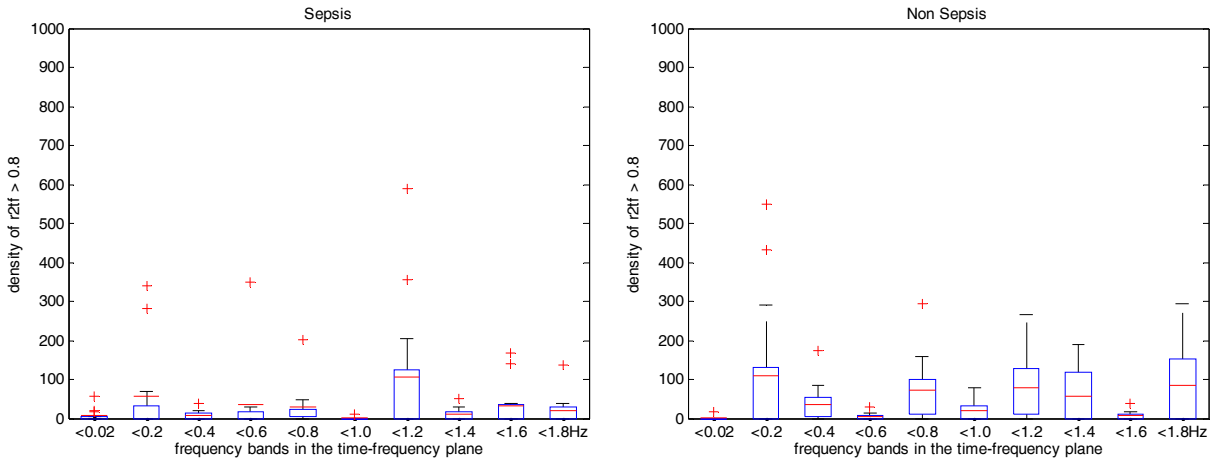

Sepsis Non-Sepsis

Fig. B2-11 Distribution of $\mathbf{r^2_{t,f}}$ between RR and original nasal respiration (greater than 0.8), Window=1024, Step=1024

In Boxplot, red line is mean value.

Table B2-3 demonstrates the results of statistical analysis for $r^2_{t,f}$ between RR and nasal respiration, in the window 1024 with step 1024.

Table B2-3 Statistical analysis for $r^2_{t,f}$ between RR and nasal respiration, Window=1024, Step=1024

Band(Hz)	Sepsis	Non Sepsis	ANOVA	KruskWall	Wilrs
0-0.02	7.2308 ± 16.6841	1.3846 ± 4.9923	0.2379	0.2704	0.2885
0.02-0.2	56.0769 ±115.2595	109.5385 ±188.1266	0.3909	0.6855	0.7055
0.2-0.4	8.6154 ± 11.3324	36.2308 ± 49.6154	0.0421	0.0445	0.0484
0.4-0.6	34.5385 ± 94.6657	5.0000 ± 8.5342	0.2736	0.1881	0.1975
0.6-0.8	29.1538 ± 53.2930	72.7692 ± 82.2559	0.1217	0.1725	0.1807
0.8-1.0	1.7692 ± 4.3235	18.5385 ± 26.0947	0.0314	0.0254	0.0275
1.0-1.2	105.6154 ±178.8689	79.2308 ±100.9762	0.6474	0.5323	0.5495
1.2-1.4	10.3077 ± 16.1987	56.8462 ± 70.3253	0.0288	0.1547	0.1630
1.4-1.6	33.6154 ± 55.3075	7.4615 ± 11.1177	0.1076	0.3446	0.3585
1.6-1.8	21.0769 ± 37.8912	83.6154 ±105.7848	0.0562	0.1995	0.2088

The level of significance was set at p value
p< 0.05 is marked in yellow

- We confirm statistically ($p<0.05$ whatever the statistical tests) that the higher correlation is retrieved in the two frequency bands for the non-sepsis group (*$0.2<f<0.4Hz$ and $0.8<f<1.0Hz$*).

We carry out the same analysis for three sizes of window in detail. All these results are reported in Appendix VII.

B2.5.3.3 Multi-Boxplot $r^2_{t,f}$ between RR and envelope of nasal respiration

The followings report the results of statistical analysis for $r^2_{t,f}$ between RR and envelope of nasal respiration frequency band by band. These qualitative findings were statistically verified. Fig. B2-12 depicts the sub-band distribution of the time-frequency correlation coefficient $r^2_{t,f}$, over a threshold set to 0.8, in the window 1024 with step 1024.

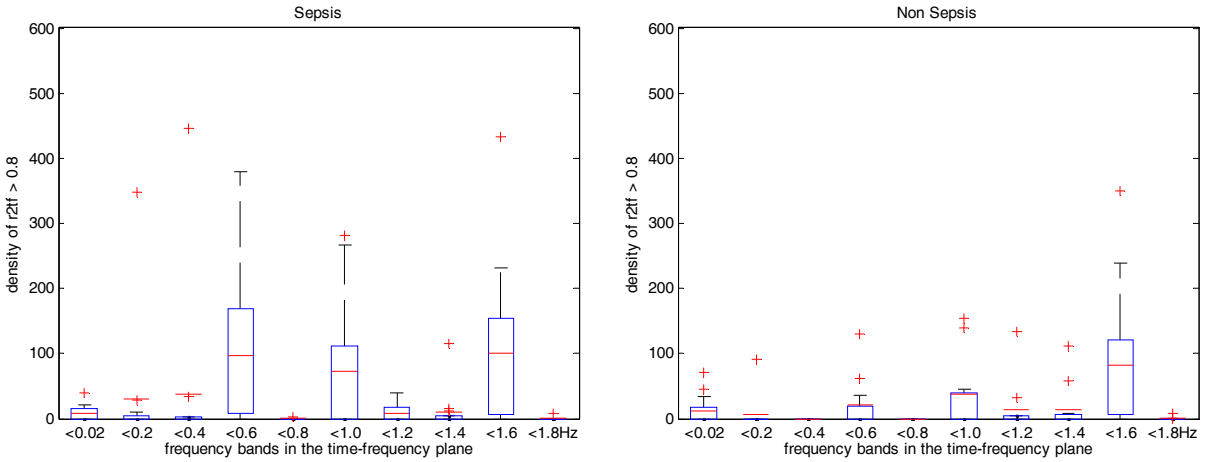

Sepsis Non-Sepsis

Fig. B2-12 Distribution of $\mathbf{r^2_{t,f}}$ between RR and envelope of nasal respiration (greater than 0.8), Window=1024, Step=1024

In Boxplot, red line is mean value.

Table B2-4 presents the results of statistical analysis for $r^2_{t,f}$ between RR and envelope of nasal respiration, in the window 1024 with step 1024.

Table B2-4 Statistical analysis for $r^2_{t,f}$ between RR and envelope of nasal respiration, Window=1024, Step=1024

Band(Hz)	Sepsis	Non Sepsis	ANOVA	KruskWall	Wilrs
0-0.02	8.7692 ± 15.2050	12.6154 ± 23.1572	0.6212	0.6946	0.7171
0.02-0.2	30.1538 ± 95.8478	7.0769 ± 25.5162	0.4098	0.0889	0.0956
0.2-0.4	37.3846 ±123.1480	0.0000 ± 0.0000	0.2846	0.0338	0.0373
0.4-0.6	97.0000 ±123.1990	20.6923 ± 37.5730	0.0431	0.0167	0.0179
0.6-0.8	0.1538 ± 0.5547	0.0000 ± 0.0000	0.3273	0.3173	0.3560
0.8-1.0	72.2308 ±102.8139	37.4615 ± 51.3235	0.2861	0.6582	0.6771
1.0-1.2	8.6923 ± 14.0735	13.6154 ± 36.9110	0.6572	0.9318	0.9545
1.2-1.4	11.0769 ± 31.9256	14.0000 ± 33.1989	0.8209	1.0000	1.0000
1.4-1.6	101.5385 ±128.5461	82.7692 ±112.1169	0.6951	0.8573	0.8775

Band(Hz)	Sepsis	Non Sepsis	ANOVA	KruskWall	Wilrs
1.6-1.8	0.6923 ± 2.4962	0.7692 ± 2.4884	0.9379	0.5791	0.6111

The level of significance was set at p value
p< 0.05 is marked in yellow

- We confirm statistically ($p<0.05$ whatever the statistical tests) that the higher correlation is retrieved in the frequency band for the sepsis group ($0.4<f<0.6Hz$).

We carry out the same analysis for three sizes of window in detail. All these results are reported in Appendix VII.

B2.6 Results and Discussion for Non-linear Methods

This section presents the results obtained for the non-linear regression coefficient (h^2). As an example, the curves of h^2 for a sepsis (figures on the left) and a non-sepsis (figures on the right) patient are plotted in Fig. B2-13 below.

Tests have been conducted to evaluate $h^2(\tau)$, considering two directions:

→ RR vs. the nasal respiratory signal (upper subfigure)

← the nasal respiratory signal vs. RR (lower subfigure)

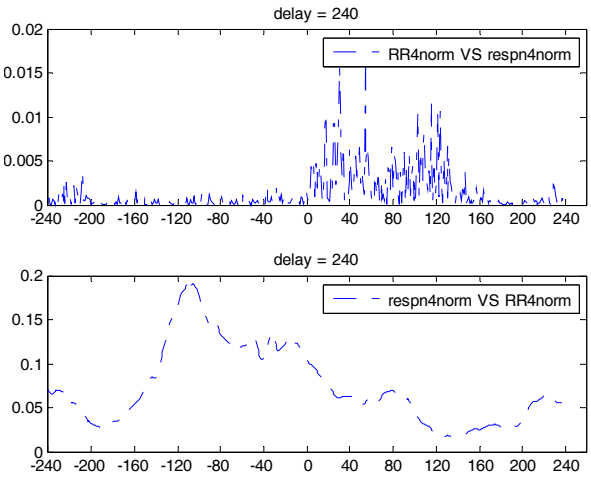

a) original

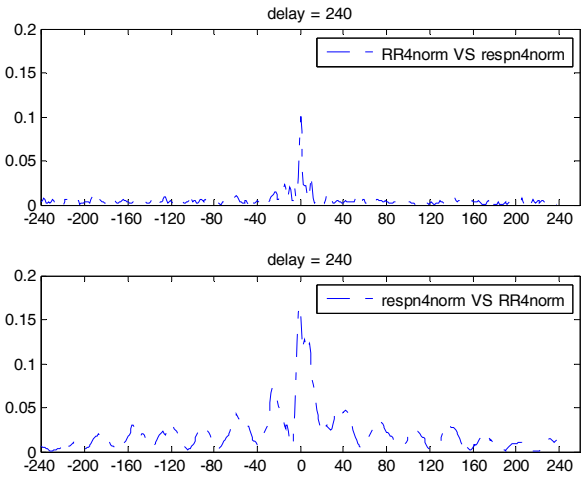

a) original

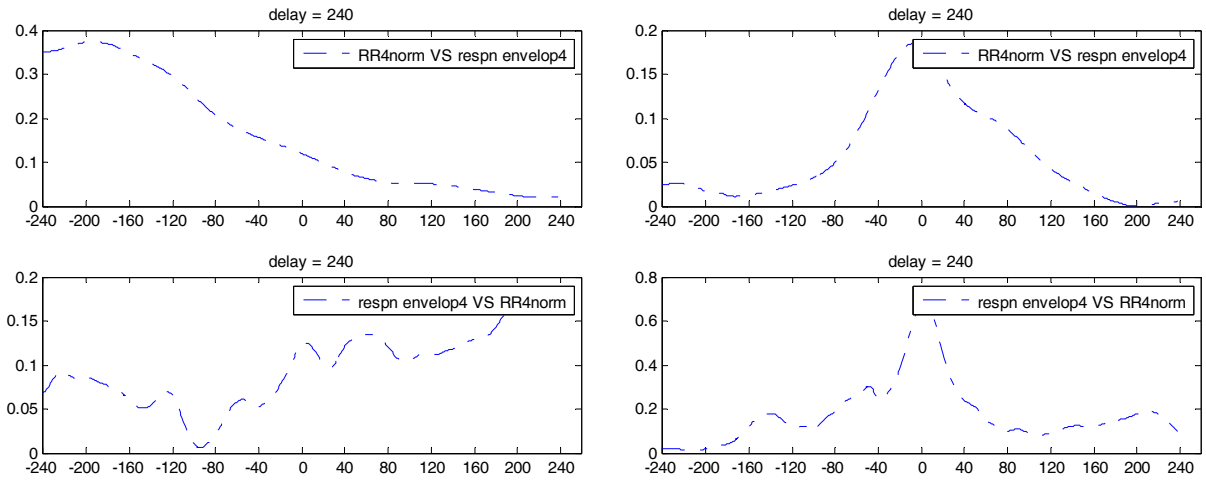

b) envelope

Sepsis

b) envelope

Non-Sepsis

Fig. B2-13 Curves of h² calculated on segments of 1024 points (around 4.3 minutes) with a delay window of (±240 points) between RR and Original/Envelope of Nasal Respiration separately. For each sub-figure, x-axis for the numbers of points and y-axis stands for the max values of h^2.

- As it is evident from Fig. B2-13, there is a big difference in the maximum values of h^2 function. The curves themselves are very different, with a great and very well-defined peak for non-sepsis case and without a precise shape, or a defined peak in sepsis baby.

It's the Table B2-5 of statistical analysis for h^2 in one direction: RR vs. nasal respiration, in the window 1024 with step 1024.

Table B2-5 Results of statistical analysis for h^2 between RR and nasal respiration, Window=1024, Step=1024

h^2	Sepsis	Non Sepsis	ANOVA	KruskWall	Wilrs
rn_raw	0.0813 ± 0.0779	0.0432 ± 0.0403	0.0000	0.0000	0.0000
rn_enp	0.4500 ± 0.2011	0.4083 ± 0.1620	0.0759	0.0937	0.0939

The level of significance was set at p value
p< 0.05 is marked in yellow

In Table B2-5, the second and third column present "Mean Value ± Standard Deviation" of sepsis and non-sepsis infants respectively. The fourth, fifth and sixth column bring forth the p value of ANOVA, Kruskal-Wallis test and Wilcoxon rank-sum test respectively in each case.

While Table B2-6 presents the statistical analysis in the other direction: nasal respiration vs. RR, in the window 1024 with step 1024.

Table B2-6 Results of statistical analysis for h^2 between nasal respiration and RR, Window=1024, Step=1024

h^2	Sepsis	Non Sepsis	ANOVA	KruskWall	Wilrs
nr_raw	0.1887 ± 0.2531	0.0975 ± 0.0737	0.0003	0.0000	0.0000
nr_enp	0.5648 ± 0.1808	0.5160 ± 0.1502	0.0225	0.0062	0.0063

The level of significance was set at p value
p< 0.05 is marked in yellow

In Table B2-6, the columns are identical to Table B2-5.

We carry out the same analysis for three sizes of window in detail. All these results are reported in Appendix VIII.

B2.7 Discussion

Here, we recall that
Linear estimates:

- ⇒ r2_rn_raw (r^2 between RR and original nasal respiration)
- ⇒ r2_rn_enp (r^2 between RR and envelope of nasal respiration)

- ⇒ Cohere_rn_raw (Coherence between RR and original nasal respiration)

- ⇒ r2tf_rn_raw_0p0_0p02 (the quantity of $r^2_{t,f}$ between RR and original nasal respiration over a threshold set to 0.8 in the sub-band $0<f<0.02$ *Hz*)
- ⇒ r2tf_rn_raw_0p02_0p2 (the quantity of $r^2_{t,f}$ between RR and original nasal respiration over a threshold set to 0.8 in the sub-band $0.02<f<0.2$ *Hz*)
- ⇒ r2tf_rn_raw_0p2_0p4 (the quantity of $r^2_{t,f}$ between RR and original nasal respiration over a threshold set to 0.8 in the sub-band $0.2<f<0.4$ *Hz*)
- ⇒ r2tf_rn_raw_0p4_0p6 (the quantity of $r^2_{t,f}$ between RR and original nasal respiration over a threshold set to 0.8 in the sub-band $0.4<f<0.6$ *Hz*)
- ⇒ r2tf_rn_raw_0p6_0p8 (the quantity of $r^2_{t,f}$ between RR and original nasal respiration over a threshold set to 0.8 in the sub-band $0.6<f<0.8$ *Hz*)
- ⇒ r2tf_rn_raw_0p8_1p0 (the quantity of $r^2_{t,f}$ between RR and original nasal respiration over a threshold set to 0.8 in the sub-band $0.8<f<1.0$ *Hz*)
- ⇒ r2tf_rn_raw_1p0_1p2 (the quantity of $r^2_{t,f}$ between RR and original nasal respiration over a threshold set to 0.8 in the sub-band $1.0<f<1.2$ *Hz*)
- ⇒ r2tf_rn_raw_1p2_1p4 (the quantity of $r^2_{t,f}$ between RR and original nasal respiration over a threshold set to 0.8 in the sub-band $1.2<f<1.4$ *Hz*)
- ⇒ r2tf_rn_raw_1p4_1p6 (the quantity of $r^2_{t,f}$ between RR and original nasal respiration over a threshold set to 0.8 in the sub-band $1.4<f<1.6$ *Hz*)
- ⇒ r2tf_rn_raw_1p6_1p8 (the quantity of $r^2_{t,f}$ between RR and original nasal respiration over a threshold set to 0.8 in the sub-band $1.6<f<1.8$ *Hz*)

⇒ r2tf_rn_enp_0p0_0p02 (the quantity of $r^2_{t,f}$ between RR and envelope of nasal respiration over a threshold set to 0.8 in the sub-band $0<f<0.02$ *Hz*)
⇒ r2tf_rn_enp_0p02_0p2 (the quantity of $r^2_{t,f}$ between RR and envelope of nasal respiration over a threshold set to 0.8 in the sub-band $0.02<f<0.2$ *Hz*)
⇒ r2tf_rn_enp_0p2_0p4 (the quantity of $r^2_{t,f}$ between RR and envelope of nasal respiration over a threshold set to 0.8 in the sub-band $0.2<f<0.4$ *Hz*)
⇒ r2tf_rn_enp_0p4_0p6 (the quantity of $r^2_{t,f}$ between RR and envelope of nasal respiration over a threshold set to 0.8 in the sub-band $0.4<f<0.6$ *Hz*)
⇒ r2tf_rn_enp_0p6_0p8 (the quantity of $r^2_{t,f}$ between RR and envelope of nasal respiration over a threshold set to 0.8 in the sub-band $0.6<f<0.8$ *Hz*)
⇒ r2tf_rn_enp_0p8_1p0 (the quantity of $r^2_{t,f}$ between RR and envelope of nasal respiration over a threshold set to 0.8 in the sub-band $0.8<f<1.0$ *Hz*)
⇒ r2tf_rn_enp_1p0_1p2 (the quantity of $r^2_{t,f}$ between RR and envelope of nasal respiration over a threshold set to 0.8 in the sub-band $1.0<f<1.2$ *Hz*)
⇒ r2tf_rn_enp_1p2_1p4 (the quantity of $r^2_{t,f}$ between RR and envelope of nasal respiration over a threshold set to 0.8 in the sub-band $1.2<f<1.4$ *Hz*)
⇒ r2tf_rn_enp_1p4_1p6 (the quantity of $r^2_{t,f}$ between RR and envelope of nasal respiration over a threshold set to 0.8 in the sub-band $1.4<f<1.6$ *Hz*)
⇒ r2tf_rn_enp_1p6_1p8 (the quantity of $r^2_{t,f}$ between RR and envelope of nasal respiration over a threshold set to 0.8 in the sub-band $1.6<f<1.8$ *Hz*)

Non-linear estimates:
⇒ h2_rn_raw (h^2 between RR and original nasal respiration)
⇒ h2_rn_enp (h^2 between RR and envelope of nasal respiration)

⇒ h2_nr_raw (h^2 between original nasal respiration and RR)
⇒ h2_nr_enp (h^2 between envelope of nasal respiration and RR)

The synthesis of all the results is reported in the following table.

Table B2-7 Synthesis of all parameters between RR and nasal respiration

	Window Size		
	1024	2048	4096
r2_rn_raw	×		
r2_rn_enp			
Cohere_rn_raw			
r2tf_rn_raw_0p0_0p02			
r2tf_rn_raw_0p02_0p2			
r2tf_rn_raw_0p2_0p4	×	×	×
r2tf_rn_raw_0p4_0p6			
r2tf_rn_raw_0p6_0p8			
r2tf_rn_raw_0p8_1p0	×		
r2tf_rn_raw_1p0_1p2			

	Window Size		
	1024	2048	4096
r2tf_rn_raw_1p2_1p4			
r2tf_rn_raw_1p4_1p6			
r2tf_rn_raw_1p6_1p8			
r2tf_rn_enp_0p0_0p02			
r2tf_rn_enp_0p02_0p2			
r2tf_rn_enp_0p2_0p4			
r2tf_rn_enp_0p4_0p6	×		
r2tf_rn_enp_0p6_0p8			
r2tf_rn_enp_0p8_1p0			
r2tf_rn_enp_1p0_1p2			
r2tf_rn_enp_1p2_1p4			
r2tf_rn_enp_1p4_1p6			
r2tf_rn_enp_1p6_1p8			
h2_rn_raw	×	×	×
h2_rn_enp			×
h2_nr_raw	×	×	×
h2_nr_enp	×		

For each case in column, these parameters whose p value less than 0.05 are marked as "×".

From Table B2-7, it is obvious that "r2tf_rn_raw_0p2_0p4", "h2_rn_raw" and "h2_nr_raw" are the most frequently selected as significant indexes during the process of statistical analysis. These three indicators are regarded as candidate parameters (highlighted in red horizontally) to discriminate between sepsis and non-sepsis. Their p values are shown in following table:

Table B2-8 p values of candidate parameters of Bi-Channel

	Window Size		
	1024	2048	4096
r2tf_rn_raw_0p2_0p4	0.0421	0.0074	0.0107
h2_rn_raw	0.0000	0.0002	0.0241
h2_nr_raw	0.0003	0.0001	0.0194

Fig. B2-11 already gave the performance of Boxplot of "r2tf_rn_raw_0p2_0p4". For "h2_rn_raw" and "h2_nr_raw", Fig. B2-14 is schematically demonstrated in boxplot, where the red lines stand for mean values of the maximum correlation index h^2 for all segments.

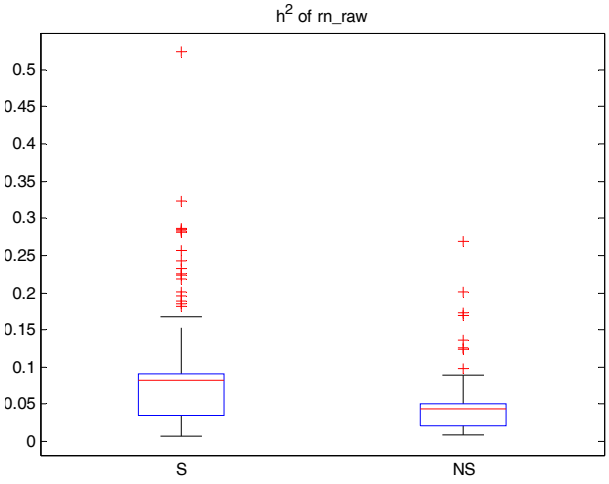

a) (Win1024, Step1024)

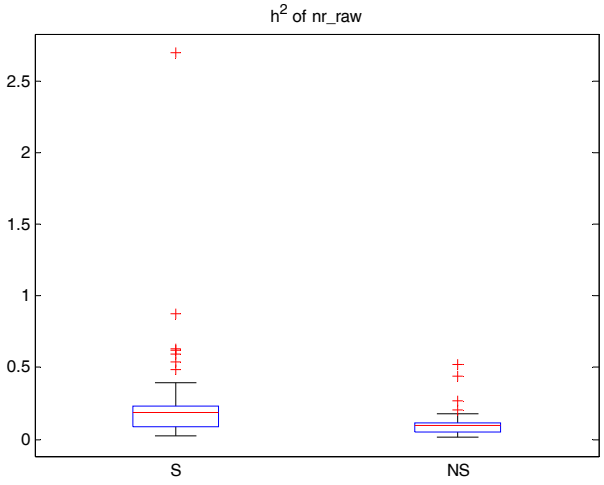

a) (Win1024, Step1024)

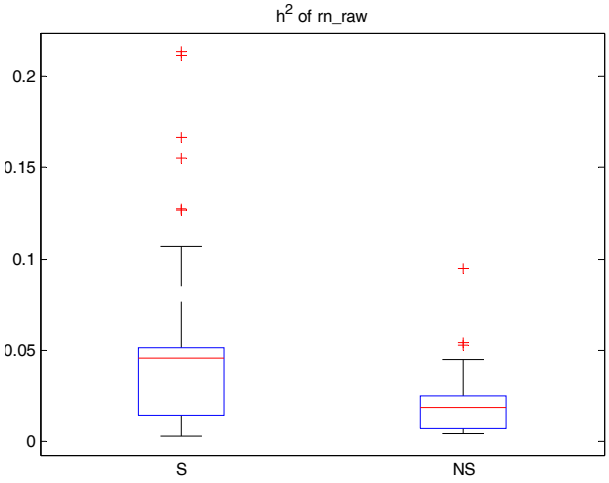

b) (Win2048, Step2048)

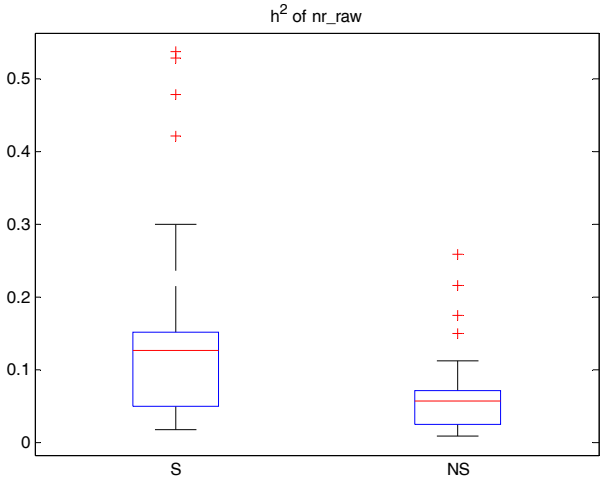

b) (Win2048, Step2048)

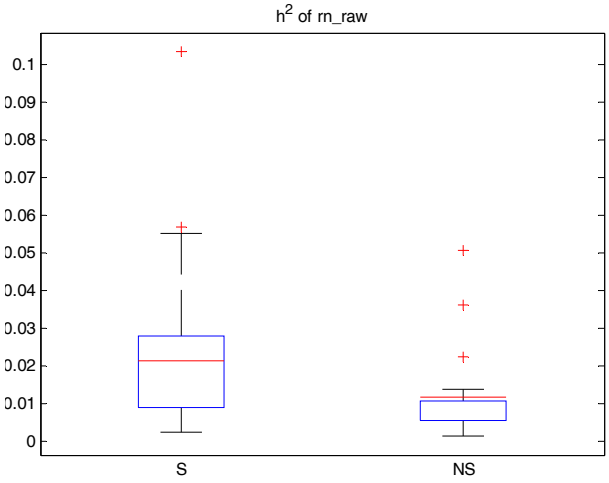

c) (Win4096, Step4096)

RR vs. Nasal Respiration

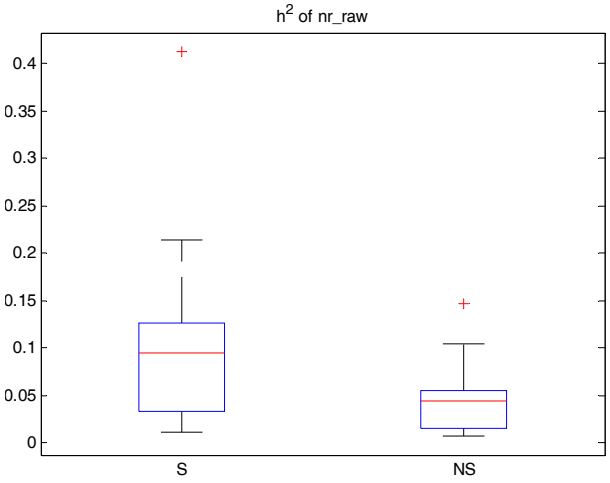

c) (Win4096, Step4096)

Nasal Respiration vs. RR

Fig. B2-14 Boxplot of optimal indexes

- In both left and right column, non-linear regression coefficient h^2 is always lower in non-sepsis infants than in sepsis ones, whichever size of windows.

B2.8 Conclusion

This chapter constitutes a new way of approaching to the problem of monitoring sepsis in the newborns. From the same cohort used for RR analysis, patients were retained, those having respiratory signals recorded. Research work on mutual influence between cardiovascular system variability and nasal respiration was carried out.

Linear and non-linear relationships have been measured. Linear indexes were correlation (r^2), coherence function (*Cohere*) and time-frequency index ($r^2_{t,f}$), while a non-linear regression coefficient (h^2) was used to analyze non-linear relationships.

Concerning linear estimates, we confirm statistically ($p<0.05$ whatever the statistical tests) that the higher correlation is retrieved in the low frequency band for the non-sepsis group between RR and nasal respiration (**r2tf_rn_raw**). Results show that the relationships are circumscribed within a particular region of the time-frequency plane ($0.2<f<0.4$ *Hz*) for the sepsis group and a different one for the non-sepsis group. In addition, several $r^2_{t,f}$ thresholds (*0.6, 07, 0.8, 0.9*) were tested and the threshold *0.8* appears the most discriminative between the two groups.

Regarding non-linear estimates, having such a clinically interesting background, accordingly they are used as mathematical and statistical tools to discriminate the two categories of sepsis and non-sepsis signals. The result obtained using the index h^2 of non-linear regression between RR and nasal respiration in two directions (**h2_rn_raw**, **h2_nr_raw**) were always significant during the entire analysis process. Furthermore, the analysis of non-linear relationship shows that the curves of maximum values of h^2 functions performance a defined peak for non-sepsis case, on the contrary, an arbitrary shape in sepsis group. This fact was retrieved for all the patients.

In conclusion, three indexes from this chapter can be viewed as complementary:

- ⇒ r2tf_rn_raw_0p2_0p4 (the quantity of $r^2_{t,f}$ between RR and original nasal respiration over a threshold set to 0.8 in the sub-band $0.2<f<0.4$ *Hz*)
- ⇒ h2_rn_raw (h^2 between RR and original nasal respiration)
- ⇒ h2_nr_raw (h^2 between original nasal respiration and RR)

They can be chosen as candidate parameters to distinguish sepsis from non-sepsis, which may be a valuable way to diagnosticate sepsis in a non-invasive way, in such delicate patients.

B2.9 Bibliography

[1] G. Baselli, S. Cerutti, F. Badilini*, et al.*, "Model for the assessment of heart period and arterial pressure variability interactions and of respiration influences," *Med Biol Eng Comput,* vol.32*(2)*, pp.143-152, Mar, 1994.

[2] F. Raschke, "Coordination in the circulatory systems," in *Temporal disorder in human oscillatory systems*, L. Rensing, U. an der Heiden, and M. C. Mackey, Eds., Berlin: Springer, 1987.

[3] F. Raschke, "The respiratory system – features of modulation and coordination in Rhythms in physiological systems ", H. Haken and H. P. Koepchen, Eds., Berlin: Springer, 1991, pp. 155-164.

[4] D. Cysarz, H. Bettermann, S. Lange*, et al.*, "A quantitative comparison of different methods to detect cardiorespiratory coordination during night-time sleep," *Biomed Eng Online,* vol.3*(1)*, p.44, Nov 25, 2004.

[5] C. A. Chapman, Y. Xu, S. Haykin*, et al.*, "Beta-frequency (15-35 Hz) electroencephalogram activities elicited by toluene and electrical stimulation in the behaving rat," *Neuroscience,* vol.86*(4)*, pp.1307-1319, Oct, 1998.

[6] M. A. Brazier, "Studies of the EEG activity of limbic structures in man," *Electroencephalogr Clin Neurophysiol,* vol.25*(4)*, pp.309-318, Oct, 1968.

[7] J. Gotman, "Interhemispheric interactions in seizures of focal onset: data from human intracranial recordings," *Electroencephalogr Clin Neurophysiol,* vol.67*(2)*, pp.120-133, Aug, 1987.

[8] R. B. Duckrow and S. S. Spencer, "Regional coherence and the transfer of ictal activity during seizure onset in the medial temporal lobe," *Electroencephalogr Clin Neurophysiol,* vol.82*(6)*, pp.415-422, Jun, 1992.

[9] P. J. Franaszczuk and G. K. Bergey, "Application of the directed transfer function method to mesial and lateral onset temporal lobe seizures," *Brain Topogr,* vol.11*(1)*, pp.13-21, Fall, 1998.

[10] P. J. Franaszczuk and G. K. Bergey, "An autoregressive method for the measurement of synchronization of interictal and ictal EEG signals," *Biol Cybern,* vol.81*(1)*, pp.3-9, Jul, 1999.

[11] A. L. Goldberger, "Non-linear dynamics for clinicians: chaos theory, fractals, and complexity at the bedside," *Lancet,* vol.347*(9011)*, pp.1312-1314, May 11, 1996.

[12] K. Ansari-Asl, J. J. Bellanger, F. Bartolomei*, et al.*, "Time-frequency characterization of interdependencies in nonstationary signals: application to epileptic EEG," *IEEE Trans Biomed Eng,* vol.52*(7)*, pp.1218-1226, Jul, 2005.

[13] T. Rantonen, J. Jalonen, J. Gronlund*, et al.*, "Increased amplitude modulation of continuous respiration precedes sudden infant death syndrome -detection by spectral estimation of respirogram," *Early Hum Dev,* vol.53*(1)*, pp.53-63, Nov, 1998.

Chapter B3
Real time detection using HRV and interrelationship between HRV and respiratory signal

B3.1 Introduction

As already mentioned elsewhere in this PhD thesis, transient episodes of apnea and bradycardia are common in preterm infants [1]. These episodes may seriously compromise oxygenation and tissue perfusion and, when they become prolonged and repetitive, they may lead to neurological morbidity or even infant death. Premature infants in Neonatal Intensive Care Units (NICU) are continuously monitored through polygraphic recording, to detect bradycardia events and to initiate quick nursing actions (manual or vibrotactile stimulation, oxygenation, ventilation through a mask or intubation) [2]. Typically, when an infant presents a bradycardia event, an alarm is generated by a monitoring device, an available nurse or physician goes to the appropriate NICU room, washes his/her hands, and applies a manual stimulation to the infant in distress. The mean intervention delay, measured from the activation of the alarm to the application of the therapy has been estimated to be around 33 seconds, with a mean manual stimulation duration of 13 seconds, in order to terminate the event of apnea-bradycardia [3]. However, even if algorithms for bradycardia detection have been developed, they are inefficient and usually produce false or late alarms.

The objective of this chapter is to add a new device to the apnea-bradycardias detection of the used monitors. The device is related to infection detection in NICU. So, we study the feasibility of its implementation in NICU with the proposed features presented from Chapter B1 and Chapter B2. Here, a new architecture for the decision level is proposed and based upon the combination of several features, also called Decision Fusion. This principle of Optimal Fusion is first described in section B3.2. In section B3.3, Receiver Operating Characteristic (ROC) space and curve are recalled. We offer experimental protocol in section B3.4. Results of Mono-Channel features and Bi-Channel features are demonstrated and discussed in section B3.5 and section B3.6 respectively. And then, the fusion of all mix features is done and synthesis discussed in section B3.7. Finally, we conclude with summary in section B3.8.

B3.2 Fusion Rules

Different fusion rules can be used to combine local detections (obtained from each algorithm) into a final decision u. Some simple rules are based on a "k out of n" function ($k<n$). Special cases of this function include the AND, the OR and the MAJOR rules. However, there has been an important effort to obtain the OPTIMAL FUSION rules, based often on the weighted combination of each local detection, that provide a higher weight to the more reliable detectors. In this work we have used the optimality criterion proposed by Chair and Varshney [4], which has been seen relevant in several studies performed in our lab (Alfredo HERNANDEZ [5], Miguel ALTUVE [6]). The principles are briefly recalled here.

B3.2.1 Preliminaries

Let us consider a binary hypothesis testing problem with the following two hypotheses:

- H_0: signal is absent
- H_1: signal is present.

The a priori probabilities of the two hypotheses are denoted by $P(H_0) = P_0$ and $P(H_1) = P_1$. As shown in Fig. B3-1, we assume that there are n detectors and the observations at each detector are denoted by y_i, $i = 1, \ldots, n$.

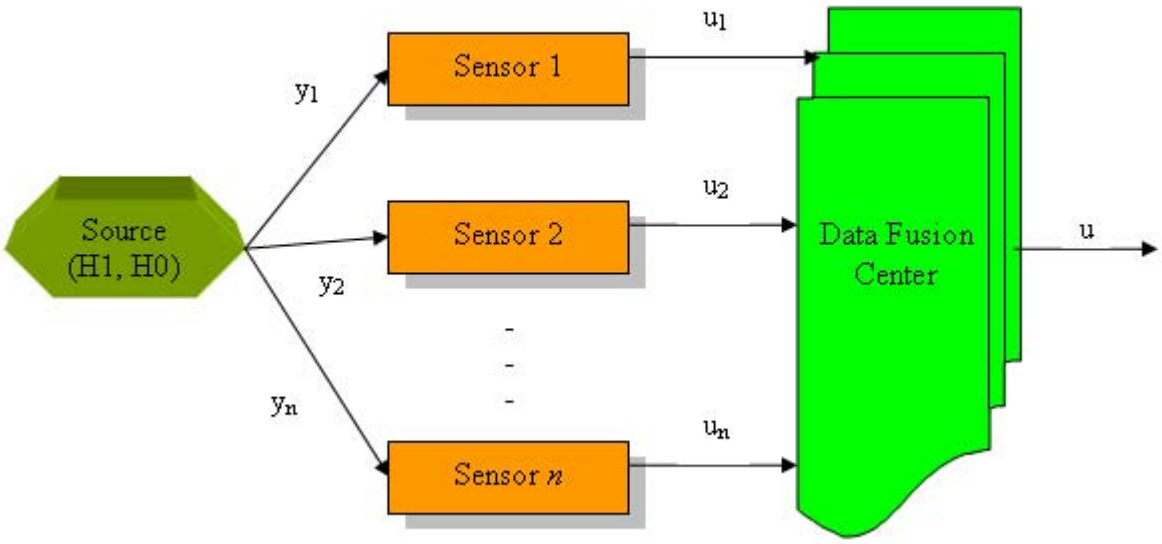

Fig. B3-1 Distributed detection system with data fusion center

We further assume that the observations at the individual detectors are statistically independent and that the conditional probability density function is denoted by
$p(y_i \mid H_j)$, $i = 1, ..., n$, $j = 1, 2$. Each detector employs a decision rule $g_i(y_i)$ to make a decision u_i, i = 1, ..., n,
where

$$u_i = \begin{cases} -1, & if\ H_0\ is\ declared \\ +1, & if\ H_1\ is\ declared \end{cases} \tag{7.1}$$

We denote the probabilities of false alarm and miss of each detector by P_{F_i} and P_{M_i}, respectively.

After processing the observations locally, the decisions u_i are transmitted to the data fusion center. The data fusion center determines the overall decision for the system u based on the individual decisions, *i.e.* ,

$$u = f(u_1, \cdots, u_n). \tag{7.2}$$

In the next section, we consider the optimization of the data fusion algorithm.

B3.2.2 Optimal Fusion

As indicated earlier, Tenney and Sandell [7] considered the Bayesian detection problem. They did not, however, consider the optimization of the data fusion rule. We consider the problem of optimization of the data fusion rule for given detectors, that is, when the individual detectors have already been designed.

Data fusion rules are often implemented as "*k* out of *n*" logical functions. This means that if *k* or more detectors decide hypothesis H_1, then the global decision is H_1, i.e.,

$$u = \begin{cases} 1, & \text{if } u_1 + u_2 + \cdots + u_n \geq 2k - n \\ -1, & \text{otherwise} \end{cases} \tag{7.3}$$

Common logical functions such as AND, OR, and majority gate are special cases of the *k* out of *n* rule. In this section, we consider a more general formulation of the data fusion problem.

The data fusion problem can be viewed as a two hypothesis detection problem with individual detector decisions being the observations. The optimum decision rule is given by the following likelihood ratio test.

$$\frac{P(u_1, \cdots, u_n / H_1)}{P(u_1, \cdots, u_n / H_0)} \underset{H_0}{\overset{H_1}{\gtrless}} \frac{P_0(C_{10} - C_{00})}{P_1(C_{01} - C_{11})} \tag{7.4}$$

The quantity on the left-hand side is the likelihood ratio and the Bayes optimum threshold is on the right-hand side. In our formulation we assume the minimum probability of error criterion, that is, $C_{00} = C_{11} = 0$, and $C_{10} = C_{01} = 1$. Therefore, we have

$$\frac{P(u/H_1)}{P(u/H_0)} \underset{H_0}{\overset{H_1}{\gtrless}} \frac{P_0}{P_1} \tag{7.5}$$

Using Bayes rule to express the conditional probabilities, substituting and simplifying, we obtain

$$\frac{P(H_1/u)}{P(H_0/u)} \underset{H_0}{\overset{H_1}{\gtrless}} 1 \tag{7.6}$$

The corresponding log-likelihood ratio test is

$$\log \frac{P(H_1/u)}{P(H_0/u)} \underset{H_0}{\overset{H_1}{\gtrless}} 0 \tag{7.7}$$

We found an expression for the left-hand side in order to implement the data fusion rule, and the result is presented as the theorem in Appendix IX.

Therefore, the data fusion rule that we used in this study can be expressed by:

$$f(u_1,\cdots,u_n)=\begin{cases}1, & if\ a_0+\sum_{i=1}^{n}a_iu_i>\lambda\\ -1, & otherwise\end{cases} \tag{7.8}$$

where the optimum weights are given by

$$\begin{aligned}a_0&=\log\frac{P_1}{P_0}\\ a_i&=\log\frac{1-P_{M_i}}{P_{F_i}},\quad if\ u_i=+1\\ a_i&=\log\frac{1-P_{F_i}}{P_{M_i}},\quad if\ u_i=-1\end{aligned} \tag{7.9}$$

The optimum data fusion rule can be implemented as shown in Fig. B3-2. As we can observe, individual detector decisions are weighted according to their reliability, that is, the weights are functions of probability of false alarm and probability of miss. The data fusion structure obtained here attempts to optimally use the individual detector decisions by forming a weighted sum and then comparing it to a threshold λ.

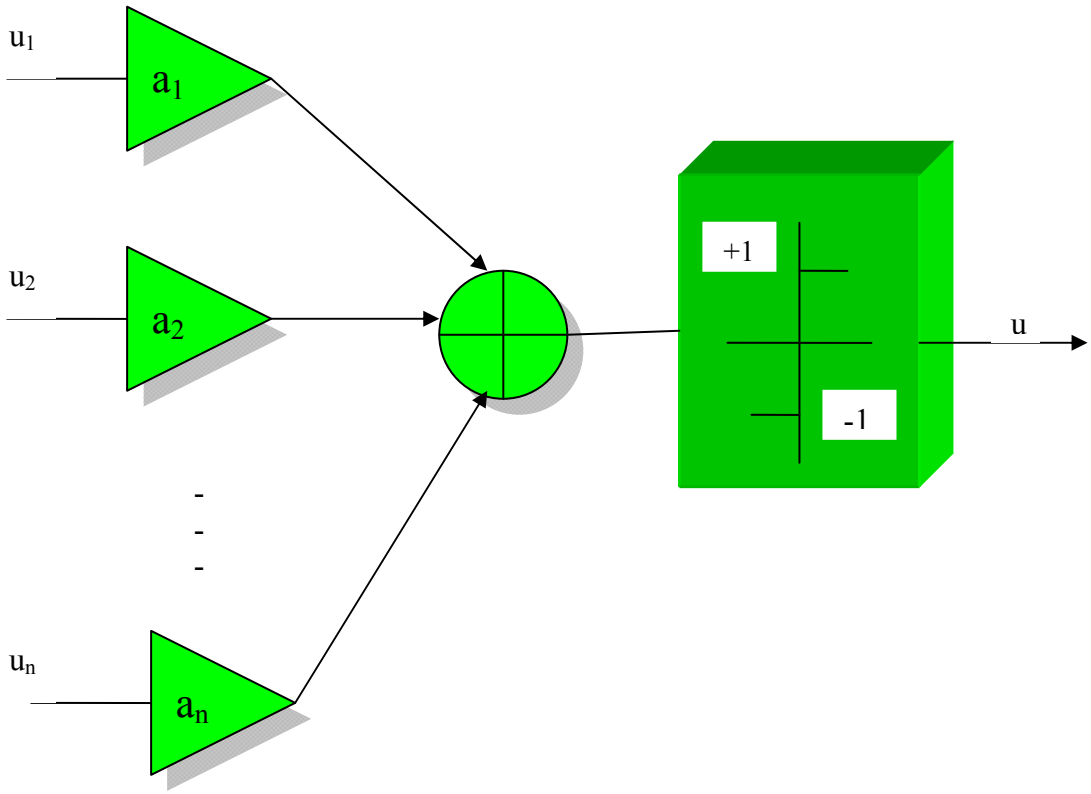

Fig. B3-2 Optimum data fusion center structure

B3.3 Receiver Operating Characteristic (ROC)

In signal detection theory, a receiver operating characteristic, or simply ROC curve, is a graphical plot which illustrates the performance of a binary classifier system as its discrimination threshold is varied. [8] The ROC is created by plotting the fraction of true positives out of the positives (TPR = true positive rate) vs. the fraction of false positives out of the negatives (FPR = false positive rate), at various threshold settings. (TPR is also known as sensitivity, and FPR is one minus the specificity or true negative rate.)

ROC analysis provides tools to select possibly optimal models and to discard suboptimal ones independently from (and prior to specifying) the cost context or the class distribution. ROC analysis is related in a direct and natural way to cost/benefit analysis of diagnostic decision making. The ROC curve was first developed by electrical engineers and radar engineers during World War II for detecting enemy objects in battle fields and was soon introduced to psychology to account for perceptual detection of stimuli. In medicine, ROC analysis has been extensively used in the evaluation of diagnostic tests. [9] [10] ROC curves are also used extensively in epidemiology and medical research and are frequently mentioned in conjunction with evidence-based medicine. In addition, ROC analysis since then has been used in radiology, biometrics, and other areas for many decades and is increasingly used in machine learning and data mining research.

B3.3.1 Basic Concept

A classification model (classifier or diagnosis) is a mapping of instances between certain classes/groups. The classifier or diagnosis result can be a real value (continuous output), in which case the classifier boundary between classes must be determined by a threshold value (for instance, to determine whether a person has hypertension based on a blood pressure measure). Or it can be a discrete class label, indicating one of the classes.

Let us consider a two-class prediction problem (binary classification), in which the outcomes are labeled either as positive (*p*) or negative (*n*). There are four possible outcomes from a binary classifier. If the outcome from a prediction is *p* and the actual value is also *p*, then it is called a true positive (TP); however if the actual value is *n* then it is said to be a false positive (FP). Conversely, a true negative (TN) has occurred when both the prediction outcome and the actual value are *n*, and false negative (FN) is when the prediction outcome is *n* while the actual value is *p*.

To get an appropriate example in a real-world problem, consider a diagnostic test that seeks to determine whether a person has a certain disease. A false positive in this case occurs when the person tests positive, but actually does not have the disease. A false negative, on the other hand, occurs when the person tests negative, suggesting they are healthy, when they actually do have the disease.

Let us define an experiment from P positive instances and N negative instances. The four outcomes can be formulated in a 2×2 contingency table or confusion matrix, as follows:

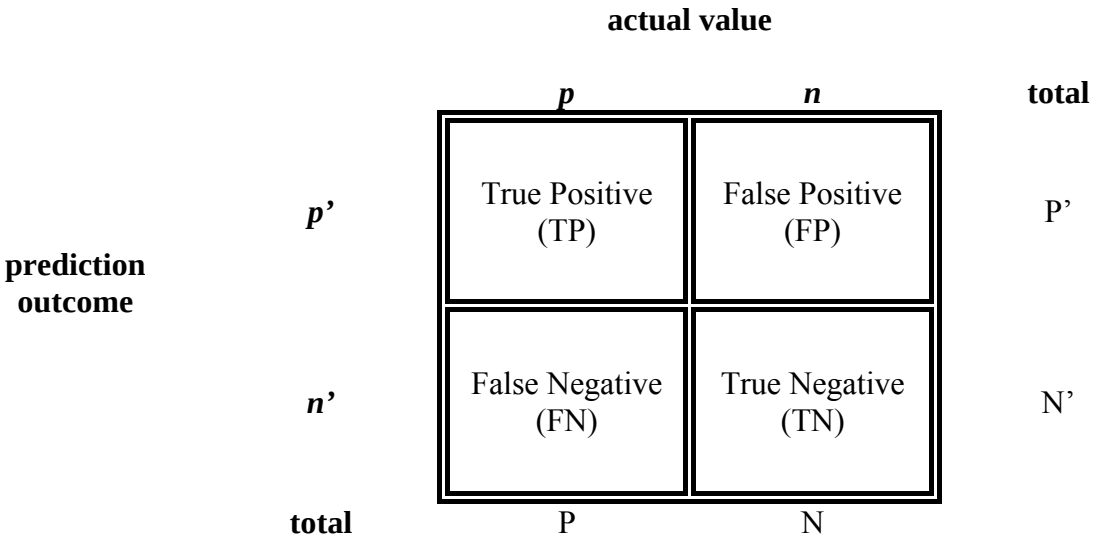

Fig. B3-3 Principle of ROC Matrix

In our research, FPR values specify Probability of False Alarm (P_{FA}), and TPR values imply Probability of Detection (P_D).

B3.3.2 ROC Space

The contingency table can derive several evaluation "metrics". To draw an ROC curve, only the TPR and FPR are needed (as functions of some classifier parameter). The TPR defines how many correct positive results occur among all positive samples available during the test. FPR, on the other hand, defines how many incorrect positive results occur among all negative samples available during the test.

An ROC space is defined by FPR and TPR as x and y axes respectively, which depicts relative trade-offs between true positive (benefits) and false positive (costs). Since TPR is equivalent with sensitivity and FPR is equal to 1 − specificity, the ROC graph is sometimes called the sensitivity vs. (1 − specificity) plot. Each prediction result or instance of a confusion matrix represents one point in the ROC space.

The best possible prediction method would yield a point in the upper left corner or coordinate (0, 1) of the ROC space, representing 100% sensitivity (no false negatives) and 100% specificity (no false positives). The (0, 1) point is also called a perfect classification. A completely random guess would give a point along a diagonal line (the so-called line of no-discrimination) from the left bottom to the top right corners (regardless of the positive and negative base rates). An intuitive example of random guessing is a decision by flipping coins (heads or tails). As the size of the sample increases, a random classifier's ROC point migrates towards (0.5, 0.5).

The diagonal divides the ROC space. Points above the diagonal represent good classification results (better than random), points below the line poor results (worse than random). Note that the output of a consistently poor predictor could simply be inverted to obtain a good predictor.

B3.4 Experimentation

The objective in this chapter was to study the feasibility of real time detection for sepsis or non-sepsis hypothesis. To reach this goal, firstly, we mix 13 sepsis and 13 non-sepsis infants and then randomly select for 50 times. For each random selection, we connect 26 segments into one long series including 30.3 hours (see Fig. B3-4). Therefore, the whole 50 time selections contain 1515 hours.

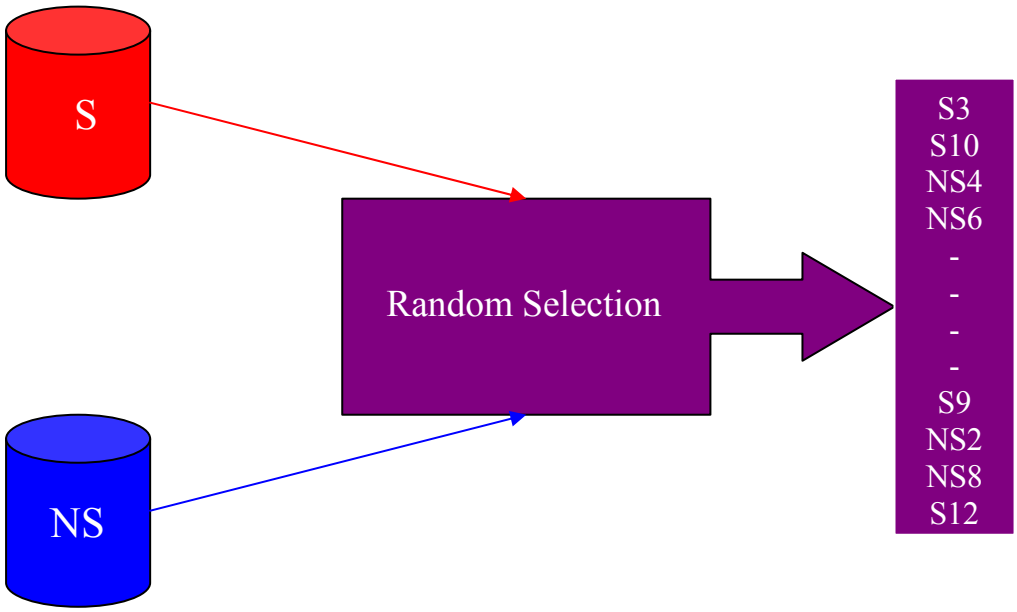

Fig. B3-4 Random Selection

Secondly, on the one hand, three features from Mono-Channel analysis in Chapter B1: alphaS (alpha Slow), alphaF (alpha Fast) and SamEn (Sample Entropy) were selected. On the other hand, three estimates from Bi-Channel analysis in Chapter B2, we denote them in the following:

⇒ r2tf_rn_raw_0p2_0p4 (the quantity of $r^2_{t,f}$ between RR and original nasal respiration over a threshold set to 0.8 in the sub-band $0.2<f<0.4$ *Hz*)

⇒ h2_rn_raw (h^2 between RR and original nasal respiration)

⇒ h2_nr_raw (h^2 between original nasal respiration and RR)

are recognized as optimal methods to distinguish sepsis from non-sepsis.

These candidate parameters are recalculated over these 50 long series in the sliding window with the same length step using three sizes 1024/2048/4096 as depicted in Fig. B3-5. Finally, we did five tests reported in Table B3-1 for these long series.

Table B3-1 Five tests for Feasibility Study

Test	Features	Explanations
Test 1	alphaS alphaF SamEn	For each long series, we compare alphaS values with 1000 thresholds and use ROC analysis in order to plot ROC curve one by one. In total, there are 50 ROC curves for alphaS. So, do the same for alphaF and SamEn.
Test 2	Optimal Fusion Mono-Channel	We combined alphaS, alphaF and SamEn by fusion rule: Optimal Fusion
Test 3	r2tf_rn_raw h2_rn_raw h2_nr_raw	For each long series, we compare r2tf_rn_raw values with 1000 thresholds and use ROC analysis in order to plot ROC curve one by one. In total, there are 50 ROC curves for r2tf_rn_raw. So, do the same for the two others.
Test 4	Optimal Fusion Bi-Channel	We combined r2tf_rn_raw, h2_rn_raw and h2_nr_raw by fusion rule: Optimal Fusion
Test 5	Optimal Fusion All	We combined all features by fusion rule: Optimal Fusion

We recall here that a window size of 1024 samples is equivalent to 4.3mins duration, 2048 samples to 8.6mins and 4096 samples to 17.2mins respectively, which is a very acceptable value in practice due to the fact actual evaluation are generally performed every 6 hours.

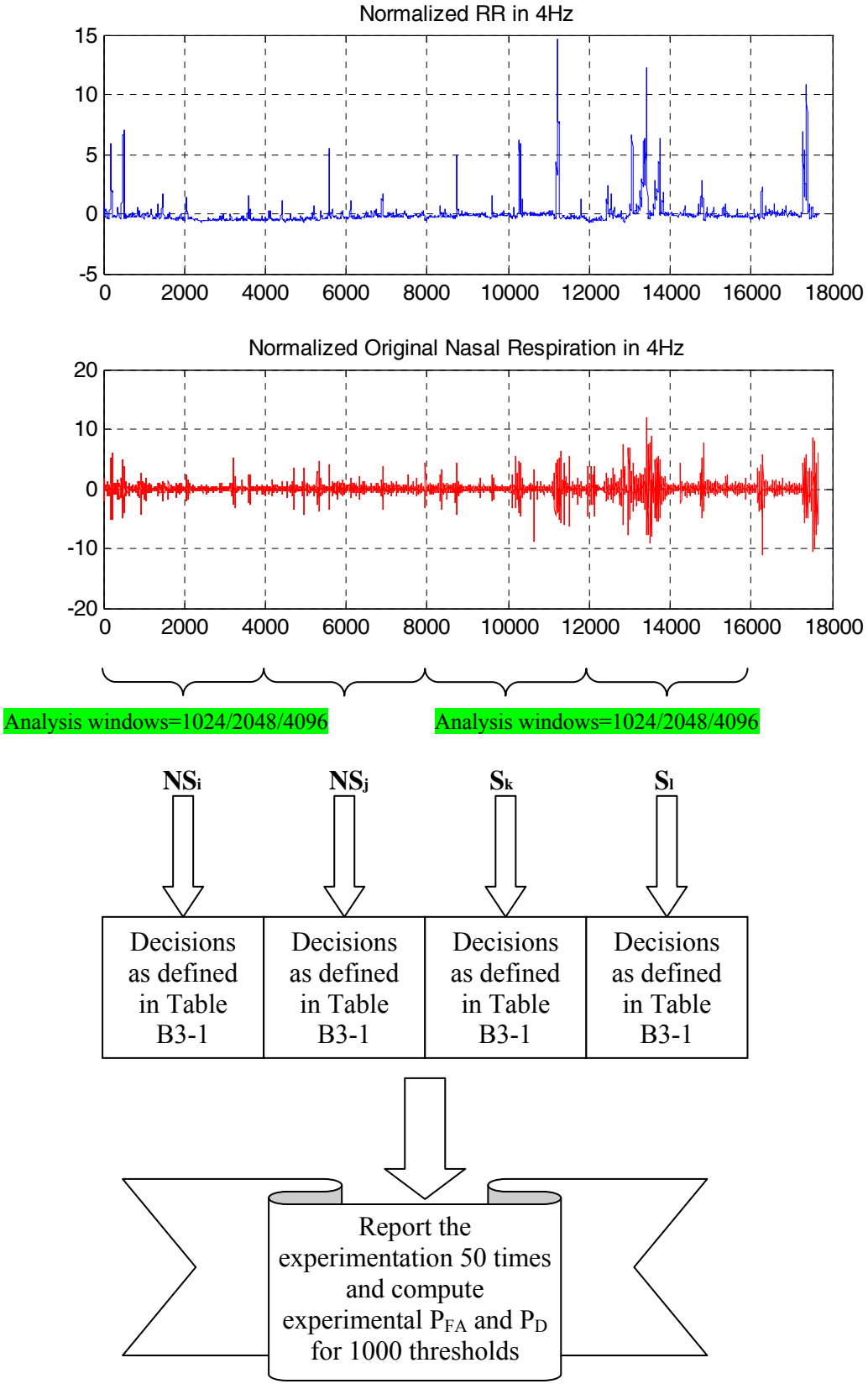

Fig. B3-5 Analysis windows over Normalized RR and Original Nasal Respiration, NS stands for non-sepsis, while S stands for sepsis

We summarized the experimental procedure in following flow chart (Fig. B3-6):

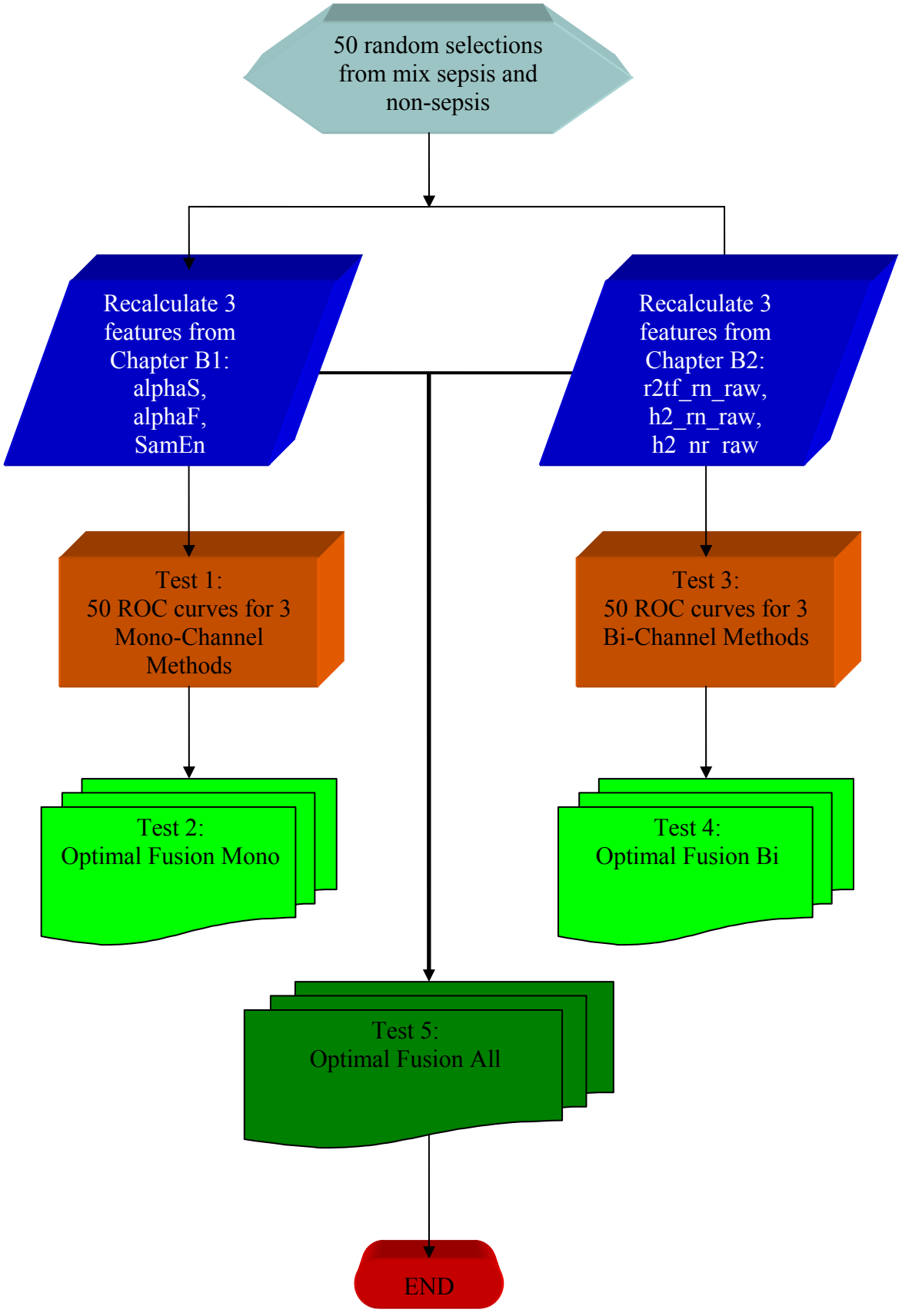

Fig. B3-6 Flow chart of ROC Analysis

B3.5 Results and Discussion of ROC analysis for RR series features

We propose here to firstly describe the results and then we discuss all the performances at the end of this chapter. Test 1 to Test 5 is reported in the following.

We retained here each time the same procedure:
i) Display of the ROC curves for the three window sizes.
ii) Comparative table of the optimal detection point.

B3.5.1 Test 1

In Chapter B1, alphaS, alphaF and SamEn are identified as optimal methods to distinguish sepsis from non-sepsis.The analysis procedure were already described in Section B2.4, and the ROC curves computed 50 times selections over three different sizes of window.

In this case, the tactic for decision making is to compare the statistic S(x) to thresholds, let

$$S(x) > \lambda \tag{7.10}$$

where S(x) is either alphaS, alphaF or SamEn.

All results are reported in Fig. B3-7, Fig. B3-8 and Fig. B3-9 respectively.

B3.5.1.1 Window=1024, Step=1024

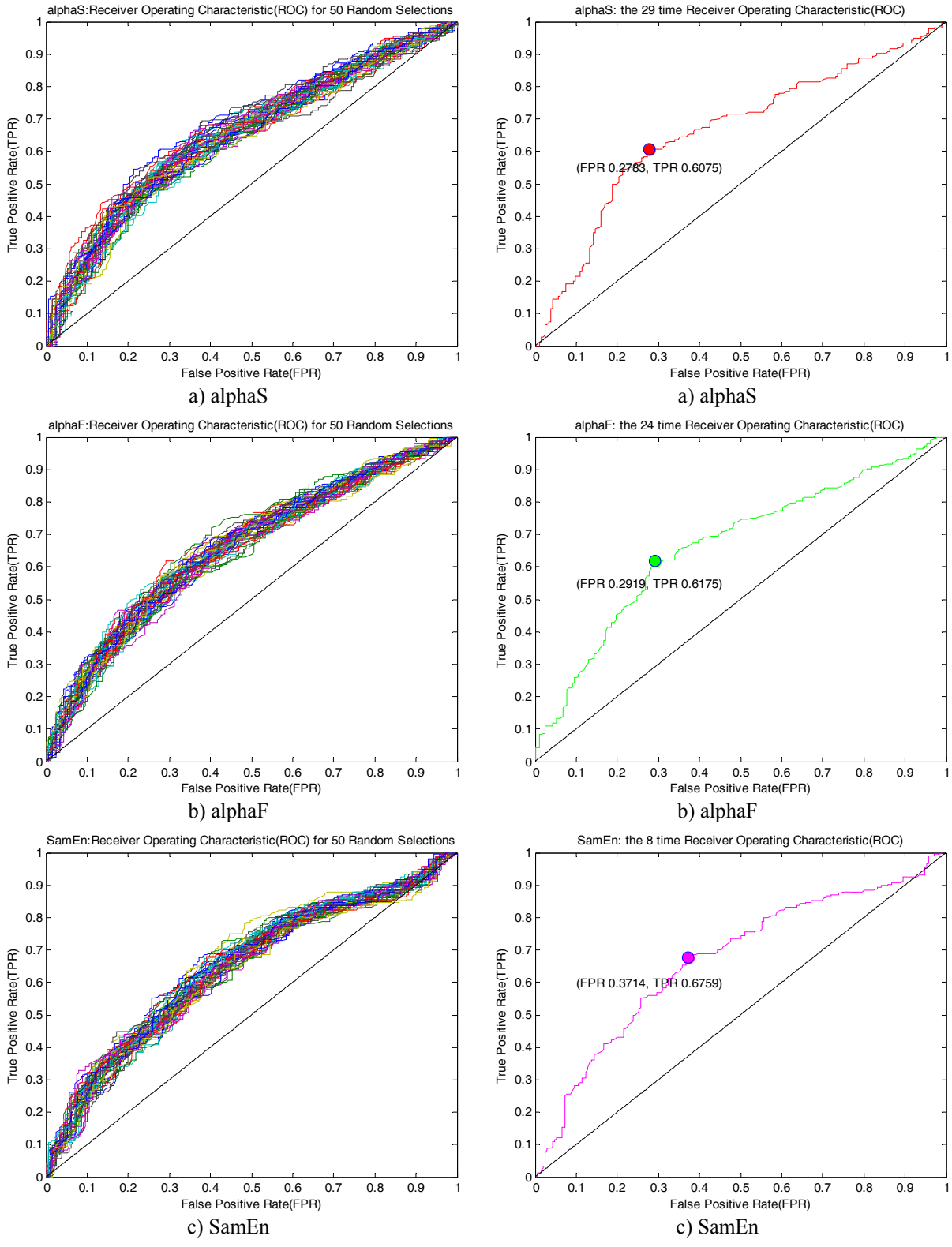

Fig. B3-7 ROC curves in Test 1, Window=1024, Step=1024

In Fig. B3-7, the left column displays 50 ROC curves for each feature, while the right column shows the nearest-upper-left ROC curve, where the points the closest to upper left corner (0, 1) is marked as round point.

B3.5.1.2 Window=2048, Step=2048

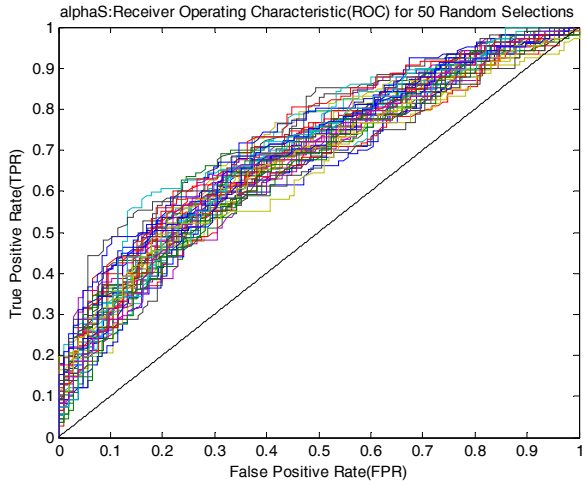

a) alphaS

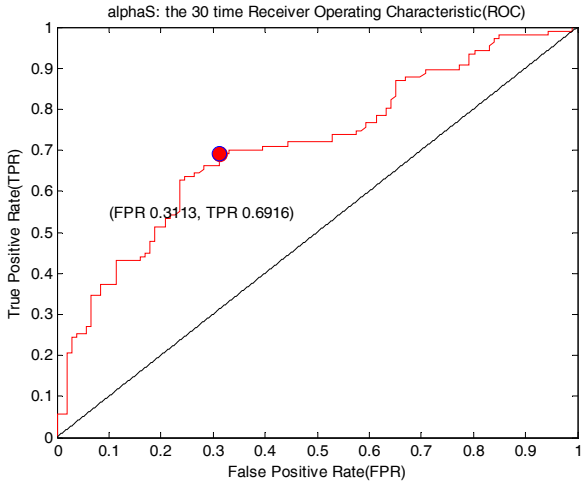

a) alphaS

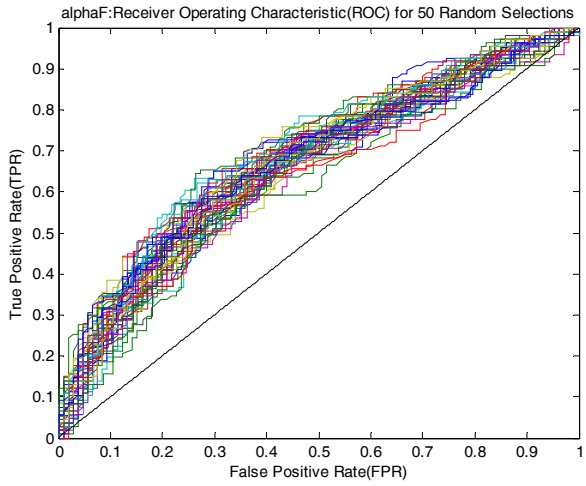

b) alphaF

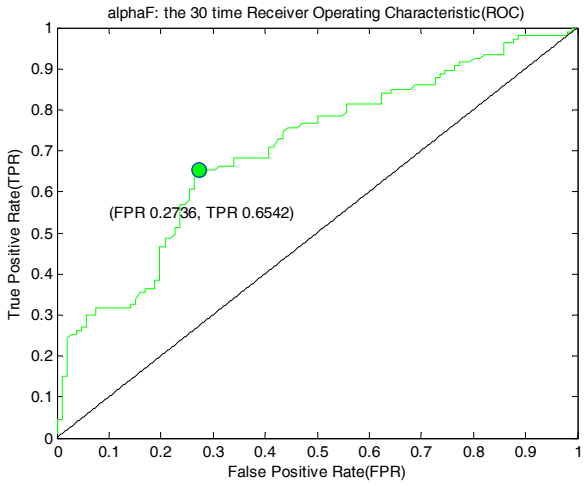

b) alphaF

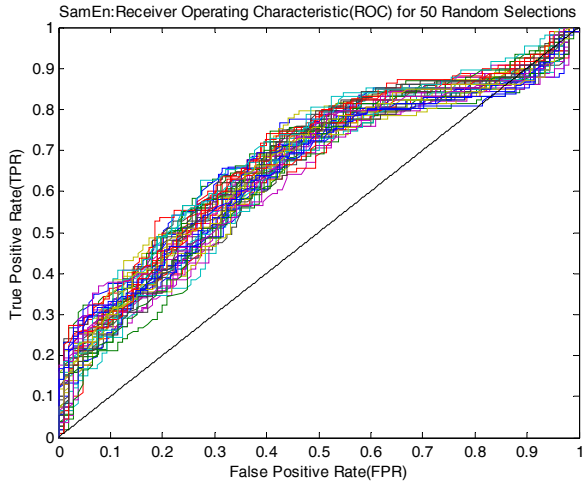

c) SamEn

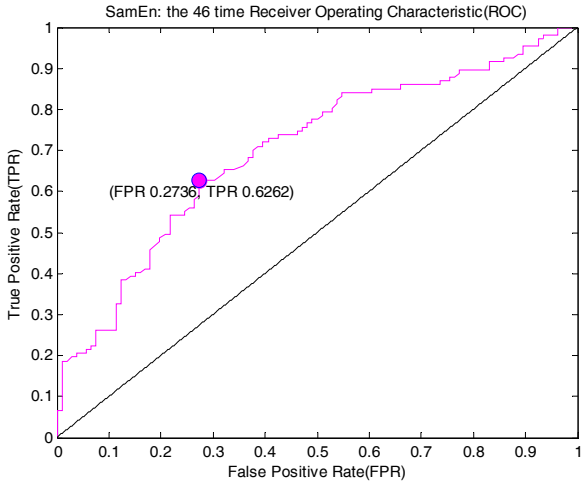

c) SamEn

Fig. B3-8 ROC curves in Test 1, Window=2048, Step=2048

B3.5.1.3 Window=4096, Step=4096

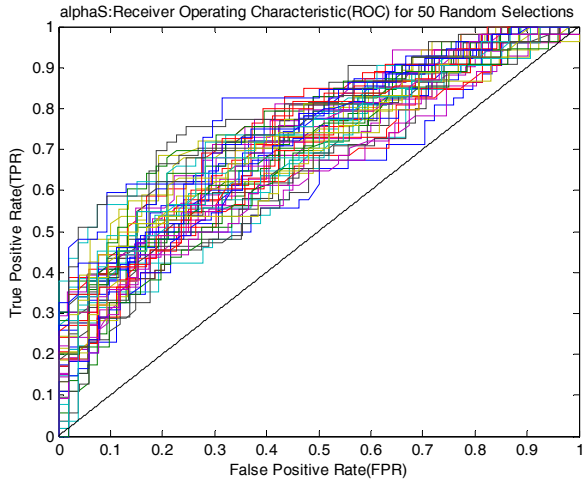

a) alphaS

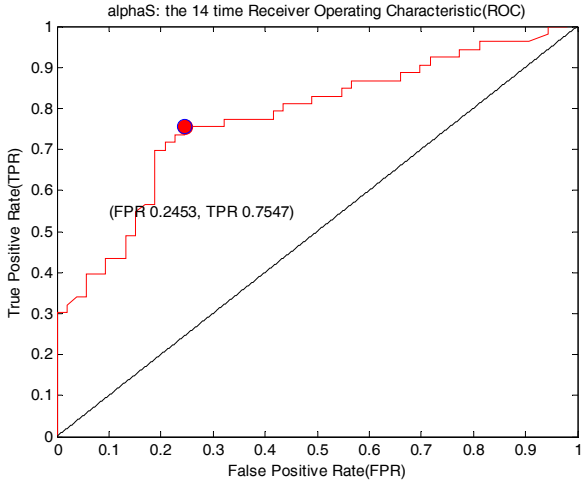

a) alphaS

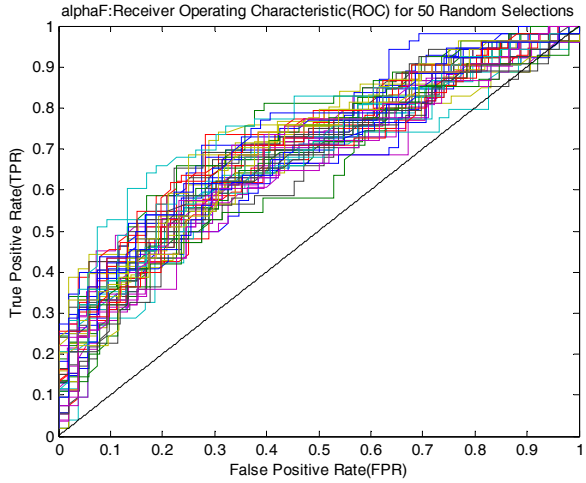

b) alphaF

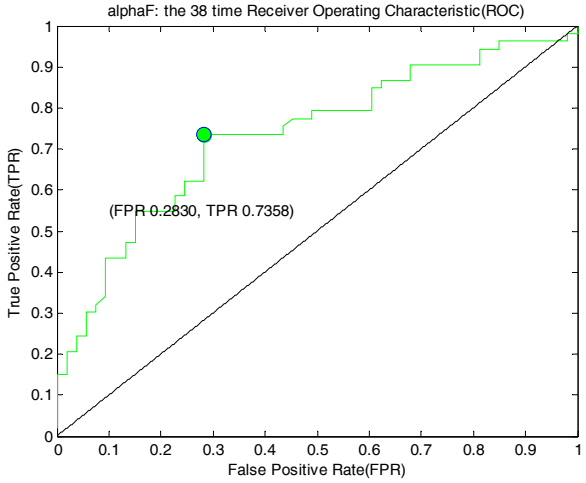

b) alphaF

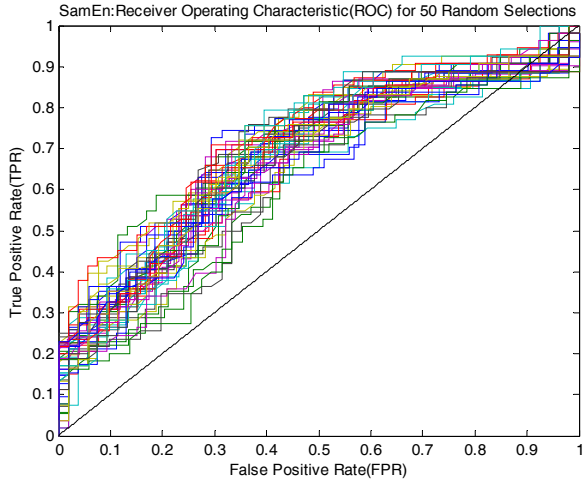

c) SamEn

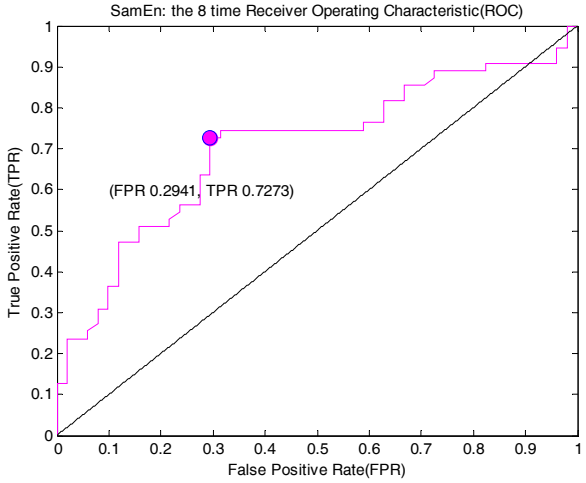

c) SamEn

Fig. B3-9 ROC curves in Test 1, Window=4096, Step=4096

B3.5.2 Test 2

We combined alphaS, alphaF and SamEn using Optimal Fusion in Mono-Channel, then its ROC curves are illustrated in Fig. B3-10.

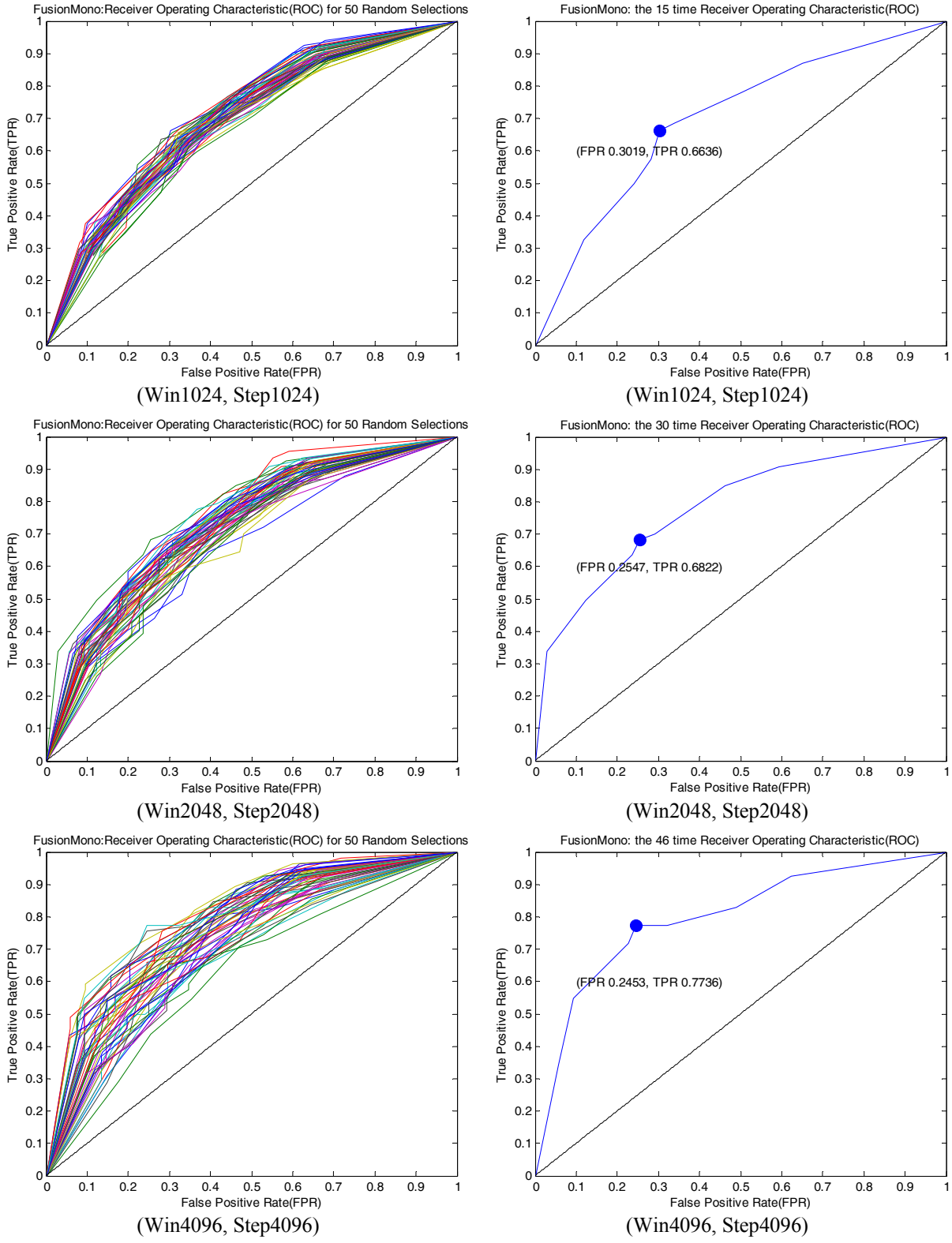

(Win1024, Step1024) (Win1024, Step1024)

(Win2048, Step2048) (Win2048, Step2048)

(Win4096, Step4096) (Win4096, Step4096)

Fig. B3-10 ROC curves in Test 2

In Fig. B3-10, the left column displays 50 ROC curves of Optimal Fusion for three features in Mono-Channel, while the right column shows the nearest-upper-left ROC curve, where the points the closest to upper left corner (0, 1) is marked as blue round point.

B3.6 Results and Discussion of ROC analysis for features of relationship between RR series and Respiration

B3.6.1 Test 3

In Chapter B2, r2tf_rn_raw_0p2_0p4, h2_rn_raw and h2_nr_raw are identified as optimal methods to distinguish sepsis from non-sepsis.

In Test 3, there are two cases:

- In the case of $r^2_{t,f}$, it counts the number of time that the value of $r^2_{t,f}$ >0.8 in frequency band [0.2 0.4], then the statistics S(x) compare this number to a threshold. The final statistic is

$$S(x) = N_{0.2}^{0.4} > \lambda \tag{7.11}$$

- In the case of h^2, the statistic *S(x)* compares the values of h^2 to thresholds, let:

$$S(x) = h^2 > \lambda \tag{7.12}$$

The experimental condition of the previous section was re-conducted here, but using two channels (HRV and respiration). Fig. B3-11, Fig. B3-12 and Fig. B3-13 depict the ROC curves of crucial estimates in Bi-channel over three different sizes of window separately.

B3.6.1.1 Window=1024, Step=1024

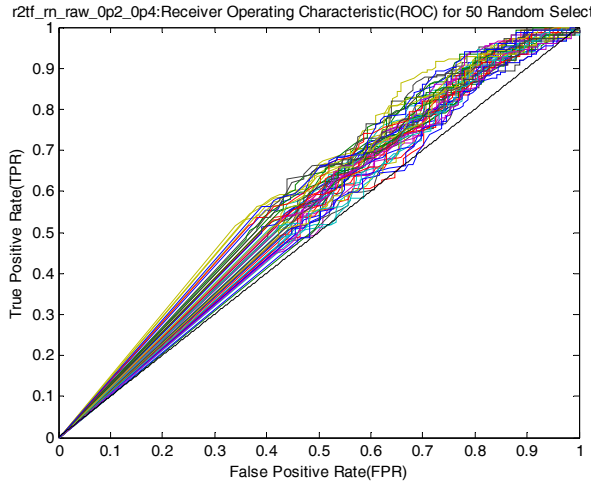

a) r2tf_rn_raw

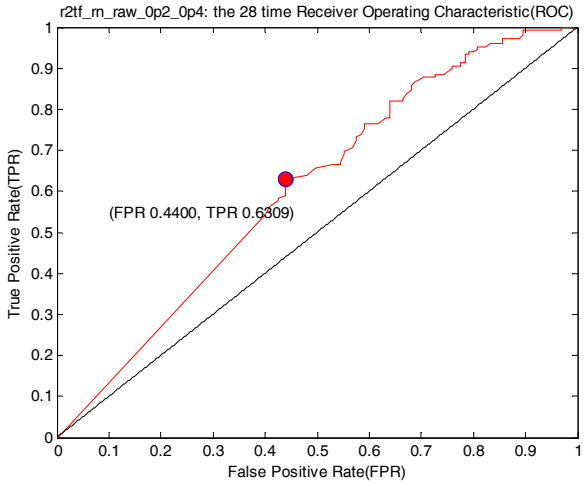

a) r2tf_rn_raw

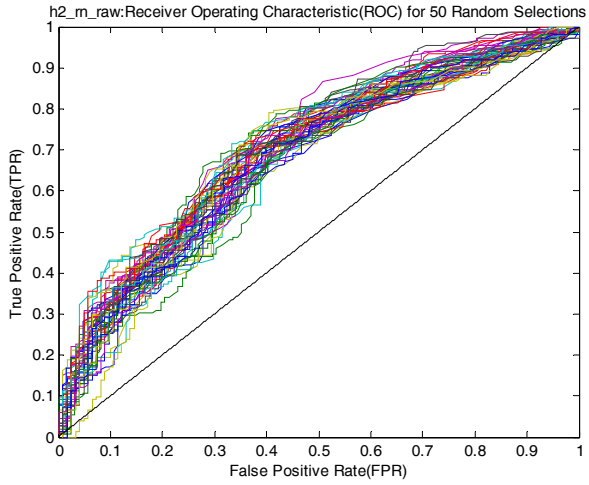

b) h2_rn_raw

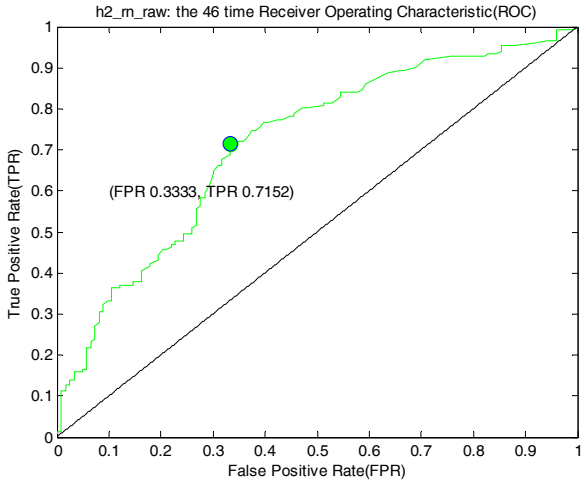

b) h2_rn_raw

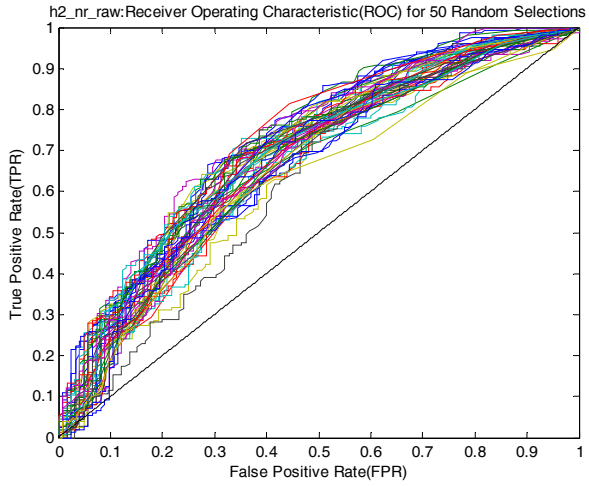

c) h2_nr_raw

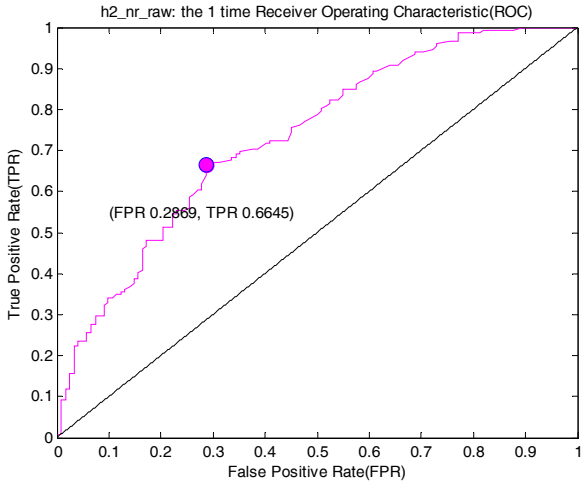

c) h2_nr_raw

Fig. B3-11 ROC curves in Test 3, Window=1024, Step=1024

B3.6.1.2 Window=2048, Step=2048

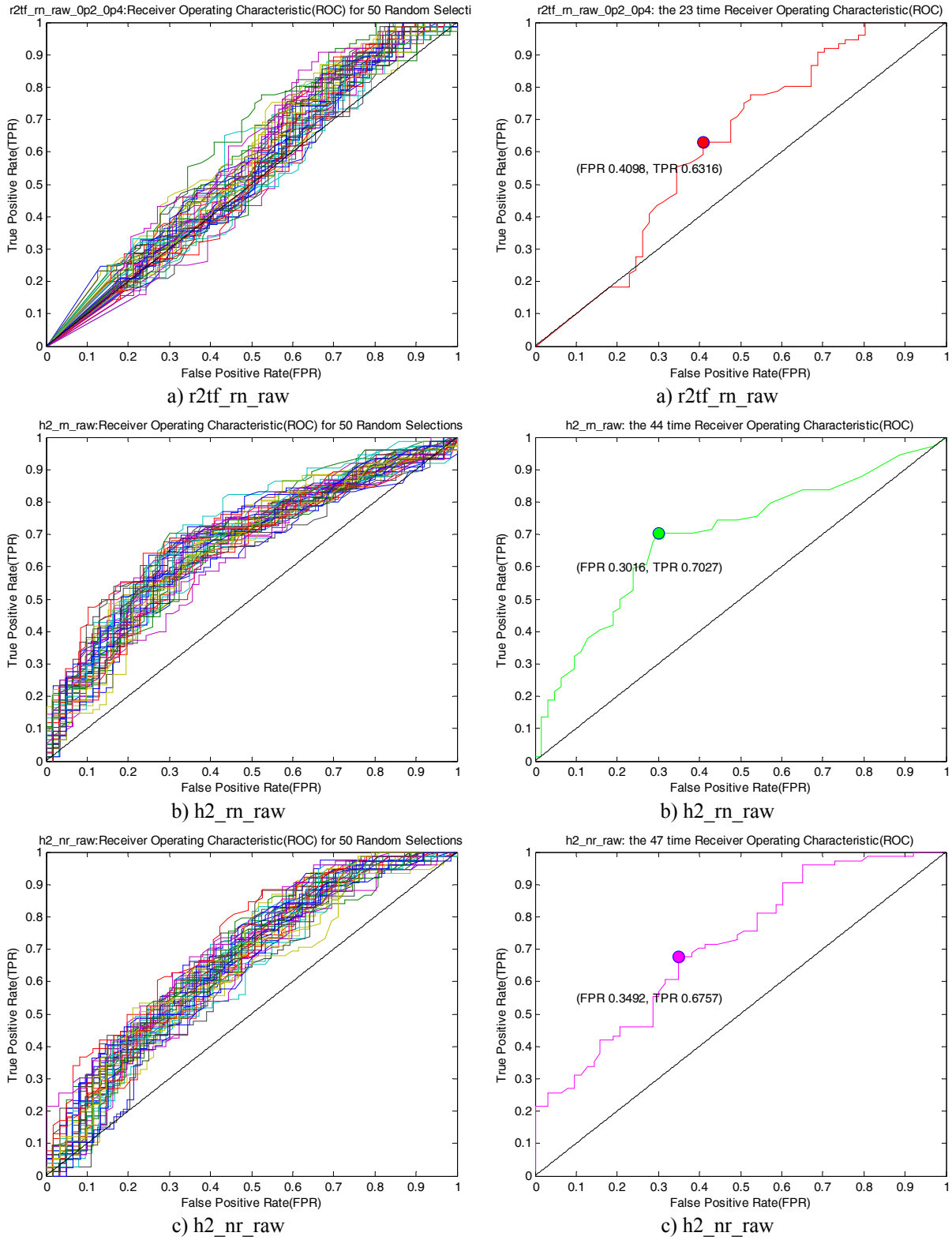

Fig. B3-12 ROC curves in Test 3, Window=2048, Step=2048

B3.6.1.3 Window=4096, Step=4096

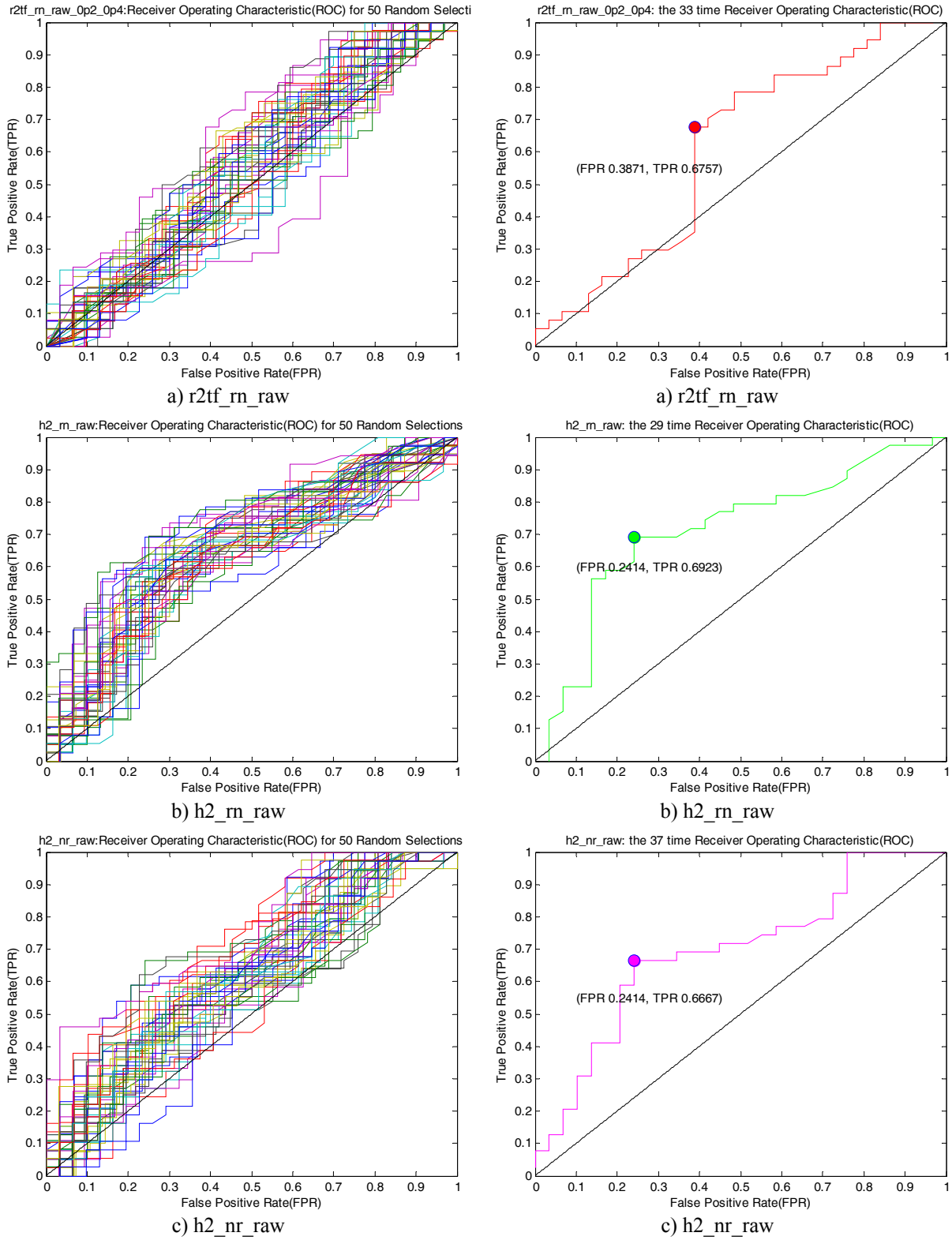

Fig. B3-13 ROC curves in Test 3, Window=4096, Step=4096

B3.6.2 Test 4

We blended r2tf_rn_raw_0p2_0p4, h2_rn_raw and h2_nr_raw using Optimal Fusion in Bi-Channel, then its ROC curves are demonstrated in Fig. B3-14.

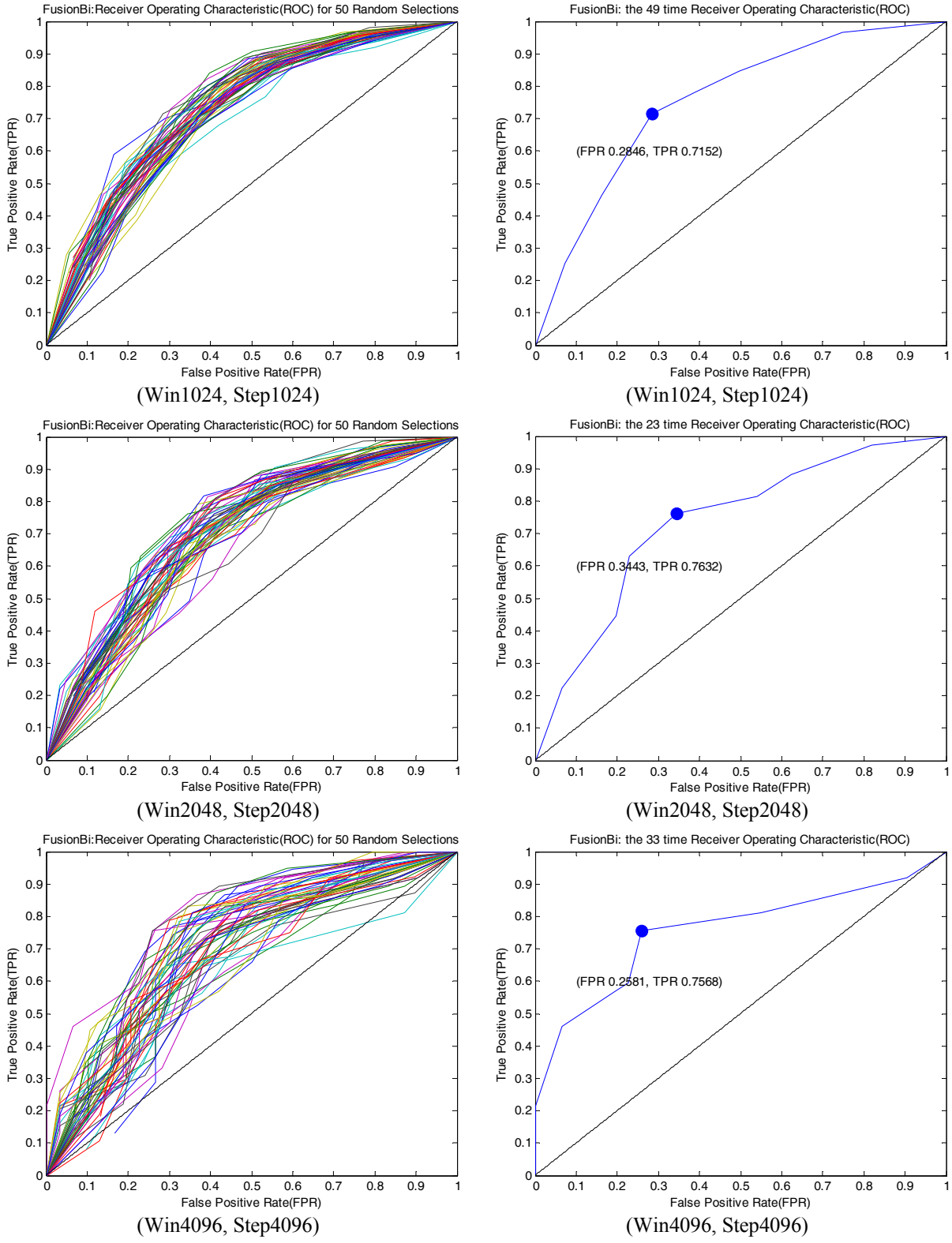

Fig. B3-14 ROC curves in Test 4

In Fig. B3-14, the left column displays 50 ROC curves of Optimal Fusion for three features in Bi-Channel, while the right column shows the nearest-upper-left ROC curve, where the points the closest to upper left corner (0, 1) is marked as blue round point.

B3.7 Synthesis and Discussion

The nearest-upper-left ROC curves of each candidate feature in Mono-Channel from Test 1 and Test 2 are redrawn in Fig. B3-15 a) and those in Bi-Channel from Test 3 and Test 4 are done in Fig. B3-15 b). Seemingly, performances are comparable and fusions look better than classic methods.

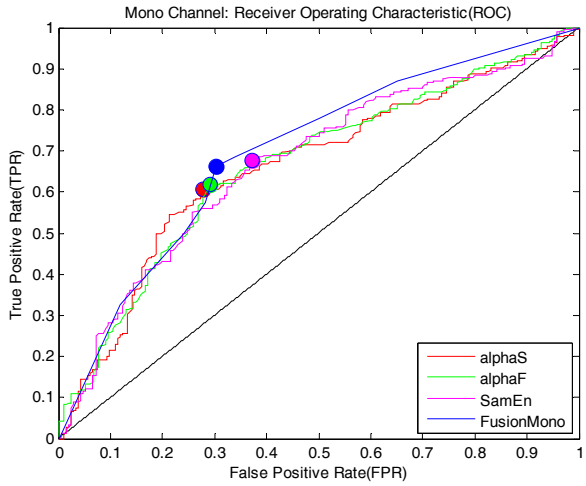

(Win1024, Step1024)

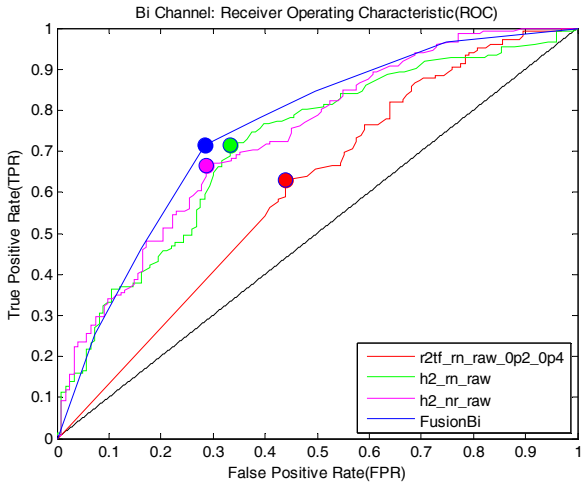

(Win1024, Step1024)

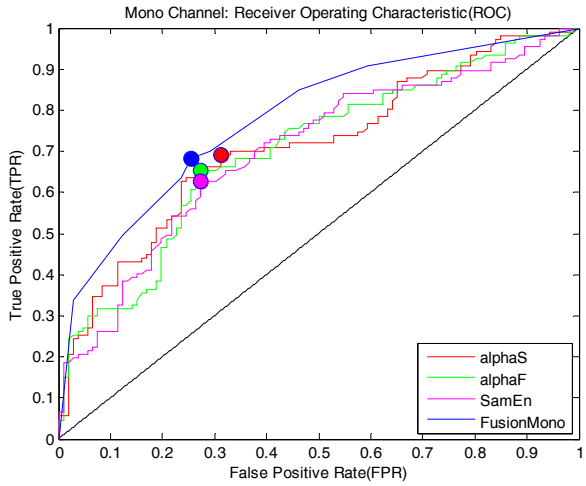

(Win2048, Step2048)

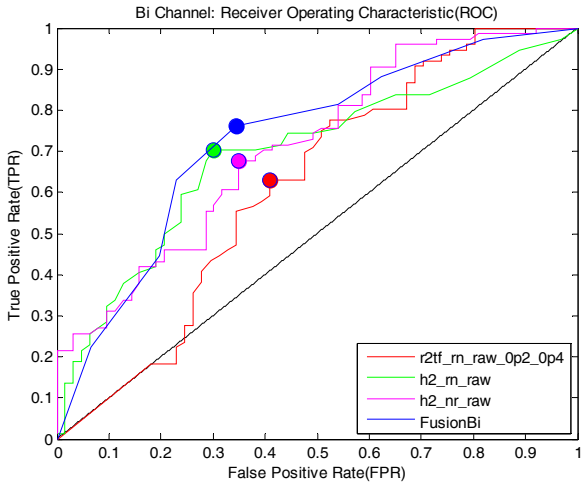

(Win2048, Step2048)

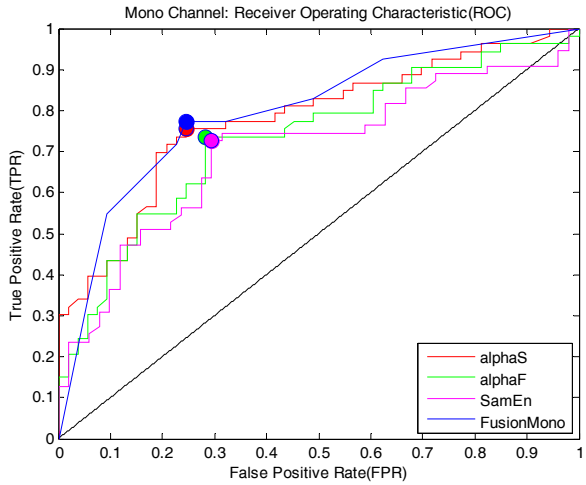

(Win4096, Step4096)

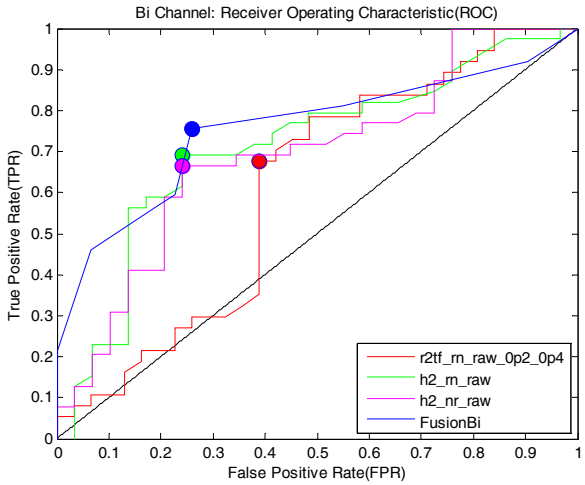

(Win4096, Step4096)

a) Mono-Channel

b) Bi-Channel

Fig. B3-15 The nearest-upper-left ROC curves, where the points the closest to upper left corner (0, 1) are marked as colourful round points

Test 5 is the results of mixed all significant features using Optimal Fusion. The following Fig. B3-16. lists ROC curves of long sequences in Test 5 and its best ROC curve for 3 kinds of window size:

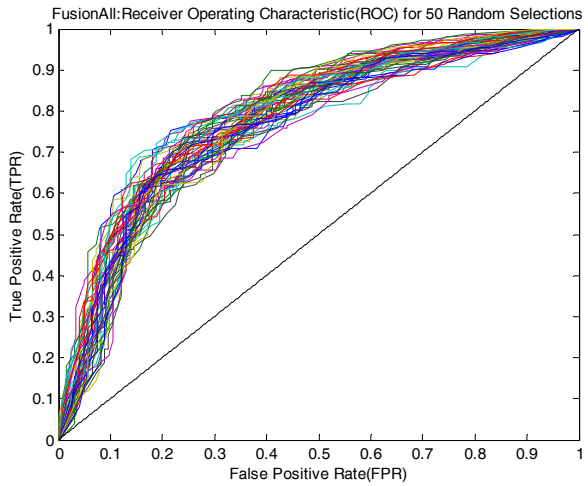

(Win1024, Step1024)

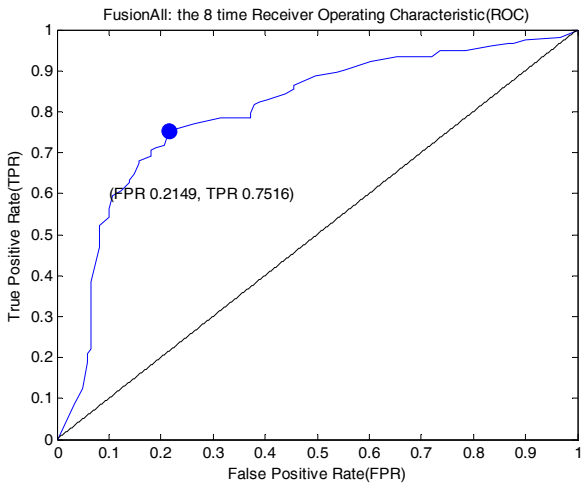

(Win1024, Step1024)

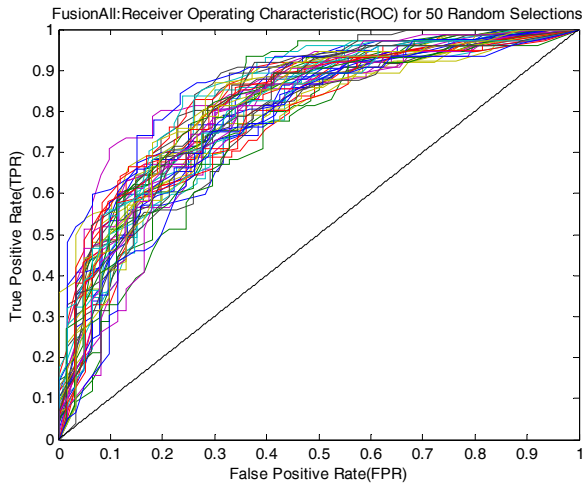

(Win2048, Step2048)

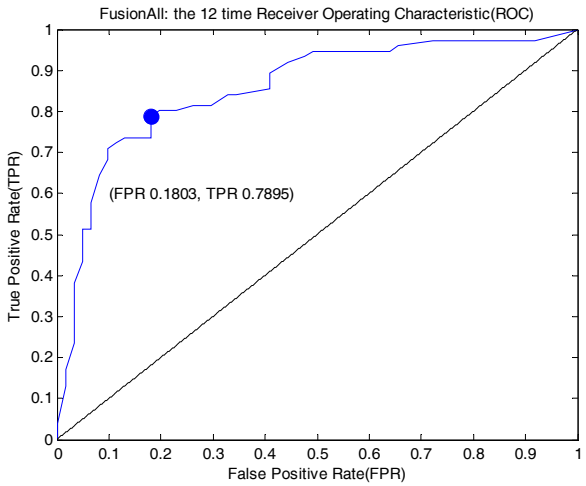

(Win2048, Step2048)

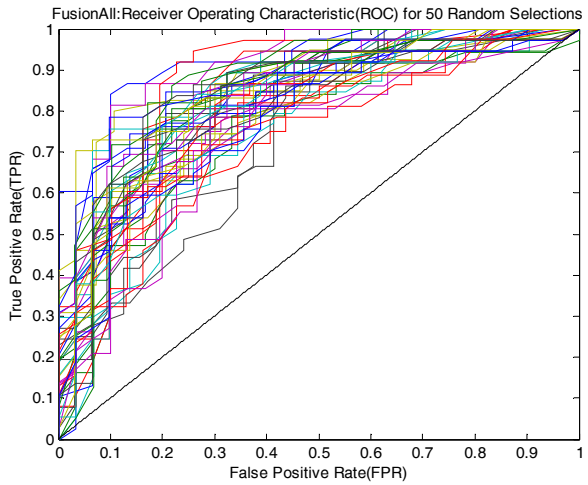

(Win4096, Step4096)

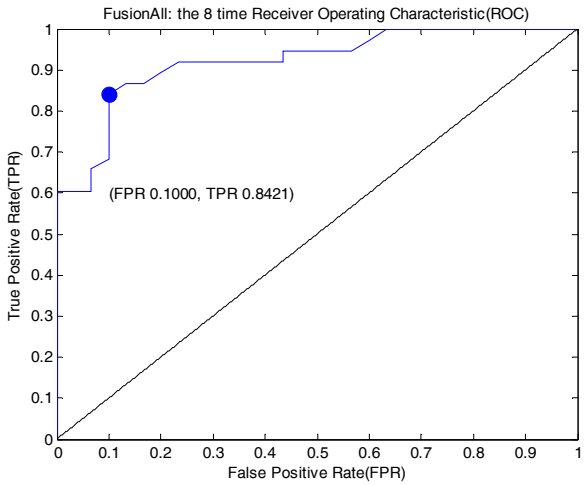

(Win4096, Step4096)

Fig. B3-16 ROC curves in Test 5

Furthermore, the important characteristics of ROC curves analysis are reported in Table B3-2, Table B3-3 and Table B3-4 in order to dig out the best method for sepsis diagnosis.

The following is the explanations of Table B3-2, Table B3-3 and Table B3-4:

- ♠ The first column indicates the type of test.
- ♠ The second column lists features of each test.
- ♠ The third column delivers FPR values, which represent P_{FA}.
- ♠ The fourth column provides TPR values, which denote P_D.
- ♠ The fifth column presents the Area Under Curve (AUC), which is the most important criteria to compare among all features. The larger the AUC is, the more convincing the decision-making method is.
- ♠ The best performance is in bold in the table.

Table B3-2 Characteristics of ROC curves, Window=1024, Step=1024

Test	Features	FPR(P_{FA})	TPR(P_D)	AUC
Test 1	alphaS	0.2783	0.6075	0.6630
	alphaF	0.2919	0.6175	0.6684
	SamEn	0.3714	0.6759	0.6648
Test 2	Optimal Fusion Mono-channel	0.3019	0.6636	0.4191
Test 3	r2tf_rn_raw_0p2_0p4	0.4400	0.6309	0.4885
	h2_rn_raw	0.3333	0.7152	0.7185
	h2_nr_raw	0.2869	0.6645	0.7359
Test 4	Optimal Fusion Bi-channel	0.2846	0.7152	0.5557
Test 5	Optimal Fusion All	0.2149	0.7516	**0.7731**

Table B3-3 Characteristics of ROC curves, Window=2048, Step=2048

Test	Features	FPR(P_{FA})	TPR(P_D)	AUC
Test 1	alphaS	0.3113	0.6916	0.7031
	alphaF	0.2736	0.6542	0.7055
	SamEn	0.2736	0.6262	0.6912
Test 2	Optimal Fusion Mono-channel	0.2547	0.6822	0.4317
Test 3	r2tf_rn_raw_0p2_0p4	0.4098	0.6316	0.5837
	h2_rn_raw	0.3016	0.7027	0.7079
	h2_nr_raw	0.3492	0.6757	0.7143
Test 4	Optimal Fusion Bi-channel	0.3443	0.7632	0.6059
Test 5	Optimal Fusion All	0.1803	0.7895	**0.7813**

Table B3-4 Characteristics of ROC curves, Window=4096, Step=4096

Test	Features	FPR(P_{FA})	TPR(P_D)	AUC
Test 1	alphaS	0.2453	0.7547	0.7593
	alphaF	0.2830	0.7358	0.7351
	SamEn	0.2941	0.7273	0.7048
Test 2	Optimal Fusion Mono-channel	0.2453	0.7736	0.4514
Test 3	r2tf_rn_raw_0p2_0p4	0.3871	0.6757	0.5763
	h2_rn_raw	0.2414	0.6923	0.7171
	h2_nr_raw	0.2414	0.6667	0.6941
Test 4	Optimal Fusion Bi-channel	0.2581	0.7568	0.7079
Test 5	Optimal Fusion All	0.1000	0.8421	**0.8246**

Furthermore, the synthesis of comparison among the three kinds of window size is reported in the following table.

Table B3-5 Comparison among the three kinds of window size

Window Size	minutes	FPR(P_{FA})	TPR(P_D)	AUC
1024	4.3	0.2149	0.7516	**0.7731**
2048	8.6	0.1803	0.7895	**0.7813**
4096	17.2	0.1000	0.8421	**0.8246**

From Table B3-5, we can see that Window 4096 has the least P_{FA} and the largest value of AUC.

From Table B3-2, Table B3-3 and Table B3-4, it is obvious that Test 5 has the least P_{FA} and the largest AUC, that is to say, both 3 features recommended from Mono-Channel and 3 features from Bi-Channel are the significant parameters. However, optimal fusion of all the different parameters rather than each parameter improves the performance. Consequently, we propose Test 5 as a new methodology.

B3.8 Conclusion

The problem of this chapter is to verify that real time detection is feasible based upon the two previous chapters:

(i) Chapter B1 based on HRV;
(ii) Chapter B2 based on HRV and respiration.

Feasibility study is carried out on the candidate parameters selected from Mono-Channel Analysis and Bi-Channel Analysis respectively, and their mixed condition. Firstly, we generate long series mixing sepsis and non-sepsis case as real time series. Accordingly, we test the sepsis

or non-sepsis hypothesis on every segment of 3 kinds of window size by 5 types of Test. Finally, we summarize characteristics of ROC curves such as P_{FA}, P_D and AUC in Table B3-2, Table B3-3 and Table B3-4 in order to compare these 5 tests and discover which the best solution is. In addition, the contrast among the three window sizes 1024/2048/4096 indicates that Window 4096 has the least P_{FA} and the largest value of AUC.

In conclusion, among five tests, the proposed Test 5 based on optimal fusion of all 6 features (alphaS, alphaF, SamEn, r2tf_rn_raw, h2_rn_raw and h2_nr_raw) shows good performance with the least P_{FA} and the largest AUC, which can be used to provide high-precision warning alerts of apnea-bradycardia in neonatal monitoring system.

B3.9 Bibliography

[1] C. F. Poets, V. A. Stebbens, M. P. Samuels*, et al.*, "The relationship between bradycardia, apnea, and hypoxemia in preterm infants," *Pediatr Res,* vol.34*(2)*, pp.144-147, Aug, 1993.

[2] A. Lowe, R. W. Jones, and M. J. Harrison, "The graphical presentation of decision support information in an intelligent anaesthesia monitor," *Artif Intell Med,* vol.22*(2)*, pp.173-191, May, 2001.

[3] R. Pichardo, J. S. Adam, E. Rosow*, et al.*, "Vibrotactile stimulation system to treat apnea of prematurity," *Biomed Instrum Technol,* vol.37*(1)*, pp.34-40, Jan-Feb, 2003.

[4] Z. Chair and P. K. Varshney, "Optimal Data Fusion in Multiple Sensor Detection Systems," *Aerospace and Electronic Systems, IEEE Transactions on,* vol.AES-22*(1)*, pp.98-101, 1986.

[5] A. I. Hernandez, G. Carrault, F. Mora*, et al.*, "Multisensor fusion for atrial and ventricular activity detection in coronary care monitoring," *Biomedical Engineering, IEEE Transactions on,* vol.46*(10)*, pp.1186-1190, 1999.

[6] Altuve. M., Carrault. G., Cruz. J.*, et al.*, "Multivariate Ecg Analysis for Apnea-Bradycardia Detection and Characterization in Preterm Infants.," *International Journal of Biomedical Engineering and Technology,* vol.5*(2-3)*, pp.247-265, 2011.

[7] R. R. Tenney and N. R. Sandell, "Detection with distributed sensors," *IEEE Transactions on Aerospace and Electronic Systems,* vol.17*(4)*, pp.501-509, July, 1981.

[8] J. A. Swets, *Signal detection theory and ROC analysis in psychology and diagnostics : collected papers*, Mahwah, NJ: Lawrence Erlbaum Associates, 1996.

[9] M. H. Zweig and G. Campbell, "Receiver-operating characteristic (ROC) plots: a fundamental evaluation tool in clinical medicine," *Clinical Chemistry,* vol.39*(4)*, pp.561-577, April 1, 1993.

[10] M. S. Pepe, *The statistical evaluation of medical tests for classification and prediction* New York: Oxford, 2003.

Chapter 8
Conclusions and Perspectives

In Chapter 8, we summarize the goal and the proposed methods of this dissertation. We also point out some possible ways to improve and extend our research in future work.

8.1 Conclusions

Late-onset sepsis, defined as a systemic infection in neonates older than 3 days, occurs in approximately 7% to 10% of all neonates and in more than 25% of very low birth weight infants who are hospitalized in NICU. In view of the high morbidity and mortality associated with infection, reliable markers are needed.

Recurrent and severe spontaneous apneas and bradycardias is one of the major clinical early indicators of systemic infection in the premature infant. It requires prompt laboratory investigation so that treatment can start without delay. Various hematological and biochemical markers have been evaluated for this indication but they are invasive procedures that cannot be repeated several times.

The objective of this dissertation was to determine if heart rate behavior, respiratory amplitude and the analysis of their relationships help to the diagnosis of infection in premature infants with cardiac decelerations via non-invasive ways. Therefore, we carried out two parts of research work in two selected groups of premature infants (sepsis vs. non-sepsis):

- Analysis for RR series
  - Analysis for relationship between RR series and respiration

First of all, we studied the RR interval series not only by distribution methods (moy, varn, skew, kurt, med, SpAs), by linear methods — time domain (SD, RMSSD) and frequency domain (p_VLF, p_LF, p_HF), but also by non-linear methods – chaos theory (alphaS, alphaF) and information theory (AppEn, SamEn, PermEn, Regul). For each method, we attempt three sizes of window 1024/2048/4096, and then compare these methods in order to find the optimal ways to distinguish sepsis premature infants from non-sepsis ones. The results show that **alphaS**, **alphaF** and **SamEn** are optimal parameters to recognize sepsis from the diagnosis of late neonatal infection in premature infants with unusual and recurrent apnea-bradycardia.

However, in sick premature infants, the mechanism is probably not just a change in RR series. The clinical findings here clearly demonstrate that HRV, respiration and their relationship could be efficient diagnosis tools and may help identifying culture-positive sepsis in a population of infants with recurrent bradycardias. From the same cohort used for RR analysis, patients were retained, those having respiratory signals recorded.

The question about the functional coupling of heart rate variability and nasal respiration is addressed. Linear and non-linear relationships have been explored. Linear indexes were correlation (r^2), coherence function (*Cohere*) and time-frequency index ($r^2_{t,f}$), while a non-linear regression coefficient (h^2) was used to analyze non-linear relationships. We calculated two

directions during evaluate the index h^2 of non-linear regression. Finally, from the entire analysis process, it is obvious that the three following indexes:

- ⇒ the quantity of $r^2_{t,f}$ between RR and original nasal respiration over a threshold set to 0.8 in the sub-band $0.2<f<0.4$ *Hz* (r2tf_rn_raw_0p2_0p4)
- ⇒ h^2 between RR and original nasal respiration (h2_rn_raw)
- ⇒ h^2 between original nasal respiration and RR (h2_nr_raw)

were complementary ways to diagnosticate sepsis in a non-invasive way, in such delicate patients.

Furthermore, feasibility study is carried out on the candidate parameters selected from Mono-Channel Analysis in Chapter B1 and Bi-Channel Analysis in Chapter B2 respectively. Firstly, we generate long series mixing sepsis and non-sepsis case as real time series. Accordingly, we test the sepsis or non-sepsis hypothesis on every segment of 3 kinds of window size by 5 types of Test. Here, an optimal fusion law is proposed and based on the mixed condition of several features. Finally, we summarize characteristics of ROC curves such as P_{FA}, P_D and AUC. By way of comparing all these tests, we discovered that a proposed test based on optimal fusion of 6 features (alphaS, alphaF, SamEn, r2tf_rn_raw, h2_rn_raw and h2_nr_raw) shows good performance with the least P_{FA} and the largest AUC, which can be used to provide high-precision warning alerts of apnea-bradycardia in neonatal monitoring system. In addition, the contrast among the three window sizes 1024/2048/4096 indicates that Window 4096 has the least P_{FA} and the largest value of AUC.

As a conclusion, we believe that the selected measures from Mono-Channel and Bi-Channel signal analysis have a good repeatability and accuracy to test for the diagnosis of sepsis via non-invasive NICU monitoring system, which can reliably confirm or refute the diagnosis of infection at an early stage.

8.2 Perspectives

Of course, there are still many possibilities to improve and extend the work in this dissertation. Here we list some perspectives:

8.2.1 Relationship between RR series and Respiration

Concerning analysis of relationship between RR series and Respiration in Chapter B2, it is valuable to attempt several new methods.

Firstly, we plan to test a new and fast nonlinear method—the ***V*** measure proposed by Cunha and Oliveira [1]. The features of this new measure when applied to biosignals are also shown using simulated time series. ***V*** was found to be twice as fast and more robust to nonlinearities than the classical cross-correlation ratio (r^2) and more than 100 times faster than the nonlinear regression coefficient (h^2), presenting similar behavior in the presence of nonlinear simulated situations. This new measure is very fast and versatile. It is appropriate to deal with nonlinear relations

presenting usually a sharp peak in the association function enabling a high degree of selectivity for maxima detection. It seems to constitute an improvement over linear methods of association which is faster and more robust to the existing nonlinearities. It can be used as an alternative to more complex nonlinear association measures when computational speed is an important feature.

Secondly, we are interested in a novel correlation coefficient based on order statistics and rearrangement inequality proposed by Xu and Chang [2]. The proposed coefficient represents a compromise between the Pearson's linear coefficient and the two rank-based coefficients, namely Spearman's rho and Kendall's tau. Theoretical derivations show that their coefficient possesses the same basic properties as the three classical coefficients. Experimental studies based on four models and six biosignals show that the coefficient performs better than the two rank-based coefficients when measuring linear associations; whereas it is well able to detect monotone nonlinear associations like the two rank-based coefficients. Extensive statistical analyses also suggest that the new coefficient has superior anti-noise robustness, small biases, and high sensitivity to changes in association, accurate time-delay detection ability, fast computational speed, and robustness under monotone nonlinear transformations.

Thirdly, synchronization index (*S*) need to be considered. Synchronization occurs when patterns involving two signals contemporaneously are repetitive. Synchronization to a periodic input can be observed when the activity of a self-sustained oscillator is perturbed by a periodic input. But synchronization can be found not only to a periodic process; examples of synchronized chaotic dynamics are given by Pecora and Carroll [3]. Quantification of the degree of synchronization (i.e. the coupling strength) between two signals is considered an important goal, as different levels of synchronization are found between the RR interval and respiration [4]. The method will be applied to quantify the degree of coupling between the RR series and the respiration signals.

8.2.2 Analysis of EEG

Apnea-bradycardia' repetition in several cases seems to be associated to a neuropsychiatric evolution's alteration valued in neonates. EEG is also an excellent tool to investigate the longitudinal course and prognostic value of amplitude integrated EEG (aEEG) in infants with neonatal sepsis [5].When used selectively through serial recordings, neonatal EEG's greatest value is its potential for prediction of short- and long-term prognosis. [6]

The EEG background, static abnormalities, and EEG maturational indices are the best prognostic factors. EEG may reflect the severity of brain injury in neonatal asphyxia, the degree of abnormalities usually being consistent with the clinical grading of hypoxic-ischemic encephalopathy (HIE). Therefore, in neonatal asphyxia, EEG background pattern especially is a valuable predictor of future neurologic outcome in combination with clinical data such as gestational age, birth weight, imaging, and HIE severity. Low birth weight amplitude of brain electrical activity, duration of interburst intervals, and sleep-wake cycle disturbance were among the most significant indexes of a poor long-term prognosis. [7]

Although some ictal discharges may have specific significance, a normal interictal EEG indicates the greatest chance of favorable outcome, even in the case of early, recurrent seizures [8]. Several studies have demonstrated the prognostic role of EEG in different diseases, ranging from neonatal seizures to asphyxia and hemorrhage. [9]

8.3 Bibliography

[1] J. P. S. Cunha and P. G. de Oliveira, "A new and fast nonlinear method for association analysis of biosignals," *IEEE TRANSACTIONS ON BIOMEDICAL ENGINEERING,* vol.47*(6)*, pp.757 - 763 2000.

[2] W. Xu, C. Chang, Y. S. Hung*, et al.*, "Order Statistics Correlation Coefficient as a Novel Association Measurement With Applications to Biosignal Analysis," *Signal Processing, IEEE Transactions on,* vol.55*(12)*, pp.5552-5563, 2007.

[3] L. M. Pecora and T. L. Carroll, "Synchronization in chaotic systems," *Physical Review Letters,* vol.64*(8)*, pp.821-824, 1990.

[4] D. Hoyer, R. Bauer, B. Walter*, et al.*, "Estimation of nonlinear couplings on the basis of complexity and predictability-a new method applied to cardiorespiratory coordination," *Biomedical Engineering, IEEE Transactions on,* vol.45*(5)*, pp.545-552, 1998.

[5] H. J. Ter Horst, M. Van Olffen, H. J. Remmelts*, et al.*, "The prognostic value of amplitude integrated EEG in neonatal sepsis and/or meningitis," *Acta Pædiatrica,* vol.99*(2)*, pp.194-200, 2010.

[6] A. Husain, "Review of neonatal EEG. ," *Am J Electroneurodiagnostic Technol,* vol.45*(1)*, pp.12-35, 2005.

[7] B. R. Tharp, "Neonatal Encephalography," *Progress in Perinatal Neurology*, pp.37-64, 1981.

[8] N. Monod, N. Pajot, and S. Guidasci, "The neonatal EEG: statistical studies and prognostic value in full-term and pre-term babies," *Electroencephalogr Clin Neurophysiol.,* vol.32*(5)*, pp.529-544, 1972.

[9] A. L. Rose and C. T. Lombroso, "A study of clinical, pathological, and electroencephalographic features in 137 full-term babies with a long-term follow-up," *Pediatrics,* vol.45*(3)*, pp.404-425, 1970.

Appendix I
Analysis of Variance

To apply the test, assume random sampling of a variate ***Y*** with equal variances, independent errors, and a normal distribution. Let n be the number of replicates (sets of identical observations) within each of ***k*** factor levels (treatment groups), and y_{ij} be the jth observation within factor level i. Also assume that the ANOVA is "balanced" by restricting n to be the same for each factor level.

Now define the sum of square terms

SST	$SST = \sum_{i=1}^{k}\sum_{j=1}^{n} y_{ij}^{\ 2} - \frac{(\Sigma_{i=1}^{k}\Sigma_{j=1}^{n} y_{ij})^{2}}{K_n}$
SSA	$SSA = \frac{1}{n}\sum_{i=1}^{k}(\sum_{j=1}^{n} y_{ij})^{2} - \frac{1}{K_n}(\sum_{i=1}^{k}\sum_{j=1}^{n} y_{ij})^{2}$
SSE	$SSE = \sum_{i=1}^{k}\sum_{j=1}^{n}(y_{ij} - \overline{y_i})^{2}$ $SSE = SST - SSA$

which are the total, treatment, and error sums of squares. Here, $\overline{y_i}$ is the mean of observations within factor level i, and $\overline{\overline{y}}$ is the "group" mean (i.e., mean of means). Compute the entries in the following table, obtaining the value corresponding to the calculated F-ratio of the mean squared values

$$F = \frac{MSA}{MSE}$$

category	°freedom	SS	mean squared	F-ratio
model	K-1	SSA	$MSA \equiv \frac{SSA}{K-1}$	$\frac{MSA}{MSE}$
error	K(n-1)	SSE	$MSE \equiv \frac{SSE}{K(n-1)}$	
total	Kn-1	SST	$MST \equiv \frac{SST}{Kn-1}$	

If the F-ratio is small, reject the null hypothesis that all means are the same for the different groups.

Appendix II
Results for Univariate Analysis

II.1 With outliers

II.1.1 Window=1024, Step=1024

We tested the link between sepsis/non-sepsis status and the parameters using ANOVA models. The experiments were performed with and without taking into account the baby effects.

The results are reported in the Table II-1 below. The following is the table of univariate analysis. With outliers, the size of analysis windows is 1024 with step 1024.

Table II-1 Univariate Analysis, p value, with outliers, Window=1024, Step=1024

	Baby effect?	Effect of group Sepsis?	
		hierarchical model with random effect baby (p-value)	model without random effect baby (p-value)
moy	0.0015 yes	0.7299	0.5455
varn	0.1856 no	0.2446	0.1931
skew	0.0110 yes	0.0273	0.0121
kurt	0.1891 no	0.1055	0.0925
med	0.0012 yes	0.9966	0.9605
SpAs	0.1005 no	0.0561	0.0282
SD	0.0442 yes	0.2243	0.1306
RMSSD	0.0511 lim	0.3243	0.1992
p_HF	0.0358 yes	0.2274	0.1084
p_LF	0.0140 yes	0.2129	0.0693
p_VLF	0.1420 no	0.8028	0.7929
alphaS	0.1002 no	0.0012	0.0007
alphaF	0.0051 yes	0.0307	0.0025
AppEn	0.0607 no	0.2745	0.2621
SamEn	0.0335 yes	0.0840	0.0556
PermEn	0.0042 yes	0.1654	0.0959
Regul	0.1159 no	0.6347	0.6841

The second column is to determine if there is an effect ‘baby’ on the parameters or if the measurements can be considered from different babies. We used mixed effect ANOVA in which the baby is a random effect such as the fact that the same baby is used several times is taken into account.

The threshold of test is 0.05. If p value is less than the threshold, baby effect is considered significant.

The third and fourth columns test whether the cardiac parameters are discriminating among infants. The p values are reported here. In the third column, we assume that there is random baby effect, considering whether this set of data is sepsis baby or not. In the fourth column, we assume

that there is no baby effect on the parameters. The p value is only calculated by using Generalized Linear Model (GLM).

We highlighted in yellow the significant results at the 5% level and in brown those up to 20%.

There are only a few parameters that seem to be related to the sepsis status. From Table II-1, we can see that the methods ‘skew’, ’kurt’, ’SpAs’, ’ alphaS’, ’alphaF’, ‘SamEn’ and ‘PermEn’ are significant. They can be introduced into a multivariate discriminant analysis or logistic regression model.

II.1.2 Window=2048, Step=2048

The results are in the Table II-2 below. The following is the table of univariate analysis. With outliers, the size of analysis windows is 2048 with step 2048.

Table II-2 Univariate Analysis, p value, with outliers, Window=2048, Step=2048

	Baby effect?	Effect of group Sepsis?	
		hierarchical model with random effect baby (p-value)	model without random effect baby (p-value)
moy	0.0017 yes	0.8083	0.7633
varn	0.0440 yes	0.5311	0.3598
skew	0.0254 yes	0.5832	0.5321
kurt	0.3141 no	0.8510	0.8216
med	0.0007 yes	0.6169	0.4366
SpAs	0.3456 no	0.8610	0.8331
SD	0.0189 yes	0.5281	0.3150
RMSSD	0.0559 lim	0.8338	0.7205
p_HF	0.0087 yes	0.6259	0.3774
p_LF	0.0066 yes	0.1808	0.0423
p_VLF	0.0275 yes	0.8180	0.6378
alphaS	0.0410 yes	0.0045	0.0009
alphaF	0.0076 yes	0.1154	0.0155
AppEn	0.0080 yes	0.0369	0.0044
SamEn	0.0122 yes	0.0507	0.0177
PermEn	0.0015 yes	0.0575	0.0123
Regul	0.0747 no	0.4257	0.3557

There are only a few parameters that seem to be related to the sepsis status. From Table II-2, we can see that the methods ’p_LF’, ’ alphaS’, ’alphaF’, ‘AppEn’, ‘SamEn’ and ‘PermEn’ are significant. They can be introduced into a multivariate discriminant analysis or logistic regression model.

II.1.3 Window=4096, Step=4096

The results are in the Table II-3 below. The following is the table of univariate analysis. With outliers, the size of analysis windows is 4096 with step 4096.

Table II-3 Univariate Analysis, p value, with outliers, Window=4096, Step=4096

	Baby effect?	Effect of group Sepsis?	
		hierarchical model with random effect baby (p-value)	model without random effect baby (p-value)
moy	0.0009 yes	0.8654	0.6066
varn	0.0494 lim	0.8738	0.4995
skew	0.4137 no	0.8583	0.8416
kurt	. yes	0.7057	0.7046
med	0.0006 yes	0.6990	0.3311
SpAs	0.0264 yes	0.1830	0.0479
SD	0.0439 yes	0.9873	0.6315
RMSSD	0.4830 no	0.3595	0.3565
p_HF	0.0037 yes	0.8113	0.6630
p_LF	0.0022 yes	0.2420	0.0773
p_VLF	0.0123 yes	0.9066	0.9202
alphaS	0.0240 yes	0.0003	<.0001
alphaF	0.0022 yes	0.0252	0.0010
AppEn	0.0075 yes	0.0043	0.0002
SamEn	0.0057 yes	0.0410	0.0081
PermEn	0.0008 yes	0.0503	0.0038
Regul	0.0318 yes	0.5016	0.3871

There are only a few parameters that seem to be related to the sepsis status. From Table II-3, we can see that the methods 'SpAs', ' alphaS', 'alphaF', 'AppEn', 'SamEn' and 'PermEn' are significant. They can be introduced into a multivariate discriminant analysis or logistic regression model.

II.2 Without outliers

II.2.1 Window=1024, Step=1024

The results are in the Table II-4 below. The following is the table of univariate analysis. Without outliers, the size of analysis windows is 1024 with step 1024.

Table II-4 Univariate Analysis, p value, without outliers, Window=1024, Step=1024

	Baby effect?	Effect of group Sepsis?	
		hierarchical model with random effect baby (p-value)	model without random effect baby (p-value)
moy	0.0019 yes	0.6968	0.5612
varn	0.0455 lim	0.9620	0.9820
skew	0.0025 yes	0.0002	<.0001

	Baby effect?	Effect of group Sepsis?	
		hierarchical model with random effect baby (p-value)	model without random effect baby (p-value)
kurt	0.0278 yes	0.0002	<.0001
med	0.0018 yes	0.8509	0.7413
SpAs	0.0577 no	0.0022	0.0005
SD	0.0172 yes	0.6232	0.4699
RMSSD	0.0248 yes	0.8832	0.6911
p_HF	0.0083 yes	0.4155	0.1396
p_LF	0.0039 yes	0.4656	0.0942
p_VLF	0.0345 yes	0.5186	0.5141
alphaS	0.0282 yes	0.0047	0.0003
alphaF	0.0226 yes	0.0128	0.0009
AppEn	0.0648 no	0.4410	0.5544
SamEn	0.2387 no	0.1931	0.1961
PermEn	0.0064 yes	0.1933	0.2717
Regul	0.3586 no	0.5258	0.4780

There are only a few parameters that seem to be related to the sepsis status. From Table II-4, we can see that the methods 'skew', 'kurt', 'SpAs', 'alphaS', 'alphaF' and 'SamEn' are significant. They can be introduced into a multivariate discriminant analysis or logistic regression model.

II.2.2 Window=2048, Step=2048

The results are in the Table II-5 below. The following is the table of univariate analysis. Without outliers, the size of analysis windows is 2048 with step 2048.

Table II-5 Univariate Analysis, p value, without outliers, Window=2048, Step=2048

	Baby effect?	Effect of group Sepsis?	
		hierarchical model with random effect baby (p-value)	model without random effect baby (p-value)
moy	yes	0.7	0.61
varn	no	0.23	0.23
skew	yes	0.19	0.16
kurt	no	0.46	0.45
med	yes	0.89	0.83
SpAs	no	0.02	0.01
SD	no	0.25	0.23
RMSSD	no	0.38	0.46
p_HF	yes	0.32	0.43
p_LF	yes	0.11	0.06
p_VLF	no	0.9	0.91
alphaS	yes	0.01	0.001
alphaF	yes	0.04	0.003
AppEn	limite	0.12	0.05
SamEn	no	0.03	0.017
PermEn	yes	0.47	0.097
Regul	no	0.84	0.67

There are only a few parameters that seem to be related to the sepsis status. From Table II-5, we can see that the methods ‘skew’, ‘SpAs’, ‘p_LF’, ‘alphaS’, ‘alphaF’, ‘AppEn’ and ‘SamEn’ are significant. They can be introduced into a multivariate discriminant analysis or logistic regression model.

II.2.3 Window=4096, Step=4096

The results are in the Table II-6 below. The following is the table of univariate analysis. Without outliers, the size of analysis windows is 4096 with step 4096.

Table II-6 Univariate Analysis, p value, without outliers, Window=4096, Step=4096

	Baby effect?	Effect of group Sepsis?	
		hierarchical model with random effect baby (p-value)	model without random effect baby (p-value)
moy	0.0018 yes	0.8024	0.7425
varn	0.0098 yes	0.1704	0.0341
skew	0.2462 no	0.4186	0.3551
kurt	0.4765 no	0.9823	0.9775
med	0.0015 yes	0.5878	0.4541
SpAs	0.0327 yes	0.0220	0.0033
SD	0.0085 yes	0.2775	0.0757
RMSSD	0.0074 yes	0.6404	0.4030
p_HF	0.0020 yes	0.7122	0.7504
p_LF	0.0037 yes	0.3408	0.1615
p_VLF	0.0476 lim	0.8464	0.8588
alphaS	0.1099 no	0.0011	0.0004
alphaF	0.0026 yes	0.0440	0.0022
AppEn	0.0167 yes	0.0006	<.0001
SamEn	0.0471 lim	0.0006	<.0001
PermEn	0.0030 yes	0.0337	0.0043
Regul	0.1101 no	0.1751	0.1104

There are only a few parameters that seem to be related to the sepsis status. From Table II-6, we can see that the methods ‘varn’, ‘SpAs’, ‘alphaS’, ‘alphaF’, ‘AppEn’, ‘SamEn’, ‘PermEn’ and ‘Regul’ are significant. They can be introduced into a multivariate discriminant analysis or logistic regression model.

Appendix III
Results for Multivariate Analysis —— Logistic Regression

III.1 With outliers

III.1.1 Window=1024, Step=1024

It's the Table III-1 of logistic regression, with outliers, analysis window=1024 with step 1024.

Table III-1 Logistic Regression, with outliers, Window=1024, Step=1024

Analysis of Maximum Likelihood Estimates					
Parameter	**DF**	**Coefficient**	**Standard Error**	**Wald Chi-Square**	**Pr > ChiSq**
Intercept	1	11.6551	8.0490	2.0967	0.1476
skew	1	-0.1631	0.4663	0.1223	0.7265
kurt	1	-0.00714	0.0453	0.0248	0.8748
SpAs	1	0.0500	0.0576	0.7534	0.3854
alphaS	1	-5.7189	2.2126	6.6811	0.0097
alphaF	1	0.1465	2.8801	0.0026	0.9594
SamEn	1	-9.9756	7.5724	1.7355	0.1877
PermEn	1	-8.5441	9.3547	0.8342	0.3611

- The first column represents the Intercept and the significant parameters chosen from Table II-1 of univariate analysis in Appendix II.
- The second column denotes the degree of freedom (DF) with each parameter.
- The third column denotes the estimated coefficients of the parameter, which are $\beta_1, \beta_2, \beta_3, \ldots, \beta_k$ in Equation (5.32)
- The fourth column denotes the standard error of the coefficient.
- The fifth column denotes the Wald Chi-Square statistic, computed as the square of the value obtained by dividing the parameter estimate by its standard error.
- The sixth column denotes the p-value (Pr > ChiSq) for the Wald Chi-square statistic with 1 DF, with a value below 0.2 indicating a significant effect of the associated model parameter if a 20 percent significance level is chosen.

From Table III-1, it is observed that alphaS and SamEn have the significant regression coefficients, which have p-values <0.2 and marked in green. Two negative regression coefficients mean that alphaS and SamEn decrease the probability of sepsis.

III.1.2 Window=2048, Step=2048

It's the Table III-2 of logistic regression, with outliers, analysis window=2048 with step 2048. These significant parameters are chosen from Table II-2 of univariate analysis in Appendix II.

Table III-2 Logistic Regression, with outliers, Window=2048, Step=2048

Analysis of Maximum Likelihood Estimates					
Parameter	**DF**	**Coefficient**	**Standard Error**	**Wald Chi-Square**	**Pr > ChiSq**
Intercept	1	21.6149	10.5761	4.1770	0.0410
p_LF	1	0.2730	0.4249	0.4129	0.5205
alphaS	1	-6.7654	2.5306	7.1473	0.0075
alphaF	1	-0.9702	3.1581	0.0944	0.7587
AppEn	1	-8.5973	6.8171	1.5905	0.2073
SamEn	1	-1.3363	8.9314	0.0224	0.8811
PermEn	1	-23.1268	15.7261	2.1627	0.1414

From Table III-2, it is observed that alphaS and PermEn have the significant regression coefficients, which have p-values <0.2 and marked in green. Two negative regression coefficients mean that alphaS and PermEn decrease the probability of sepsis.

III.1.3 Window=4096, Step=4096

It's the Table III-3 of logistic regression, with outliers, analysis window=4096 with step 4096. These significant parameters are chosen from Table II-3 of univariate analysis in Appendix II.

Table III-3 Logistic Regression, with outliers, Window=4096, Step=4096

Analysis of Maximum Likelihood Estimates					
Parameter	**DF**	**Coefficient**	**Standard Error**	**Wald Chi-Square**	**Pr > ChiSq**
Intercept	1	27.0433	15.2359	3.1505	0.0759
SpAs	1	0.0261	0.0396	0.4354	0.5094
alphaS	1	-12.1747	3.6775	10.9603	0.0009
alphaF	1	-0.0989	4.5916	0.0005	0.9828
AppEn	1	-16.9164	11.6551	2.1066	0.1467
SamEn	1	-14.4850	13.3648	1.1747	0.2784
PermEn	1	-18.7703	17.1643	1.1959	0.2741

From Table III-3, it is observed that alphaS and AppEn have the significant regression coefficients, which have p-values <0.2 and marked in green. Two negative regression coefficients mean that alphaS and AppEn decrease the probability of sepsis.

III.2 Without outliers

III.2.1 Window=1024, Step=1024

It's the Table III-4 of logistic regression, without outliers, analysis window=1024 with step 1024. These significant parameters are chosen from Table II-4 of univariate analysis in Appendix II.

Table III-4 Logistic Regression, without outliers, Window=1024, Step=1024

Analysis of Maximum Likelihood Estimates					
Parameter	**DF**	**Coefficient**	**Standard Error**	**Wald Chi-Square**	**Pr > ChiSq**
Intercept	1	-12.1413	10.5073	1.3352	0.2479
skew	1	-3.7032	1.7232	4.6184	0.0316
kurt	1	0.5575	0.2293	5.9110	0.0150
SpAs	1	1.8309	0.7506	5.9493	0.0147
alphaS	1	-7.4428	3.2870	5.1273	0.0236
alphaF	1	9.6729	7.2557	1.7773	0.1825
SamEn	1	-37.0885	25.8890	1.6839	0.1882

From Table III-4, it is observed that skew, kurt, SpAs, alphaS, alphaF and SamEn have the significant regression coefficients, which have p-values <0.2 and marked in green. Positive regression coefficients mean that kurt, SpAs and alphaF increase the probability of sepsis, while negative regression coefficients mean that skew, alphaS and SamEn decrease the probability of sepsis.

Among these 6 variables, the largest regression coefficient means that SamEn strongly influences the probability of sepsis, while a near-zero regression coefficient means that kurt has little influence on the probability of sepsis.

III.2.2 Window=2048, Step=2048

It's the Table III-5 of logistic regression, without outliers, analysis window=2048 with step 2048. These significant parameters are chosen from Table II-5 of univariate analysis in Appendix II.

Table III-5 Logistic Regression, without outliers, Window=2048, Step=2048

Analysis of Maximum Likelihood Estimates					
Parameter	**DF**	**Coefficient**	**Standard Error**	**Wald Chi-Square**	**Pr > ChiSq**
Intercept	1	-1.0472	17.7273	0.0035	0.9529
skew	1	-2.3937	1.0994	4.7406	0.0295
SpAs	1	0.6450	0.2721	5.6208	0.0177
p_LF	1	-0.9800	0.9483	1.0680	0.3014
alphaS	1	-18.7639	7.4643	6.3193	0.0119
alphaF	1	16.9458	9.7327	3.0315	0.0817
AppEn	1	33.3132	30.7536	1.1734	0.2787
SamEn	1	-35.0995	27.8890	1.5839	0.2082

From Table III-5, it is observed that skew, SpAs, alphaS and alphaF have the significant regression coefficients, which have p-values <0.2 and marked in green. Two positive regression coefficients mean that SpAs and alphaF increase the probability of sepsis, while two negative regression coefficients mean that skew and alphaS decrease the probability of sepsis.

Among these 4 variables, the largest regression coefficient means that alphaS strongly influences the probability of sepsis, while a near-zero regression coefficient means that SpAs has little influence on the probability of sepsis.

III.2.3 Window=4096, Step=4096

It's the Table III-6 of logistic regression, without outliers, analysis window=4096 with step 4096. These significant parameters are chosen from Table II-6 of univariate analysis in Appendix II.

Table III-6 Logistic Regression, without outliers, Window=4096, Step=4096

Analysis of Maximum Likelihood Estimates					
Parameter	**DF**	**Coefficient**	**Standard Error**	**Wald Chi-Square**	**Pr > ChiSq**
Intercept	1	18.4547	21.5344	0.7344	0.3915
varn	1	-0.00026	0.000885	0.0831	0.7732
SpAs	1	0.0889	0.0903	0.9691	0.3249
alphaS	1	-11.2460	5.9626	3.5573	0.0593
alphaF	1	-0.2933	5.5059	0.0028	0.9575
AppEn	1	-2.6563	24.8865	0.0114	0.9150
SamEn	1	-29.2534	33.4121	0.7666	0.3813
PermEn	1	-17.2851	22.4517	0.5927	0.4414
Regul	1	9.0125	17.7172	0.2588	0.6110

From Table III-6, it is observed that alphaS has the significant regression coefficient, which has p-values <0.2 and marked in green. A negative regression coefficient means that alphaS decreases the probability of sepsis.

Appendix IV
Results for Multivariate Analysis —— Stepwise Regression

IV.1 With outliers

IV.1.1 Window=1024, Step=1024

It's the Table IV-1 of stepwise regression, with outliers, analysis window=1024 with step 1024.

Table IV-1 Stepwise Regression, with outliers, Window=1024, Step=1024

Summary of Stepwise Selection								
	Effect			Number	Score	Wald		Variable
Step	Entered	Removed	DF	In	Chi-Square	Chi-Square	Pr > ChiSq	Label
1	alphaS		1	1	11.0066		0.0009	alphaS
2	SamEn		1	2	6.6081		0.0102	SamEn

Analysis of Maximum Likelihood Estimates					
Parameter	DF	Estimate	Standard Error	Wald Chi-Square	Pr > ChiSq
Intercept	1	6.1324	1.7289	12.5808	0.0004
alphaS	1	-5.3019	1.5784	11.2835	0.0008
SamEn	1	-11.6893	4.8646	5.7740	0.0163

For the upper table:

- The first column denotes the number of step.
- The second column represents the variables added to the model.
- The third column represents the variables removed from the model.
- The fourth column denotes the degree of freedom (DF) with each parameter.
- The fifth column count on the number of the added variables.
- The sixth column denotes the Score Chi-Square statistic.
- The seventh column denotes the Wald Chi-Square statistic.
- The eighth column denotes the p-value (Pr > ChiSq) for the Score/Wald Chi-square statistic with 1 DF.
- The ninth column denotes Variable Label.

For the down table

- The first column represents the Intercept and the significant parameters chosen from Stepwise Selection in the upper table.

- The second column denotes the DF with each parameter.
- The third column denotes the estimated coefficients of the parameter.
- The fourth column denotes the standard error of the coefficient.
- The fifth column denotes the Wald Chi-Square statistic, computed as the square of the value obtained by dividing the parameter estimate by its standard error.
- The sixth column denotes the p-value (Pr > ChiSq) for the Wald Chi-square statistic with 1 DF.

Among all the parameters, ‘alphaS’ and ‘SamEn’ are chosen as significant predictive variables by using stepwise regression.

IV.1.2 Window=2048, Step=2048

It’s the Table IV-2 of stepwise regression, with outliers, analysis window=2048 with step 2048.

Table IV-2 Stepwise Regression, with outliers, Window=2048, Step=2048

Summary of Stepwise Selection								
	Effect			Number	Score	Wald		Variable
Step	Entered	Removed	DF	In	Chi-Square	Chi-Square	Pr > ChiSq	Label
1	alphaS		1	1	10.5101		0.0012	alphaS
2	PermEn		1	2	8.2362		0.0041	PermEn

Analysis of Maximum Likelihood Estimates					
Parameter	DF	Estimate	Standard Error	Wald Chi-Square	Pr > ChiSq
Intercept	1	24.9272	7.6916	10.5029	0.0012
alphaS	1	-7.3475	2.3004	10.2021	0.0014
PermEn	1	-28.0728	10.5029	7.1441	0.0075

Among all the parameters, ‘alphaS’ and ‘PermEn’ are chosen as significant predictive variables by using stepwise regression.

IV.1.3 Window=4096, Step=4096

It’s the Table IV-3 of stepwise regression, with outliers, analysis window=4096 with step 4096.

Table IV-3 Stepwise Regression, with outliers, Window=4096, Step=4096

Summary of Stepwise Selection								
	Effect			Number	Score	Wald		Variable
Step	Entered	Removed	DF	In	Chi-Square	Chi-Square	Pr > ChiSq	Label
1	alphaS		1	1	16.2963		<.0001	alphaS
2	SamEn		1	2	13.0092		0.0003	SamEn
3	AppEn		1	3	4.6201		0.0316	AppEn
4		AppEn	1	2		3.4910	0.0617	AppEn

Analysis of Maximum Likelihood Estimates					
Parameter	DF	Estimate	Standard Error	Wald Chi-Square	Pr > ChiSq
Intercept	1	14.7236	3.7491	15.4235	<.0001
alphaS	1	-13.1390	3.4558	14.4553	0.0001
SamEn	1	-31.5450	9.8542	10.2475	0.0014

Among all the parameters, ‘alphaS’ and ‘SamEn’ are chosen as significant predictive variables by using stepwise regression.

IV.2 Without outliers

IV.2.1 Window=1024, Step=1024

It’s the Table IV-4 of stepwise regression, without outliers, analysis window=1024 with step 1024.

Table IV-4 Stepwise Regression, without outliers, Window=1024, Step=1024

Summary of Stepwise Selection								
	Effect			Number	Score	Wald		Variable
Step	Entered	Removed	DF	In	Chi-Square	Chi-Square	Pr > ChiSq	Label
1	kurt		1	1	15.4348		<.0001	kurt
2	alphaS		1	2	6.0667		0.0138	alphaS
3	p_VLF		1	3	11.3656		0.0007	p_VLF

Analysis of Maximum Likelihood Estimates					
Parameter	**DF**	**Estimate**	**Standard Error**	**Wald Chi-Square**	**Pr > ChiSq**
Intercept	1	-18.7611	8.6438	4.7109	0.0300
kurt	1	0.3930	0.1206	10.6107	0.0011
p_VLF	1	-2.2262	0.7512	8.7829	0.0030
alphaS	1	23.7444	8.0431	8.7151	0.0032

Among all the parameters, ‘kurt’, ‘p_VLF’ and ‘alphaS’ are chosen as significant predictive variables by using stepwise regression.

IV.2.2 Window=2048, Step=2048

It’s the Table IV-5 of stepwise regression, without outliers, analysis window=2048 with step 2048.

Table IV-5 Stepwise Regression, without outliers, Window=2048, Step=2048

Summary of Stepwise Selection								
	Effect			**Number**	**Score**	**Wald**		**Variable**
Step	**Entered**	**Removed**	**DF**	**In**	**Chi-Square**	**Chi-Square**	**Pr > ChiSq**	**Label**
1	**alphaS**		1	1	9.9321		0.0016	alphaS
2	**SpAs**		1	2	7.5252		0.0061	SpAs
3		**SpAs**	1	1		3.8242	0.0505	SpAs

Analysis of Maximum Likelihood Estimates					
Parameter	**DF**	**Estimate**	**Standard Error**	**Wald Chi-Square**	**Pr > ChiSq**
Intercept	1	5.9008	2.1885	7.2702	0.0070
alphaS	1	-6.6680	2.3695	7.9188	0.0049

Among all the parameters, ‘alphaS’ is chosen as significant predictive variables by using stepwise regression.

IV.2.3 Window=4096, Step=4096

It's the Table IV-6 of stepwise regression, without outliers, analysis window=4096 with step 4096.

Table IV-6 Stepwise Regression, without outliers, Window=4096, Step=4096

Summary of Stepwise Selection								
	Effect			Number	Score	Wald		Variable
Step	Entered	Removed	DF	In	Chi-Square	Chi-Square	Pr > ChiSq	Label
1	AppEn		1	1	14.6433		0.0001	AppEn
2	alphaS		1	2	7.8846		0.0050	alphaS

Analysis of Maximum Likelihood Estimates					
Parameter	DF	Estimate	Standard Error	Wald Chi-Square	Pr > ChiSq
Intercept	1	14.8063	4.2478	12.1495	0.0005
alphaS	1	-9.0556	3.6030	6.3169	0.0120
AppEn	1	-39.5236	13.7163	8.3031	0.0040

Among all the parameters, 'alphaS' and 'AppEn' are chosen as significant predictive variables by using stepwise regression.

Appendix V
Results for Correlation Index (r^2)

V.1 Window=1024, Step=1024

The cross-correlation (r^2) between the RR and the respiratory series was computed (only for nasal channel) over the range of -240 to 240 sample lags (1 minute) and it was normalized to have $r^2(0)=1$.

The maximum r^2 values for each sequence were registered as well as the delay time at which these values occurred. Table V-1 reports the results of statistical analysis for r^2 between RR and nasal respiration on the entire population, in the window 1024 with step 1024.

Table V-1 Results of statistical analysis for r^2 between RR and nasal respiration, Window=1024, Step=1024

r^2	Sepsis	Non Sepsis	ANOVA	KruskWall	Wilrs
rn_raw	0.0800 ± 0.0872	0.0450 ± 0.0383	0.0001	0.0011	0.0011
rn_enp	0.5135 ± 0.1980	0.4953 ± 0.1825	0.4528	0.4374	0.4379

The level of significance was set at p value
p< 0.05 is marked in yellow

In Table V-1, the second and third column present "Mean Value ± Standard Deviation" of sepsis and non-sepsis infants respectively. The fourth, fifth and sixth column bring forth the p value of ANOVA, Kruskal-Wallis test and Wilcoxon rank-sum test respectively in each case.

- For the original nasal respiration and its envelope, correlation index r^2 is higher in sepsis infants than in non-sepsis ones. That is to say, sepsis condition doesn't influence on the original nasal respiration signal and its envelope.

V.2 Window=2048, Step=2048

It's the Table V-2 of statistical analysis for r^2 between RR and nasal respiration, in the window 2048 with step 2048.

Table V-2 Results of statistical analysis for r^2 between RR and nasal respiration, Window=2048, Step=2048

r^2	Sepsis	Non Sepsis	ANOVA	KruskWall	Wilrs
rn_raw	0.0649 ± 0.0774	0.0384 ± 0.0336	0.0241	0.0551	0.0554
rn_enp	0.4447 ± 0.2016	0.4104 ± 0.1611	0.3231	0.3821	0.3836

The level of significance was set at p value
p< 0.05 is marked in yellow

- For the original nasal respiration and its envelope, correlation index r^2 is higher in sepsis infants than in non-sepsis ones. That is to say, sepsis condition doesn't influence on the original nasal respiration signal and its envelope.

V.3 Window=4096, Step=4096

It's the Table V-3 of statistical analysis for r^2 between RR and nasal respiration, in the window 4096 with step 4096.

Table V-3 Results of statistical analysis for r^2 between RR and nasal respiration, Window=4096, Step=4096

r^2	Sepsis	Non Sepsis	ANOVA	KruskWall	Wilrs
rn_raw	0.0520 ± 0.0653	0.0323 ± 0.0263	0.2195	0.3626	0.3683
rn_enp	0.4040 ± 0.1887	0.3382 ± 0.1393	0.2012	0.2418	0.2461

The level of significance was set at p value
$p < 0.05$ is marked in yellow

- For the original nasal respiration and its envelope, correlation index r^2 is higher in sepsis infants than in non-sepsis ones. That is to say, sepsis condition doesn't influence on the original nasal respiration signal and its envelope.

Appendix VI
Results for Coherence function (*Cohere*)

VI.1 Window=1024, Step=1024

Coherence is a function of frequency with values between 0 and 1 that indicate how well the input (the RR signal) corresponds to the output (the respiratory signal) at each frequency.

The squared coherence estimate of the system has been computed using Welch's averaged periodogram method.

A vector divides RR and Respiration signals into overlapping sections of 64 or 32 points (depending on the signal length, here 64 is selected), and then windows each section with this vector (hamming window).

As final results, the cumulative sum of the coherence values upon the frequency band of interest (VLF = 0.002 —0.02 Hz), normalized (divided by N points, correspondent to the frequency band points, here N=256) to give a value between 0 and 1, was recorded as:

$$\frac{1}{N}\sum_{f=0.002}^{0.02} C_{RRresp}(f) \qquad \text{(VI.1)}$$

Table VI-1 shows the results of statistical analysis for Coherence between RR and nasal respiration, in the window 1024 with step 1024.

Table VI-1 Results of statistical analysis for *Cohere* between RR and nasal respiration, Window=1024, Step=1024

Cohere	Sepsis	Non Sepsis	ANOVA	KruskWall	Wilrs
rn_raw	0.4375 ± 0.1693	0.4149 ± 0.1542	0.2742	0.2668	0.2672

In Table VI-1, the second and third column present "Mean Value ± Standard Deviation" of sepsis and non-sepsis infants respectively. The fourth, fifth and sixth column bring forth the p value of ANOVA, Kruskal-Wallis test and Wilcoxon rank-sum test respectively in each case.

- For original nasal respiration, coherence index is higher in sepsis infants than in non-sepsis ones. That is to say, sepsis condition doesn't influence on the original nasal respiration signal and its envelope.

VI.2 Window=2048, Step=2048

Table VI-2 shows the results of statistical analysis for Coherence between RR and nasal respiration, in the window 2048 with step 2048.

Table VI-2 Results of statistical analysis for *Cohere* between RR and nasal respiration, Window=2048, Step=2048

Cohere	Sepsis	Non Sepsis	ANOVA	KruskWall	Wilrs
rn_raw	0.2940 ± 0.1534	0.2868 ± 0.1535	0.8037	0.7127	0.7147

- For original nasal respiration, coherence index is higher in sepsis infants than in non-sepsis ones. That is to say, sepsis condition doesn't influence on the original nasal respiration signal and its envelope.

VI.3 Window=4096, Step=4096

Table VI-3 shows the results of statistical analysis for Coherence between RR and nasal respiration, in the window 4096 with step 4096.

Table VI-3 Results of statistical analysis for *Cohere* between RR and nasal respiration, Window=4096, Step=4096

Cohere	Sepsis	Non Sepsis	ANOVA	KruskWall	Wilrs
rn_raw	0.1971 ± 0.1342	0.2241 ± 0.1611	0.5357	0.8965	0.9051

- For original nasal respiration, coherence index is lower in sepsis infants than in non-sepsis ones. Therefore, sepsis condition seems to destroy the informative content of the signal, consequently influence the coherence properties with the original nasal respiration signal.

Appendix VII
Results for Local Linear Correlation Coefficient ($r^2_{t,f}$)

VII.1 Window=1024, Step=1024

VII.1.1 Multi-Boxplot $r^2_{t,f}$ between RR and original nasal respiration

The following section reports the results of statistical analysis for $r^2_{t,f}$ between RR and original nasal respiration frequency band by band. These qualitative findings were statistically verified. Fig. VII-1 depicts the sub-band distribution of the time-frequency correlation coefficient $r^2_{t,f}$, over a threshold set to 0.8, in the window 1024 with step 1024.

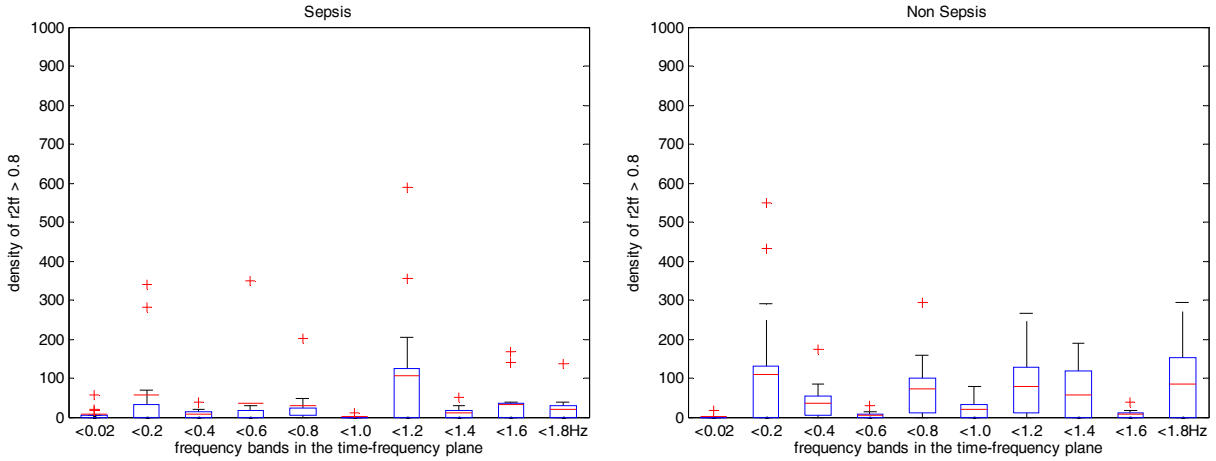

Fig. VII-1 Distribution of $r^2_{t,f}$ between RR and original nasal respiration (greater than 0.8), Window=1024, Step=1024

In Boxplot, red line is mean value.

Table VII-1 demonstrates the results of statistical analysis for $r^2_{t,f}$ between RR and nasal respiration, in the window 1024 with step 1024.

Table VII-1 Statistical analysis for $r^2_{t,f}$ between RR and nasal respiration, Window=1024, Step=1024

Band(Hz)	Sepsis	Non Sepsis	ANOVA	KruskWall	Wilrs
0-0.02	7.2308 ± 16.6841	1.3846 ± 4.9923	0.2379	0.2704	0.2885
0.02-0.2	56.0769 ±115.2595	109.5385 ±188.1266	0.3909	0.6855	0.7055
0.2-0.4	8.6154 ± 11.3324	36.2308 ± 49.6154	0.0421	0.0445	0.0484
0.4-0.6	34.5385 ± 94.6657	5.0000 ± 8.5342	0.2736	0.1881	0.1975
0.6-0.8	29.1538 ± 53.2930	72.7692 ± 82.2559	0.1217	0.1725	0.1807
0.8-1.0	1.7692 ± 4.3235	18.5385 ± 26.0947	0.0314	0.0254	0.0275
1.0-1.2	105.6154 ±178.8689	79.2308 ±100.9762	0.6474	0.5323	0.5495

Band(Hz)	Sepsis	Non Sepsis	ANOVA	KruskWall	Wilrs
1.2-1.4	10.3077 ± 16.1987	56.8462 ± 70.3253	0.0288	0.1547	0.1630
1.4-1.6	33.6154 ± 55.3075	7.4615 ± 11.1177	0.1076	0.3446	0.3585
1.6-1.8	21.0769 ± 37.8912	83.6154 ±105.7848	0.0562	0.1995	0.2088

The level of significance was set at p value
p< 0.05 is marked in yellow

- We confirm statistically (p<0.05 whatever the statistical tests) that the higher correlation is retrieved in the two frequency bands for the non-sepsis group (*0.2<f<0.4Hz and 0.8<f<1.0Hz*).

VII.1.2 Multi-Boxplot $r^2_{t,f}$ between RR and envelop of nasal respiration

The followings report the results of statistical analysis for $r^2_{t,f}$ between RR and envelop of nasal respiration frequency band by band. These qualitative findings were statistically verified. Fig. VII-2 depicts the sub-band distribution of the time-frequency correlation coefficient $r^2_{t,f}$, over a threshold set to 0.8, in the window 1024 with step 1024.

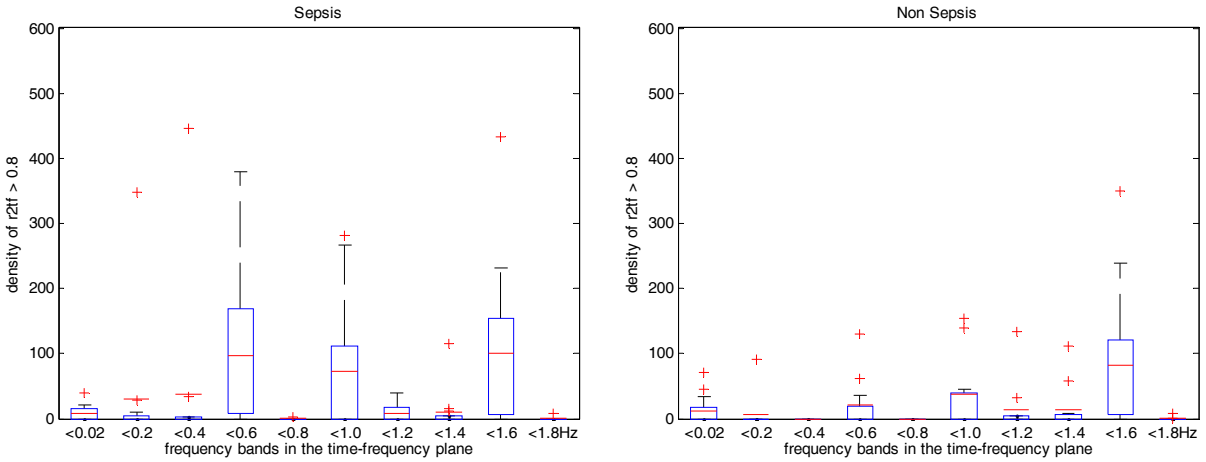

Sepsis Non-Sepsis

Fig. VII-2 Distribution of $r^2_{t,f}$ between RR and envelope of nasal respiration (greater than 0.8), Window=1024, Step=1024

In Boxplot, red line is mean value.

Table VII-2 presents the results of statistical analysis for $r^2_{t,f}$ between RR and envelop of nasal respiration, in the window 1024 with step 1024.

Table VII-2 Statistical analysis for $r^2_{t,f}$ between RR and envelop of nasal respiration, Window=1024, Step=1024

Band(Hz)	Sepsis	Non Sepsis	ANOVA	KruskWall	Wilrs
0-0.02	8.7692 ± 15.2050	12.6154 ± 23.1572	0.6212	0.6946	0.7171
0.02-0.2	30.1538 ± 95.8478	7.0769 ± 25.5162	0.4098	0.0889	0.0956
0.2-0.4	37.3846 ±123.1480	0.0000 ± 0.0000	0.2846	0.0338	0.0373
0.4-0.6	97.0000 ±123.1990	20.6923 ± 37.5730	0.0431	0.0167	0.0179
0.6-0.8	0.1538 ± 0.5547	0.0000 ± 0.0000	0.3273	0.3173	0.3560
0.8-1.0	72.2308 ±102.8139	37.4615 ± 51.3235	0.2861	0.6582	0.6771
1.0-1.2	8.6923 ± 14.0735	13.6154 ± 36.9110	0.6572	0.9318	0.9545
1.2-1.4	11.0769 ± 31.9256	14.0000 ± 33.1989	0.8209	1.0000	1.0000
1.4-1.6	101.5385 ±128.5461	82.7692 ±112.1169	0.6951	0.8573	0.8775
1.6-1.8	0.6923 ± 2.4962	0.7692 ± 2.4884	0.9379	0.5791	0.6111

The level of significance was set at p value
p< 0.05 is marked in yellow

- We confirm statistically (p<0.05 whatever the statistical tests) that the higher correlation is retrieved in the frequency band for the sepsis group (*0.4<f<0.6Hz*).

VII.2 Window=2048, Step=2048

VII.2.1 Multi-Boxplot $r^2_{t,f}$ between RR and original nasal respiration

Fig. VII-3 depicts the sub-band distribution of the time-frequency correlation coefficient $r^2_{t,f}$, over a threshold set to 0.8, in the window 2048 with step 2048.

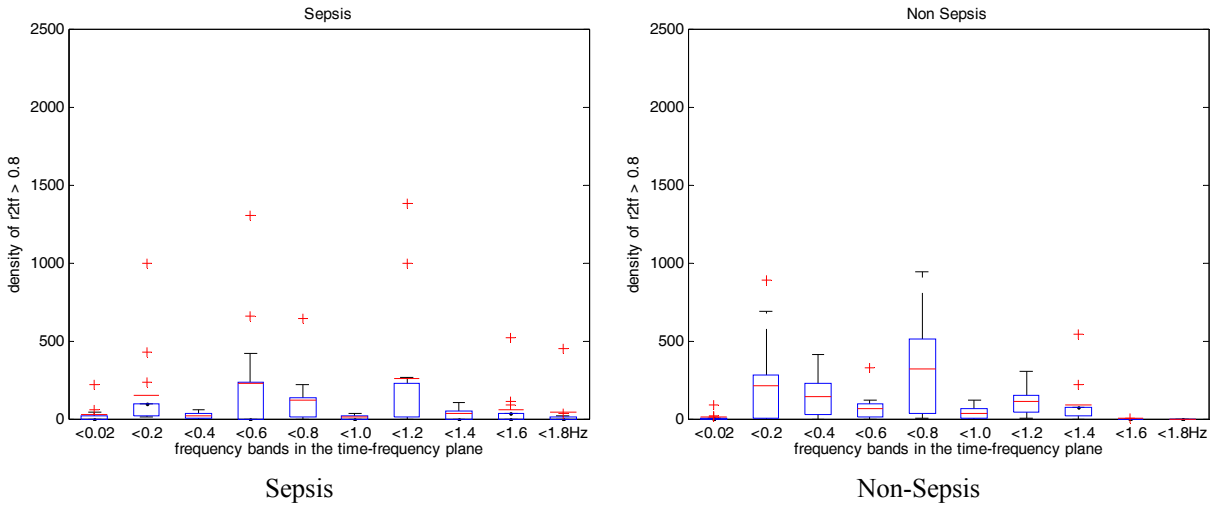

Sepsis Non-Sepsis

Fig. VII-3 Distribution of $r^2_{t,f}$ between RR and original nasal respiration (greater than 0.8), Window=2048, Step=2048

Table VII-3 demonstrates the results of statistical analysis for $r^2_{t,f}$ between RR and nasal respiration, in the window 2048 with step 2048.

Table VII-3 Statistical analysis for $r^2_{t,f}$ between RR and nasal respiration,Window=2048, Step=2048

Band(Hz)	Sepsis	Non Sepsis	ANOVA	KruskWall	Wilrs
0-0.02	25.7692 ± 60.6055	9.3846 ± 25.4740	0.3778	0.5768	0.5995
0.02-0.2	149.1538 ±282.2180	211.0000 ±302.9101	0.5951	0.6626	0.6813
0.2-0.4	21.1538 ± 18.8938	140.0000 ±145.1626	0.0074	0.0158	0.0169
0.4-0.6	225.0769 ±379.1566	68.0769 ± 87.6170	0.1587	0.6618	0.6806
0.6-0.8	117.5385 ±171.3941	319.1538 ±313.1724	0.0529	0.0858	0.0906
0.8-1.0	9.0769 ± 12.3319	37.0000 ± 42.3084	0.0315	0.0539	0.0573
1.0-1.2	260.6154 ±427.6366	108.0000 ± 85.9787	0.2192	0.9386	0.9591
1.2-1.4	31.4615 ± 36.5208	86.8462 ±146.9818	0.1998	0.2074	0.2168
1.4-1.6	56.8462 ±142.7421	0.0769 ± 0.2774	0.1645	0.0478	0.0518
1.6-1.8	39.9231 ±124.0272	0.0000 ± 0.0000	0.2572	0.0338	0.0373

The level of significance was set at p value
p< 0.05 is marked in yellow

- We confirm statistically (p<0.05 whatever the statistical tests) that the higher correlation is retrieved in the low frequency band for the non-sepsis group (*0.2<f<0.4Hz*).

VII.2.2 Multi-Boxplot $r^2_{t,f}$ between RR and envelop of nasal respiration

Fig. VII-4 depicts the sub-band distribution of the time-frequency correlation coefficient $r^2_{t,f}$, over a threshold set to 0.8, in the window 2048 with step 2048.

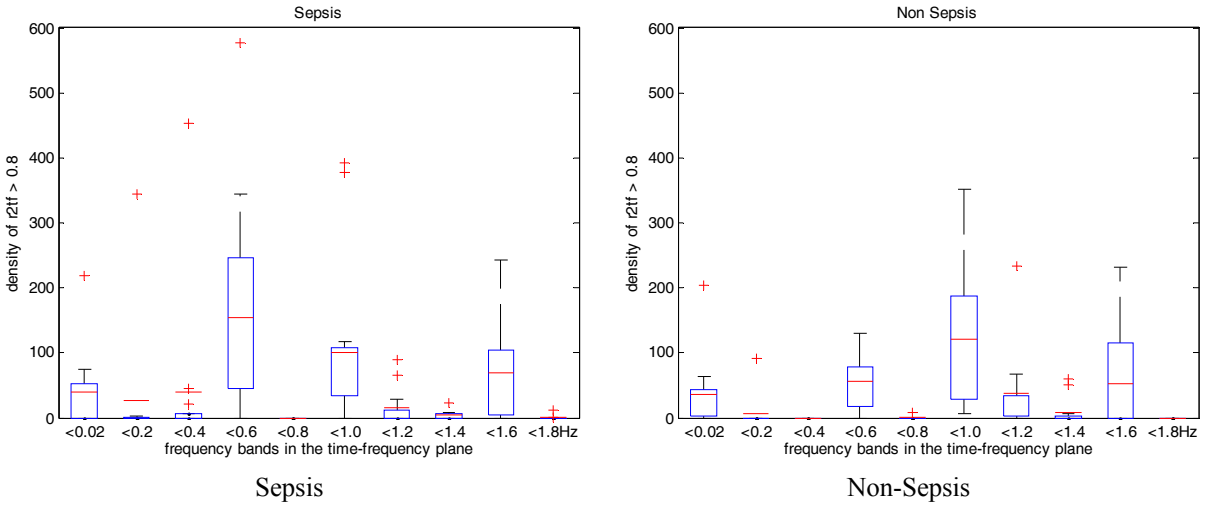

Sepsis Non-Sepsis

Fig. VII-4 Distribution of $r^2_{t,f}$ between RR and envelope of nasal respiration (greater than 0.8), Window=2048, Step=2048

Table VII-4 presents the results of statistical analysis for $r^2_{t,f}$ between RR and envelop of nasal respiration, in the window 2048 with step 2048.

Table VII-4 Statistical analysis for $r^2_{t,f}$ between RR and envelop of nasal respiration, Window=2048, Step=2048

Band(Hz)	Sepsis	Non Sepsis	ANOVA	KruskWall	Wilrs
0-0.02	39.4615 ± 59.9689	36.7692 ± 54.0450	0.9053	0.9171	0.9378
0.02-0.2	26.8462 ± 95.5954	7.0769 ± 25.5162	0.4782	0.1678	0.1796
0.2-0.4	40.3077 ±125.0329	0.0000 ± 0.0000	0.2565	0.0338	0.0373
0.4-0.6	153.9231 ±170.0140	56.6154 ± 42.9467	0.0568	0.1653	0.1733
0.6-0.8	0.0000 ± 0.0000	0.6923 ± 2.4962	0.3273	0.3173	0.3560
0.8-1.0	101.1538 ±130.2061	120.3846 ±110.6545	0.6885	0.5553	0.5726
1.0-1.2	15.4615 ± 28.9471	37.1538 ± 62.1314	0.2651	0.1355	0.1425
1.2-1.4	4.1538 ± 6.8172	9.0769 ± 20.5526	0.4204	0.5384	0.5579
1.4-1.6	68.4615 ± 77.4689	52.1538 ± 74.8608	0.5902	0.2628	0.2741
1.6-1.8	1.0000 ± 3.3166	0.0000 ± 0.0000	0.2878	0.1492	0.1655

The level of significance was set at p value
p< 0.05 is marked in yellow

- No frequency band has significant correlation

VII.3 Window=4096, Step=4096

VII.3.1 Multi-Boxplot $r^2_{t,f}$ between RR and original nasal respiration

Fig. VII-5 depicts the sub-band distribution of the time-frequency correlation coefficient $r^2_{t,f}$, over a threshold set to 0.8, in the window 4096 with step 4096.

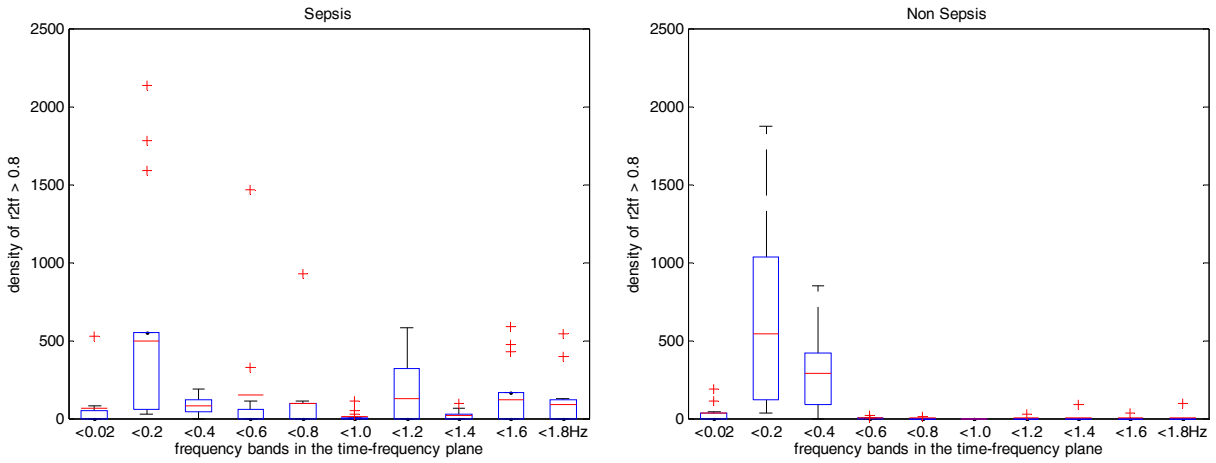

Sepsis Non-Sepsis

Fig. VII-5 Distribution of $r^2_{t,f}$ between RR and original nasal respiration (greater than 0.8), Window=4096, Step=4096

Table VII-5 demonstrates the results of statistical analysis for $r^2_{t,f}$ between RR and nasal respiration, in the window 4096 with step 4096.

Table VII-5 Statistical analysis for $r^2_{t,f}$ between RR and nasal respiration,Window=4096, Step=4096

Band(Hz)	Sepsis	Non Sepsis	ANOVA	KruskWall	Wilrs
0-0.02	64.3846 ±141.4735	32.2308 ± 56.0344	0.4536	0.4715	0.4881
0.02-0.2	499.1538 ±770.1144	543.0000 ±579.0105	0.8710	0.2282	0.2382
0.2-0.4	81.6923 ± 54.8625	291.6154 ±267.9439	0.0107	0.0210	0.0224
0.4-0.6	150.5385 ±405.6141	2.0769 ± 4.6630	0.1994	0.2214	0.2335
0.6-0.8	97.9231 ±253.0334	0.7692 ± 2.7735	0.1790	0.0478	0.0518
0.8-1.0	14.0769 ± 32.0558	0.0000 ± 0.0000	0.1264	0.0716	0.0792
1.0-1.2	128.2308 ±208.9969	2.2308 ± 8.0432	0.0400	0.1091	0.1176
1.2-1.4	18.6923 ± 33.6684	7.0769 ± 25.5162	0.3314	0.1680	0.1798
1.4-1.6	120.4615 ±217.3590	2.9231 ± 10.5393	0.0633	0.1091	0.1176
1.6-1.8	90.6154 ±176.0334	7.3077 ± 26.3483	0.1045	0.1091	0.1176

The level of significance was set at p value
p< 0.05 is marked in yellow

- We confirm statistically (p<0.05 whatever the statistical tests) that the higher correlation is retrieved in the low frequency band for the non-sepsis group (*0.2<f<0.4Hz*).

VII.3.2 Multi-Boxplot $r^2_{t,f}$ between RR and envelop of nasal respiration

Fig. VII-6 depicts the sub-band distribution of the time-frequency correlation coefficient $r^2_{t,f}$, over a threshold set to 0.8, in the window 4096 with step 4096.

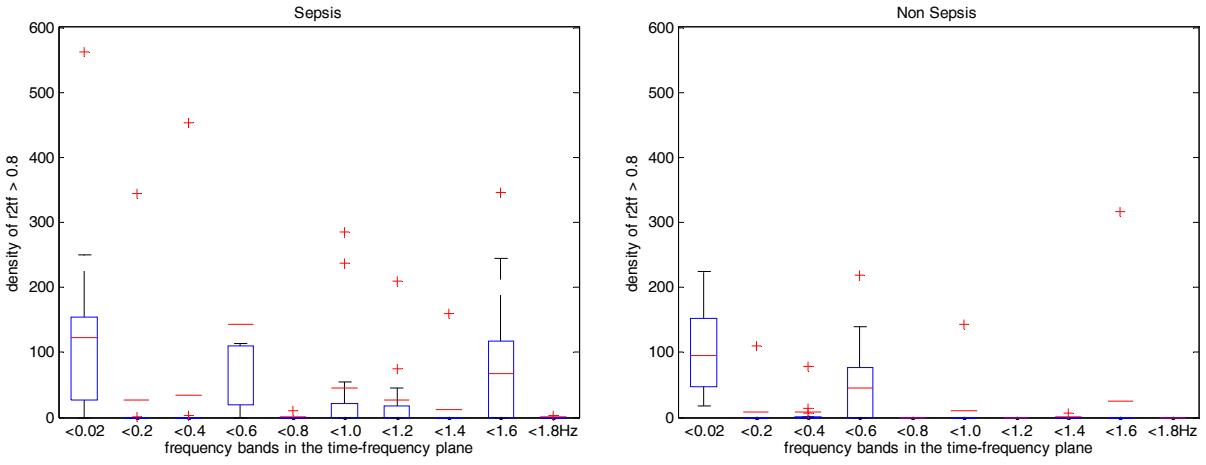

Sepsis Non-Sepsis

Fig. VII-6 Distribution of $r^2_{t,f}$ between RR and envelope of nasal respiration (greater than 0.8), Window=4096, Step=4096

Table VII-6 presents the results of statistical analysis for $r^2_{t,f}$ between RR and envelop of nasal respiration, in the window 4096 with step 4096.

Table VII-6 Statistical analysis for $r^2_{t,f}$ between RR and envelop of nasal respiration, Window=4096, Step=4096

Band(Hz)	Sepsis	Non Sepsis	ANOVA	KruskWall	Wilrs
0-0.02	123.4615 ±152.6312	95.0769 ± 64.4120	0.5425	0.7976	0.8175
0.02-0.2	26.6154 ± 95.6631	8.3846 ± 30.2312	0.5186	0.5481	0.5793
0.2-0.4	35.0000 ±125.5946	7.6154 ± 21.5543	0.4460	0.6281	0.6548
0.4-0.6	142.2308 ±239.7172	45.6154 ± 70.9678	0.1763	0.0888	0.0938
0.6-0.8	0.8462 ± 3.0509	0.0000 ± 0.0000	0.3273	0.3173	0.3560
0.8-1.0	45.6923 ± 97.3827	11.0769 ± 39.9384	0.2473	0.0766	0.0825
1.0-1.2	26.0000 ± 59.5987	0.0000 ± 0.0000	0.1288	0.0338	0.0373
1.2-1.4	12.3077 ± 44.3760	0.4615 ± 1.6641	0.3457	0.9558	1.0000
1.4-1.6	66.9231 ±117.1832	24.3077 ± 87.6426	0.3042	0.1680	0.1798
1.6-1.8	0.1538 ± 0.5547	0.0000 ± 0.0000	0.3273	0.3173	0.3560

The level of significance was set at p value
p< 0.05 is marked in yellow

- No frequency band has significant correlation

Appendix VIII
Results for Non-linear Regression Coefficient (h^2)

This Appendix presents the results obtained for the non-linear regression coefficient (h^2). Tests have been conducted to evaluate $h^2(\tau)$, considering two directions:

→ RR vs. the nasal respiratory signal
← the nasal respiratory signal vs. RR

VIII.1 Window=1024, Step=1024

It's the Table VIII-1 of statistical analysis for h^2 in one direction: RR vs. nasal respiration, in the window 1024 with step 1024.

Table VIII-1 Results of statistical analysis for h^2 between RR and nasal respiration, Window=1024, Step=1024

h^2	Sepsis	Non Sepsis	ANOVA	KruskWall	Wilrs
rn_raw	0.0813 ± 0.0779	0.0432 ± 0.0403	0.0000	0.0000	0.0000
rn_enp	0.4500 ± 0.2011	0.4083 ± 0.1620	0.0759	0.0937	0.0939

The level of significance was set at p value
$p < 0.05$ is marked in yellow

In Table VIII-1, the second and third column present "Mean Value ± Standard Deviation" of sepsis and non-sepsis infants respectively. The fourth, fifth and sixth column bring forth the p value of ANOVA, Kruskal-Wallis test and Wilcoxon rank-sum test respectively in each case.

While Table VIII-2 presents the statistical analysis in the other direction: nasal respiration vs. RR, in the window 1024 with step 1024.

Table VIII-2 Results of statistical analysis for h^2 between nasal respiration and RR, Window=1024, Step=1024

h^2	Sepsis	Non Sepsis	ANOVA	KruskWall	Wilrs
nr_raw	0.1887 ± 0.2531	0.0975 ± 0.0737	0.0003	0.0000	0.0000
nr_enp	0.5648 ± 0.1808	0.5160 ± 0.1502	0.0225	0.0062	0.0063

The level of significance was set at p value
$p < 0.05$ is marked in yellow

In Table VIII-2, the columns are identical to Table VIII-1.

In the case of (Win1024, Step1024), the non-linear relationship between HRV and respiration signals is calculated as non-linear regression coefficient (h^2). From these results, we can discover that

√ h2_rn_raw (h^2 between RR and original nasal respiration)
√ h2_nr_raw (h^2 between original nasal respiration and RR)
√ h2_nr_enp (h^2 between envelop of nasal respiration and RR)
can discriminate sepsis from non-sepsis.

VIII.2 Window=2048, Step=2048

It's the Table VIII-3 of statistical analysis for h^2 in one direction: RR vs. nasal respiration, in the window 2048 with step 2048.

Table VIII-3 Results of statistical analysis for h^2 between RR and nasal respiration, Window=2048, Step=2048

h^2	Sepsis	Non Sepsis	ANOVA	KruskWall	Wilrs
rn_raw	0.0454 ± 0.0470	0.0190 ± 0.0165	0.0002	0.0001	0.0001
rn_enp	0.3226 ± 0.1870	0.2656 ± 0.1424	0.0729	0.1265	0.1272

The level of significance was set at p value
p< 0.05 is marked in yellow

In Table VIII-3, the columns are identical to Table VIII-1.

While Table VIII-4 presents the statistical analysis in the other direction: nasal respiration vs. RR, in the window 2048 with step 2048.

Table VIII-4 Results of statistical analysis for h^2 between nasal respiration and RR, Window=2048, Step=2048

h^2	Sepsis	Non Sepsis	ANOVA	KruskWall	Wilrs
nr_raw	0.1253 ± 0.1165	0.0563 ± 0.0509	0.0001	0.0000	0.0000
nr_enp	0.4114 ± 0.1906	0.3593 ± 0.1962	0.1504	0.0680	0.0684

The level of significance was set at p value
p< 0.05 is marked in yellow

In Table VIII-4, the columns are identical to Table VIII-1.

In the case of (Win2048, Step2048), the non-linear relationship between HRV and respiration signals is calculated as non-linear regression coefficient (h^2). From these results, we can discover that
√ h2_rn_raw (h^2 between RR and original nasal respiration)
√ h2_nr_raw (h^2 between original nasal respiration and RR)
can discriminate sepsis from non-sepsis

VIII.3 Window=4096, Step=4096

It's the Table VIII-5 of statistical analysis for h^2 in one direction: RR vs. nasal respiration, in the window 4096 with step 4096.

Table VIII-5 Results of statistical analysis for h^2 between RR and nasal respiration, Window=4096, Step=4096

h^2	Sepsis	Non Sepsis	ANOVA	KruskWall	Wilrs
rn_raw	0.0214 ± 0.0215	0.0117 ± 0.0123	0.0241	0.0256	0.0263
rn_enp	0.2904 ± 0.1945	0.1675 ± 0.0891	0.0135	0.0355	0.0364

The level of significance was set at p value
p< 0.05 is marked in yellow

In Table VIII-5, the columns are identical to Table VIII-1.

While Table VIII-6 presents the statistical analysis in the other direction: nasal respiration vs. RR, in the window 4096 with step 4096.

Table VIII-6 Results of statistical analysis for h^2 between nasal respiration and RR, Window=4096, Step=4096

h^2	Sepsis	Non Sepsis	ANOVA	KruskWall	Wilrs
nr_raw	0.0944 ± 0.0857	0.0436 ± 0.0370	0.0194	0.0105	0.0109
nr_enp	0.3616 ± 0.2357	0.2444 ± 0.1532	0.0628	0.1238	0.1264

The level of significance was set at p value
p< 0.05 is marked in yellow

In Table VIII-6, the columns are identical to Table VIII-1.

In the case of (Win4096, Step4096), the non-linear relationship between HRV and respiration signals is calculated as non-linear regression coefficient (h^2). From these results, we can discover that

- √ h2_rn_raw (h^2 between RR and original nasal respiration)
- √ h2_rn_enp (h^2 between RR and envelop of nasal respiration)
- √ h2_nr_raw (h^2 between original nasal respiration and RR)

can discriminate sepsis from non-sepsis

Appendix IX
Theorem in Optimal Fusion

THEOREM. *Given n detectors and the corresponding quantities as defined previously, we have*

$$\log\frac{P(H_1/u)}{P(H_0/u)} = \log\frac{P_1}{P_0} + \sum_{S_+}\log\frac{1-P_{M_i}}{P_{F_i}} + \sum_{S_-}\log\frac{P_{M_i}}{1-P_{F_i}} \tag{IX.1}$$

where S_+ is the set of all i such that u_i = + 1 and S_- is the set of all i such that u_i = -1.

PROOF. We have

$$P(H_1/u) = \frac{P(H_1,u)}{P(u)} = \frac{P_1}{P(u)}\prod_{S_+}P(u_i=+1/H_1)\bullet\prod_{S_-}P(u_i=-1/H_1) = \frac{P_1}{P(u)}\prod_{S_+}(1-P_{M_i})\bullet\prod_{S_-}P_{M_i} \tag{IX.2}$$

In a similar manner,

$$P(H_0/u) = \frac{P_0}{P(u)}\prod_{S_-}(1-P_{F_i})\bullet\prod_{S_+}P_{F_i} \tag{IX.3}$$

Thus

$$\log\frac{P(H_1/u)}{P(H_0/u)} = \log\frac{P_1}{P_0} + \sum_{S_+}\log\frac{1-P_{M_i}}{P_{F_i}} + \sum_{S_-}\log\frac{P_{M_i}}{1-P_{F_i}} \tag{IX.4}$$

which completes the proof.

Résumé
Le sepsis tardif, défini comme une infection systémique chez les nouveaux nés âgés de plus de 3 jours, survient chez environ 7% à 10% de tous les nouveau-nés et chez plus de 25% des nouveau-nés de très faible poids de naissance qui sont hospitalisés dans les unités de soins intensifs néonatals (USIN). Compte tenu du taux élevé de morbidité et de mortalité associée à l'infection, des marqueurs fiables de cette infection sont nécessaires.
L'objectif de cette thèse est de déterminer si la variabilité du rythme cardiaque (VRC), la respiration et l'analyse de leurs relations aident au diagnostic de l'infection chez les nouveau-nés prématurés par des moyens non invasifs en USIN.
Tout d'abord, la RC a été étudiée, non seulement par des méthodes de distribution (moy, varn, skew, kurt, med, SpAs), par les méthodes linéaires: le domaine temporel (SD, RMSSD) et dans le domaine fréquentiel (p_VLF, p_LF, p_HF), mais aussi par les méthodes non–linéaires: la théorie du chaos (alphaS, alphaF) et la théorie de l'information (AppEn, SamEn, PermEn, Regul). Pour chaque méthode, trois tailles de fenêtre 1024/2048/4096 ont été étudiées afin d'identifier les meilleures façons de distinguer les bébés sepsis des non-sepsis. Les résultats montrent que les indices alphaS, alphaF et SamEn sont les paramètres optimaux pour séparer les deux populations.
La question du couplage fonctionnel entre la VRC et la respiration nasale a été ensuite adressée. Des relations linéaires et non-linéaires ont été explorées. Les indices linéaires sont la corrélation (r^2), l'indice de la fonction de cohérence (*Cohere*) et la corrélation temps-fréquence ($r^2_{t,f}$) , tandis que le coefficient de régression non-linéaire (h^2) a été utilisé pour analyser des relations non-linéaires. Nous avons évalué les deux directions de couplage pendant l'évaluation de l'indice h^2 de régression non-linéaire. Les analyses démontrent que les relations non linéaires dans les deux directions de couplage ainsi que les relations dans le plan temps-fréquence se modifient avec l'infection et représentent de fait des moyens complémentaires pour le diagnostic du sepsis de façon non-invasive chez ces patients fragiles.
En outre, l'étude de faisabilité de la détection du sepsis en USIN en temps quasi-réel est réalisée sur la base des paramètres jugés discriminants. Nous avons montré que le test proposé, basé sur la fusion optimale des six indices (alphaS, alphaF et SamEn, 2 paramètres de couplages non linéaire et couplage dans le plan temps-fréquence) conduit à de bonnes performances statistiques, présente une bonne répétabilité et permet de mettre en place un test en vue du diagnostic non invasif et précoce du sepsis.

Mots-clés: Unités de soins intensifs néonatals (USIN), nouveau-nés prématurés, sepsis, non-sepsis, variabilité du rythme cardiaque (VRC), respiration, couplage fonctionnel entre VRC et respiration nasale, fusion optimale

Abstract
Late-onset sepsis, defined as a systemic infection in neonates older than 3 days, occurs in approximately 7% to 10% of all neonates and in more than 25% of very low birth weight infants who are hospitalized in Neonatal Intensive Care Units (NICU). In view of the high morbidity and mortality associated with infection, reliable markers are needed.
Recurrent and severe spontaneous apneas and bradycardias (AB) is one of the major clinical early indicators of systemic infection in the premature infant. It requires prompt laboratory investigation so that treatment can start without delay. Various hematological and biochemical markers have been evaluated for this indication but they are invasive procedures that cannot be repeated several times.
The objective of this Ph.D dissertation was to determine if heart rate variability (HRV), respiration and the analysis of their relationships help to the diagnosis of infection in premature infants via non-invasive ways in NICU. Therefore, we carried out Mono-Channel (MC) and Bi-Channel (BC) Analysis in two selected groups of premature infants: sepsis (S) vs. non-sepsis (NS).
Firstly, we studied the RR series not only by distribution methods (moy, varn, skew, kurt, med, SpAs), by linear methods: time domain (SD, RMSSD) and frequency domain (p_VLF, p_LF, p_HF), but also by non-linear methods: chaos theory (alphaS, alphaF) and information theory (AppEn, SamEn, PermEn, Regul). For each method, we attempt three sizes of window 1024/2048/4096, and then compare these methods in order to find the optimal ways to distinguish S from NS. The results show that **alphaS**, **alphaF** and **SamEn** are optimal parameters to recognize sepsis from the diagnosis of late neonatal infection in premature infants with unusual and recurrent AB.
The question about the functional coupling of HRV and nasal respiration is addressed. Linear and non-linear relationships have been explored. Linear indexes were correlation (r^2), coherence function (*Cohere*) and time-frequency index ($r^2_{t,f}$), while a non-linear regression coefficient (h^2) was used to analyze non-linear relationships. We calculated two directions during evaluate the index h^2 of non-linear regression. Finally, from the entire analysis process, it is obvious that the three indexes (**r2tf_rn_raw_0p2_0p4**, **h2_rn_raw** and **h2_nr_raw**) were complementary ways to diagnosticate sepsis in a non-invasive way, in such delicate patients.
Furthermore, feasibility study is carried out on the candidate parameters selected from MC and BC respectively. We discovered that the proposed test based on optimal fusion of 6 features shows good performance with the largest Area Under Curves (AUC) and the least Probability of False Alarm (P_{FA}).
As a conclusion, we believe that the selected measures from MC and BC signal analysis have a good repeatability and accuracy to test for the diagnosis of sepsis via non-invasive NICU monitoring system, which can reliably confirm or refute the diagnosis of infection at an early stage.

Keywords: Neonatal intensive care units (NICU), premature newborns, sepsis, non-sepsis, autonomic nervous system (ANS), heart rate variability (HRV), respiratory system, respiration, linear methods, non-linear methods, statistical analysis, feasibility study, optimal fusion, receiver operating characteristic (ROC), clinical decision making, medical informatics, prediction